2004

A Novel Subfamily of Three StAR-Related Lipid Transfer Proteins That Are Differentially-Regulated and Function in Intracellular Cholesterol Metabolism

Raymond E. Soccio

A novel subfamily of three StAR-related lipid transfer proteins that are differentially-regulated and function in intracellular cholesterol metabolism

A thesis presented to the faculty of
The Rockefeller University
in partial fulfillment of the requirements for
the degree Doctor of Philosophy

by

Raymond E. Soccio

Dedicated to my wife Leslie

"There is something fascinating about science. One gets such wholesale returns of conjecture out of such a trifling investment of fact."

-Mark Twain

ACKNOWLEDGEMENTS

I would like to express my sincere gratitude to the many people who helped make this thesis work possible. First and foremost, my research advisor ***Jan Breslow*** was the best mentor any young scientist could aspire to have. His unfailing support, his wise counsel, and his gentle encouragement were always very much appreciated. I can almost forgive him for being a Yankees fan. I thank all members of the ***Breslow lab*** past and present for their help and friendship over the past four years, but I must acknowledge three in particular. First, ***Rachel Adams*** was a research assistant indispensable in performing many of the experiments described here. Her diligence and positive attitude were key to this work. Second, ***Effie Sehayek*** helped me start in the lab and provided guidance throughout. Third, my fellow MD-PhD student ***Kara Maxwell*** was always there to discuss ideas or collaborate on experiments. I must also thank members of the ***Stoffel lab***, our floormates who enriched our lab meetings and working environment. It really was a pleasure working with everyone.

I was also fortunate to have a number of wonderful collaborators. ***Joerg Heyer*** helped with the initial microarray experiment, which led to the rest of this work. ***Michael Romanowski*** and ***Stephen Burley*** solved the X-ray crystal structure of StarD4. ***Elliot Perens*** and ***Shai Shaham*** introduced me to the world of nematode worms. ***Patricia Morris*** generously provided reagents and expertise in the field of fertility.

I must also thank several other scientists. Of course, I thank my thesis committee, ***Markus Stoffel***, ***Bob Roeder***, ***Jeff Friedman***, and ***Fred Maxfield***, for their patience and guidance. ***Jonathan Smith***, ***Mike Sinensky***, ***Ed Fisher***, ***Ira Tabas***, and ***Alan Tall*** also spent hours listening to my work and offered very useful suggestions over the years. I also thank my undergraduate research advisor ***Grace Gill***, for helping start me on this path.

The administration and staff, both ***Olaf Andersen*** and the Tri-Institutional MD-PhD program and ***Sid Strickland*** and the Rockefeller Graduate School, were a model of efficiency and kept things running smoothly through the entire educational process.

I extend my heartfelt thanks to my family and friends for their unwavering love and support, especially my parents, ***Raymond and Lorraine Soccio***, and my second parents, ***Louis and Margaret Castelo***, my sister ***Stacey***, my siblings-in-law ***Janet, Kimbery, Michael, John, and Dino***. Most of all, I thank my wife and soul-mate. ***Leslie***, everything we've done, we've done together. Words cannot express my gratitude.

TABLE OF CONTENTS

List of Tables x
List of Figures xiv
List of Abbreviations xv
Abstract 1
Chapter 1: Introduction 2
Cholesterol Regulation of Gene Expression 3
The sterol regulatory element binding proteins (SREBPs) 3
The liver X receptors (X) 6
The generation and metabolism of oxysterols 9
The endoplasmic reticulum stress response 12
Intracellular Cholesterol Transport 16
Cholesterol biosynthesis and precursor sterol transport 17
Cholesterol transport from ER to plasma membrane 19
Cholesterol transport from plasma membrane to ER 20
Cholesterol transport from late endosomes and Niemann Pick C 22
Cholesterol transport via the endocytic recycling compartment 25
Cholesterol transport to mitochondria 27
Potential transport by caveolin 28
Potential transport by sterol carrier protein-2 29
Potential roles of oxysterol binding proteins 31
Intracellular transport of cholesterol metabolites 32
The START gene family 33
The START domain structure 34
The steroidogenic acute regulatory protein 35
The MLN64 protein 37
The PCTP subfamily 38
The acyl CoA thioesterase subfamily 40
The RhoGAP subfamily 41
The high molecular weight StarD9 protein 42
Evolution of the START domain 43
Perspective 44

Chapter 2: Discovery of the StarD4 subfamily 45
Dietary cholesterol cDNA microarray experiment..... 45
Identification of the StarD4 gene and its tissue expression pattern..... 47
StarD4 regulation by dietary cholesterol..... 50
A subfamily of START genes including StarD4, StarD5, and StarD6.....51
Tissue expression of StarD5 and StarD6..... 55
Purification and crystallization of recombinant mouse StarD4 protein.....57
The StarD4 X-ray crystal structure..... 60
The *C. elegans* gene K02D3.2..... 64
Expression of a K02D3.2 GFP reporter in *C. elegans*.....66
Chapter summary..... 68

Chapter 3: Regulation of StarD4 and StarD5 Expression..... 69
StarD4 and StarD5 are not highly regulated during steroidogenesis..... 69
Regulation of StarD4 expression by sterols..... 70
StarD4 is induced in nSREBP transgenic mice..... 71
The StarD4 promoter 73
Identification of the StarD4 promoter SRE by reporter transfection..... 75
StarD4 and StarD5 are not LXR target genes..... 80
StarD5 activation in cholesterol-loaded macrophages under ER stress.....81
StarD5 activation in ER stressed NIH-3T3 cells..... 83
StarD5 promoter reporter studies 84
Chapter Summary..... 86

Chapter 4: StarD4 and StarD5 in Intracellular Cholesterol Metabolism 87
Localization of StarD4 and StarD5 throughout cells..... 87
Cell culture assay for StAR-like steroidogenic activity..... 89
Site-directed mutations in cavity salt bridges of StarD4 and MLN64..... 91
Tom20 fusion proteins localizing START proteins to mitochondria..... 92
Effects of START domain overexpression on SREBP activity..... 94
Effects of START domain overexpression on LXR activity..... 95
Targetting construct for StarD4 knockout mice..... 98
Chapter Summary..... 100

Chapter 5: StarD6 expression in male germ cells 101

StarD6 is not expressed in steroidogenic Leydig cells 101

StarD6 expression is absent in germ cell-deficient testis 102

Expression of StarD6 in male germ cells 103

5' RACE analysis of StarD6 105

The StarD6 promoter 107

Targeting construct for StarD6 knockout 109

Chapter summary 110

Chapter 6: Discussion and Future Directions 111

Models of StarD4 and StarD5 activity in the three functional assays 111

Comparison of the StarD4 subfamily to other START proteins 113

StarD4: an SREBP-2 target gene with potential roles in cholesterol synthesis or uptake 117

StarD5: an ER stress activated gene with potential roles in ER function 121

StarD6: a male germ cell specific gene with potential roles in fertility 124

K02D3.2: The only StarD4 subfamily gene in *C. elegans* 127

Future Directions 130

Conclusion 137

Chapter 7: Materials and Methods 138

Animals and diets 138

cDNA microarrays 139

Real-Time Quantitative RT-PCR (qPCR) 140

Northern Blotting 141

General cloning and PCR 142

Rapid amplification of cDNA ends (RACE) 143

Recombinant protein expression and crystallization 144

C. elegans K02D3.2 cloning and GFP reporter 145

Cell Culture, media, and treatments 146

Transient transfection experiments 147

START expression plasmids....148
StarD4 and Star5 luciferase reporters....151
Other reporter and expression plasmids....153
Antibodies, Western blots, and immunofluorescence....153
Additional methods....155
Knockout and transgenic mouse constructs....155
Data analysis and statistics....158

References....159

Publications and Manuscripts....186

LIST OF FIGURES

Figure 1.1 Gene activation by SREBPs upon cholesterol depletion 4

Figure 1.2 Gene activation by LXRs upon cholesterol excess 7

Figure 1.3 The generation and metabolism of oxysterols 10

Figure 1.4 Three ER stress response pathways 12

Figure 1.5 Three mechanisms of cholesterol transfer between membranes 17

Figure 1.6 ER cholesterol transport pathways 22

Figure 1.7 Endosomal cholesterol transport pathways 27

Figure 1.8 Phylogenetic analysis and domain structure of the START protein family 34

Figure 1.9 The START domain X-ray crystal structure 35

Figure 2.1 Liver cholesterol levels increase upon cholesterol feeding 46

Figure 2.2 Microarray analysis of liver gene expression in response to dietary cholesterol 46

Figure 2.3 Single nucleotide polymorphisms (SNPs) in the mouse StarD4 coding region 48

Figure 2.4 Mis-spliced human StarD4 RT-PCR products 49

Figure 2.5 Multiple tissue northern blots of mouse StarD4 49

Figure 2.6 Regulation of StarD4 expression by dietary cholesterol 50

Figure 2.7 StarD4 regulation in a time course of cholesterol feeding 51

Figure 2.8 Multiple alignment of human START domains 52

Figure 2.9 Subfamilies of START-domain containing proteins 53

Figure 2.10 Evidence for a mouse StarD6 processed pseudogene 54

Figure 2.11 Exonic organization of StarD4, StarD5, and StarD6 55

Figure 2.12 Multiple tissue northern blots of StarD5 and StarD6 56

Figure 2.13 Dietary cholesterol does not affect liver StarD5 or MLN64 expression 56

Figure 2.14 Expression and purification of recombinant mouse StarD4 protein 58

Figure 2.15 Gel filtration of recombinant mouse StarD4 59

Figure 2.16 Optimization of mouse StarD4 crystallization conditions 59

Figure 2.17 Overview the StarD4 X-ray crystal structure 60

Figure 2.18 StarD4 and MLN64 have similar START structures 61

Figure 2.19 The StarD4 lipid binding cavity 62

Figure 2.20 Examples of hydrophobic amino acids lining the StarD4 lipid-binding cavity 62

Figure 2.21 Salt bridges in START domain lipid binding cavities 64

Figure 2.22 cDNA cloning of the *C. elegans* StarD4 subfamily member K02D3.2 65

Figure 2.23 Expression of a K02D3.2 promoter GFP reporter in *C. elegans* 67

Figure 3.1 START domain gene regulation in steroidogenesis 69

Figure 3.2 StarD4 is sterol-regulated in cultured 3T3 fibroblasts 70

Figure 3.3 StarD4 is sterol-regulated in cultured Hepa-1 hepatoma cells 71

Figure 3.4 StarD4 expression is activated in nSREBP-2 transgenic mouse liver 72

Figure 3.5: Anti-StarD4 antibody shows increased expression of the endogenous protein in nSREBP-2 transgenic liver 73

Figure 3.6 Analysis of mouse StarD4 by 5' Rapid Amplification of cDNA ends (RACE) 73

Figure 3.7 Alignment of mouse and human StarD4 proximal promoter sequences 74

Figure 3.8 A potential enhancer region conserved between mouse and human StarD4 75

Figure 3.9 Regulation of the mouse StarD4 luciferase reporter by sterol and statin treatment 76

Figure 3.10 StarD4 luciferase reporters with longer promoters show similar regulation 76

Figure 3.11 Regulation of StarD4 reporters with site-directed mutations in potential sterol regulatory elements 77

Figure 3.12 StarD4 SRE-B mutant reporters show defective sterol-regulation 78

Figure 3.13 Additional mutagenesis studies of the mouse StarD4 promoter 79

Figure 3.14 StarD4 and StarD5 are not LXR target genes 80

Figure 3.15 An Xbp1 splicing assay shows ER stress in free cholesterol-loaded macrophages 82

Figure 3.16 StarD5 expression is induced in free cholesterol-loaded macrophages 82

Figure 3.17 StarD5 expression is increased in NIH 3T3 cells by tunicamycin treatment 83

Figure 3.18 StarD5 is induced by ER stressors but not heat shock 84

Figure 3.19 The StarD5 proximal promoter lacks a consensus ER stress response element 85

Figure 3.20 A mouse StarD5 proximal promoter luciferase reporter is not activated by ER stress 86

Figure 4.1 A GFP-StarD4 fusion protein localizes throughout cells 87

Figure 4.2 FLAG-tagged StarD4 and StarD5 proteins localize throughout cells 88

Figure 4.3 StarD4 and StarD5 have StAR-like activity in the cell culture steroidogenesis assay 90

Figure 4.4 Steroidogenic activities of StarD4 and MLN64 salt bridge mutant proteins 91

Figure 4.5 Steroidogenic activities of Tom20-START fusion proteins 93

Figure 4.6 START proteins including StarD4 and StarD5 repress SRE reporter activity 94

Figure 4.7 START proteins including StarD4 and StarD5 stimulate LXRE reporter activity 95

Figure 4.8 LXRE reporter stimulation activities of StarD4 salt bridge mutant proteins 96

Figure 4.9 LXRE reporter stimulation by Tom20-START fusion proteins 97

Figure 4.10 Conditioned media from START expressing cells does not stimulate an LXRE reporter in other cells 98

Figure 4.11 Targeting construct for a StarD4 conditional knockout mouse 99

Figure 5.1 StarD6 is not expressed in the steroidogenically active MA-10 Leydig tumor cell line 101

Figure 5.2 Testis StarD6 expression is absent in Kit W/Wv germ cell deficient mice 103

Figure 5.3 Testis StarD6 expression increases during puberty in mice and rats 104

Figure 5.4 In isolated rat testis somatic and germ cells, StarD6 mRNA is expressed in germ cells at all stages of development 104

Figure 5.5 Mouse StarD6 mRNA is expressed in germ cells and seminiferous tubules at all stages 105

Figure 5.6 Rapid Amplification of cDNA ends (5' RACE) results for mouse and human StarD6 106

Figure 5.7 Mis-spliced human StarD6 RACE and RT-PCR products 107

Figure 5.8 Conserved region of the mouse and human StarD6 proximal promoters 108

Figure 5.9 Targeting construct for a StarD6 knockout mouse 109

Figure 6.1 StarD4 and StarD5 showed activity in three functional assays 111

Figure 6.2 Model for StarD4 and StarD5 activity via generation of 27-hydroxycholesterol 112

Figure 6.3 Alignment of known SREs with StarD4 functional SRE-B and other potential SREs 118

Figure 6.4 Four potential functions of StarD4 consistent with SREBP-2 gene regulation 121

Figure 6.5 Four potential functions of StarD5 consistent with ER stress gene regulation 123

Figure 6.6 Four sterols with potential roles in male germ cells, perhaps requiring StarD6 126

LIST OF TABLES

Table 1.1 Nomenclature and chromosomal locations of the 15 mammalian START genes 33

Table 2.1 Six genes down-regulated two-fold or more by dietary cholesterol 47

Table 2.2 Gene information for StarD4, StarD5, and StarD6 from mouse and human 53

Table 7.1 Primers for genotyping SREBP transgenic mice 139

Table 7.2 TaqMan quantitative RT-PCR primers for normalizer and START genes 141

Table 7.3 TaqMan quantitative RT-PCR primers for SREBP, LXR, and ER stress target genes 142

Table 7.4 Primers for 5' RACE analysis of mouse and human StarD4 and StarD6 143

Table 7.5 RT-PCR primers for cloning the K02D3.2 cDNA 145

Table 7.6 Primers for the K02D3.2 GFP reporter 146

Table 7.7 Primers for cloning the FLAG-START expression plasmids 149

Table 7.8 Mutagenic primers for StarD4 and MLN64 salt bridge mutants 150

Table 7.9 PCR Primers for cloning StarD4 and StarD5 reporters 151

Table 7.10 Mutagenic primers for StarD4 promoter elements 152

Table 7.11 Additional RT-PCR primers for mouse Xbp1 and human StarD6 155

Table 7.12 Primers for knockout targeting constructs and transgenes 157

LIST OF ABBREVIATIONS

3β-HSD	3β-hydroxysteroid dehydrogenase
7DHCR	7-dehydrocholesterol reductase
ABC	ATP binding cassette transporter
Apo	Apolipoprotein
ACAT	Acyl-coenzyme A:cholesterol acyltransferase
ATF	Activating transcription factor
CAH	Congenital adrenal hyperplasia
CETP	Cholesterol ester transfer protein
CTX	Cerebrotendinous xanthomatosis
Cyp	Cytochrome P450
Cyp27	Sterol 27-hydroxylase
Cyp39	24-hydroxycholesterol 7α-hydroxylase
Cyp46	Cholesterol 24-hydroxylase
Cyp7A1	Cholesterol 7α-hydroxylase
Cyp7B1	Oxysterol 7α-hydroxlase
DHE	Dihydroergosterol
DLC-1	Deleted in liver cancer 1
DR4	Direct repeat 4
ER	Endoplasmic reticulum
ERC	Endocytic recycling compartment
ERSE	ER stress response element
EST	Expressed sequence tag cDNA clone
FAS	Fatty acid synthase
FLAG	FLAG epitope tag
FPP	Farnesyl pyrophosphate
FXR	Farnesyl X receptor
GAPDH	Glyceraldehyde-3-phosphate dehydrogenase
GPBP	Goodpasture antigen binding protein
HDL	High density lipoprotein
HMG CoA	Hydroxymethylglutaryl coenzyme A
HMGR	HMG CoA reductase
HMGS	HMG CoA synthase
IBABP	Ileal bile acid binding protein
IMM	Inner mitochondrial membrane
LDL	Low density lipoprotein
LXR	Liver X receptor
MENTAL	MLN64 N-terminal domain
MENTHO	MLN64 N-terminal homologue
MLN64	Metastatic lymph node 64
NF-Y	Nuclear Factor Y
NPC	Niemann Pick C
NS	Not significant
OMM	Outer mitochondrial membrane
ORF	Open reading frame
ORP	OSBP-related protein
OSBP	Oxysterol binding protein

P450scc	P450 side chain cleavage enzyme (Cyp11A1)
PC	Phophatidylcholine
PCR	Polymerase chain reaction
PCTP	Phophatidylcholine transfer protein (intracellular)
PERK	Pancreatic endoplasmic reticulum kinase
PH	Pleckstrin homology
PLTP	Phospholipid transfer protein (plasma)
PM	Plasma membrane
PPAR	Peroxisome proliferator activated receptor
qPCR	Real time quantitative RT-PCR
RACE	Rapid amplification of cDNA ends
RhoGAP	Rho GTPase activating protein
RT	Reverse transcriptase
RXR	Retinoid X receptor
S1P	Site 1 protease
S2P	Site 2 protease
SAM	Sterile alpha motif
SCAP	SREBP cleavage activating protein
SCP-2	Sterol carrier protein 2
SHP	Small heterodimeric partner
SPF	Supernatant protein factor
SRB-1	Scavenger receptor B-1
SRE	Sterol regulatory element
SREBP	Sterol regulatory element binding protein
StAR	Steroidogenic acute regulatory protein
StarD	START domain containing
START	StAR-related lipid transfer
Tom20	Transporter outer mitochondrial membrane 20
UPR	Unfolded protein response
UTR	Untranslated region
VLDL	Very low density lipoprotein
YY1	Ying Yang 1

Abstract

This thesis describes the discovery, cloning, and initial characterization of StarD4, a sterol-regulated gene encoding a StAR-related lipid transfer (START) protein, and its two close homologues, StarD5 and StarD6. StarD4 was identified using cDNA microarrays, as liver StarD4 expression decreased three-fold in mice fed a high cholesterol diet. StarD4 was also sterol-regulated in cultured cells, and a functional sterol regulatory element (SRE) was identified in its promoter. StarD4 was preferentially activated in mouse liver by SREBP-2 rather than SREBP-1, supporting a role in cholesterol rather than fatty acid metabolism. The X-ray crystal structure of StarD4 was solved, revealing a hydrophobic lipid binding cavity as described for other START domains. StarD5 and StarD6 were identified by homology to StarD4, and these three genes constituted a novel subfamily most similar to the cholesterol-binding START domains of StAR and MLN64. StarD4 and StarD5 were ubiquitously expressed with highest mRNA levels in liver, while StarD6 expression was limited to male germ cells of the testis. StarD5 was not activated by SREBP or LXR transcription factors, well-characterized regulators of cholesterol metabolism, but rather by the ER stress response, a recently-described means by which cholesterol regulates gene expression. The nematode *C. elegans* has one StarD4 subfamily protein, K02D3.2. Reporter studies indicated that this gene was not regulated by cholesterol or ER stress, and it was only expressed in hypodermal seam cells of embryos and larvae. Overexpression of StarD4 and StarD5 revealed functional activity in three cell culture assays: (1) StAR-like activation of steroidogenesis by the mitochondrial P450 side chain cleavage enzyme, (2) repression of an SREBP-regulated reporter, and (3) activation of an LXR-regulated reporter. The START domains of StAR and MLN64 were active in these assays, while the related phosphatidylcholine transfer protein (PCTP) was an inactive negative control. Based on these results, the novel StarD4 subfamily is likely to play roles in the intracellular transport and metabolism of cholesterol.

Chapter 1: Introduction

Cholesterol is a 27-carbon, four-ringed planar lipid that plays key roles in health and disease. It is a fundamental component of cell membranes, where it packs with fatty acyl chains of phosholipids to increase bilayer rigidity (Tabas, 2002a). Lipid rafts, membrane microdomains that coalesce to form platforms for signal transduction, are enriched in cholesterol and sphingolipids (Simons and Ehehalt, 2002). Cholesterol, along with its precursors and metabolites, also functions in cell signaling events regulating diverse processes including fertility. Some proteins are covalently modified with cholesterol, notably the Hedgehog morphogen that plays vital roles in patterning during embryonic development (Jeong and McMahon, 2002). Cholesterol also is the substrate for biosynthesis of all steroid hormones and bile acids. Mammals obtain cholesterol from both dietary sources and endogenous *de novo* synthesis. While cholesterol is essential for normal physiology of cells and organisms, cholesterol surplus has pathological effects. Excess cellular free cholesterol is cytotoxic, and excess biliary cholesterol causes gallstones (Portincasa et al., 2003). Elevated plasma low density lipoprotein (LDL) cholesterol is a major risk factor for atherosclerotic vascular disease, resulting in coronary heart disease and stroke (Steinberg and Gotto, 1999). These are the leading causes of death among Americans, accounting for 39% of deaths, compared to 23% for cancer and 38% for all other causes. Cholesterol has also been linked to the pathogenesis of Alzheimer's disease (Puglielli et al., 2003). Therefore, cholesterol homeostasis must be finely regulated to assure adequate supply and proper distribution of this essential lipid, yet to avoid excess and mislocalization which can be toxic.

Cholesterol Regulation of Gene Expression

Most regulation of cholesterol homeostasis is at the level of gene transcription, though there are examples of post-transcriptional regulation (Edwards and Ericsson, 1999). Two transcription factor families, the sterol regulatory element binding proteins (SREBPs) and liver X receptors (LXRs), are implicated in gene regulation by cholesterol and its oxysterol metabolites (Schoonjans et al., 2000). When sterols are low, SREBPs activate genes involved in the synthesis and uptake of cholesterol and fatty acids (Horton et al., 2002). Conversely, when sterols are in excess, LXRs activate target genes involved in cholesterol efflux and reverse cholesterol transport (Repa and Mangelsdorf, 2002). Recently, cholesterol was shown to activate a third transcriptional pathway, as free cholesterol-loaded macrophages trigger the endoplasmic reticulum (ER) stress response (Feng et al., 2003a).

The sterol regulatory element binding proteins: SREBPs share a common tripartite structure: (1) an N-terminal basic helix-loop-helix leucine zipper transcription factor domain, (2) a central membrane anchor with two transmembrane α-helices, and (3) a C-terminal regulatory domain that binds the SREBP cleavage activating protein (SCAP) (Brown and Goldstein, 1999). When cellular sterols are abundant, SREBPs are retained in the ER membrane in a complex with SCAP and the ER retention protein Insig-1 or Insig-2 (Figure 1.1). SCAP has a sterol-sensing domain and undergoes a conformation change upon ER cholesterol depletion, releasing Insig and allowing the SREBP-SCAP complex to translocate to the Golgi apparatus (Yang et al., 2002). In the Golgi, the site 1 and site 2 proteases (S1P and S2P) cleave SREBP to release the N-terminal transcription factor (nSREBP) into the cytosol. Upon translocation to the nucleus, nSREBPs bind promoter sterol regulatory elements (SREs) and cooperate with other transcription factors like NF-Y to

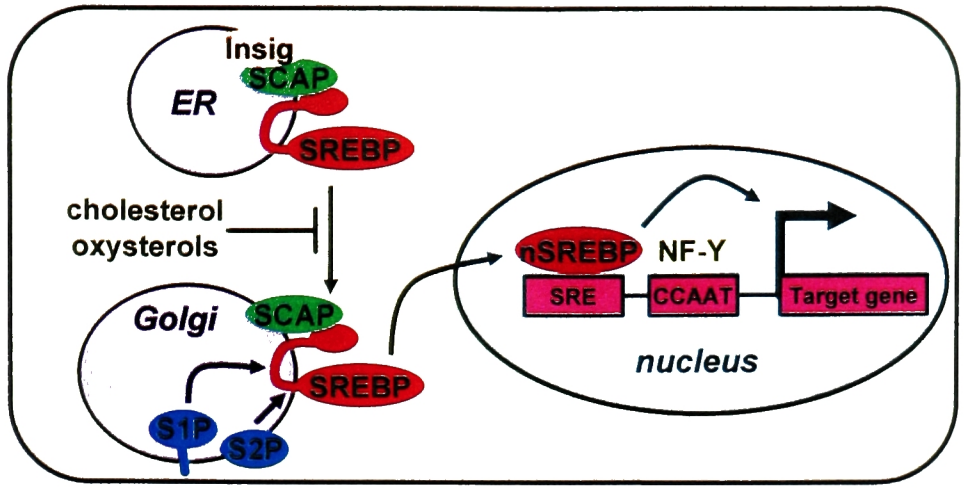

Figure 1.1: Gene activation by SREBPs upon cholesterol depletion.

When cellular cholesterol or certain oxysterols are abundant, SREBPs remain in the ER as inactive precursors associated with SCAP and Insig. When sterols are scarce, SCAP releases Insig allowing SREBP-SCAP trafficking to the Golgi apparatus, where the site 1 and site 2 proteases (S1P and S2P) cleave SREBP. This releases the N-terminal transcription factor nSREBP, which translocates to the nucleus and binds promoter SREs. nSREBPs cooperate with other factors like NF-Y to activate transcription of target genes involved in the synthesis and uptake of cholesterol and fatty acids.

activate target genes (Edwards et al., 2000). nSREBPs are inactivated by polyubiquitination and proteosomal degradation (Hirano et al., 2001), as well as covalent attachment of the small ubiquitin-related modifier SUMO-1 (Hirano et al., 2003).

Localization of SREBPs to the ER reflects the important regulatory role this compartment plays in cholesterol homeostasis. Though the surface areas of the plasma membrane (PM) and ER are similar in many cells, 60-80% of total cellular cholesterol is in PM while only 0.5-1% is in ER (Maxfield and Wustner, 2002). However, the cholesterol-poor ER is exquisitely sensitive to changes in cellular cholesterol levels: modest ~50% changes in PM cholesterol (by addition or removal with cyclodextrin) result in large 10-fold changes in ER cholesterol (Lange et al., 1999). In addition to affecting SCAP-SREBP, ER cholesterol also regulates two important enzymes in cholesterol metabolism. First, ER cholesterol accelerates the degradation of HMG CoA reductase (HMGR), the rate-limiting enzyme in cholesterol biosynthesis, by promoting association of its sterol-sensing domain

with Insig-1 (Sever et al., 2003). Second, ER cholesterol allosterically activates the acyl-coenzyme A:cholesterol acyltransferase (ACAT) enzyme, which generates cholesterol esters for storage in cytosolic lipid droplets (Chang et al., 1998).

There are two SREBP genes that encode three distinct proteins: SREBP-1a, SREBP-1c, and SREBP-2. Alternative promoters of the same gene generate SREBP-1a and SREBP-1c, which differ only in the length of their N-terminal transactivation domains. SREBP-1a is a stronger transcriptional activator, but SREBP-1c is the predominant form of SREBP-1 expressed in liver. Transgenic mice have been developed with liver overexpression of each truncated nuclear SREBP, such that target genes are constitutively activated (Horton et al., 2002). nSREBP-1a preferentially activates genes for lipogenic enzymes like fatty acid synthase (FAS), resulting in a 26-fold increase in the rate of hepatic fatty acid synthesis but only a 5-fold increase in cholesterol synthesis (Shimano et al., 1996). nSREBP-1c weakly activates the same genes, giving a 4-fold increase in fatty acid synthesis and no change in cholesterol synthesis (Shimano et al., 1997). Conversely, nSREBP-2 transgenic mice increase hepatic cholesterol synthesis 28-fold and fatty acid synthesis only 4-fold, reflecting preferential activation of cholesterogenic enzymes like HMGR (Horton et al., 1998). Proteolytic cleavage of SREBP-1 and SREBP-2 is differentially regulated in rodent models: drugs that deplete cholesterol cause increased processing of SREBP-2 but not SREBP-1 (Sheng et al., 1995; Shimomura et al., 1997), while dietary polyunsaturated fatty acids decrease processing of SREBP-1 but not SREBP-2 (Xu et al., 2002). SREBPs are also differentially regulated at the level of transcription. Most significantly, only the SREBP-1c transcript is regulated by LXRs, insulin, and glucagon (Repa et al., 2000a), and SREBP-1 expression in adipocytes is repressed by the hormone leptin (Soukas et al., 2000).

While SREBP-1 primarily regulates fatty acid metabolism and SREBP-2 primarily regulates cholesterol metabolism, there appears to be considerable cross-talk. In *Drosophila*,

there is only one SREBP whose cleavage is regulated by phosphatidylethanolamine, indicating that the SREBP pathway evolved to monitor cell membrane lipids and regulate synthesis accordingly (Dobrosotskaya et al., 2002). SREBPs also mediate the effects of statins, a widely-used class of drugs to lower LDL cholesterol. By inhibiting hepatic HMGR and cholesterol synthesis, statins stimulate SREBP-mediated activation of the LDL receptor, resulting in clearance of plasma LDL cholesterol.

The liver X receptors: The two mammalian LXRs, LXRα and LXRβ, are encoded by separate genes. LXRα is expressed only in liver, adipose tissue, intestine, kidney, and macrophages, while LXRβ is more widely expressed. LXRs belong to the nuclear hormone receptor family, which have N-terminal DNA binding domains and C-terminal domains responsible for ligand binding, dimerization, and transcriptional regulation. LXRs form obligate heterodimers with retinoid X receptors (RXRs) and bind direct repeat 4 (DR4) motifs in promoters (Repa and Mangelsdorf, 2000). LXR/RXR is constitutively bound to target promoters associated with transcriptional corepressors (Hu et al., 2003; Wagner et al., 2003). Ligand binding causes a conformational change (Farnegardh et al., 2003), releasing corepressors and binding coactivators to activate transcription (Figure 1.2). Ligands for either LXR or RXR will activate transcription by LXR/RXR, and combinations act synergistically. RXR ligands alone non-specifically activate other heterodimeric nuclear receptors (Repa et al., 2000b). Oxysterols are specific LXR agonists, though the physiologically relevant ligands are uncertain, as described in the next section.

Most known LXR target genes function in reverse cholesterol transport, a process by which high density lipoproteins (HDL) transport cholesterol from peripheral cells to the liver, where it is excreted in bile as free cholesterol or bile acids (Repa and Mangelsdorf, 2002). This pathway likely accounts for the major atheroprotective effects of HDL. Consistent with

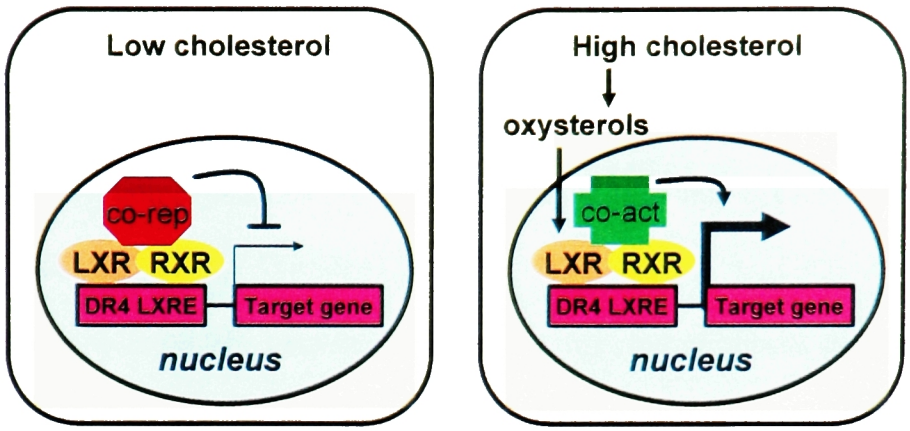

Figure 1.2: Gene activation by LXRs upon cholesterol excess.

LXRs bind to direct repeat 4 (DR4) elements as obligate heterodimers with RXR, recruiting co-repressors to suppress target gene expression. When cholesterol is abundant, oxysterols are generated and serve as LXR agonists, causing the release of co-repressors and recruitment of co-activators. LXR target genes are generally involved in cholesterol efflux and reverse cholesterol transport.

LXR activation of reverse cholesterol transport, multiple studies have shown that LXR activation inhibits atherosclerosis, while LXR deficiency in macrophages increases lesion formation (Tontonoz and Mangelsdorf, 2003).

In macrophages, LXRs activate the ATP binding cassette transporter ABCA1 (Costet et al., 2000), which mediates cholesterol efflux to nascent HDL. Other macrophages LXR targets like ABCG1 (Venkateswaran et al., 2000) and the apolipoprotein E/C-I/C-IV/C-II gene cluster (Mak et al., 2002) may also function in this efflux pathway. Two plasma lipid transfer proteins that remodel HDL particles, CETP (Luo and Tall, 2000) and PLTP (Laffitte et al., 2003), are LXR targets. In liver, LXRs activate expression of scavenger receptor B-1 (SRB-1), which mediates selective uptake of cholesterol from HDL (Malerod et al., 2002), and ABCG5 and ABCG8, which secrete free cholesterol into the bile (Yu et al., 2003). In the intestine, LXRs activate ABCA1, ABCG5, and ABCG8 to decrease absorption of dietary cholesterol. LXRα, but not LXRβ, positively feeds back on its own transcription (Li et al., 2002), potentially amplifying these responses. Several species differences in LXR target genes between humans and mice have been described: (1) only mice show LXR activation of

hepatic cholesterol 7α-hydroxylase (Cyp7A1), which initiates the conversion of cholesterol to bile acids (Agellon et al., 2002), (2) mice lack CETP, and (3) human macrophages show much stronger activation of ABCG1, ApoE, and LXRα in response to LXR ligands (Laffitte et al., 2001; Lund et al., 2003).

There is also cross-talk between LXRs and other transcriptional pathways in lipid metabolism. LXRs stimulate fatty acid synthesis by activating SREBP-1c expression (Repa et al., 2000a), causing hypertriglyceridemia and hepatic steatosis in mice treated with synthetic LXR ligands (Schultz et al., 2000). However, arachidonate and other unsaturated fatty acids serve as competitive inhibitors of LXR activation, result in negative feedback on SREBP-1c (Ou et al., 2001). Consistent with LXR activation of SREBP-1c, LXRα knockout mice show lower hepatic expression of SREBP-1 and its target genes (Peet et al., 1998). However, these mice also show higher expression of SREBP-2 and its target genes, suggesting that LXRs may repress SREBP-2 and cholesterol synthesis by an unknown mechanism (Millatt et al., 2003). Cholesterol synthesis may reciprocally inhibit LXRs, as the intermediate geranylgeranyl pyrophosphate blocks LXR activation by preventing co-activator recruitment (Forman et al., 1997; Gan et al., 2001). There is also cross-talk between LXRs and peroxisome proliferator activated receptors (PPARs), which also heterodimerize with RXR but are activated by fatty acid ligands. PPARδ and perhaps PPARα activate transcription of LXRα (Millatt et al., 2003), and there is reciprocal competition between PPARs and LXRs at the level of target gene promoters (Ide et al., 2003; Yoshikawa et al., 2003). LXR activation of rodent Cyp7A1 is blocked by small heterodimeric partner (SHP), which binds the promoter indirectly and is induced by the bile acid-activated FXR nuclear receptor (Goodwin et al., 2000; Lu et al., 2000). Lipid metabolism thus appears finely regulated by a complex web of interactions among SREBPs, LXRs, PPARs, FXRs, and other transcription factors.

The generation and metabolism of oxysterols: Oxysterols, 27-carbon hydroxylated derivatives of cholesterol, are present at very low levels *in vivo* but have at least three important functions (Russell, 2000). First, oxysterols are intermediates in the hepatic synthesis of bile acids, which proceeds via the classic pathway initiated by microsomal Cyp7A1 and the alternative pathway initiated by mitochondrial sterol 27-hydroxylase (Cyp27) (Fuchs, 2003). Second, oxysterols are transport forms of cholesterol, allowing movement in plasma from peripheral tissues to the liver for elimination (Bjorkhem, 2002). This process may be an HDL-independent pathway for reverse cholesterol transport. Cyp27 in peripheral tissues, especially alveolar macrophages, generates 27-hydroxycholesterol which travels to the liver for bile acid synthesis starting with Cyp7B1 (oxysterol 7α-hydroxlase). Likewise, microsomal Cyp46 (cholesterol 24-hydroxylase) in brain generates 24(S)-hydroxycholesterol, which crosses the blood-brain barrier, travels to the liver, and is converted to bile acids via a pathway initiated by Cyp39 (24-hydroxycholesterol 7α-hydroxylase). Third, some oxysterols also function as positive regulators of LXRs and negative regulators of SREBPs. Most oxysterols can serve multiple roles in cholesterol metabolism (Figure 1.3).

Many natural and synthetic oxysterols have been tested *in vitro* for LXR activation (Janowski et al., 1999; Janowski et al., 1996), but the physiological molecules are uncertain and may differ among tissues. 24(S)-hydroxycholesterol is a high affinity LXR ligand, but it is only produced in the brain, its levels elsewhere are low, and hepatic Cyp39 rapidly inactivates it as an LXR ligand (Russell, 2000). 24(S),25-epoxycholesterol, produced by a shunt in the cholesterol biosynthetic pathway, is also a high affinity LXR ligand (Spencer et al., 2001). Statin drugs, which inhibit cholesterol synthesis at mevalonate generation, block activation of LXRE reporter constructs by LXR/RXR (Forman et al., 1997) and decrease transcription of the LXR-target SREBP-1c in hepatoma cells (DeBose-Boyd et al., 2001). In

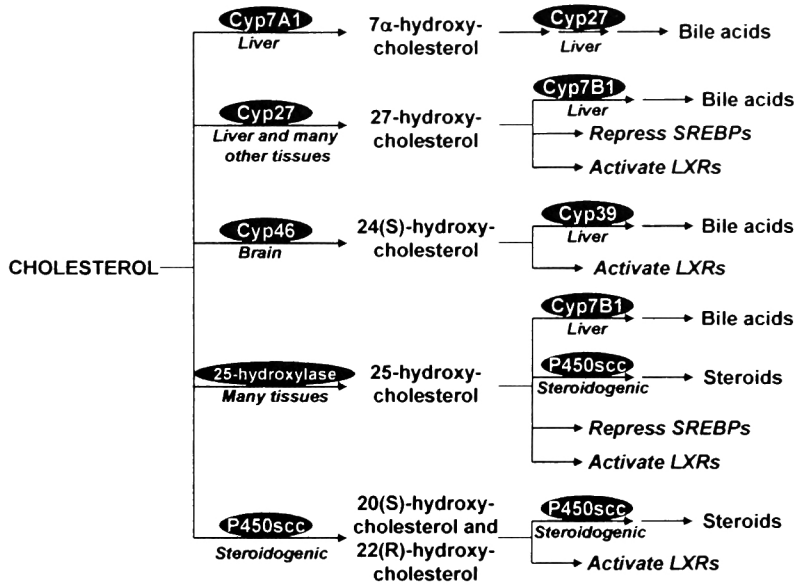

Figure 1.3: The generation and metabolism of oxysterols.

Various tissue-specific hydroxylase enzymes convert cholesterol to oxysterols, which have several fates. They serve as intermediates in the generation of bile acids and steroid hormones. The brain and other peripheral tissues use oxysterols as transport forms of cholesterol, which are delivered to liver for bile acid synthesis and excretion. Oxysterols also regulate SREBP and LXR transcription factors.

both cases, mevalonate or LXR agonists overcome statin-mediated inhibition, consistent with an endogenous LXR ligand like 24(S),25-epoxycholesterol generated by cholesterol biosynthesis. However, it is unclear whether this oxysterol is produced in non-hepatic cells. Two other high affinity LXR ligands, 22(R)-hydroxycholesterol and 20(S)-hydroxy-cholesterol, are made only in steroidogenic tissues as transient intermediates in the three-step activity of the P450 side chain cleavage enzyme (P450scc/Cyp11A1) (Miller, 2002). Given the limited distribution and low levels of high affinity LXR agonists, the relevant oxysterols may actually be weaker agonists like 25- and 27-hydroxycholesterol.

27-hydroxycholesterol, the most abundant oxysterol in plasma, is a potent repressor of SREBP processing and a weak partial LXR agonist. Cholesterol loading of macrophages activates LXR targets and results in dose-dependent generation of 27-hydroxycholesterol, but not any high affinity LXR ligands (Fu et al., 2001). In the human disease cerebrotendinous xanthomatosis (CTX), mutations in Cyp27 result in defective bile acid synthesis, cholesterol

accumulation in multiple tissues, and premature atherosclerosis (Bjorkhem, 2002). Cholesterol accumulation could indicate defective elimination from cells as 27-hydroxy-cholesterol, but it could also reflect defective generation of oxysterol LXR ligands to stimulate cholesterol efflux. Consistent with the latter hypothesis, cells from CTX patients fail to activate the LXR target ABCA1 in response to cholesterol-loading, but activate it normally when supplied with exogenous 24(S),25-epoxycholesterol (Fu et al., 2001). This supports a role for 27-hydroxycholesterol in macrophage LXR activation, but others have questioned the physiological relevance of this oxysterol (Bjorkhem, 2002).

25-hydroxycholesterol has similar effects on SREBPs and LXRs to 27-hydroxy-cholesterol. Most tissues express low levels of cholesterol 25-hydroxylase, a non-P450 transmembrane protein localized to ER and Golgi (Lund et al., 1998). 25-hydroxycholesterol can be a substrate for the synthesis of bile acids via Cyp7B1 (Russell, 2000) or steroid hormones via P450scc (Lukyanenko et al., 2001). Since 25-hydroxycholesteol is the most potent negative regulator of SREBP processing, it was thought that SCAP may sense this oxysterol. However, recent data indicate that SCAP senses cholesterol itself, as it undergoes a conformational change in response to cholesterol but not 25- or 27-hydroxycholesterol (Brown et al., 2002). Likewise, even though oxysterols increase ACAT activity in cells, cholesterol itself was shown to be the most potent allosteric activator of this enzyme *in vitro* (Zhang et al., 2003). Therefore, oxysterols may affect the ER regulatory compartment indirectly by causing intracellular cholesterol transport to the ER.

It is also notable that cholesterol, oxysterols, and steroids can also be sulfonated by specific sulfotransferase enzymes (Javitt et al., 2001). The physiological function of this modification is uncertain, but oxysterol sulfates are LXR antagonists (Song et al., 2001) and cholesterol sulfates inhibit steroid hormone production (Xu and Lambeth, 1989).

The endoplasmic reticulum stress response: When ER function is perturbed by unfolded proteins, ER stress signals are transduced to the nucleus to activate gene transcription by three routes (Figure 1.4): the PERK-ATF4, IRE1-Xbp1, and ATF6 pathways (Harding et al., 2002; Kaufman, 2002). In one pathway, the ER transmembrane kinase PERK, after stress-induced dimerization and autophosphorylation, phosphorylates the translation factor eIF2α to transiently inhibit global protein translation, thus reducing ER protein load. However, some mRNAs are translated more efficiently in this condition, including the ATF4 transcription factor that activates ER stress target genes. In the second pathway, the ER membrane protein IRE-1 has a cytosolic ribonuclease domain that, upon ER stress, mediates non-traditional splicing of the Xbp1 mRNA, allowing synthesis of this transcription factor. In the third pathway, the ER membrane protein ATF6 translocates to the Golgi upon ER stress, where it is cleaved analogous to SREBPs by the proteases S1P and S2P to yield an active nuclear transcription factor.

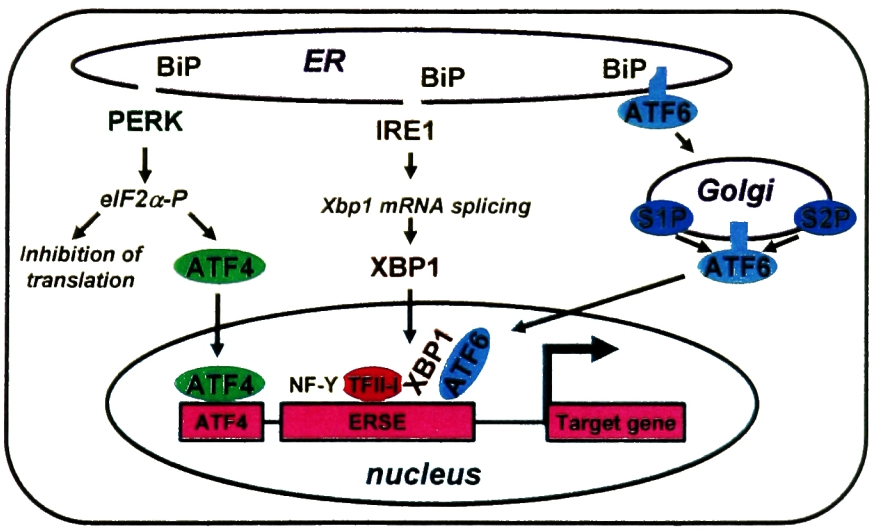

Figure 1.4: Three ER stress response pathways.

ER stress signals are transduced to the nucleus via three parallel pathways, activating the ATF4, Xbp1, and ATF6 transcription factors. The PERK pathway transiently inhibits global translation but activates translation of ATF4. IRE1 mediates non-traditional splicing of the Xbp1 mRNA to increase its synthesis, while ATF6 is activated by proteolysis in the Golgi similar to SREBP processing. The ER chaperone BiP negatively regulates all three pathways, which may converge in the nucleus with complex interactions on target gene promoters with ER stress response elements (ERSEs).

BiP, an ER-resident Hsp70-family chaperone, may be the master UPR regulator, as luminal BiP binds and inhibits activation of PERK, IRE-1, and ATF6 (Kaufman, 2002). Misfolded proteins in the ER sequester BiP, resulting in activation of all three pathways. The ER stress response is often referred to as the unfolded protein response (UPR), since known stress agents disrupt ER protein folding. For instance, tunicamycin inhibits N-linked glycosylation, reducing agents block disulfide bond formation, and the calcium pump blocker thapsigargin or the calcium ionophore A23187 cause dysfunction of calcium-dependent ER chaperones. Known UPR target genes function to ameliorate these stresses, including ER chaperones like BiP and RAMP4 (Yamaguchi et al., 1999), ER calcium pumps like SERCA2b (Hojmann Larsen et al., 2001), and components of the secretory pathway and ER-associated protein degradation (ERAD) (Travers et al., 2000). However, prolonged or severe ER stress results in apoptosis via multiple mechanisms, including expression of the pro-apoptotic transcription factor CHOP and activation of the ER procaspase-12 (Ma et al., 2002).

The three ER stress transcription factors, ATF4, Xbp1, and ATF6, belong to the basic leucine zipper family, and several studies have addressed their promoter binding sites. Some target genes have ER stress response elements (ERSEs) with the tripartite structure CCAAT-N_9-CCACG, where the 9 bp spacer is GC-rich (Roy and Lee, 1999; Yoshida et al., 1998). The three elements of this ERSE bind to NF-Y, TFII-I, and ATF6, respectively (Parker et al., 2001; Yoshida et al., 2001b). Xbp1 appears to act at the same element as ATF6 (Yoshida et al., 2001a), but some target genes only respond to Xbp1 (Yoshida et al., 2003), and these factors may form homo- or heterodimers. An alternate ERSE-II has been described with an inverted CCAAT box spaced one nucleotide from the putative ATF6/Xbp1 site (ATTGG-N-CCACG) (Kokame et al., 2001). The promoters for CHOP and BiP both contain ERSEs as well as additional elements to bind ATF4 (Luo et al., 2003; Ma et al., 2002). Further studies

are necessary to clarify the roles of the different ER stress transcription factors, and to identify the responsible elements in target genes that lack consensus ERSEs.

The two main functions of the ER are protein secretion and lipid synthesis, so lipids may also affect ER stress. A microarray study of tunicamycin-treated yeast identified multiple phospholipid biosynthetic enzymes as UPR targets (Travers et al., 2000). Conversely, inhibition of phospholipid synthesis in CHO cells induces CHOP and apoptosis, though BiP activation was not observed (van der Sanden et al., 2003). ER cholesterol has been linked to protein secretion, as excess cholesterol inhibits protein translocation by rough microsomes *in vitro* (Nilsson et al., 2001). ER membrane proteins like the translocon are likely adapted to the low cholesterol environment of the ER. Less protein translocation might be expected to reduce ER stress, but cholesterol-induced dysfunction of other ER proteins like calcium pumps would certainly activate the UPR. It is also notable that SREBPs and ATF6 are cleaved by the same Golgi proteases. Their regulation is thought to be independent, since sterol depletion activates SREBPs but not ATF6, and ATF6 cleavage is SCAP-independent (Ye et al., 2000). However, they may be coordinately regulated in some cases, as some ER stressors in HepG2 cells activate the UPR as well as SREBP-target genes (Werstuck et al., 2001). In response to high ER cholesterol, SREBP processing is repressed, while recent evidence described below indicates that the UPR is activated.

The ER is thought to handle excess cholesterol primarily by ACAT-mediated esterification. It may also accommodate some excess free cholesterol via its large surface area and ability to synthesize phospholipids, thus maintaining an acceptable cholesterol:phospholipid ratio (Blanchette-Mackie, 2000; Tabas, 2002b). When cultured macrophages are loaded with free cholesterol, via treatment with acetylated LDL and an ACAT inhibitor, the phospholipid biosynthetic response is overwhelmed and apoptosis ensues (Tabas, 2002b). It was initially proposed that excess PM cholesterol triggers this

apoptotic response (Kellner-Weibel et al., 1999), but directly loading the PM with cholesterol does not trigger cell death (Feng et al., 2003a). Furthermore, this apoptosis is markedly inhibited in two experimental systems that prevent LDL-derived cholesterol from reaching the ER, but allow it to reach the PM (Feng et al., 2003a).

Since ER cholesterol was strongly implicated in macrophage apoptosis, Feng, Tabas, and coworkers showed that cholesterol-loaded macrophages trigger the UPR, activating IRE-1, PERK, ATF4, Xbp1, and CHOP (Feng et al., 2003a). These macrophages have depleted ER calcium stores, suggesting that ER calcium pumps are indeed cholesterol-sensitive and the proximal cause for UPR activation. The UPR is initially protective, as PERK knockout macrophages are more susceptible to apoptosis upon cholesterol loading. However, CHOP induction ultimately causes apoptosis, as CHOP knockout macrophages are resistant to apoptosis upon cholesterol loading. Macrophages in atherosclerotic lesions show elevations in CHOP, so ER stress is likely relevant to macrophage apoptosis *in vivo* (Feng et al., 2003a). Furthermore, NPC1-heterozygous ApoE-deficient mice, which have defective cholesterol trafficking to ER, show less apoptosis in atherosclerotic lesions (Feng et al., 2003b). The macrophage ER stress model also provides a mechanism whereby hyperhomocysteinemia, an independent risk factor for atherosclerosis, could contribution to lesion formation, as homocysteine can activate the UPR (Werstuck et al., 2001). The connection between cholesterol and ER stress is a new field of research, and it is still unclear whether it extends to other cells types besides macrophages. It is clear that ER cholesterol can trigger the UPR, so along with SREBPs and LXRs, ER stress marks a third way that cholesterol can impinge on gene regulation.

Intracellular Cholesterol Transport

Cholesterol must be synthesized by a multi-enzyme pathway, transported between compartments within cells, moved in and out of cells by transmembrane proteins, and transported in the plasma by lipoproteins. While many relevant genes and pathways in cholesterol metabolism have been identified, molecular understanding of intracellular cholesterol transport has lagged behind. Due in part to technical difficulties such as measuring cholesterol levels of intracellular membranes, many features of intracellular cholesterol transport are only vaguely understood.

There are three general ways cholesterol can move between intracellular compartments (Figure 1.5) (Maxfield and Wustner, 2002; Prinz, 2002). Cholesterol is transported in the membranes of intracellular vesicles, and these movements typically require ATP and an intact cytoskeleton. Cholesterol can spontaneously desorb from membranes, but it is only sparingly soluble in water and will usually return to the same membrane. However, if different membranes are closely juxtaposed, perhaps brought together by specialized proteins, then cholesterol may transfer between them by diffusion or by movement along contact sites. Non-vesicular cholesterol transport is also mediated by diffusible carrier proteins, with hydrophobic cavities to bind cholesterol and transport it across the aqueous cytosol. For any given pathway, several transport mechanisms may act simultaneously or redundantly, making their relative contributions difficult to determine.

Cholesterol shuttles among cellular locations, including the major compartment in the PM, the site of synthesis in the ER, and the site of uptake in the endocytic pathway (Simons and Ikonen, 2000). There are marked asymmetries in cholesterol concentration among intracellular membranes, despite transport pathways that might be expected to equilibrate cholesterol distribution. Transport vesicles may have active sorting mechanisms to exclude

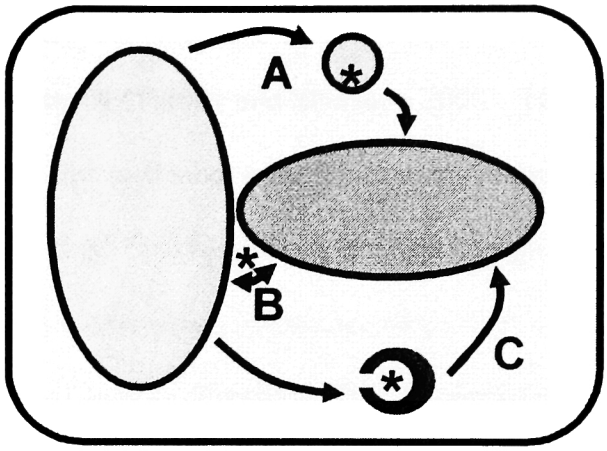

Figure 1.5: Three mechanisms of cholesterol transfer between membranes. Cholesterol (*) is highly hydrophobic and requires special transport mechanisms between subcellular compartments. (A) Cholesterol can move in the membranes of vesicles. (B) Cholesterol can transfer between two closely juxtaposed membranes. (C) Hydrophobic cavity lipid transfer protein can shuttle cholesterol between membranes.

or incorporate cholesterol (Prinz, 2002), and intracellular shuttling proteins must have specificity in targeting. Specificity could arise from interactions with receptor proteins on target membranes; alternatively membranes may have intrinsic differences in ability to accept cholesterol (Maxfield and Wustner, 2002). It is uncertain how intracellular gradients between compartments are formed and maintained, and how cholesterol moves with and against these gradients. Even within the same subcellular compartment, there may be different pools of cholesterol with different kinetics of mobilization to various pathways.

Cholesterol biosynthesis and precursor sterol transport: The early steps in cholesterol biosynthesis from acetyl CoA produce mevalonate, which is phosphorylated to generate isoprenoids that condense to give 15-carbon farnesyl pyrophosphate (FPP). FPP is the precursor for dolichol, heme, ubiquinone, and isoprenylated proteins, as well as the 30-carbon linear squalene. Squalene cyclization generates the four-ringed sterol lanosterol, which is modified by 9 enzymes in 19 steps (rearranging double bonds and removing three methyl groups from the α-face of the rings) to generate the 27-carbon cholesterol. The post-lanosterol enzymatic steps are independent of one another, and they occur in different sequences to generate a number of sterol intermediates (Phillips and Johnson, 1998). Pre-lanosterol sterol biosynthesis is essential for viability, as squalene synthase knockout mice

die by fetal day 12.5 even when the maternal diet is supplemented with squalene or cholesterol (Tansey and Shechter, 2000). However, inborn errors in post-lanosterol synthesis allow live births but generally result in congenital anomalies and mental retardation. Defects in the final enzyme of cholesterol synthesis, 7-dehydrocholesterol reductase (7DHCR), cause Smith-Lemli-Opitz syndrome, while five other human malformation syndromes have other enzyme defects (Porter, 2002). Precursor sterols fail to substitute for cholesterol, and their accumulation has deleterious effects, underscoring the exquisite adaptation of the cholesterol molecule. Precursors abundance varies widely among cell types, and certain precursors may have physiological functions (Lusa et al., 2003). For instance, 7-dehydrocholestereol is converted to vitamin D in skin, and other precursors activate meiosis in the gonads.

The ER is the primary site of cholesterol synthesis (Reinhart et al., 1987). Some reactions and enzymes also localize to peroxisomes (Olivier et al., 2000), though cells lacking functional peroxisomes appear to have normal cholesterol synthesis (Hogenboom et al., 2002). Precursors like zymosterol also reach the PM, and rapidly return to the ER for conversion to cholesterol (Lange et al., 1991). Therefore, hydrophobic intermediates in cholesterol synthesis may move among compartments like ER, PM, and peroxisomes, or even between domains of the same compartment. There was an extensive literature in the 1970s and 1980s on soluble proteins that stimulate enzymatic steps of cholesterol biosynthesis. Sterol-carrier protein 2 (SCP-2) was originally purified as an activator of 7DHCR activity in liver microsomes *in vitro*, but it binds many other lipids and its *in vivo* role is unclear (Seedorf et al., 2000). The supernatant protein factor (SPF), which increases squalene epoxidase activity, was recently cloned and structurally characterized as a member of the CRAL-TRIO lipid binding family (Shibata et al., 2001; Stocker et al., 2002). However, SPF also shows ligand promiscuity, binding phosphatidylinositol and γ-tocopherol with higher affinity than squalene (Panagabko et al., 2003). Cholesterol biosynthesis likely

requires cytosolic transport proteins for hydrophobic precursor sterols, but none have been definitively described to date.

Cholesterol transport from ER to PM: Newly synthesized cholesterol can be metabolically labeled by adding ^{3}H-acetate to cells, and its arrival at the PM is typically assayed by cholesterol oxidase susceptibility or extraction with cyclodextrin (Lange, 1998). Since the ER is cholesterol-poor, nascent cholesterol moves against a steep concentration gradient to reach the PM. However, some have speculated this gradient may not exist if ER cholesterol only exchanges with the minority of PM cholesterol outside of lipid rafts (Simons and Ikonen, 2000). In certain cells types, precursor sterols also reach the PM, and there are marked differences in rates of arrival among precursors and cholesterol, perhaps confounding interpretation of some experiments (Lusa et al., 2003).

Vesicular transport along the protein secretory pathway is one possible path from ER to PM, and there is evidence that the cholesterol-enriched lipid rafts assemble in the Golgi (Simons and Ikonen, 2000). Energy poisons or low temperature inhibit the rapid ER to PM transport of nascent cholesterol (DeGrella and Simoni, 1982; Urbani and Simoni, 1990), supporting a vesicular mechanism. However, inconsistent with vesicles, disruption of actin filaments or microtubules has no effect on ER to PM transport (Kaplan and Simoni, 1985). Furthermore, the drug Brefeldin A, which causes Golgi disassembly and fusion with ER, blocks over 90% of protein secretion but only decreases nascent cholesterol transport by ~20% in the same cells (Heino et al., 2000; Urbani and Simoni, 1990). Therefore, while vesicular transport through the Golgi may bring some nascent cholesterol to the PM, it is not the major pathway.

Most ER to PM cholesterol movement bypasses the Golgi, but the molecular mechanisms are uncertain. While some have proposed nontraditional vesicles (Urbani and

Simoni, 1990), non-vesicular transport by membrane contacts or shuttling proteins is more likely. Contact sites between ER and PM could allow sterol transfer (Menon, 2002), and yeast data indicate that ER subfractions near the PM are enriched with sterol and phospholipid biosynthetic enzymes (Pichler et al., 2001). However, in mammalian cells, the phagocytosis of latex beads promotes ER-PM contact but fails to increase cholesterol arrival at the PM (Lusa et al., 2003). As described later, cytosolic shuttling by caveolin complexes or SCP-2 has been proposed, and other hydrophobic cavity proteins could play important roles in ER to PM cholesterol transport.

Cholesterol transport from PM to ER: Arrival of cholesterol at the ER is typically measured by cholesterol ester formation by the ER-localized ACAT enzyme. There are two variations of this assay, the *in vivo* rate of esterification and the more quantitative *in vitro* run-off assay (Lange et al., 1999). It is clear that cholesterol travels from PM to ER via a different route than nascent cholesterol leaving the ER (Field et al., 1998), as PM to ER transport is sensitive to cytoskeletal inhibitors and requires intermediate filaments (Liscum and Munn, 1999). It has been proposed that only non-raft cholesterol in the liquid disordered phase of the PM is transported to the ER (Simons and Ikonen, 2000). Consistent with the hypothesis, the bacterial enzyme sphingomyelinase digests the sphingolipids of lipid rafts, releasing cholesterol for esterification via an ATP-independent vesicularization of 15-30% of the PM (Zha et al., 1998). The oxysterol 25-hydroxycholesterol also increases ER cholesterol by an unknown mechanism (Lange, 1998), resulting in decreased SREBP processing and activation ACAT as described earlier.

The Golgi and/or the endocytic pathway may be intermediates in PM to ER cholesterol transport (Neufeld, 1998), but data have been inconsistent. In yeast, PM to ER sterol transport is independent of the protein secretory pathway through the Golgi (Prinz,

2002). In Niemann-Pick C (NPC) or U18666A-treated cells, which accumulate cholesterol in late endosomes as described in the next section, cholesterol esterification is defective in response to sphingomyelinase, but normal in response to 25-hydroxycholesterol (Lange et al., 2000; Neufeld et al., 1996; Underwood et al., 1996). In these NPC cells, newly synthesized cholesterol reaches the PM normally, but its return to the ER for esterification is markedly defective (Cruz and Chang, 2000; Reid et al., 2003). However, other groups have shown that PM cholesterol reaches ACAT normally in NPC cells (Wojtanik and Liscum, 2003). Given this conflicting data, PM cholesterol may take at least two paths to the ER: a vesicular route via the endosomes or Golgi and a potentially non-vesicular alternative route (Simons and Ikonen, 2000; Underwood et al., 1998; Wojtanik and Liscum, 2003).

Two mutant CHO cell lines have been described with defective cholesterol transport to the ER, but no defects in other transport pathways. Mutant cells designated 3-6 have normal PM cholesterol levels, but defective PM to ER cholesterol movement both basally and in response to sphingomyelinase, suggesting altered lipid raft organization (Liscum, 1998). A similar phenotype was observed in Nrel-4 cells that cannot synthesize plasmalogens, special phospholipids of unknown function with *sn*-1 vinyl ether bonds to long chain fatty alcohols. In these cells, delivery of cholesterol to the ER is specifically blocked and rescued by restoration of plasmalogen synthesis (Munn et al., 2003). Both 3-6 and Nrel-4 mutant cells still increase ACAT activity in response to 25-hydroxycholesterol, but the phenotypes are distinct. The 3-6 mutant was identified in a screen for resistance to amphotericin B, an antibiotic that kills cells by forming pores in the cholesterol-rich PM, while Nrel-4 cells are sensitive like normal CHO cells (Munn et al., 2003). The mutated gene in 3-6 cells has not been cloned and the role of plasmalogens is unclear, so cholesterol movement to the ER remains poorly understood. Figure 1.6 summarizes ER cholesterol transport pathways.

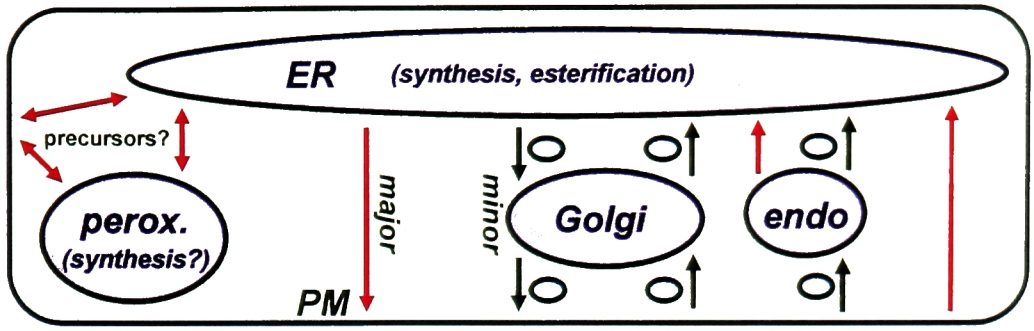

Figure 1.6: ER cholesterol transport pathways.

The ER is the site of cholesterol synthesis and esterification. Synthesis may also occur in peroxisomes, and cholesterol precursors may shuttle among and within compartments (left). Movement of nascent cholesterol from ER to PM proceeds primarily via a Golgi-independent pathway, though vesicular transport through the Golgi may account for some transport (middle). Likewise, there may be multiple routes from PM to ER, only some requiring endosomes (endo) and Golgi vesicles (right). Red arrows indicate candidate pathways for non-vesicular transport.

Cholesterol transport from late endosomes and Niemann Pick C: LDL binds to cell surface LDL receptors for endocytosis in clathrin-coated pits, and LDL cholesterol esters are hydrolyzed in the endocytic pathway. This newly hydrolyzed free cholesterol can be metabolically labeled by introducing ^{3}H- or ^{14}C-cholesterol esters into LDL. Most of this cholesterol appears back at the PM, where it can subsequently move to the ER for re-esterification, though about one third of endocytosed cholesterol moves directly to the ER bypassing the PM (Liscum and Munn, 1999). Therefore, cholesterol follows at least two pathways from endosomes to ER, one PM-dependent and the other PM-independent, and their relative contributions may vary in different cells types or conditions. The PM-dependent pathway uses the Golgi as an intermediate, consistent with filipin electron microscopy studies (Blanchette-Mackie and Pentchev, 1998). Furthermore, Brefeldin A blocks the PM-dependent pathway, causing all LDL-derived cholesterol to bypass the PM for direct delivery to ER. This result indicates either that the PM-independent pathway can substitute completely, or that cholesterol normally bound for the PM is delivered to the merged Golgi-ER (Blanchette-Mackie, 2000). Endosome to ER cholesterol transport was

initially described as vesicular, since it was inhibited by actin polymerization, ionophores that affect vesicle sorting, and energy poisons (Skiba et al., 1996; Underwood et al., 1998). However, these studies may have only assayed the PM and Golgi-dependent pathway, and it is possible that the PM-independent pathway is non-vesicular.

The fatal neurodegenerative disease Niemann Pick C (NPC) is an autosomal recessive lipid storage disorder characterized by intracellular free cholesterol accumulation in most tissues. Neurons accumulate glycosphingolipids rather than cholesterol, but both lipids are found in rafts, so the pathway defective in NPC may normally mobilize multiple raft components (Simons and Ikonen, 2000). Most intracellular cholesterol in NPC cells appears in multilamellar storage bodies, a hybrid compartment derived from late endosomes (Mukherjee and Maxfield, 1999), though accumulation in the Golgi has also been observed (Blanchette-Mackie, 2000). Late endosomes are normally dynamic multivesicular structures, but they become static, enlarged, and cholesterol-rich in NPC cells (Ko et al., 2001). While LDL is considered the primary source of this intracellular cholesterol, newly synthesized cholesterol also accumulates at a slower rate (Cruz et al., 2000). The NPC phenotype can be reproduced by treatment of normal cells with progesterone or hydrophobic amines (class II amphiphiles) like U18666A. The mechanism of U18666A action is unknown, though U18R mutant CHO cells are resistant to it (Liscum and Collins, 1991), and a putative membrane protein binding site has been described but not identified (Underwood et al., 1996).

Despite increased cholesterol content, NPC cells have repressed ACAT activity, high LDL receptor activity, and elevated cholesterol synthesis, all of which suggest low cholesterol in the ER regulatory pool. NPC cells are resistant to amphotericin B, so it was proposed that they have low PM cholesterol reflected in the ER (Lange et al., 1999). However, NPC cells have normal PM cholesterol, and amphotericin B resistance is due to sequestration of drug in the intracellular cholesterol-rich compartments, thus protecting the

PM (Lange et al., 2002). Recent data show that NPC cells also have normal ER cholesterol levels, but that they fail to repress SREBPs and activate LXRs in response to LDL (Frolov et al., 2003). These defects in transcriptional regulation in NPC cells correlate with up to 90% decreased generation of 25- and 27-hydroxycholeterol from LDL-cholesterol, and addition of these oxysterols corrects the cholesterol accumulation. Therefore, defective oxysterol generation and transcriptional regulation of cholesterol homeostasis may contribute to the NPC phenotype.

Two NPC disease complementation groups were identified, and both causative genes have been cloned. NPC1 is a late endosomal membrane protein with 13 predicted transmembrane segments, including a sterol sensing domain like those found in SCAP, HMGR, 7DHCR, and Patched, the receptor for Hedgehog (Prinz, 2002). NPC1 also shows homology to bacterial permeases, and NPC1 expression in *E. coli* increases the uptake of fatty acids, though not cholesterol in this assay (Davies et al., 2000). NPC2 is a soluble cholesterol-binding protein that resides in the lumen of late endosomes and lysosomes (Friedland et al., 2003; Naureckiene et al., 2000). Mutant NPC1 proteins that fail to reach late endosomes also cause mislocalization of NPC2 (Blom et al., 2003). NPC1 and NPC2 could directly participate in the vesicular or non-vesicular trafficking of cholesterol from late endosomes, or they could function indirectly as regulatory cholesterol sensors (Prinz, 2002). The M87 mutant CHO cell line shows an NPC-like cholesterol-rich compartment despite wild type NPC1 and NPC2 and normal NPC1-containing multivesicular late endosomes (Frolov et al., 2001), but the defective gene has not been cloned. Other genes, such as the hydrophobic cavity protein MLN64 described below, also may function in the NPC pathway.

There has been conflicting data on the transport defect in NPC cells. Two independent groups found that LDL-derived cholesterol rapidly arrives at the PM for cyclodextrin extraction, surprisingly even in NPC cells (Cruz et al., 2000; Lange et al., 2000).

A model was proposed in which the early PM cholesterol is re-internalized to a "cholesterol sorting compartment," and its subsequent movement back to the PM or to the ER is defective in NPC cells (Cruz et al., 2000). However, another group found no evidence for early appearance of LDL-cholesterol at the PM, suggesting the early cyclodextrin-extracted cholesterol may actually represent an internal pool diverted to the PM by treatment (Wojtanik and Liscum, 2003). Indeed, one of the original groups recently found this to be the case by using a revised cyclodextrin protocol and other methods (Sugii et al., 2003).

Based on this recent data, a consensus model for NPC is emerging. LDL-derived cholesterol esters are hydrolyzed early in the endocytic pathway, since the acid lipase enzyme was recently localized to an early acidic compartment, rather than to NPC1-containing late endosomes and lysosomes as previously assumed (Sugii et al., 2003). Free cholesterol in this early compartment can be extracted by prolonged cyclodextrin treatment, but it is not normally delivered to the PM. Instead, it enters the cyclodextrin-inaccessible late compartment, likely the multivesicular late endosomes, and egress of free cholesterol from this site is defective in NPC cells. The defect may only be slight, as even a small imbalance between influx and efflux would result in the observed cholesterol accumulation (Lange et al., 2002). In normal cells, late endosomal cholesterol may be transported directly to other compartments like PM, ER, and mitochondria, or it could first move to the endocytic recycling compartment (ERC) before subsequent transport (Wojtanik and Liscum, 2003).

Cholesterol transport via the endocytic recycling compartment: The ERC contains proteins and lipids that recycle from sorting endosomes to the plasma membrane. There is no enyzmatic assay for ERC cholesterol, but compositional data suggest cholesterol enrichment in this compartment (Gagescu et al., 2000; Hornick et al., 1997). Recent experiments have strongly implicated the ERC in cholesterol transport using the analog dihydroergosterol

(DHE), a naturally fluorescent yeast sterol that can be directly imaged in living cells (Mukherjee et al., 1998). These DHE studies, confirmed with ^{3}H-cholesterol, show that the ERC is the major intracellular sterol storage organelle in CHO cells (Hao et al., 2002). Cholesterol is transported from ERC to PM via the same vesicles that carry recycling proteins (Hao et al., 2002). Consistent with this observation, cells overexpressing Rab11, a small GTPase that inhibits recycling endosomes, accumulate cholesterol along with recycling markers in enlarged ERC organelles (Holtta-Vuori et al., 2002). However, cholesterol transport from the PM to the ERC is likely non-vesicular, as it is rapid and ATP-independent (Hao et al., 2002). DHE studies of polarized HepG2 hepatoma cells gave similar results, showing vesicular and non-vesicular sterol transport and the apical recycling compartment as the major storage site (Wustner et al., 2002).

Dissecting the role of the ERC in cholesterol transport is an exiting new field of research. While the ERC may be involved in NPC disease, current data suggests distinct pathways. NPC cells are rescued by overexpression of Rab7 or Rab9, GTPases implicated in late endosomal trafficking, but not Rab11, the inhibitor of ERC recycling endosomes (Choudhury et al., 2002). Notably, NPC1-deficient cells transfected with NPC1 clear cholesterol from late endosomes even when cholesterol is trapped in the ERC due to Rab11 overexpression (Holtta-Vuori et al., 2002). Rab11-mediated ERC cholesterol accumulation decreases basal ACAT activity ~50% but does not affect esterification of PM cholesterol delivered via cyclodextrin, suggesting that only some cholesterol transport to the ER proceeds via the ERC (Holtta-Vuori et al., 2002). Other transport pathways to and from the ERC remain to be described, as well as the mechanism of rapid non-vesicular cholesterol transport from the PM to the ERC. Figure 1.7 summarizes endosomal cholesterol transport pathways.

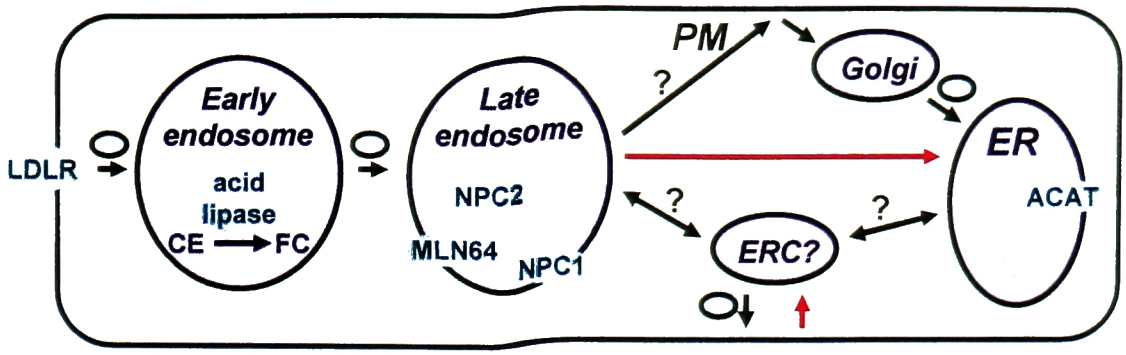

Figure 1.7: Endosomal cholesterol transport pathways.

LDL-derived cholesterol esters (CE) are hydrolyzed by acid lipase, and the free cholesterol (FC) leaves endosomes via a pathway involving the NPC proteins and MLN64. This cholesterol is re-esterified by ACAT in the ER. Endosomal cholesterol reaches the ER via a PM- and Golgi-dependent route or a direct route. The ERC is a major cholesterol storage compartment, and may serve as an intermediate in many transfer pathways. Red arrows indicate candidate pathways for non-vesicular transport.

Cholesterol transport to mitochondria: Mitochondria are considered cholesterol-poor organelles, with the outer mitochondrial membrane containing more cholesterol than the inner (Cheng et al., 1985). Two important cholesterol-metabolizing P450 enzymes reside on the matrix side of the inner mitochondrial membrane, sterol 27-hydroxylase (Cyp27) and the steroidogenic P450scc enzyme. Transport of cholesterol to P450scc is mediated by the hydrophobic cavity transfer protein StAR, which is described in detail below. P450scc and StAR are limited to steroidogenic cells, so other related transport proteins may deliver cholesterol to the widely expressed Cyp27 enzyme.

The source of mitochondrial cholesterol for steroidogenesis is unclear and may vary in different cells or conditions. In adrenocortical cells, HDL cholesterol taken up via SRB-1 appears to be the predominant substrate (Imachi et al., 1999). In MA-10 Leydig cells, steroidogenic stimulation causes increased internalization of PM cholesterol to a compartment resembling late endosomes (Choi and Freeman, 1998). NPC1 mutations or U18666A inhibit steroidogenic utilization of LDL-derived cholesterol *in vitro* (Watari et al., 2000), but NPC1 knockout mice use HDL cholesterol normally for steroidogenesis (Xie et

al., 2000). This may be analogous to the situation in the livers of NPC1 knockout mice, in which LDL cholesterol accumulates in a metabolically inactive pool, while cholesterol from HDL is metabolized normally (Xie et al., 2000). Cytosolic lipid droplets may also provide cholesterol to mitochondria, as full length StAR interacts with hormone sensitive lipase in adrenal cells, perhaps stimulating cholesterol ester hydrolysis and mobilization (Shen et al., 2003). Multiple cholesterol pools can contribute to steroidogenesis, but one compartment may still be the immediate proximal source for cholesterol that is delivered to mitochondria.

Potential transport by caveolin: Caveolin is an acylated integral membrane protein essential for the formation of caveolae, a subset of lipid rafts with characteristic flask shapes in electron micrographs. Caveolin is also soluble in multiple compartments including the cytosol, and it binds cholesterol and fatty acids (Liu et al., 2002). Pulse chase studies show that nearly all nascent cholesterol reaching the PM after 10 minutes is in caveolae, while after 60 minutes it is in non-caveolar PM (Smart et al., 1996). Cultured lymphocytes lacking caveolae exhibit relatively slow initial appearance of nascent cholesterol at the PM, but transfection of caveolin-1 increases the initial rate ~4-fold (Smart et al., 1996). However, caveolin is not essential, as similar amounts of nascent cholesterol reach the PM in transfected and untransfected cells by 1 hour. Further studies have identified a cytosolic complex containing caveolin, cholesterol, and three immunophilin chaperone proteins: cyclophilin A, cyclophilin 40, and heat shock protein 56 (Hsp56). Disruption of this complex with cyclosporin A in NIH 3T3 cells was reported to almost completely block transfer of nascent cholesterol to PM (Uittenbogaard et al., 1998). This marked inhibition is surprising given strong evidence for non-caveolin pathways, and another group showed no effect of cyclosporin A on nascent cholesterol transport in BHK cells under similar conditions (Heino et al., 2000).

Treatment of cells expressing the selective uptake receptor SRB-1 with HDL results in formation of a different cytosolic caveolin complex, containing HDL-derived cholesterol esters, caveolin, cyclophilin A, cyclophilin 40, and annexin II rather than Hsp56 (Uittenbogaard et al., 2002). Studies with caveolin mutants showed that acylation at cysteine 133 is required for formation of the annexin II complex (Uittenbogaard et al., 2002), while acylation at 143 and 156 is required for the Hsp56 complex (Uittenbogaard and Smart, 2000). These caveolin-cholesterol-chaperone complexes may represent novel intracellular lipid particles analogous to plasma lipoproteins (Liu et al., 2002). Indeed, earlier studies of nascent cholesterol transport suggested a lipid-rich low density transport intermediate (Urbani and Simoni, 1990). In addition, soluble caveolin may coat cytosolic lipid storage droplets (Pol et al., 2001). Given these important potential functions, it is quite surprising that caveolin-1 knockout mice, which also fail to express caveolin-2 and lack caveolae in all non-muscle cells, are viable (Prinz, 2002).

Potential transport by sterol carrier protein-2: The SCP-2 gene has two initiation sites that produce distinct proteins, the 58kD SCP-x and 15kD pro-SCP-2, both of which are cleaved to generate 13kD SCP-2. SCP-x cleavage is partial and generates a 45kD fragment, while pro-SCP-2 cleavage is complete and removes a 20 amino acid presequence (Gallegos et al., 2001). The 45kD N-terminal portion of SCP-x is a thiolase that breaks down straight-chain and branched chain fatty acyl-CoAs as well as bile acid precursors (Seedorf et al., 2000). SCP-x and SCP-2 proteins are found at varying levels in nearly all tissues, and both contain a peroxisomal targeting motif. SCP-x and its 45kD fragment appear completely localized in peroxisomes, while as much as half of SCP-2 is outside of peroxisomes in the cytosol, ER, mitochondria, and lysosomes (Gallegos et al., 2001).

SCP-2 binds many lipids, including fatty acids, fatty acyl-CoAs, phospholipids, cholesterol, and other sterols (Gallegos et al., 2001). SCP-2 is also called non-specific lipid transfer protein, as it transfers these lipids between membranes *in vitro*. The past 20 years have produced data supporting some role for SCP-2 in nearly every intracellular cholesterol transport pathway, involving lysosomes, ER, mitochondria, PM, and other compartments (Gallegos et al., 2001). Recent reports have similarly proposed myriad functions for SCP-2 in the metabolism of phospholipids (Schroeder et al., 2003; Starodub et al., 2000) and fatty acids (Atshaves et al., 2003; Murphy, 2002). Given so many potential functions, it is difficult to discern which may be physiological.

Studies of SCP-2 deficient cells may help in this regard. Peroxisome deficiency, which occurs in Zellweger syndrome, results in near absence of SCP-2. Such cells have normal trafficking of LDL-derived cholesterol to the ER and PM (Johnson and Reinhart, 1994), indicating that SCP-2 is not essential for the endosomal transport pathway involving NPC proteins. In contrast, the initial appearance of newly synthesized cholesterol at the PM after 10 minutes is decreased in cells lacking SCP-2 due to peroxisome-deficiency or SCP-2 antisense treatment (Puglielli et al., 1996). However, analogous to the studies of caveolin, there is no defect at 20 minutes, indicating that SCP-2 is not essential for this transport. Furthermore, SCP knockout mice are viable, and all the primary defects can be explained by absence of the SCP-x peroxisomal thiolase activity (Seedorf et al., 2000). More subtle defects in hepatic cholesterol metabolism and biliary cholesterol secretion have been reported, supporting some role for SCP-2 in cholesterol transport (Fuchs et al., 2001). However, these cholesterol defects may be secondary to major alterations in peroxisome function and fatty acid metabolism. Definitive proof that SCP-2 functions physiologically in cholesterol transport has been elusive.

Potential roles of oxysterol binding proteins: The oxysterol binding protein (OSBP) binds 25-hydroxycholesterol and other oxysterols, and was originally purified as a candidate for transcriptional regulation of cholesterol homeostasis (Taylor and Kandutsch, 1985). The SREBP-SCAP pathway proved to mediate this regulation, and the function of OSBP remains uncertain. OSBP has an oxysterol binding domain and a Pleckstrin homology (PH) domain that mediates membrane association (Lehto and Olkkonen, 2003). OSBP overexpression slightly decreases ACAT activity and increases cholesterol synthesis, suggesting some effect on the ER regulatory pool, and these effects require the PH domain (Lagace et al., 1997). OSBP is normally localized in the cytoplasm, probably on vesicles, but it relocates to the Golgi apparatus upon 25-hydroxycholesterol treatment (Ridgway et al., 1992). OSBP is also phosphorylated in a Golgi-dependent manner, but this modification does not appear to affect localization or ligand binding (Ridgway et al., 1998a). Other treatments that alter cholesterol transport affect Golgi localization and/or phosphorylation of OSBP, including cholesterol starvation, sphingomyelinase treatment, cyclodextrin extraction of PM cholesterol, and U18666A or NPC mutations (Mohammadi et al., 2001; Ridgway et al., 1998b; Storey et al., 1998). Since OSBP is clearly sensitive to cholesterol levels and trafficking, it may function in these pathways. Oxysterols are more hydrophilic than cholesterol and unlikely to require shuttling proteins, so OSBP is thought to serve a regulatory function in vesicular trafficking, oxysterol availability, or some other process.

An OSBP-related protein (ORP) family has been described, with 12 members in humans and 7 in yeast (Lehto and Olkkonen, 2003). All ORP proteins have ligand binding domains, most have PH domains, and alternative splicing is common (-S designates short forms and -L long forms). Proteins closely related to OSBP may bind oxysterols, as shown for the nearest homolog ORP4, while other ligands are likely for more divergent family members (Lehto and Olkkonen, 2003). Little is known about the function and localization of

mammalian ORPs, but two have been implicated in cholesterol metabolism. ORP4-S associates with vimentin intermediate filaments and decreases esterification of LDL-derived cholesterol by ~40% when overexpressed (Schroeder et al., 2001). Most interestingly, OSP1-L localizes to the surface of late endosomes, is induced ~100-fold upon differentiation of monocytes to macrophages, and its overexpression enhances LXRα reporter activation (Johansson et al., 2003).

Intracellular transport of cholesterol metabolites: Cholesterol is metabolized to bile acids and steroid hormones, and these molecules may also require intracellular transport mechanisms in specialized cell types. Transmembrane transport proteins for bile acids have been characterized in the apical and basolateral membranes of hepatocytes and enterocytes, but less is understood about intracellular bile acid trafficking. The weight of evidence suggests non-vesicular transport and several cytosolic bile acid binding proteins have been identified, including 3α-hydroxysteroid dehydrogenase (3α-HSD) and the ileal bile acid binding protein (IBABP), though transport has not been demonstrated (Agellon and Torchia, 2000). IBABP is transcriptionally activated in enterocytes by bile acids via the FXR nuclear receptor (Grober et al., 1999), but it is not expressed in liver. Intermediates in either pathway of bile acid biosynthesis may also shuttle between compartments in hepatocytes (Agellon and Torchia, 2000).

Even less is known about intracellular movements of steroid hormones. Since they typically circulate in plasma bound to proteins, it is possible that they also bind to intracellular transport proteins in addition to their cognate nuclear receptors. However, there is only indirect evidence for intracellular steroid transport pathways, such as their transport across epithelial cells (Fujise et al., 2002) and along neuronal axons (Frolkis and Tanin, 1999).

The START gene family

Two proteins that function in intracellular cholesterol transport, StAR and MLN64, belong to the family of StAR-related lipid transfer (START) proteins. START domains are ~210 amino acid lipid binding domains implicated in intracellular lipid transport, lipid metabolism, and cell signaling events. These domains are found in an extensive protein family, including START domain-only and multi-domain proteins, but lipid ligands have only been identified in a few cases (Ponting and Aravind, 1999; Soccio and Breslow, 2003). The human and mouse genomes each have 15 genes encoding START domains (Table 1.1), and phylogenetic analysis divides the family into six subfamilies (Figure 1.8). The novel subfamily of StarD4, StarD5, and StarD6 is the subject of this thesis. The remaining introduction will address the current state of knowledge about other START domain proteins.

StarD name	other names	mouse	human
StarD1	***StAR***	8, 24.5 Mb	8, 37.4 Mb
	StAR pseudogene	-	13, 59.8 Mb
StarD2	***PCTP***	11, 90.7 Mb	17, 53.6 Mb
StarD3	***MLN64***, es64, CAB1	11, 99.1 Mb	17, 37.3 Mb
StarD4	CRSP	18, 33.4 Mb	5,110.5 Mb
StarD5	none	7, 73.3 Mb	15, 77.6 Mb
StarD6	none	18, 70.8 Mb	18, 52.0 Mb
	StarD6 pseudogene	10, 56.8 Mb	-
StarD7	GTT1	2,128.3 Mb	2, 94.7 Mb
StarD8	KIAA0189-RhoGAP	X, 81.9 Mb	X, 64.1 Mb
StarD9	KIAA1300	2,121.1 Mb	15, 38.4 Mb
StarD10	PCTP-like, SDCCAG28, CGI-5	7, 91.1 Mb	11, 74.8 Mb
StarD11	***GPBP***, COL4A3BP	13, 93.9 Mb	5, 73.5 Mb
StarD12	***DLC-1***, Arhgap7, p122-RhoGA	8, 35.5 Mb	8, 12.7 Mb
StarD13	GT650, 4902678-RhoGAP	5,150.3 Mb	13, 31.7 Mb
(StarD14)	***CACH***	13, 88.9 Mb	5, 80.8 Mb
(StarD15)	***THEA***, BFIT, KIAA0707	4,104.5 Mb	1, 54.8 Mb

Table 1.1: Nomenclature and chromosomal locations of the 15 mammalian START genes.
The gene names in bold italics are used in the text. All human START genes except CACH and THEA have been assigned formal names START domain containing (StarD), but some common names are widely used. Physical map positions (chromosome, position in megabases) in the mouse and human genomes are based on the Ensembl database, 2 Dec 2002 revision (www.ensembl.org). Pseudogenes have been described for human StAR (Sugawara et al., 1995a) and mouse StarD6 (Soccio et al., 2002).

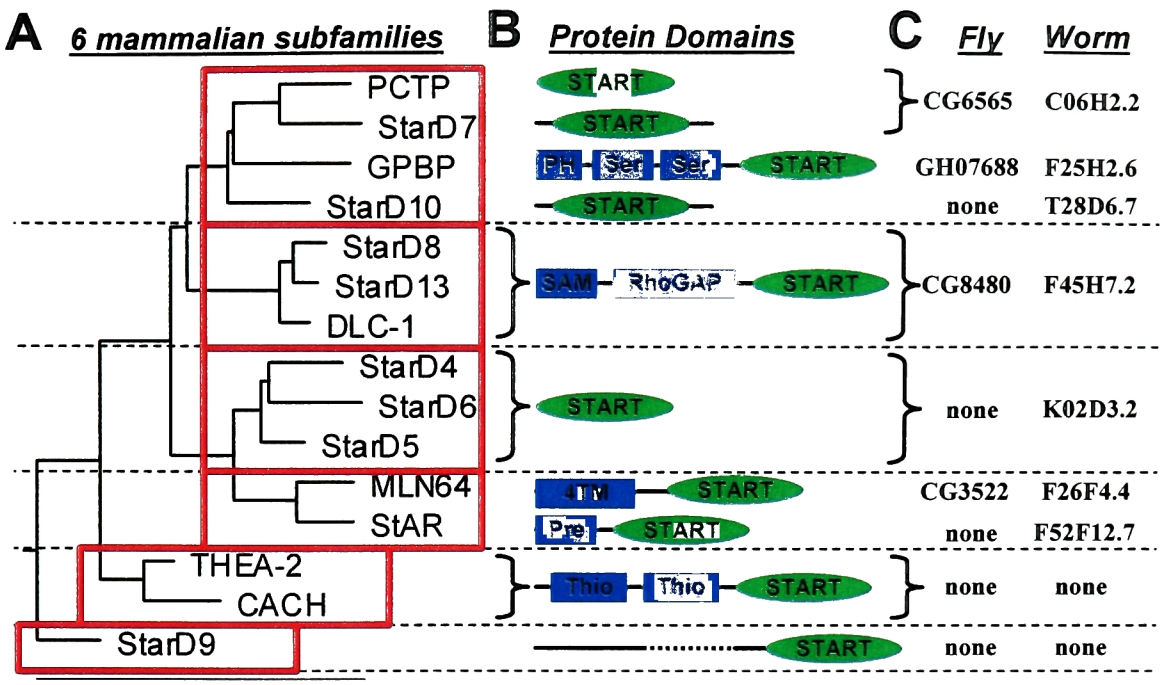

Figure 1.8: Phylogenetic analysis and domain structure of the START protein family.
(A) The 15 human START domains were aligned using ClustalW, and the resulting phylogenetic tree divides the family into six subfamilies. (B) The domain organization is shown for each protein or subfamily, with the START domain in green and other domains in blue (PH, Pleckstrin homology; Ser, serine-rich; SAM, sterile alpha motif; RhoGAP, Rho GTPase activating protein; 4TM, four transmembrane; Pre, mitochondrial presequence; Thio: acyl CoA thioesterase). (C) The START proteins from *Drosophila melanogaster* (fly) and *C. elegans* (worm) most closely resemble certain mammalian proteins or protein subfamilies.

The START domain structure: X-ray crystal structures have been solved for the MLN64 START domain (Tsujishita and Hurley, 2000), StarD4 (Romanowski et al., 2002), and phosphatidylcholine transfer protein (PCTP) (Roderick et al., 2002). All three share the same helix-grip fold (Iyer et al., 2001), with α-helices at the N- and C-termini separated by nine β-strands and two shorter α-helices. The curved β-sheet forms a deep pocket with the C-terminal α-helix acting as a lid, resulting in an internal hydrophobic cavity (Figure 1.9). The START structure differs from other hydrophobic cavity lipid binding proteins, such as SCP-2 (Choinowski et al., 2000), SPF (Stocker et al., 2002), phosphatidylinositol transfer protein (Yoder et al., 2001), and the fatty acid binding protein (FABPs) (Bernlohr et al., 1997). The

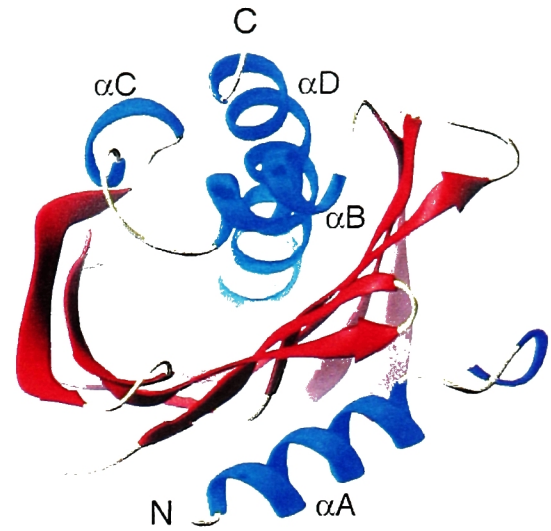

Figure 1.9: The START domain X-ray crystal structure.
Like other START structures, StarD4 has four α-helices (A-D, blue) and nine β-strands (red) that form a U-shaped sheet. The C-terminal αD helix may open or unfold to allow lipid binding in the internal hydrophobic cavity.

PCTP structure was reported with a phosphatidylcholine (PC) molecule in the cavity (Roderick et al., 2002), while the MLN64 and StarD4 structures contain cavities large enough to accommodate a cholesterol ligand (Romanowski et al., 2002). Lipid entry or egress would require a major conformational change, most likely opening or unfolding of the C-terminal α-helix lid. In fact, this helix of PCTP is implicated in membrane binding and PC extraction (Feng et al., 2000). Furthermore, StAR can form partially unfolded states (Christensen et al., 2001) and decreases its helical content upon binding a cholesterol analogue (Petrescu et al., 2001). Modeling of StAR using structure-based thermodynamics shows that an open-lid conformational state can exist at equilibrium, and that cholesterol binding and lid closure significantly stabilize the complex (Mathieu et al., 2002).

The steroidogenic acute regulatory protein: The rate-limiting step in steroidogenesis is StAR-mediated delivery of cholesterol to the P450scc enzyme, which resides on the matrix side of the inner mitochondrial membrane (IMM) and converts cholesterol to pregnenolone (Miller and Strauss, 1999; Stocco, 2001). After stimulation by pituitary trophic hormones, acute steroidogenesis results from phosphorylation of pre-existing StAR and rapid synthesis of new StAR (Miller and Strauss, 1999). When StAR is mutated in humans with lipoid

congenital adrenal hyperplasia (CAH) (Bose et al., 1996) or in knockout mice (Caron et al., 1998), there are marked defects in the synthesis of adrenal and gonadal steroids, as well as cholesterol accumulation in cytosolic lipid droplets of steroidogenic cells. Early studies did not detect StAR mRNA in other steroidogenic organs such as placenta and brain (Sugawara et al., 1995a), but more sensitive assays have recently shown StAR expression in both tissues (King et al., 2002; Koh et al., 2002). Increased StAR expression has even been observed in glial brain tumors, perhaps implicating StAR in tumorigenesis (Kim et al., 2003). StAR null fetuses produce normal levels of placental progesterone (Bose et al., 1996), suggesting the existence of alternate steroidogenic mechanisms. StAR-independent steroidogenesis is also key to the favored two-hit model of lipoid CAH, which explains the clinical manifestations based on different times of onset for StAR-dependent steroidogenesis in testis (fetal), adrenal gland (postnatal), and ovary (puberty) (Miller, 2002; Miller and Strauss, 1999).

In order for P450scc to act, cholesterol must get to the outer mitochondrial membrane (OMM), across the intermembranous space, and to the IMM. StAR is synthesized as a 37 kD protein, but the N-terminal presequence directs mitochondrial import before being cleaved in the matrix, leaving a 30 kD protein. Despite its final matrix localization, StAR most likely acts at the OMM (Bose et al., 2002). In transfection assays and studies with isolated mitochondria, StAR lacking the presequence (N-62 StAR) has equivalent activity to full-length StAR (Arakane et al., 1998; Arakane et al., 1996). In studies using StAR fusions to mitochondrial proteins, StAR at the OMM facing the cytosol is fully active, while StAR in the intermembranous space or matrix is inactive (Bose et al., 2002). StAR could simply drop-off cholesterol, or alter the OMM to facilitate cholesterol desorption to the IMM (Miller and Strauss, 1999). An alternate view is that StAR must be imported to act, since data supporting an OMM site of action rely on non-physiological isolated mitochondria or transfection of non-steroidogenic cells (Jefcoate, 2002).

If StAR acts at the OMM, then the purpose of its presequence and mitochondrial import is unclear. StAR can act as a cholesterol transfer protein *in vitro*, as N-62 StAR selectively transfers sterols from donor liposomes to acceptor mitochondria (Kallen et al., 1998). However, N-62 StAR lacks target specificity, as other acceptors include trypsin-treated mitochondria, endoplasmic reticulum (ER), and phospholipid vesicles (Kallen et al., 1998; Tuckey et al., 2002). Therefore, the presequence may direct cholesterol transfer to mitochondria in preference to other organelles (Miller and Strauss, 1999). In addition, import may rapidly inactivate StAR (Bose et al., 2002), as StAR undergoes proteolytic degradation in mitochondria (Granot et al., 2002). Mitochondrial proteins such as the peripheral-type benzodiazepine receptor (PBR) and PAP7 have also been implicated in StAR function (Hauet et al., 2002), and a novel StAR binding protein (SBP) was recently cloned by yeast two-hybrid (Sugawara et al., 2003), so future studies of these proteins may shed additional light on the function of StAR.

The MLN64 protein: MLN64 was cloned as a gene amplified in breast, gastric and esophageal cancers (Akiyama et al., 1997; Tomasetto et al., 1995). While MLN64 could play a causative role in tumorigenesis (Moog-Lutz et al., 1997; Watari et al., 1997), amplification likely reflects close genomic proximity (within 36kB) to the oncogene c-Erb-b2 (Her2/neu) (Tomasetto et al., 1995), which is invariantly co-amplified (Watari et al., 1997). The N-terminus of MLN64 includes four transmembrane helices, while the C-terminal START domain is 37% identical to StAR (Moog-Lutz et al., 1997). Like StAR, the isolated MLN64 START domain binds (Tsujishita and Hurley, 2000) and transfers (Zhang et al., 2002a) cholesterol *in vitro*, and stimulates steroidogenesis when co-transfected with P450scc (Bose et al., 2000; Watari et al., 1997).

MLN64 expression is detected in all tissues (Watari et al., 1997), and it is a candidate for StAR-independent steroidogenesis. However, the transmembrane domain of MLN64 localizes it to late endosomes with the START domain facing the cytosol (Alpy et al., 2001; Zhang et al., 2002a). Given this localization, full-length MLN64 is relatively inactive in steroidogenesis assays, but proteolysis could release the START domain allowing delivery of cholesterol to mitochondria (Watari et al., 1997). Supporting this notion, antibodies against the MLN64 START domain detect full-length protein and prominent smaller bands in placenta and transfected cells (Watari et al., 1997).

MLN64 also functions in cholesterol mobilization from endosomes via the Niemann-Pick C (NPC) pathway. Since MLN64 co-localizes with NPC1, endosomal cholesterol could move sequentially from luminal NPC2, through NPC1, to MLN64, and finally to a cytosolic acceptor (Strauss et al., 2002). MLN64 mutations have not been reported in NPC disease, but overexpression of the MLN64 transmembrane domain with no START domain results in an NPC phenocopy, with cholesterol accumulation in enlarged endosomes (Zhang et al., 2002a). A similar phenotype is observed upon overexpression of MENTHO (MLN64 N-terminal domain homologue), an endosomal membrane protein of unknown function, which is 70% identical to the MLN64 transmembrane domain but lacks a START domain (Alpy et al., 2002).

The PCTP subfamily: While PCTP, StarD7, StarD10, and Goodpasture antigen binding protein (GPBP) form a subfamily based on phylogenetic analysis, the four genes do not appear as closely related as other subfamilies. Unlike the other subfamilies, the four PCTP subfamily genes do not share a common exonic organization or homology outside the START domain. In the PCTP structure, 28 residues in the hydrophobic cavity contact PC (Roderick et al., 2002), and 20 of these are identical or similar in StarD7, including 9 of the

11 aromatics. This suggests that StarD7 may also bind PC, while StarD10 and GPBP exhibit much less similarly at these key residues (only 1 and 3 of the 11 aromatics conserved, respectively), suggesting different ligands.

PCTP is an extremely specific lipid binding protein, as it promotes intermembrane transfer of PC but not other phospholipids or sterols (Wirtz, 1991). PCTP is a cytosolic protein, though one report indicates relocation to mitochondria upon clofibrate treatment. This relocation occurs in endothelial cells but not hepatoma cells, and requires a putative phosphorylation site at serine 110 (de Brouwer et al., 2002). PCTP is widely expressed with highest levels in liver (Cohen et al., 1999), and a function has been proposed in the selective secretion of PC into bile. However, PCTP knockout mice were reported to have normal biliary PC levels, but even wild-type adults in this study had very low liver PCTP protein levels compared to newborn pups (van Helvoort et al., 1999). PCTP may also play a role in cellular lipid efflux via ABCA1, which forms plasma HDL by efflux of phospholipids and cholesterol to ApoAI (Tall et al., 2002). PCTP overexpression results in a dose dependent acceleration of this efflux, suggesting that PCTP replenishes the cell membrane with PCs that have been removed by ABCA1 (Baez et al., 2002).

Little is known of StarD7 and StarD10, which have short extensions of non-START sequence at their N- and C-termini. There are no StarD7 publications, but ~800 expressed sequence tag cDNAs (ESTs) indicate abundant and widespread expression. StarD10 mRNA is detectable by Northern Blot in testis, liver, kidney, and intestine (Yamanaka et al., 2000), and there are ~700 ESTs from many tissues. In testis, StarD10 mRNA is expressed in germ but not somatic cells, and the protein localizes to sperm tails (Yamanaka et al., 2000).

The widely expressed GPBP has an N-terminal PH domain, two serine-rich domains, and a C-terminal START domain (Raya et al., 1999). GPBP binds and phosphorylates Goodpasture (GP) antigen, the C-terminus of human collagen IV α3, which is the target of

autoantibodies in GP syndrome (Raya et al., 1999). PH domains mediate interactions, and the GPBP PH and first serine-rich domains are sufficient for binding GP antigen (Raya et al., 1999). GPBP lacks a conventional serine/threonine kinase domain, but the START domain is more likely a regulatory lipid binding domain than a catalytic site. GPBP mRNA is alternatively spliced and the most abundant form (GPBPΔ26) lacks the second serine rich domain (Raya et al., 2000). Antibodies that recognize the rarer full length protein but not GPBPΔ26 stain endothelial basement membranes - particularly in renal glomeruli and lung alveoli, which are affected in GP syndrome - and show markedly increased staining in skin biopsies from patients with dermatologic autoimmune conditions (Raya et al., 2000). GPBP is thus implicated in human autoimmune diseases, but other roles are likely as GPBP is conserved in other mammals lacking the GP antigen, and even in *Drosophila* and *C. elegans*.

The acyl CoA thioesterase subfamily: Cytosolic acetyl CoA hydrolase (CACH) and thioesterase adipose-associated (THEA) each have two type II acyl CoA thioesterase domains and a C-terminal START domain. Multiple subcellular compartments contain acyl CoA thioesterases, which hydrolyze acyl-CoAs to free fatty acids. Several are regulated by PPAR nuclear receptors and nutritional factors, yet their precise roles in lipid metabolism remain undefined (Hunt and Alexson, 2002).

CACH has high hydrolase activity for acetyl-CoA (C_2), low activity for short chain acyl-CoAs (C_4-C_6), but no activity for medium (C_{12}) and long (C_{16}) chain acyl-CoAs (Suematsu et al., 2001). Rat CACH activity is detected only in liver and kidney cytosol (Matsunaga et al., 1985), and hepatic activity is regulated in several metabolic states. First, both starvation and a fat-free diet increase activity, suggesting that CACH regulates acetyl CoA levels for fatty acid oxidation and synthesis (Matsunaga et al., 1985). Second, activity is increased by cholesterol feeding or by cholesterol synthesis inhibitors, both of which

decrease cholesterol synthesis and may increase levels of the precursor acetyl CoA (Ebisuno et al., 1988). Third, activity is elevated in acute streptozotocin-induced diabetes, but insulin injection prevents this elevation (Ebisuno et al., 1988). Finally, a PPARα agonist elevates CACH activity 3-fold (Nakanishi et al., 1993), indicating it may be a PPAR target gene.

Though the thioesterase domains of THEA and CACH are ~60% identical, no acetyl-CoA hydrolase activity is detectable for recombinant THEA (Suematsu et al., 2001), which instead hydrolyzes medium and long chain acyl-CoAs (Adams et al., 2001). Humans produce two THEA splice variants, which vary in relative abundance among tissues and encode different C-termini (Adams et al., 2001). THEA-1 and THEA-2 could differ in lipid binding since their START domains have different C-terminal α-helix lids. Only the THEA-2 C-terminus resembles CACH, and mice express only THEA-2. In mouse brown adipose tissue, THEA mRNA is induced by cold exposure, suppressed by warmth, and decreased 2.5-fold in genetically obese (*ob/ob*) mice compared to lean littermates (Adams et al., 2001). THEA maps to the Dietary obese 1 (*Do1*) locus on mouse chromosome 4, syntenic to an obesity locus in the Quebec Family Study on human 1p32 (Adams et al., 2001). THEA may thus play a role in energy metabolism and obesity.

The RhoGAP subfamily: Rho family small GTPases signal in actin cytoskeletal organization and other cellular processes, and Rho GTPase activating proteins (RhoGAPs) stimulate GTP hydrolysis to inactivate signaling (Ridley, 2001). The human genome encodes over 50 RhoGAPs, three of which have START domains. Deleted in liver cancer 1 (DLC-1), StarD8, and StarD13 are ~50% identical proteins, each with an N-terminal sterile alpha motif (SAM, a protein interaction domain found in many signaling proteins), a RhoGAP domain, and a C-terminal START domain. There are no publications on StarD8 and StarD13, which could share redundant functions with DLC-1 or be expressed in different

tissues. There are two potential connections between RhoGAPs and cholesterol metabolism: Rho proteins have been implicated in regulating the activity of LXRs (Gan et al., 2001), while related Rab proteins regulate vesicular cholesterol transport in the endosomal compartment as described earlier (Choudhury et al., 2002).

The widely expressed tumor suppressor DLC-1 is often deleted homozygously in primary hepatocellular carcinomas and breast tumors (Yuan et al., 2003). Deletion or loss of expression is found in many tumor cell lines from liver, breast, colon, and prostate (Yuan et al., 2003). DLC-1 transfection inhibits growth of DLC-1 negative hepatoma and breast carcinoma lines, preventing *in vivo* tumorigenicity of the latter (Ng et al., 2000; Yuan et al., 2003). *In vitro* studies identified two potential signaling functions for rat DLC-1, activation of phospholipase C-δ1 and RhoGAP activity for RhoA (Homma and Emori, 1995). Phospholipase C-δ1 induces Ca^{2+} release, and cells microinjected with DLC-1 show a rapid rise in intracellular Ca^{2+} (Sekimata et al., 1999). RhoA affects the cytoskeleton, and DLC-1 transfected cells round and detach from the plate, changes blocked by dominant active RhoA. The SAM and START domains of DLC-1 are dispensable for this cytoskeletal reorganization (Sekimata et al., 1999), though they could play roles at physiological expression levels.

The high molecular weight StarD9 protein: StarD9 is in sequence databases as a partial 1820 amino acid human coding sequence (Nagase et al., 2000) with a C-terminal START domain but no defined N-terminus. The 5' exon in the partial cDNA has at least 4000 bp of coding sequence, and upstream genomic sequence shows up to 9995 bp of coding sequence in this exon. (An exon with ~10 kb of coding sequence is atypical, but the mouse gene shares this feature.) Although additional 5' exons are possible, this large exon and ten 3' exons constitute an ORF of 11,334 bp, encoding a 413 kD protein. In this very large

predicted protein, only the START domain exhibits homology to other proteins. EST evidence suggests StarD9 is predominantly expressed in the nervous system.

Evolution of the START domain: The distribution of START proteins in completely sequenced genomes shows the evolutionary history of this domain (Iyer et al., 2001). The pathogenic bacterium *Pseudomonas aeruginosa* PA1579 gene is similar to mammalian PCTP, suggesting horizontal acquisition from hosts since there are no START genes in other prokaryotes (Romanowski et al., 2002). START domains are also absent in the budding yeast *Saccharomyces cerevisiae*, a unicellular eukaryote. The slime mold *Dictyostelium discoideum* has the CheaterA START protein, indicating the domain was present in the common ancestor to multicellular eukaryotes (Iyer et al., 2001). CheaterA also includes WD40 and F-box domains, suggesting a role in protein ubiquitination, and CheaterA mutants preferentially form spores rather than stalks (Ennis et al., 2000). The plant *Arabidopsis thaliana* has 20 START genes, 16 of which are fused to homeodomains, suggesting that ligand binding to these transcription factors may regulate plant development (Ponting and Aravind, 1999). In animals, mammals have 15 START genes, while the fruit fly *Drosophila melanogaster* has only four, which most closely resemble mammalian MLN64, GPBP, PCTP/StarD7, and a RhoGAP. The nematode *Caenorhabditis elegans* has three additional START genes – most similar to StAR, StarD10, and StarD5 – for a total of seven (see Figure 1.9). START genes have also been described in animals without completely sequenced genomes, including a START protein in the silkworm *Bombyx mori* that binds carotenoids (Tabunoki et al., 2002).

Perspective

By binding lipid ligands, START domains could function in net lipid transfer between subcellular compartments or in lipid regulation of cellular signaling events. START proteins likely play significant roles in lipid metabolism, fertility, atherosclerosis, autoimmune disease, and cancer, making them potential drug targets. There has been significant recent progress in the study of some START proteins, while others are essentially uncharacterized and demand further investigation. Given the roles of StAR and MLN64 in cholesterol metabolism, other related START proteins could also play roles in intracellular sterol transport. Here we describe the cloning, structure, and regulated expression of the StarD4 subfamily of three START proteins, and present data that these proteins function in intracellular cholesterol metabolism.

Chapter 2: Discovery of the StarD4 subfamily

Dietary cholesterol cDNA microarray experiment: Our initial experiment sought to identify novel hepatic genes regulated by dietary cholesterol. Most previous studies of cholesterol-regulated genes have used cultured cells and genetically modified mice (Horton et al., 2002), but we used a physiologically relevant model of cholesterol feeding to intact wild type mice. We assayed gene expression in liver since it is the central organ in cholesterol metabolism (Dietschy and Turley, 2002). Hepatocytes synthesize a large fraction of whole body cholesterol, store cholesterol esters in lipid droplets, and convert cholesterol to bile acids, which are excreted in bile along with free cholesterol. In the metabolism of plasma lipoproteins, the liver is responsible for uptake of dietary cholesterol in chylomicron remnants, re-secretion of cholesterol in very low density lipoproteins (VLDL), apolipoprotein synthesis, and uptake of cholesterol from LDL and HDL.

Known SREBP and LXR target genes do not explain many aspects of cholesterol metabolism, such as the responsiveness of plasma cholesterol levels to dietary cholesterol. Therefore, we hypothesized that relevant genes could be identified by their differential regulation. To identify such genes, we considered PCR-based methods including differential display (Liang and Pardee, 1992), serial analysis of gene expression (SAGE) (Velculescu et al., 1995), suppression subtractive hybridization (Diatchenko et al., 1996), selective amplification via biotin- and restriction-mediated enrichment (SABRE) (Lavery et al., 1997), and representational differential analysis (Hubank and Schatz, 1999). We attempted some of these techniques before choosing cDNA microarrays, a relatively novel technique at the time with many advantages over previous methods (Brown and Botstein, 1999). By collaborating with the laboratory of Raju Kucherlapati, we obtained glass slide cDNA microarrays (Cheung et al., 1999) with ~9000 mouse ESTs representing ~6000 genes.

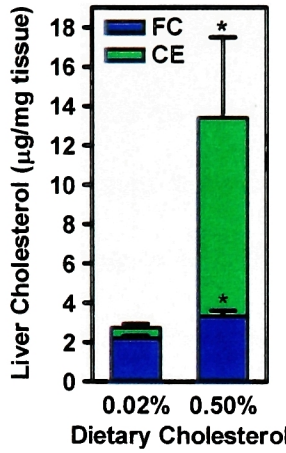

Figure 2.1: Liver cholesterol levels increase upon cholesterol feeding.

Six week-old C57BL/6 male mice were fed a chow-based diet containing 0.02% or 0.50% cholesterol (wt/wt) for three weeks (n=5 per group). Livers were extracted and total cholesterol and free cholesterol (FC) were measured by gas chromatography, while cholesterol esters (CE) were calculated as the difference. *P<0.01

Our experimental comparison was C57BL/6 male mice fed a chow diet low (0.02%) or high (0.50%) in cholesterol for three weeks. The high cholesterol diet raised liver total cholesterol almost 5-fold, with most of the increase in cholesterol esters but also a significant increase in free cholesterol (Figure 2.1). RNA was extracted from mice on each diet and used to probe cDNA microarrays (Figure 2.2). As others have reported (Lee et al., 2000), the results from a single microarray hybridization are unreliable, so we performed three

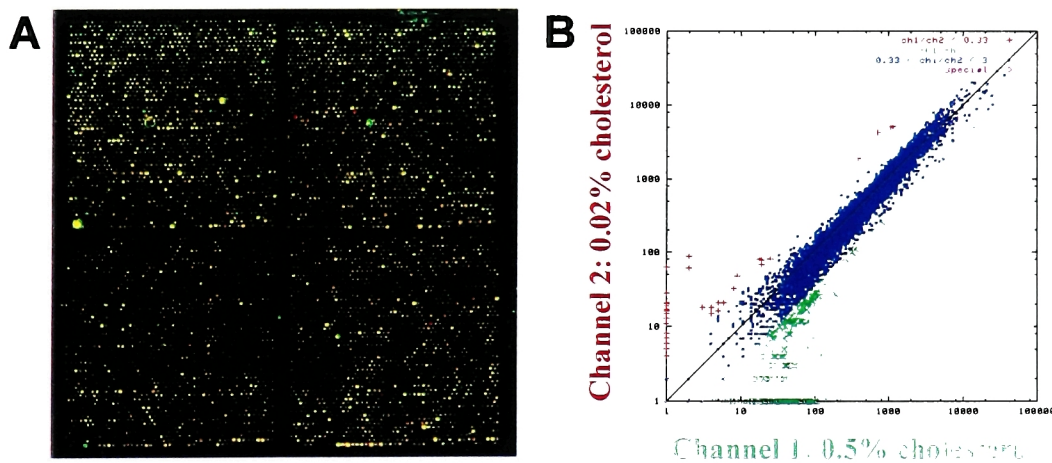

Figure 2.2: Microarray analysis of liver gene expression in response to dietary cholesterol.

RNA was prepared from livers of mice fed chow diets with 0.02% or 0.50% cholesterol. cDNA was synthesized incorporating Cy3 (red) or Cy5 (green) fluorophores, and the labeled cDNA probes were competitively hybridized to glass slide cDNA microarrays. (A) A merged image of the red and green fluorescence from a representative array. Unregulated genes appear as yellow spots. (B) A representative scatter plot of red and green fluorescence intensity for each array spot. There was noise at low signal intensities (<100), but cholesterol-regulated genes were identified above this background.

independent feeding experiments with duplicate hybridizations for a total of six microarrays. Among the six genes on the array that were down-regulated more than two-fold by dietary cholesterol, five were known SREBP-target genes involved in cholesterol or fatty acid biosynthesis (Horton et al., 2002), thus validating our microarray approach. The sixth gene was an expressed sequence tag (EST AA239481) representing a novel gene (Table 2.1). A similar dietary cholesterol microarray experiment was performed by Kara Maxwell using Affymetrix oligonucleotide arrays, and this study found these six genes and many others that are down- and up-regulated by cholesterol (Maxwell et al., 2003).

Mean Fold	GenBank		fold decrease on six arrays					
Decrease	Accession	Gene Product	1a	1b	2a	2b	3a	3b
4.6	AA237469	Isopentyl diphosphate isomerase	3.3	7.6	2.4	3.6	4.9	5.9
2.8	***AA239481***	***novel EST (StarD4)***	***3.6***	***2.3***	***4.8***	***1.6***	***2.8***	***1.9***
2.6	AA268608	Squalene epoxidase	3.2	2.7	2.8	1.3	2.9	(44)
2.5	AA061468	HMG CoA synthase	2.6	0.9	5.2	2.0	2.4	2.1
2.0	AA116513	Fatty acid synthase	1.4	1.7	2.0	2.8	2.3	2.0
2.0	AA500330	Farnesyl pyrophosphate synthase	1.2	1.7	2.0	2.8	2.3	2.0

Table 2.1: Six genes down-regulated two-fold or more by dietary cholesterol.
Experiments 1-3 each compared liver gene expression in a pair of individual mice fed different diets (0.02% versus 0.5% cholesterol). Each experiment was performed on duplicate arrays (a, b) by reversing the Cy3 and Cy5 probe labeling. Due to variability within and between experiments, the following criteria were used for regulated genes: expression differed 2-fold or greater on at least 4 of the 6 arrays with the higher expression level at least 25% over background. For each of the six genes down-regulated by the high cholesterol diet, the fold regulation on each array is shown, as well the average from all six (the outlying value in parenthesis was eliminated)

Identification of the StarD4 gene and its tissue expression pattern: To identify the novel cholesterol-regulated gene, EST AA239481 was obtained and its 1114 bp insert sequenced. There were no long protein-coding regions in any reading frame, suggesting the sequence was 3' untranslated region (3' UTR). BLAST searches placed the EST sequence on a mouse BAC clone (AC020796), about 3 kb downstream of a 230 bp coding sequence homologous to START genes. This 230 bp sequence (the coding part of exon 6) was in multiple mouse ESTs, allowing assembly of a 675 bp open reading frame (ORF) by *in silico* EST walking.

The mouse gene encodes a 224 amino acid protein consisting almost entirely of a START domain, so it was named START domain containing 4 (StarD4). The human StarD4 orthologue encodes 205 amino acids, with a shorter N-terminus, 87% identical to the mouse protein. Both genes have six exons, and they are located on mouse chromosome 18 at 12cM and the syntenic region of human 5q22.

Mouse and human StarD4 ORFs were RT-PCR amplified from liver, cloned, and sequence-verified. The sequence of mouse StarD4 from C57BL/6 disagreed with some ESTs at positions 121 and 152. Since other ESTs agreed with the C57BL/6 sequence, StarD4 was cloned from a second inbred mouse strain, FVB. Sequencing confirmed that these nucleotides are polymorphic between strains, and that these single nucleotide polymorphisms (SNPs) result in amino acid substitutions at positions 41 and 51 (Figure 2.3). Based on the StarD4 crystal structure described later, side chains at both positions are on the protein surface and do not contribute to the lipid-binding cavity, so it is uncertain whether they have

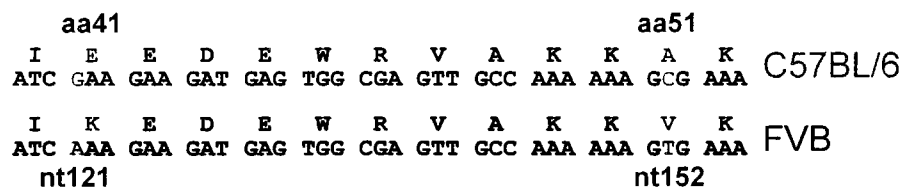

Figure 2.3: Single nucleotide polymorphisms (SNPs) in the mouse StarD4 coding region.
Multiple independent RT-PCR reactions were performed to amplify the liver StarD4 ORF from two inbred mouse strains, C57BL/6 and FVB. cDNAs were sequenced for each strain, revealing SNPs at nucleotides (nt) 121 and 152. Both SNPs result in amino acid (aa) coding differences.

functional consequences. RT-PCR amplification of human StarD4 gave the expected ORF (arrowhead) and additional products (Figure 2.4a). Several of these were cloned and sequenced, revealing mis-spliced StarD4 RNAs that included sequence from intron 5 or excluded exons (Figure 2.4b). Such products were not amplified from mouse liver and likely reflect heterogeneous nuclear RNA in the commercial human liver RNA template, rather than alternative splicing.

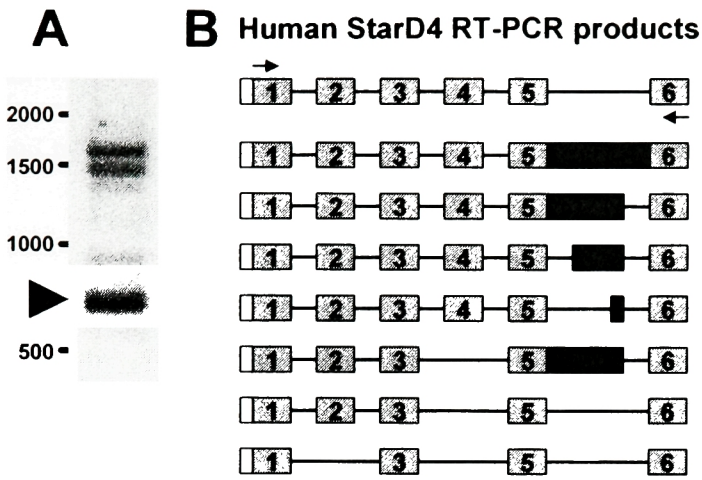

Figure 2.4: Mis-spliced human StarD4 RT-PCR products.

RT-PCR primers (arrows) in the human StarD4 coding sequence were used to amplify this gene by from a commercial source of human liver RNA. (A) The major RT-PCR product was the expected StarD4 band (arrowhead), but there were other bands. (B) These products were sequenced, revealing mis-spliced mRNAs which could not encode the StarD4 START domain.

Northern blots were performed to verify that the array EST and ORF sequences were part of the same mRNA (Figure 2.5a). On a mouse multiple tissue northern blot, a StarD4 ORF probe hybridized to a predominant mRNA at ~5.5 kb in all eight tissues with the highest levels in liver and kidney, in addition to several smaller mRNAs (Figure 2.5b). The array EST insert probe also hybridized to this ~5.5 kb mRNA with the same relative tissue

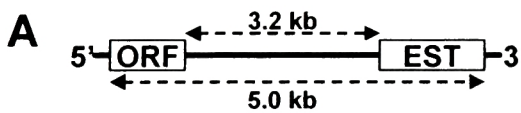

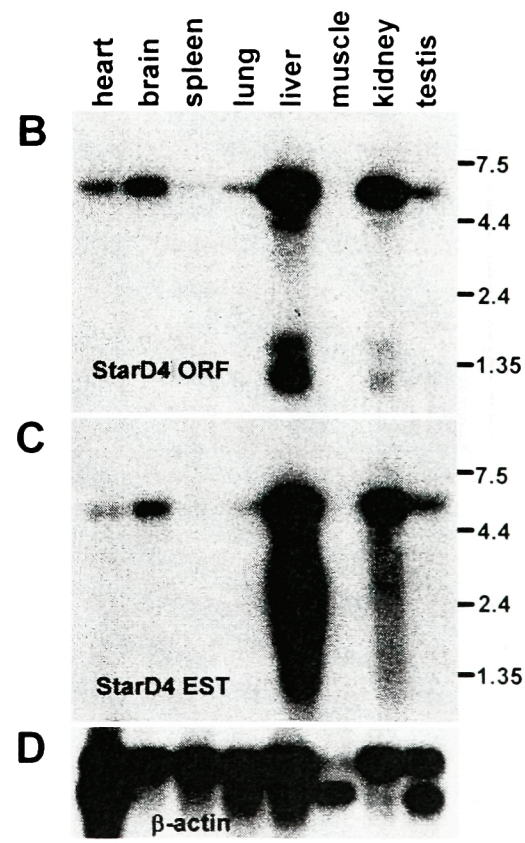

Figure 2.5: Multiple tissue northern blots of mouse StarD4.

(A) The predicted mouse StarD4 mRNA was at least 5 kb long with 3.2 kb of 3' UTR between the ORF and EST AA239481 sequence. A mouse multiple tissue northern blot was hybridized with three probes: (B) StarD4 ORF, (C) EST AA239481 insert, or (D) β-actin loading control. The major StarD4 mRNA was ~5.5 kb, and smaller transcripts were also detected. Longer exposures revealed StarD4 expression in skeletal muscle.

levels (Figure 2.5c), consistent with the predicted mRNA. Subsequent EST cloning and annotations by the various genome projects have confirmed our descriptions of the mouse and human StarD4 genes.

StarD4 regulation by dietary cholesterol: To confirm the microarray result that StarD4 expression is cholesterol-regulated, we used other methods to assay gene expression. On Northern blots, liver StarD4 expression was decreased ~3-fold upon cholesterol feeding (Figure 2.6a). We also designed real-time quantitative RT-PCR (qPCR) primer and probe sets for mouse StarD4, one set in the ORF spanning exons 1 and 2, and another in the 3' UTR of exon 6. In multiple cholesterol feeding experiments, a consistent 50-70% decrease in liver StarD4 expression was observed in both male and female mice using either probe set, and representative examples are shown in Figure 2.6b. StarD4 expression was not regulated by dietary cholesterol in non-hepatic tissues such as kidney and heart, though there was higher expression in the kidney (Figure 2.6c) consistent with the multiple tissue Northern.

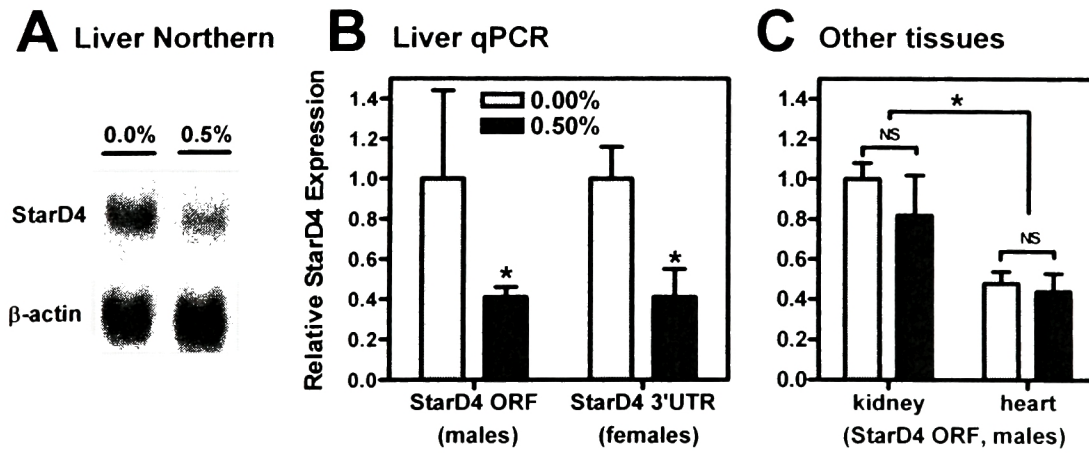

Figure 2.6: Regulation of StarD4 expression by dietary cholesterol.

C57BL/6 mice were fed a semi-synthetic diet with 0.00% or 0.50% cholesterol (wt/wt) for one week before extraction of tissue RNA. (A) A Northern blot of liver RNA shows a 3-fold decrease in StarD4 relative to loading control β-actin. (B) Two different quantitative RT-PCR probes for mouse StarD4 showed similar down-regulation by cholesterol feeding in male and female mice (n=5 per group). (C) No significant regulation of StarD4 was observed in kidney or heart (n=3 per group). Normalized to cyclophin, *P<0.05. NS=not significant

Expression of the known SREBP target genes HMGR and squalene expoxidase was also decreased by cholesterol feeding in liver but not peripheral tissues (data not shown).

In addition, Kara Maxwell performed a time course experiment of feeding a semi-synthetic 0.50% cholesterol diet for one week, revealing a difference in regulation of SREBP-1 versus SREBP-2 target genes (Maxwell et al., 2003). SREBP-2 target genes in cholesterol metabolism (i.e. HMGR) are completely down-regulated after only one day of cholesterol feeding, while SREBP-1 targets in fatty acid metabolism (i.e. FABP5) take several days. When StarD4 expression was analyzed in this time course (Figure 2.7), its expression was decreased after only one day of feeding, consistent with SREBP-2 target genes and a role in cholesterol metabolism. Further studies in Chapter 3 confirmed that StarD4 is an SREBP-2 target.

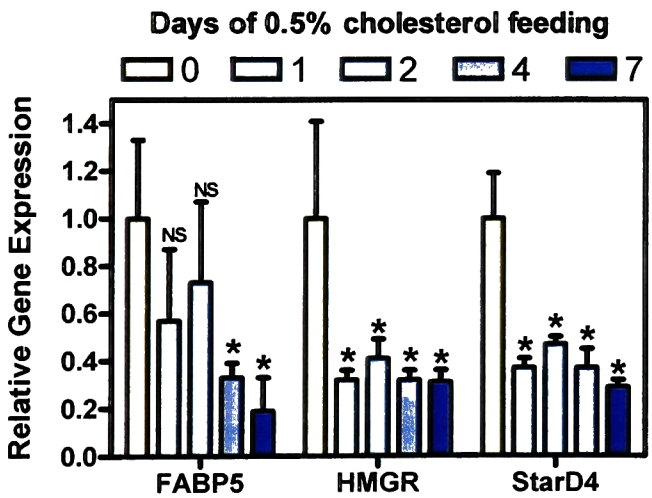

Figure 2.7: StarD4 regulation in a time course of cholesterol feeding. C57BL/6 male mice were fed a semisynthetic 0.5% cholesterol diet for the indicated number of days (n=4 mice per group). Liver RNA was analyzed for expression of FABP5, HMGR, and StarD4 by qPCR and normalized to cyclophilin. *P<0.05

A subfamily of START genes including StarD4, StarD5, and StarD6: BLAST searches against whole genome and EST databases identified 15 START domain-containing genes, which are described in the introduction. The START domain protein sequences were aligned to reveal some highly conserved amino acids across the entire family (Figure 2.8): Trp29, Trp79, Arg114, Asp/Glu115, and Arg147 (based on human StarD4 numbering). Notably, we

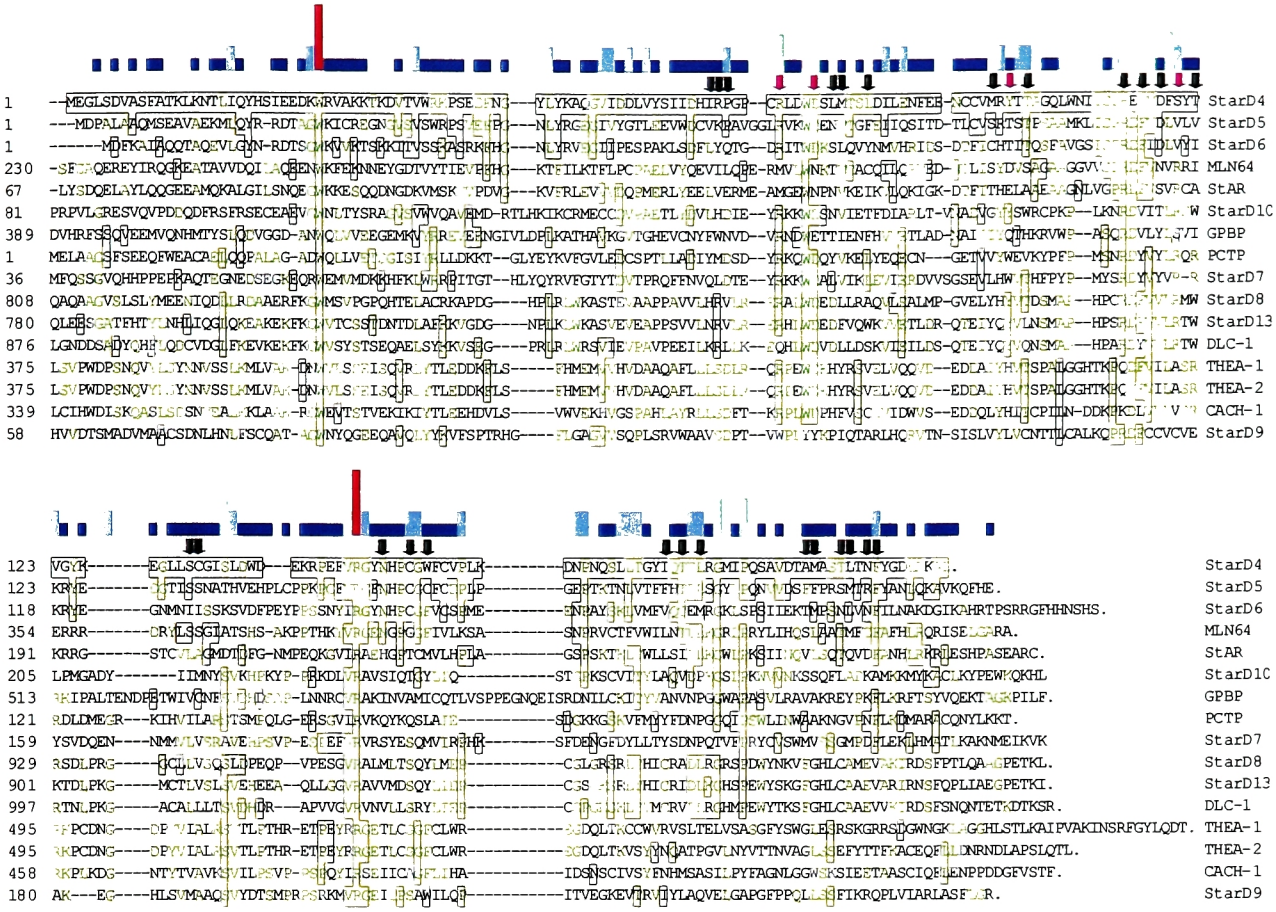

Figure 2.8: Multiple alignment of human START domains.

The amino acid sequence of 16 human START domains (15 genes, 2 splice variants of THEA) were aligned using ClustalW. The colored bars above the alignment indicate positions with strong consensus. Amino acid agreements with StarD4 are boxed, while agreements with consensus are colored yellow. The black arrows indicate residues that contribute side chain atoms to the lipid binding based on the mouse StarD4 X-ray crystal structure. The violet arrows indicate positions with charged residues that form salt bridges in the predominantly hydrophobic cavity.

found two other novel START proteins, subsequently named StarD5 and StarD6, which were highly similar to StarD4. In a phylogenetic analysis, these three proteins clearly form a subfamily among START proteins, with the most related subfamily containing the known cholesterol-binding proteins StAR and MLN64 (Figure 2.9a). Comparing each protein sequence pairwise, StarD4, StarD5, and StarD6 are ~30% identical; they share ~20% identity with StAR and MLN64, and less identity to other START subfamilies (Figure 2.9b).

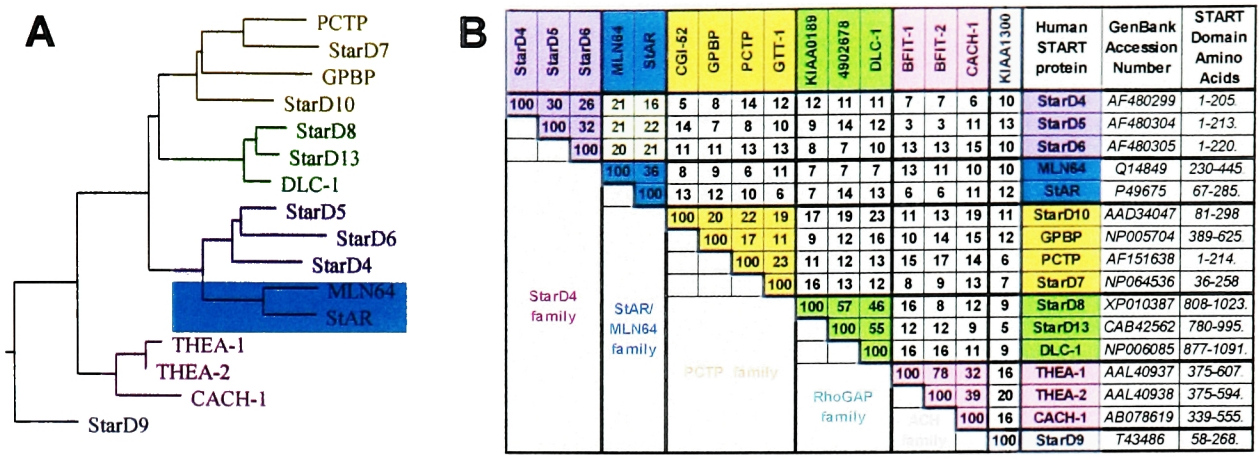

StarD4	StarD5	StarD6	MLN64	StAR	CGI-62	GPBP	PCTP	GTT-1	KIAA0189	4902678	DLC-1	BFIT-1	BFIT-2	CACH-1	KIAA1300	Human START protein	GenBank Accession Number	START Domain Amino Acids
100	30	26	21	16	5	8	14	12	12	11	11	7	7	6	10	StarD4	AF480299	1-205.
	100	32	21	22	14	7	8	10	9	14	12	3	3	11	13	StarD5	AF480304	1-213.
		100	20	21	11	11	13	13	8	7	10	13	13	15	10	StarD6	AF480305	1-220.
			100	36	8	9	6	11	7	7	7	13	11	10	10	MLN64	Q14849	230-445
				100	13	12	10	6	7	14	13	6	6	11	12	StAR	P49675	67-285.
					100	20	22	19	17	19	23	11	13	19	11	StarD10	AAD34047	81-298
						100	17	11	9	12	16	10	14	15	12	GPBP	NP005704	389-625
							100	23	11	12	13	15	17	14	6	PCTP	AF151638	1-214.
								100	16	13	12	8	9	13	7	StarD7	NP064536	36-258
									100	57	46	16	8	12	9	StarD8	XP010387	808-1023.
										100	55	12	12	9	5	StarD13	CAB42562	780-995.
											100	16	16	11	9	DLC-1	NP006085	877-1091.
												100	78	32	16	THEA-1	AAL40937	375-607.
													100	39	20	THEA-2	AAL40938	375-594.
														100	16	CACH-1	AB078619	339-555.
															100	StarD9	T43486	58-268.

Figure 2.9: Subfamilies of START domain containing proteins.

(A) A phylogenetic tree based on the multiple alignment reveals six subfamilies: PCTP-like (orange), RhoGAP domain-containing (green), the StarD4 subfamily (violet), StAR/MLN64 (blue), acyl CoA thioesterase domain-containing (pink), and StarD9 (gray). (B) The percent amino acid identity for each pairwise comparison. Yellow indicates the similarity between the StarD4 and StAR/MLN64 subfamilies.

The human and mouse sequences for StarD4, StarD5, and StarD6 were analyzed *in silico* using resources available publicly via the National Center for Biotechnology Information (www.ncbi.nlm.nih.gov) or commercially via Celera Genomics (www.celera.com). Full-length coding sequences, Unigene clusters, and chromosomal positions were determined (Table 2.2). The three genes do not reside together in a cluster, but the mouse and human orthologues for each gene reside in syntenic chromosomal regions. Based on the Online Mendelian Inheritance in Man (OMIM) database (Hamosh et al., 2002), none of these genes reside at known disease-associated loci. While there is only one copy per genome

	mStarD4	hStarD4	mStarD5	hStarD5	mStarD6	hStarD6
GenBank Accession	AF480297-8	AF480299	AF480302	AF480304	AF480303	AF480305
Unigene cluster	Mm.23344	Hs.162205	Mm.25702	Hs.172803	Mm.83623	Hs.374669
Celera gene	mCG21663	hCG37443	mCG8260	hCG27342	mCG9256	hCG1643548
Chromosome	18	5q22	7	15q26	18	18q21
Genetic Map	12 cM	116-121 cM	41 cM	72-77 cM	44 cM	71-83 cM
mRNA length	~5.5 kb	~5.5,4.5 kb	~3.0,1.5 kb	~3.0,1.5 kb	~1.5 kb	~1.5 kb
ORF length	675 bp	618 bp	642 bp	642 bp	702 bp	663 bp
Protein length	224 aa	205 aa	213 aa	213 aa	233 aa	220 aa

Table 2.2: Gene information for StarD4, StarD5, and StarD6 from mouse and human

of StarD4 and StarD5, there is a mouse StarD6 gene with introns on chromosome 18 and a nearly identical intron-less sequence on chromosome 10, likely a processed pseudogene. Mouse StarD6 ORF PCR primers in different exons amplified a strong ~700 bp product from testis cDNA as well as genomic DNA (Figure 2.10), confirming the presence of this intron-less sequence.

Figure 2.10: Evidence for a mouse StarD6 processed pseudogene.
Primers that amplify the mouse StarD6 coding sequence detect this sequence in testis cDNA as well as genomic DNA, but not in a negative control reaction without template.

To determine the exonic organization of each gene, cDNA contigs and genomic sequences were aligned to reveal introns that followed the GT-AG rule. The StarD4 subfamily genes were remarkably similar, with most splice junctions conserved (Figure 2.11). The exonic organization is different for other START genes, supporting a distinct StarD4 subfamily. Mouse StarD4 has 12 amino acids encoded by exon 1, but this exon is non-coding in human StarD4 and there are no corresponding sequences in StarD5 or StarD6. Upstream in-frame stop codons allowed identification of initiator codons in StarD4 and StarD6. No upstream stop codons were found in StarD5, but there were no upstream exons in over 180 mouse and human Unigene ESTs, indicating the first ATG was the start codon. The mouse StarD6 mRNA has a long, multi-exon 5' UTR with multiple initiation codons, and such upstream AUGs may function as regulators of translation (Morris and Geballe, 2000). While most other START proteins have additional N-terminal domains, StarD4, StarD5, and StarD6 are 205-233 amino acid proteins consisting almost entirely of START domains.

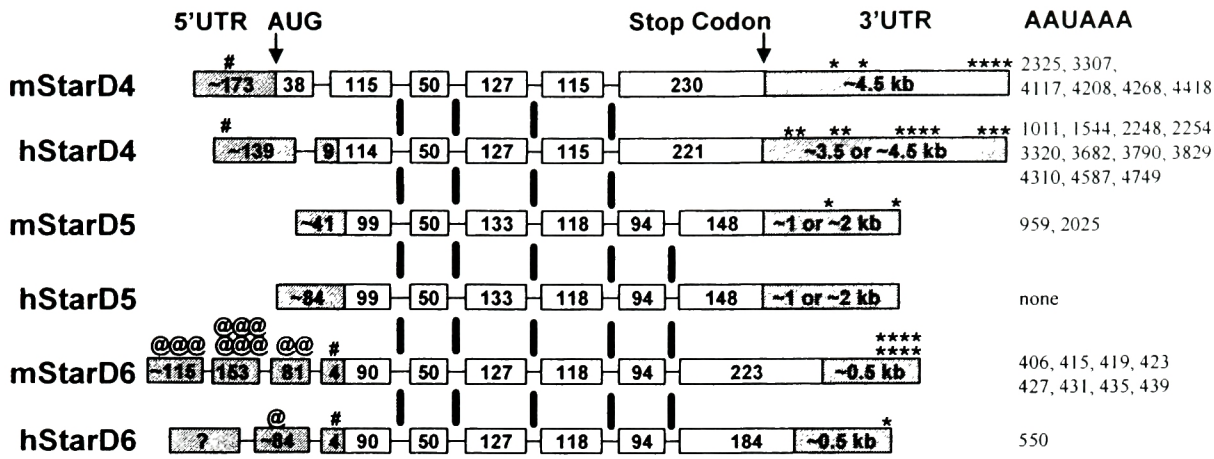

Figure 2.11: Exonic organization of StarD4, StarD5, and StarD6.

Exons for the mouse and human genes, represented as boxes with lengths in nucleotides, were determined by alignment of cDNA with genomic DNA. Vertical bars show splice junctions that are conserved among the genes. Coding sequences are white and untranslated regions (UTR) are gray. The 5' UTR lengths were based on the longest 5' sequences in each Unigene cluster, while the 3' UTR lengths were estimated based on Northern blot mRNA sizes (Table 2.2). The symbols are: #, first upstream in-frame stop codon in 5' UTR; @, upstream AUG codon in 5' UTR; *, poly-A signal (AAUAAA) in the 3' UTR. The distance from the stop codon for each poly-A signal is indicated at the far right. The 5' end of hStarD6 was uncertain based on very little available sequence data.

Tissue expression of StarD5 and StarD6: StarD5 and StarD6 ORFs were RT-PCR amplified and cloned from mouse liver and testis, respectively, and used to probe multiple tissue Northern blots. Like StarD4, StarD5 mRNA was most abundant in liver and kidney, but detectable in all tissues tested (Figure 2.12a). In contrast, StarD6 expression was restricted to testis in both mice and humans, and expression was not detected in the ovary (Figure 2.12b-c). Whereas the predominant StarD4 transcript was ~5.5 kb (see Figure 2.5), there were two major StarD5 transcripts at ~3 kb and ~1.5kB. StarD6 Northern blots consistently gave a wide band at ~1.5 kb, suggesting multiple transcripts around this length. These mRNA lengths revealed by Northern (Table 2.2) are consistent with the positions of AAUAAA polyadenylation signals in the 3' UTRs (see Figure 2.11), and multiple messages appear to represent alternative sites of RNA polyadenylation and cleavage.

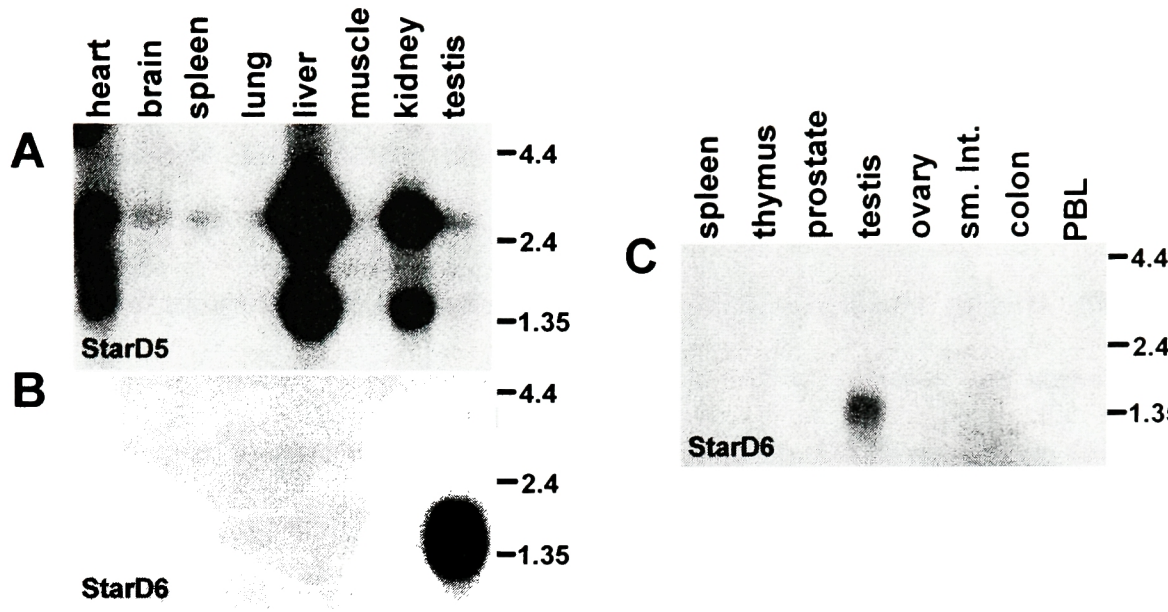

Figure 2.12: Multiple tissue Northern blots of StarD5 and StarD6.

(A) Mouse blot hybridized with mouse StarD5 ORF probe. (B) Mouse blot hybridized with mouse StarD6 ORF probe. (C) Human blot hybridized with mouse StarD6 ORF probe (sm. int.=small intestine, PBL=peripheral blood leukocyte).

Since StarD5 showed similar tissue distribution to StarD4, we measured its expression by qPCR in control and cholesterol-fed mouse livers. In this experiment, we also assayed MLN64, a widely expressed cholesterol-binding START protein, but not StAR and StarD6, which are not expressed in liver. Neither StarD5 nor MLN64 expression was regulated in mouse liver upon cholesterol feeding, while StarD4 was decreased as expected (Figure 2.13).

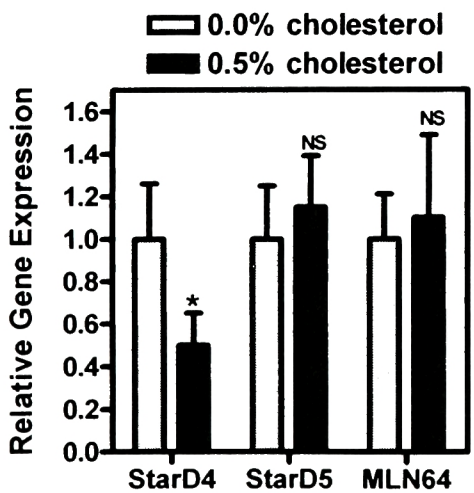

Figure 2.13: Dietary cholesterol does not affect liver StarD5 or MLN64 expression.

C57BL/6 mice were fed a semisynthetic diet with 0.00% or 0.50% cholesterol (w/w) for one week before extraction of liver RNA (n=5 per group). Expression of StarD4, StarD5, and MLN64 was assayed by quantitative RT-PCR and normalized to cyclophin A. *P<0.05, NS=not significant vs. 0.0% cholesterol.

Purification and crystallization of recombinant mouse StarD4 protein: In collaboration with Michael Romanowski and Stephen Burley at Rockefeller University, we sought to express recombinant StarD4 in bacteria and solve its X-ray crystal structure. We cloned and sequence-verified the mouse (C57BL/6 strain) StarD4 ORF as an in-frame fusion with glutathione S-transferase (GST) in a lac-inducible bacterial expression plasmid. When bacteria were transformed and induced with IPTG, a ~55 kD protein was expressed, consistent with the predicted molecular weight of the GST-StarD4 fusion protein (Figure 2.14a, arrow).

A summary of the subsequent purification of StarD4 is shown in Figure 2.14b. When bacteria were lysed (lane 1), most GST-StarD4 was soluble in the supernatant (lane 2). Fast performance liquid chromatography (FPLC) was performed against a glutathione affinity column, and most proteins flowed through (lane 3) while the ~55 kD GST-StarD4 bound the column and was eluted (lane 4). Next, the GST moiety (~30 kD) was cleaved from StarD4 (~26 kD) to give two bands (lane 5). To separate GST, a second FPLC was performed with a glutathione affinity column, and StarD4 flowed through (lane 6). After dialysis, an insoluble pellet formed that contained some StarD4 as well as contaminating proteins that were not previously apparent (lane 7). The supernatant of this dialysis contained StarD4 and a higher molecular weight contaminant (lane 8), so preparative high performance liquid chromatography (HPLC) was performed against an anion exchange column (lanes 9). StarD4 eluted as a compact peak (Figure 2.14c) that was isolated as the ~26 kD purified protein (lane 10), smaller than ~30 kD GST as predicted (lane 11). By matrix-associated laser desorption mass spectrometry (MALDI-MS), the purified protein was 25957 Da, compared to the predicted 25891 Da. This difference of 66 Da was likely within the error of the measurement, so further MS analysis was not pursued.

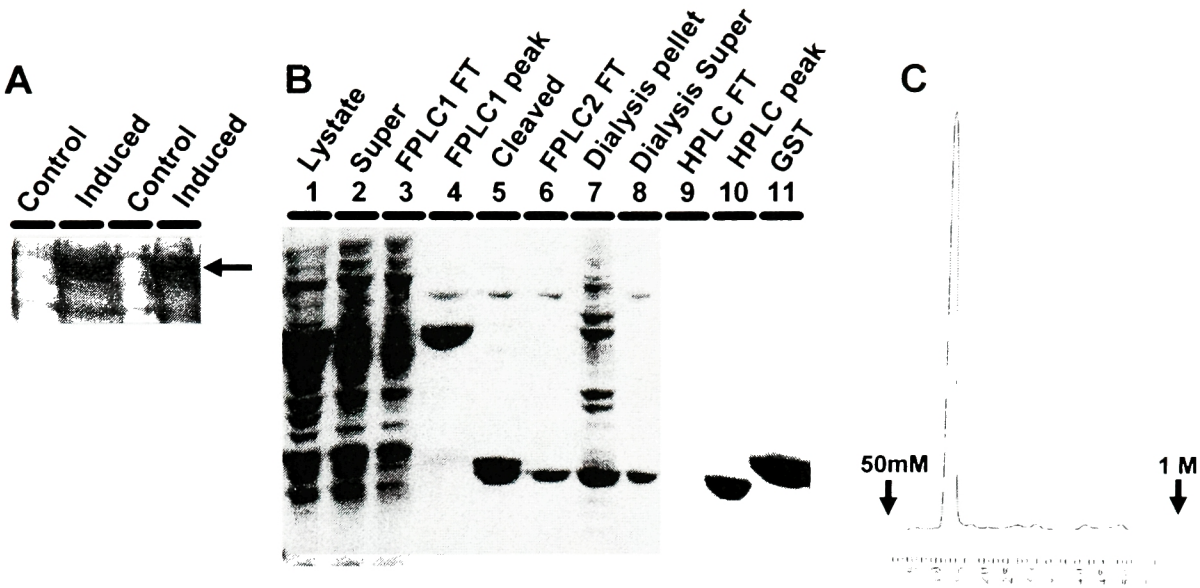

Figure 2.14: Expression and purification of recombinant mouse StarD4 protein.
(A) Bacteria were transformed with an inducible expression plasmid for GST-fused StarD4. Whole cell lysates were run on SDS-PAGE and stain with Coomassie blue. Induced cells show a ~55kD protein (arrow) consistent with GST-StarD4. (B) Coomassie gel summarizing the purification of recombinant mouse StarD4, see text for details. (C) On sepharose Q anion exchange HPLC, a sharp StarD4 peak eluted between 230-297mM KCl.

To determine whether StarD4 is a monomer or a multimer in solution, we performed gel filtration of the purified protein. Relative to monomeric standards of 25, 43, and 67 kD (Figure 2.15a), the peak for StarD4 elution was at 56.4 mL near the 25kD marker (Figure 2.15b-c). Based on the standard curve (Figure 2.15d) StarD4 had an apparent M.W. of 26.8 kD, consistent with the predicted monomeric M.W. of 26.0 kD. The StarD4 peak did show a slight shoulder to the left, indicating some higher order structures like dimers and trimers, such as the faint band visible at 49 mL elution volume (Figure 2.13b-c), but these accounted for quantitatively very little of the total StarD4. Therefore, StarD4 behaves predominantly like a monomer in solution.

To obtain crystals of StarD4 protein, we subjected it to a standard screen of crystallization solutions. In one condition, disordered crystals formed within an hour (Figure 2.14a). To obtain more suitable crystal morphology, we optimized the temperature (4°C was better than room temperature), pH (0.1 M sodium cacodylate pH 6.5 gave crystals, but pH

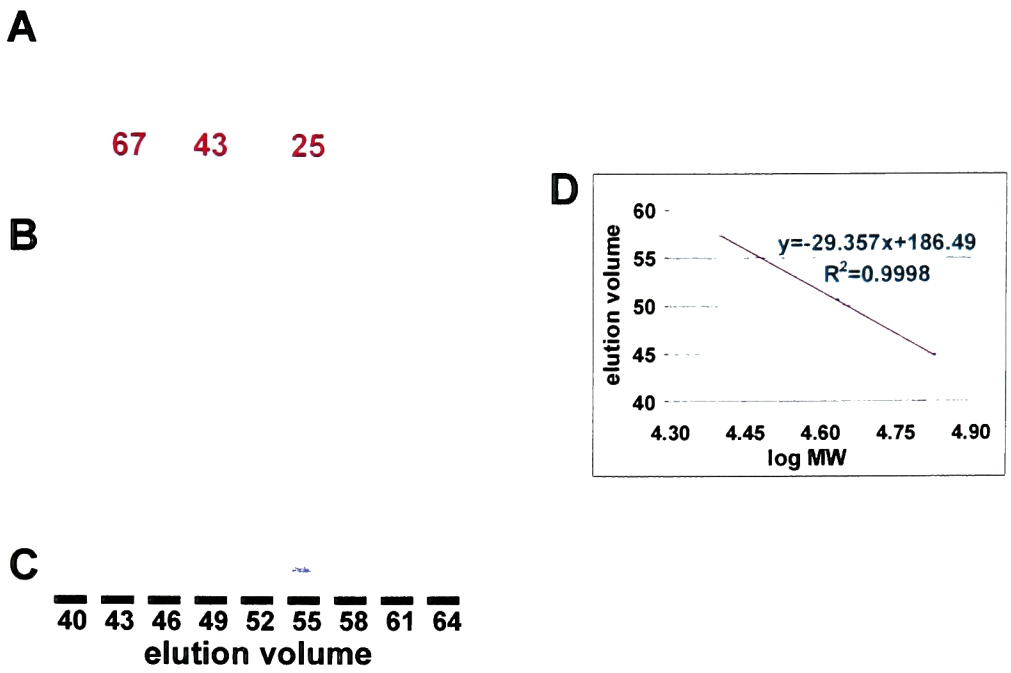

Figure 2.15: Gel filtration of recombinant mouse StarD4.

(A) Tracing of absorbance at 280 nm (A280) for three monomeric standards (67, 43, 25 kD) run over a GF75 size exclusion chromatography column. (B) A280 elution profile of recombinant StarD4, with the peak at 56.6 mL. (C) SDS-PAGE gel of fractions collected each 3 mL. (D) Based on this standard curve, StarD4 had a molecular weight of 26.8 kD, consistent with the predicted monomer of 26.0 kD.

5.6 or 7.5 did not), salt (0.2 M magnesium acetate but not 0.0 or 0.3 M), polyethylene glycol 8000 (11% was best), glycerol (22% was best, Figure 2.14b-d), and time of growth (2 days was best). The final crystals were hexagonal rods with excellent morphology (Figure 2.16e). When crystallization was attempted in the same conditions with 1 μg/ml cholesterol in 0.1% ethanol, the morpholgy deteriorated to crystals with splintered ends (Figure 2.16f).

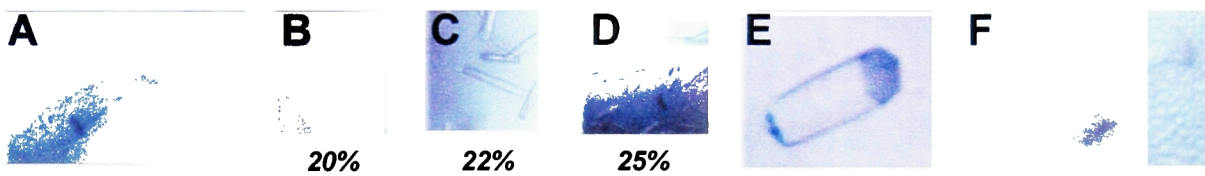

Figure 2.16: Optimization of mouse StarD4 crystallization conditions.

(A) Purified mStarD4 formed disordered crystals in one condition of a standard crystal screen. Crystallization conditions were subsequently optimized. (B-D) Optimization of glycerol concentration, in which 22% gave the most ordered crystals. (E) Higher magnification image of a StarD4 crystal in the optimal crystallization solution. (F) When 1 μg/ml cholesterol in 0.1% ethanol (final concentrations) was added to this solution, crystal morphology deteriorated.

Subsequent studies of PCTP by others showed that lipid vesicles were necessary to load a recombinant START protein with lipid ligand before crystallalization (Roderick et al., 2002).

The StarD4 X-ray crystal structure: Michael Romanowski collected diffraction data from optimized seleno-methionine StarD4 crystals and solved the X-ray crystal structure of StarD4 at 2.2 Å resolution (Romanowski et al., 2002). The StarD4 secondary structure (Figure 2.17a, 2.18a) consists of an N-terminal α-helix (αA, dark blue), 3 β-strands (β1-3, light blue), 2 shorter α -helixes (αB and αC, cyan), seven β-strands (β4-10, green, yellow, and orange), and a long C-terminal α-helix (αD, red). The ten β-strands form an antiparallel twisted β-sheet, making a U-shaped cavity with the C-terminal α-helix acting as a lid (Figure 2.17b). The N-terminal 23 amino acids of mouse StarD4, 17 of which are absent in human StarD4 (see above), were disordered and not part of the crystal structure. Amino acids highly conserved among the whole START protein family (see Figure 2.8) tended to occur at junctions in the secondary structure: Trp45 right before β1, Trp95 at the end of αC, and Arg130 at the start of β6. The StarD4 structure is very similar to that solved for MLN64 (Figure 2.17c, 2.18). The root mean squared deviation (RMSD) for the two α-carbon

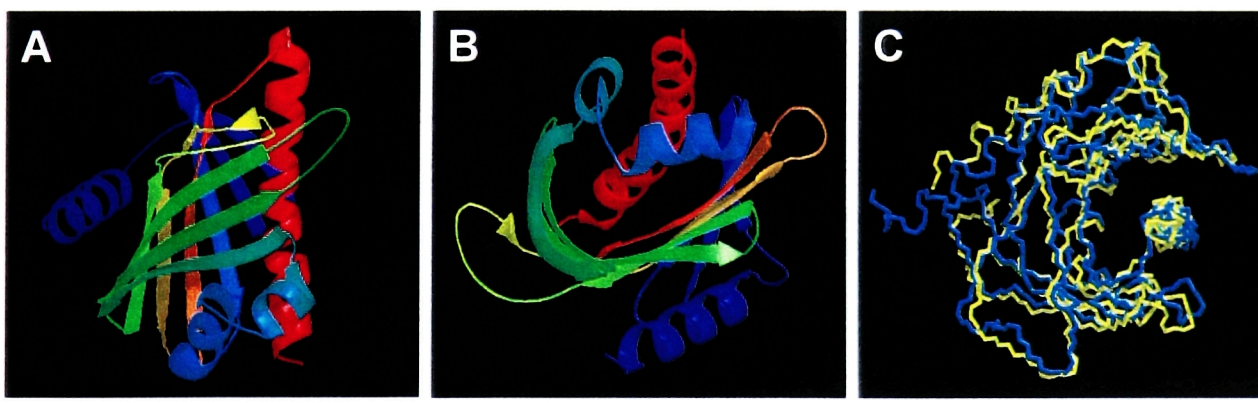

Figure 2.17: Overview the StarD4 X-ray crystal structure

(A-B) Ribbon diagrams of the StarD4 structure in two orientations, with the N-terminus blue and the C-terminus red. (C) Backbone tracing of the previously solved MLN64 START domain structure (blue) (Tsujishita and Hurley, 2000) superimposed with StarD4 (yellow).

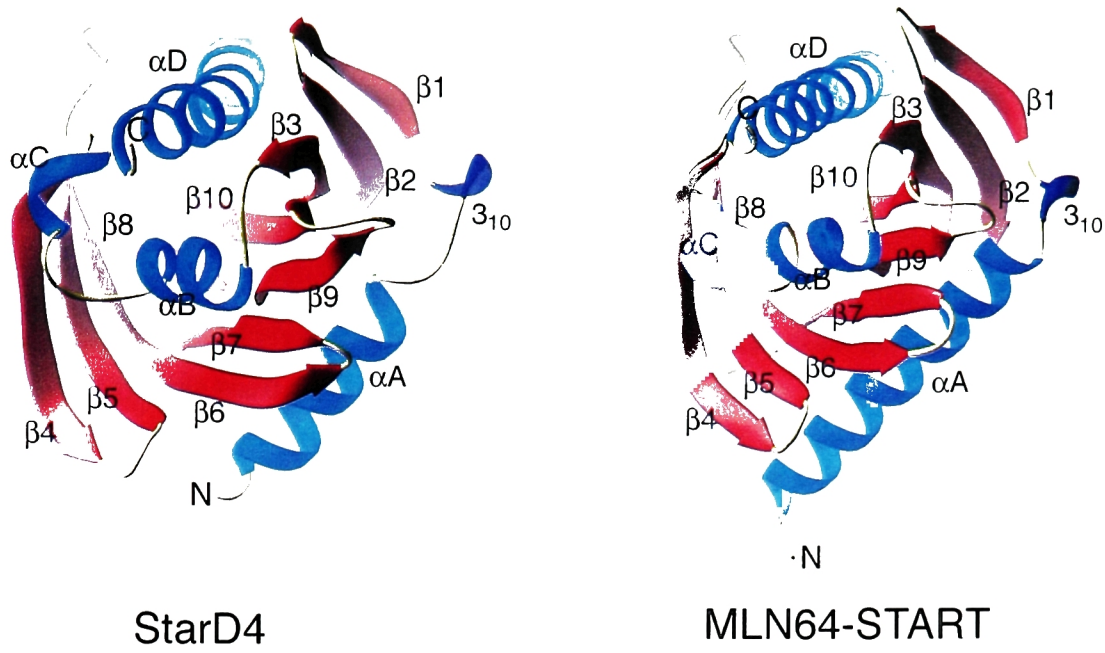

Figure 2.18: StarD4 and MLN64 have similar START structures

Despite sharing only 21% amino acid identity, mouse StarD4 and the human MLN64 START domain have the same secondary structure elements and protein fold.

backbones was 1.7 Å. The compact globular START domain fold has been classified as a helix-grip fold, since the C-terminal α-helix is "gripped" by the folded β-sheet.

The key feature of the START structure is the cavity lined by predominantly hydrophobic residues (Figure 2.19a), also called the lipid-binding tunnel since there are two small openings accessible to the outside. Hydrophobic lipids bind in this cavity, as phosphatidylcholine was co-crystallized with PCTP (Roderick et al., 2002). The volume of the MLN64 cavity was previously reported as ~1900 $Å^3$, but Michael Romanowski showed that this calculation was in error and measured the correct cavity volumes for StarD4 and MLN64 as 847 +/- 106 $Å^3$ and 848+/- 107 $Å^3$, respectively. This volume is consistent with the binding of one cholesterol molecule, which is reported to occupy 741 $Å^3$ (Schroeder et al., 1993). The cavities of StarD4 and MLN64 were similar overall in size and shape (Figure 2.19b), and cholesterol could be modeled into either cavity in two orientations (Figure 2.19c).

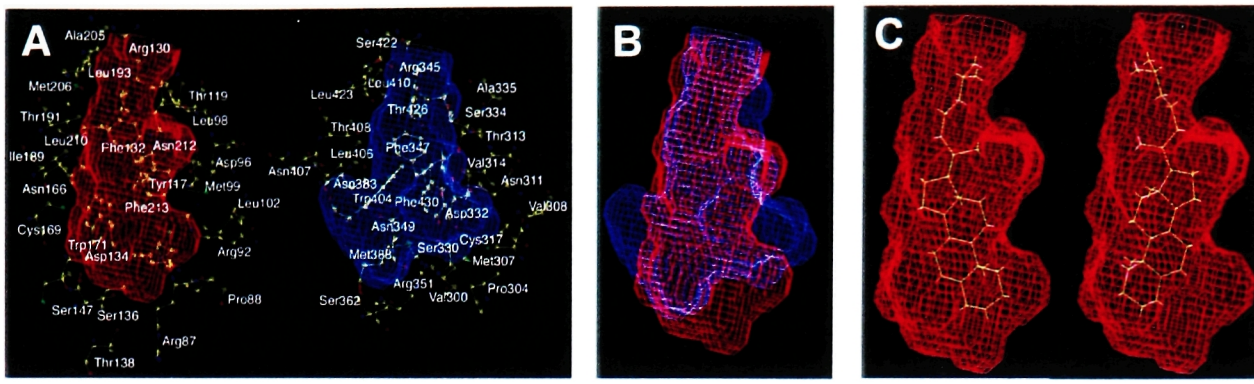

Figure 2.19: The StarD4 lipid binding cavity.

(A) Cavity volume plots for StarD4 (red) and the MLN64 START domain (blue), with cavity-lining amino acid residues shown. (B) Superposition of the StarD4 and MLN64 cavities. (C) Cholesterol (yellow) can be modeled in two orientations into the StarD4 cavity.

The residues lining the cavity are predominantly hydrophobic, though there are some polar and even charged side chains. For example, at the C-terminus of StarD4 both β9 and αD contribute side chains to the cavity, and these residues are more hydrophobic than those that face the surface (Figure 2.20a-b). Indeed, the C-terminal αD appears to be an amphipathic helix with a polar face and a non-polar face (Figure 2.20c), and amphipathic helices in apolipoproteins have been strongly implicated in membrane binding and lipid extraction (Saito et al., 2003). It is thought that ligand specificity arises from the amino acid side chains that contribute atoms to the cavity lining. In this regard, we attempted

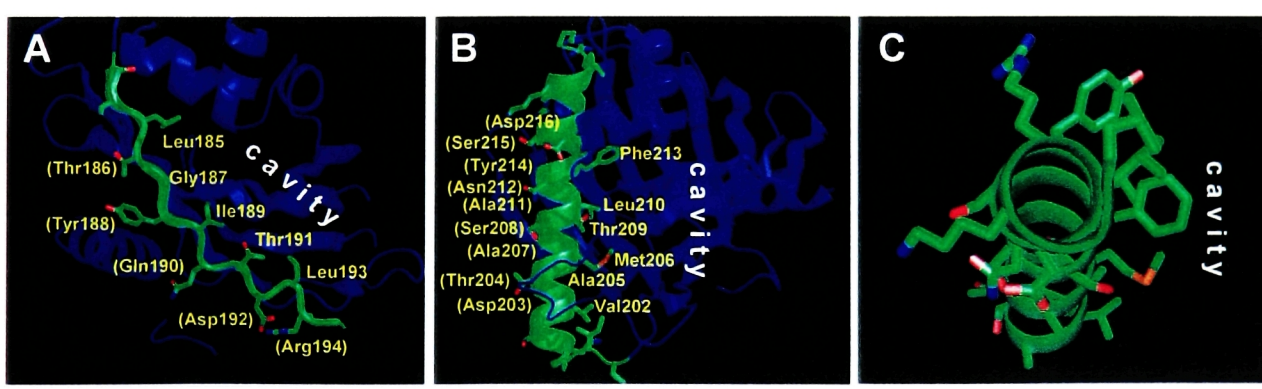

Figure 2.20: Examples of hydrophobic amino acids lining the StarD4 lipid-binding cavity.

On β-sheet 8 (A) and α-helix D (B) of StarD4, the residues facing the cavity are generally more hydrophobic than those facing the surface. (C) α-helix D appears to be an amphipathic helix with polar and non-polar faces.

comparisons of the cavity-lining residues in the structures of StarD4, MLN64, and PCTP StarD4 agreed with the cholesterol-binding MLN64 at some positions, but with PCTP at others, and many positions were divergent among the three. When these comparisons were extended to other START domains with unknown ligands, the analysis was further complicated (see arrows in Figure 2.8). No patterns were apparent in the conservation of cavity residues, except for four positions involving charged amino acid residues that form salt bridges.

In the short αC helix of StarD4, the charged side chains of Arg92 and Asp96 are within 2.9Å of each other and form a salt bridge (Figure 2.21a), while the corresponding positions in MLN64 are uncharged side chains, Met307 and Asn311. On the START protein multiple alignment, only StAR and MLN64 proteins have Met-Asn at this position, while most others have the Arg-Asp salt bridge (Figure 2.21b). Therefore, these positions were previously proposed as "likely lipid specificity determinants," with the Met-Asn pair determining cholesterol binding while the Arg-Asp salt bridge could help bind other lipids (Tsujishita and Hurley, 2000). We disagree with this prosposal, which predicts that the StarD4 subfamily would not bind sterols. (Chapter 4 presents data that strongly implicate StarD4 and StarD5 in intracellular cholesterol metabolism.) The second difference is the salt bridge in MLN64 between β5 and β6, Asp332 and Arg351. StAR has a corresponding Glu-Arg salt bridge, while no other START domains have this charge pair (Figure 2.21b). Five START domains have only the Arg, perhaps resulting in an unbalanced positive charge in the lipid binding pocket. In summary, StAR and MLN4 are the only START domains with a salt bridge between β5 and β6, while most other START domains including the StarD4 subfamily have a salt bridge in αC that is absent in StAR/MLN64. We describe experiments in Chapter 4 that test the functional relevance of these salt bridges.

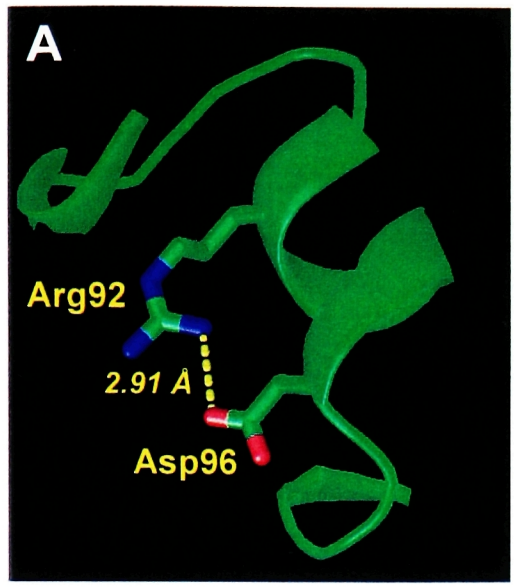

B

	αC 92	αC 96	β5 117	β6 136
StarD4	Arg	Asp	Tyr	Ser
StarD5	Arg	Asp	Thr	Val
StarD6	Arg	Asp	Thr	Val
StAR	Met	Asn	Glu	Arg
MLN64	Met	Asn	Asp	Arg
PCTP	Arg	Asp	Trp	Arg
StarD7	Arg	Asp	Trp	Arg
StarD10	Arg	Asp	Tyr	Arg
GPBP	Arg	Glu	Gln	Ser
DLC-1	Gln	Asp	Tyr	Arg
StarD8	Arg	Asp	Tyr	Arg
StarD13	Arg	Asp	Tyr	Arg
THEA	Arg	Asp	His	Ala
CACH	Arg	Asp	His	Val
StarD9	Trp	Tyr	Leu	Cys

Figure 2.21: Salt bridges in START domain lipid binding cavities.

(A) The StarD4 structure shows a salt bridge between two charged side chains on α-helix C. (B) MLN64 lacks charged residues these positions (corresponding to amino acids 92 and 96 in mouse StarD4), but has a different salt between charged residues on β-sheets 5 and 6 (corresponding to StarD4 117 and 136). These salt bridge positions were compared for all 15 START domains. Positive residues are blue, negative are red, and neutral are black.

The C. elegans gene K02D3.2: In our analysis of the START gene family in non-mammalian genomes (see Figure 1.8), we noted one putative StarD4 subfamily member, named K02D3.2, in the nematode worm *C. elegans*. As annotated in WormBase (Harris et al., 2003) by computer algorithms, the predicted K02D3.2 protein had 60 extra amino acids (positions 40-100) that failed to align with other START domains. This excess sequence was encoded by predicted exon 2 and the start of exon 3. Since there were no cDNA sequences for K02D3.2 described in EST databases, we hypothesized that the splice junctions may have been mis-annotated. PCR primers in exons 1, 3, 6, and 8 of the predicted gene (Figure 2.21a) were used to amplify K02D3.2 from a *C. elegans* cDNA library. The forward primer at the end of predicted exon 3 gave the expected PCR products, but PCR products from the exon 1 forward primer were ~200 bp shorter than predicted (Figure 2.21b). Cloning and sequencing of these PCR products confirmed that the annotated second and third exons were incorrect,

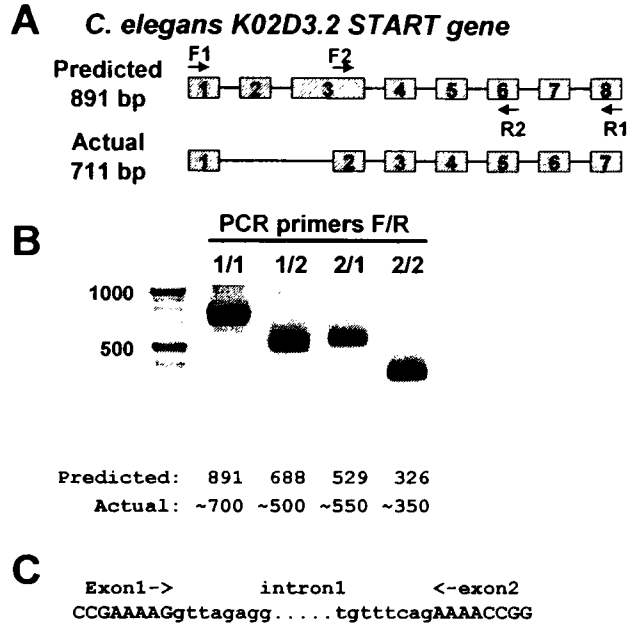

D

StarD4	18%
StarD5	23%
StarD6	17%
StAR	12%
MLN64	4%
PCTP	14%
StarD7	15%
StarD10	12%
GPBP	9%
DLC-1	10%
StarD8	8%
StarD13	11%
THEA2	9%
CACH	5%
StarD9	10%

Figure 2.22: cDNA cloning of the *C. elegans* StarD4 subfamily member K02D3.2.
(A) K02D3.2 was annotated as an 8 exon gene with an 891 bp ORF, but the encoded START domain would be interrupted by non-START amino acid sequence. Forward (F1 and F2) and reverse (R1 and R2) PCR primers were used to clone the K02D3.2 cDNA. The actual gene encodes a typical START domain via 7 exons and a 711 bp ORF. (B) RT-PCR results. (C) The correct splice junction between exons 1 and 2 of K02D3.2. (D) K02D3.2 protein sequence was aligned with the 15 human START domains, and the percent identity for each pairwise comparison is shown.

with 180 extra nucleotides not present in the actual mRNA. The correct exonic organization and the exon 1 to exon 2 splice junction are shown (Figure 2.21a, c).

K02D3.2 appears to encode a 236 amino acid protein consisting entirely of a START domain. While additional exons upstream of the predicted first exon cannot be ruled out, there is an in-frame stop codon at -42 from the ATG in genomic sequence. Since the forward primer starting at +1 in the ORF amplified PCR products with either reverse primer, we attempted PCRs with two additional forward primers. One was at -68 to -44 from the ATG, and the other was splice leader 1 (SL1), a 22 nucleotide sequence that is *trans*-spliced to the 5' ends of 60% of worm mRNAs (Ferguson et al., 1996). Both of these primers failed to amplify K02D3.2 product (data not shown), suggesting that its 5' UTR does not extend to -68 from the ATG and is not modified with SL1. The predicted K02D3.2 protein was

compared to the 15 mammalian START domains by multiple alignment, and it showed 23% identity to StarD5, 18% to StarD4, 17% to StarD6, and less identity to other START domains (Figure 2.21d).

***Expression of a K02D3.2 GFP reporter in* C. elegans:** Since worms have only one member of the StarD4 subfamily, K02D3.2 may be functionally orthologous to one of the three mammalian genes. K02D3.2 could thus show similar regulated gene expression to StarD4 (cholesterol-regulated), StarD5 (ER stress-regulated as described in Chapter 3), or StarD6 (sperm-specific as described in Chapter 5). To test this hypothesis, we generated reporter worms expressing GFP under control of the K02D3.2 regulatory elements.

A 2.8 kB fragment of K02D3.2, spanning from the 5' flanking region (-2700 from the ATG, just downstream of the preceding gene, tRNA K11E4.t1) into the first exon, was cloned by PCR from genomic DNA. This fragment was subcloned as a GFP reporter, such that a fusion protein between the first 38 amino acids of K02D3.2 and GFP was expressed. In collaboration with Elliot Perens and Shai Shaham, we microinjected this construct into worms and generated lines carrying the reporter as an extrachromosomal array. The GFP reporter showed strong expression in the hypodermal seam cells in embryos (starting at the 3-fold stage, Figure 2.23c), early and late larvae (Figure 2.22a-b), but not adult worms (data not shown). Seam cells are present in pairs bilaterally along the sides and secrete cuticle that coats the worm. No other cell types showed detectable reporter expression.

We grew K02D3.2 reporter worms on media lacking cholesterol, which would induce expression of a sterol-regulated gene like mammalian StarD4, or containing tunicamycin, which would induce expression of an ER-stress regulated gene like mammalian StarD5. However, these treatments had no effect on reporter expression, which remained strong in embryonic and larval seam cells but absent in adults (data not shown). Since the K02D3.2

reporter was not expressed in male germ cells like StarD6, nor regulated like StarD4 or StarD5, it does not appear to be a clear orthologue for any of the three mammalian genes.

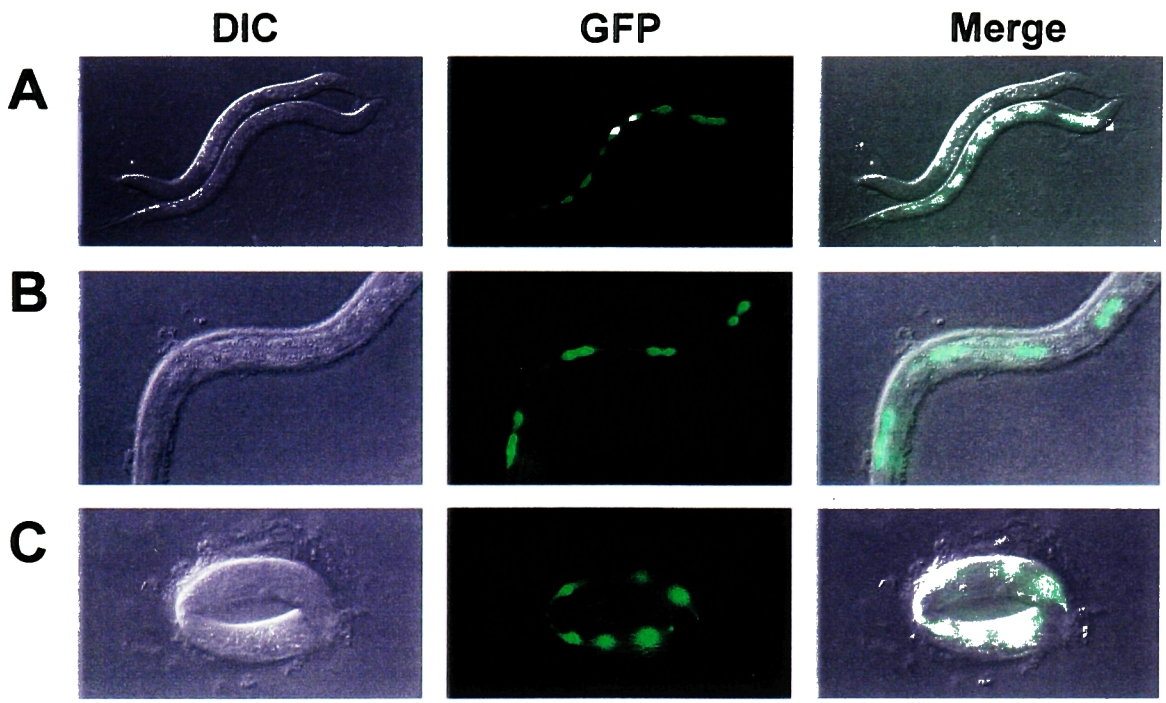

Figure 2.23: Expression of a K02D3.2 promoter GFP reporter in *C. elegans*.

A GFP reporter driven by the K02D3.2 5' flanking region was microinjected into *C. elegans* and maintained as an extrachromosomal array. Worms were imaged by differential interference contrast (DIC) and fluorescence compound (GFP) microscopy. Adult worms showed no reporter expression. (A) An L1/L2 larva shows reporter expression along its lateral side in a string of about ten cells, identified as seam cells based on morphology and location. Paired GFP-expressing seam cells were present on the opposite side. (B) A close-up image of an L3/L4 larva, showing pairs of seam cells that recently divided. (C) Seam cell reporter expression in an embryo at the three-fold stage.

Chapter summary: This chapter describes the initial discovery of StarD4 using microarrays, as StarD4 expression in mouse liver was down-regulated by cholesterol feeding. The X-ray crystal structure of StarD4 was solved, showing a predominantly hydrophobic lipid-binding cavity like other START domain structures. Analysis of genomic and cDNA sequence databases identified the entire mammalian START gene family, including two close StarD4 homologues, StarD5 and StarD6. StarD4 and StarD5 were widely expressed with highest levels in the liver, but StarD5 was not cholesterol-regulated like StarD4. StarD6 expression was limited to the testis. *C. elegans* has one StarD4 subfamily gene, but a K02D3.2 GFP reporter did not show regulated expression like any of the three mammalian genes. Instead, this gene appeared specifically expressed in embryonic and larval seam cells

Chapter 3: Regulation of StarD4 and StarD5 Expression

StarD4 and StarD5 are not highly regulated during steroidogenesis: In steroidogenic cells, pituitary trophic hormones signal via cAMP and induce StAR expression to high levels (Stocco, 2001). When steroidogenesis was activated in MA-10 mouse Leydig tumor cells by a cAMP analog, StAR mRNA expression increased 45-fold as expected, while expression of MLN64 was unchanged (Figure 3.1). StarD4 was induced almost 3-fold, as was the SREBP target gene HMGR. The StarD4 induction by cAMP was similar to the induction in these cells by serum-free media (data not shown), a treatment well known to activate SREBPs. Activation of SREBP target genes in steroidogenesis likely reflects increased demand for *de novo* cholesterol synthesis, since cholesterol is the substrate for steroid production. StarD5 expression was unchanged upon steroidogenic stimulation, while StarD6 expression was undetectable in MA-10 cells (see Figure 5.1). Therefore, StAR is highly regulated by steroidogenic stimuli, but the StarD4 subfamily did not show similar regulation.

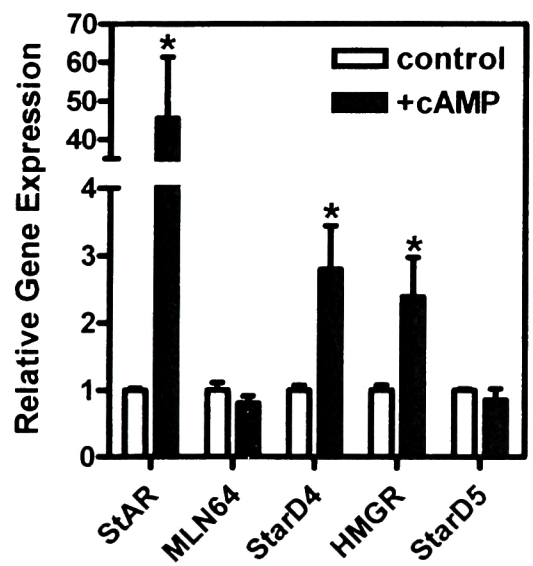

Figure 3.1: START domain gene regulation in steroidogenesis.
Mouse MA-10 Leydig tumor cells were cultured in control media or 8-bromo-cAMP (n=3 wells each) to stimulate steroid hormone production. After 20 hours, RNA was extracted and analyzed for gene expression by qPCR normalized to cyclophilin. *P<0.05 vs.control.

Regulation of StarD4 expression by sterols: StarD4 and StarD5 are also widely expressed in non-steroidogenic tissues, so we decided to study their regulation in the mouse NIH 3T3

fibroblasts. When these cells were cultured in 25-hydroxycholesterol and cholesterol (sterols) to repress SREBP activation, StarD4 expression decreased 4.3-fold compared to the control media (Figure 2.2a). 3T3 cells were also cultured in the drug mevinolin/lovastatin (statin) to inhibit cholesterol synthesis, deplete cellular cholesterol, and activate SREBPs. Statin treatment increased StarD4 expression 3.4-fold relative to control media and almost 15-fold relative to sterol-containing media. A similar pattern of gene regulation was observed for several known SREBP-target genes such as HMGR (Figure 3.2b). This is consistent with SREBP regulation of StarD4, while StarD5 and MLN64 showed no sterol regulation in NIH 3T3 cells (Figure 3.2c). Since the initial microarray experiment revealed StarD4 down-regulation by dietary cholesterol in mouse liver, we performed the same treatments in mouse Hepa-1 hepatoma cells. Again, StarD4 and HMGR mRNA levels were decreased by sterols and increased by statin, while StarD5 expression was not regulated (Figure 3.3).

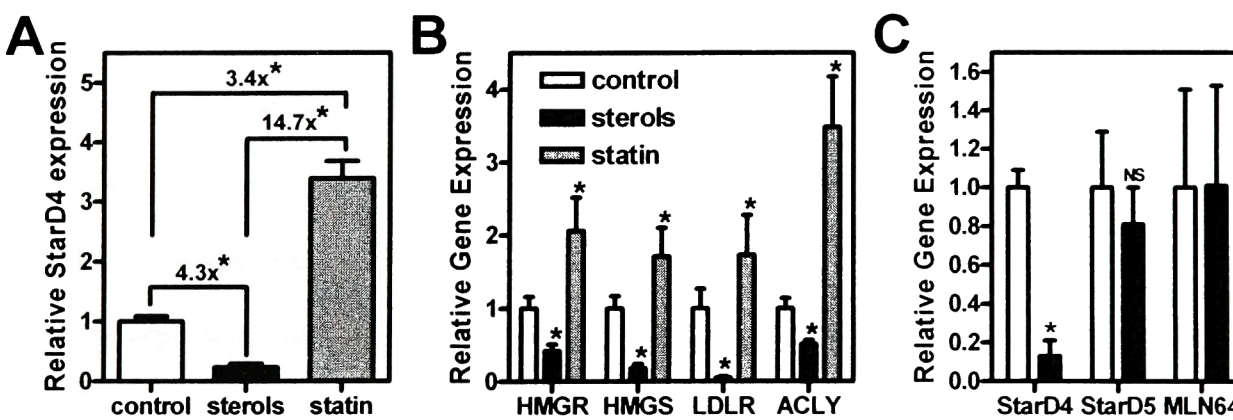

Figure 3.2: StarD4 is sterol-regulated in cultured 3T3 fibroblasts.

NIH 3T3 cells were cultured for 18-20 hours in three different media (n=4 wells each): control (DMEM with 10% lipoprotein-depleted serum), sterols (plus 1μg/mL 25-hydroxycholesterol and 10μg/mL cholesterol), or statin (plus 1μg/mL mevinolin/ lovastatin). RNA was extracted an analyzed for gene expression by qPCR normalized to cyclophilin. (A) Sterol-regulated expression of StarD4. (B) Sterol-regulated expression of other SREBP-target genes HMG CoA reductase (HMGR) and synthase (HMGS), the LDL receptor (LDLR), and ATP citrate lyase (ACLY). (C) Lack of sterol regulation for StarD5 and MLN64. *P<0.05 vs. control.

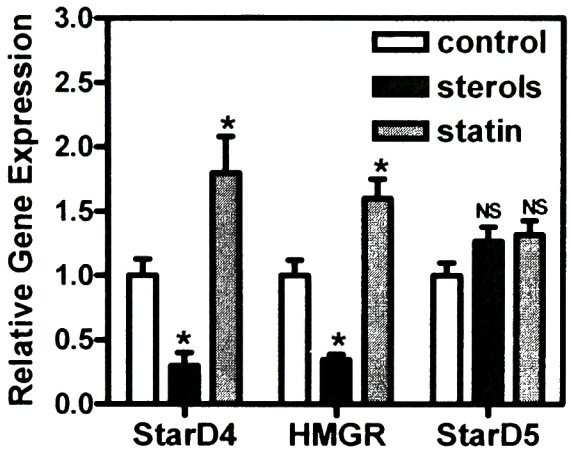

Figure 3.3: StarD4 is sterol-regulated in cultured Hepa-1 hepatoma cells.
Hepa-1 cells were cultured for 18-20 hours in the three media described above (n=3 wells each). RNA was extracted and analyzed for gene expression by qPCR normalized to cyclophilin. *P<0.05 vs. control.

StarD4 is induced in nSREBP transgenic mice: To confirm that StarD4 is a target for SREBP transactivation, we used transgenic mice overexpressing active truncated nuclear SREBPs (nSREBPs). These mice show constitutive activation of target genes: SREBP-1a preferentially activates genes involved in fatty acid synthesis and metabolism, while SREBP-2 preferentially activates genes involved in cholesterol metabolism (Horton et al., 2002). The SREBP-1 target fatty acid binding protein 5 (FABP5) (Maxwell et al., 2003) was strongly induced by nSREBP-1a and only weakly induced by nSREBP-2. The control SREBP-2 target HMG CoA synthase (HMGS) was strongly induced by SREBP-2 and also induced by SREBP-1a. Additional control SREBP-1 and SREBP-2 targets also showed this expected pattern of regulation (data not shown). Others have shown the same results by Northern blot for panels of SREBP targets, with cholesterol-related genes strongly upregulated by SREBP-2 and SREBP-1a, but lipogenesis-related genes only regulated by SREBP-1a (Amemiya-Kudo et al., 2002). StarD4 expression was induced five-fold in nSREBP-2 transgenics (P<0.01) but only two-fold in nSREBP-1a transgenics (P=NS) (Figure 3.4). This pattern of regulation is consistent with SREBP-2 regulation, so StarD4 is an SREBP-2 target likely to function in cholesterol metabolism.

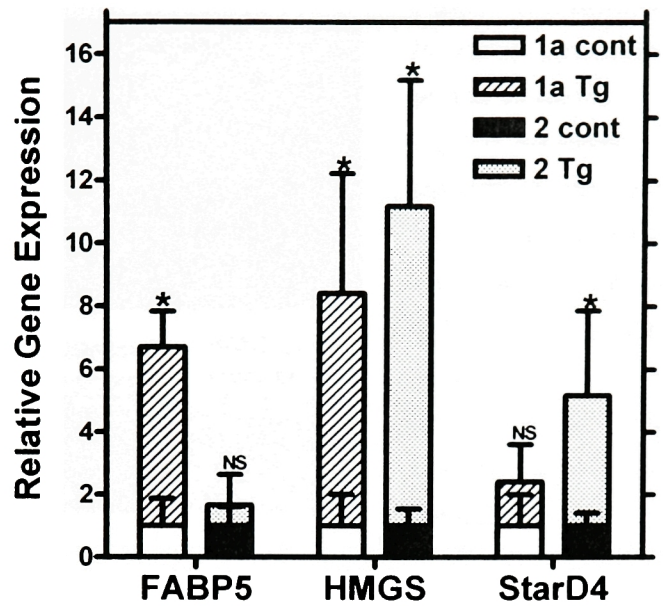

Figure 3.4: StarD4 expression is activated in nSREBP-2 transgenic mouse liver.
Expression of StarD4 and control genes was analyzed by qPCR in the livers nSREBP-1a and nSREBP-2 transgenic male mice (Tg) (n=5 per group) and compared to non-transgenic littermate controls (cont). Expression is normalized to β-actin, and expression in the wild type littermate controls was set equal to one for each gene. *P<0.05 vs. control, NS=not significant

Affinity-purified rabbit polyclonal antibodies against mouse StarD4 peptides were also generated. One antibody was against amino acids 52-67, including β2 and the loops that precede and follow it (Figure 3.5b), and this epitope was not conserved in StarD5, StarD6, or other START domains. In a Western blot from lysates of human embryonic kidney (HEK 293) cells, this antibody detected high molecular weight background bands but not a ~25 kD band representing StarD4. This probably indicates relatively low StarD4 expression in these cells, since the epitope was 100% conserved between mouse and human StarD4. When the cells were transfected with an expression plasmid for FLAG-tagged mouse StarD4, but not for other START proteins like PCTP, a band was detected at the predicted size (Figure 3.5a). A ~25 kD band was also detected in mouse liver extracts, and this band was clearly induced in the livers of nSREBP-2 transgenic mice (Figure 3.5c). Therefore, SREBP-2 activation in mouse liver results in increased StarD4 mRNA and protein.

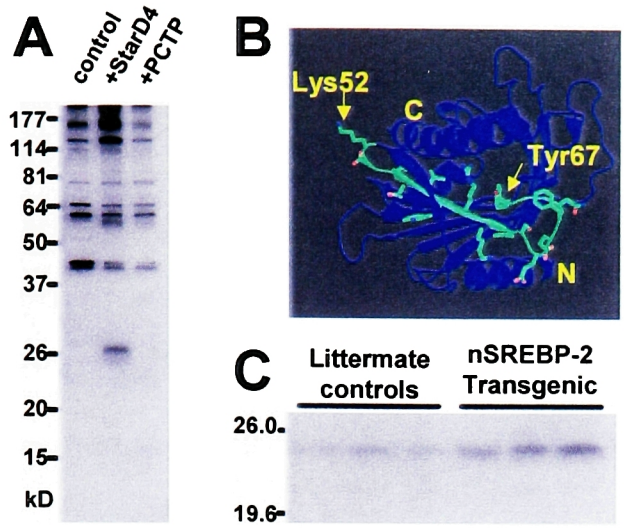

Figure 3.5: Anti-StarD4 antibody shows increased expression of the endogenous protein in nSREBP-2 transgenic liver.
(A) The polyclonal anti-StarD4 antibody was tested by Western blot on lysates from HEK 293 cells untransfected (control) or transfected with StarD4 or PCTP expression plasmids. (B) The location of the 52-67 antigenic peptide (green) in β-sheet 2 of the StarD4 structure. (C) Anti-StarD4 Western blot of liver protein extracts from control and nSREBP-2 transgenic mice.

The StarD4 promoter: StarD4 mRNA expression is sterol-regulated like SREBP-target genes, an effect likely mediated by a promoter SRE. To locate the StarD4 promoter by defining the 5' mRNA end, we performed 5' RNA ligase-mediated rapid amplification of cDNA ends (5' RLM-RACE) on mouse liver RNA (Figure 3.6). Sequencing 25 RACE products revealed 8 initiation sites 104-149 bp upstream of the ATG codon, with the most common being –137A (10/25) and –107A (8/25). –137A was defined as the +1 site for numbering the mouse promoter (Figure 3.7). 5' RLM-RACE analysis of human liver StarD4

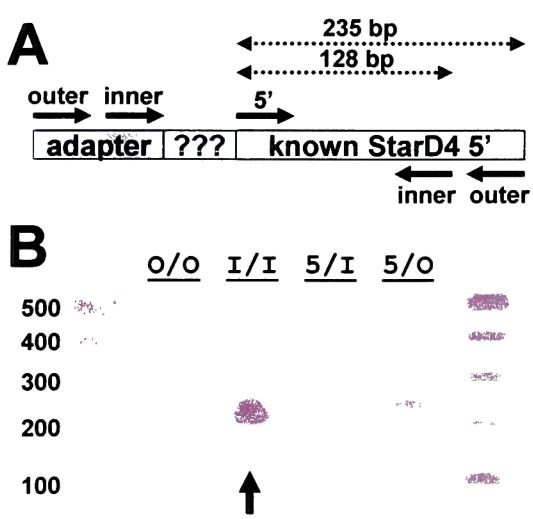

Figure 3.6: Analysis of mouse StarD4 by 5' Rapid Amplification of cDNA ends (RACE).
(A) Design of RNA-ligase mediated 5' RACE. An adaptor sequence was ligated to the 5' end of decapped mRNA and cDNA was synthesized. Primers in the adaptor and in the known StarD4 sequence were used for nested PCR. (B) Agarose gel of PCR products with forward/reverse primer combinations (I=inner, O=outer, 5=StarD4 5'). The outer (O/O) PCR was used as template for the subsequent PCR reactions. The inner (I/I) RACE PCR products (arrow) were cloned and sequenced. The control 5' primer gave the expected bands

also revealed multiple initiation sites, with the most common being –131G from the end of exon 1 (8/12 clones) (Figure 3.7). As predicted, the human StarD4 gene differed from the mouse gene, with its ATG start codon located in the second exon resulting in a protein 16 amino acids shorter at the N-terminus. There is no consensus TATA box in either StarD4 promoter, consistent with multiple initiation sites in TATA-less genes (Ince and Scotto, 1995). Several other SREBP-target genes have TATA-less promoters and multiple intitiation sites, including HMGR (Reynolds et al., 1984) and 7DHCR (Kim et al., 2001).

Mouse sequence from -350 to -100 is 68% identical to sequence from –281 to –10 in the human promoter (Figure 3.7). This high sequence identity for non-coding DNA indicates

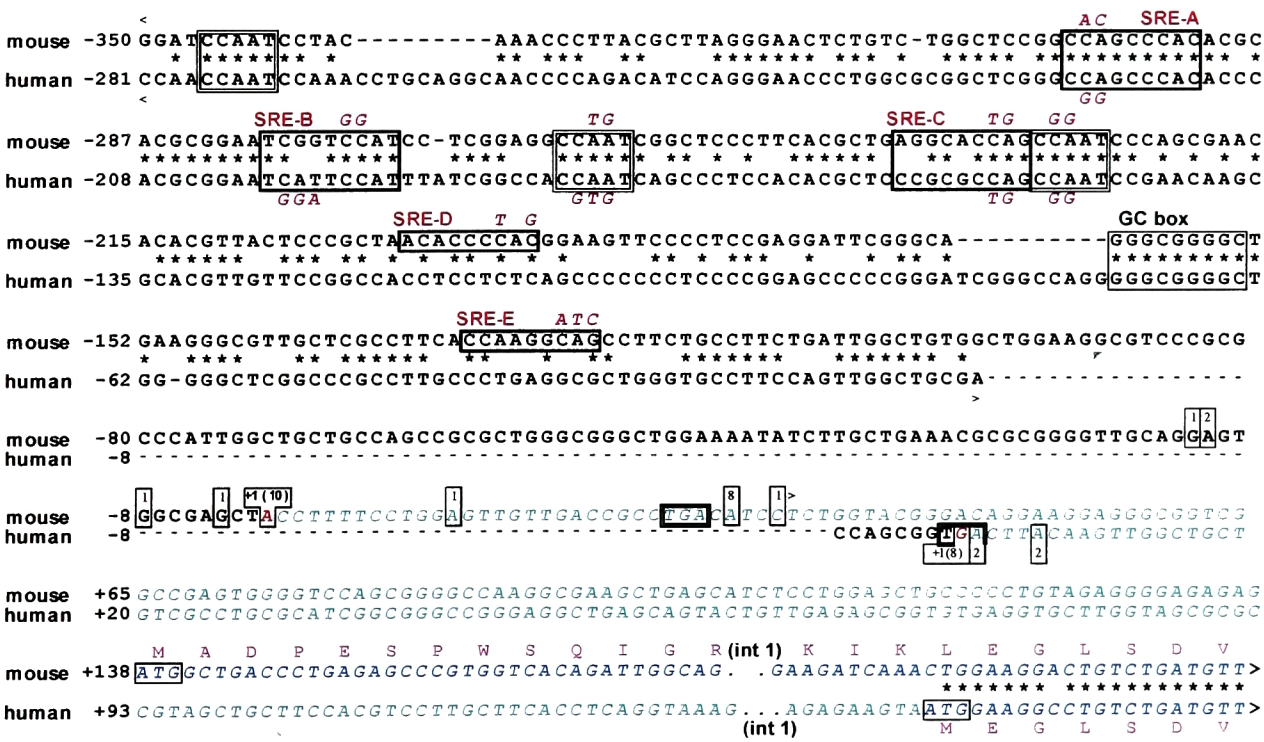

Figure 3.7: Alignment of mouse and human StarD4 proximal promoter sequences.
Nucleotides conserved between the species are indicated by (*). Promoter sequence is black, 5' untranslated region is green, and StarD4 coding sequence in exons 1 and 2 is blue (interrupted by intron 1). Transcription start sites identified by 5'RACE are shown in boxes with the number of RACE clones indicated (total n=25 for mouse, n=12 for human). The most common start sites (red) were designated +1 for promoter numbering. Potential promoter elements are indicated: sterol regulatory elements (SREs) and CCAAT and GC boxes. Sequences of the StarD4 reporter constructs (mouse -350/+34 and human -291/-9) are between the (<) and (>) symbols. Site-directed mutations are indicated in violet.

the presence of conserved gene regulatory elements. There are three conserved CCAAT boxes and two GC boxes, potential binding sites for NF-Y and Sp1, respectively. There are also three conserved sequences resembling SREs (called A, B, and C) at -300, -279, and -239 in the mouse promoter. Two additional potential SREs (D and E) at mouse -199 and -132 are not conserved in the human promoter.

In addition to the StarD4 proximal promoter, a more distal region was also conserved at –1.1 kB in mouse and –1.8 kb in human StarD4. In this stretch of ~100bp, there was over 80% interspecies nucleotide identity (Figure 3.8). No SREs were apparent by inspection, though TRANSFAC analysis (Matys et al., 2003) yielded approximately 100 other potential factor-binding sites. This conserved upstream sequence may represent an enhancer element.

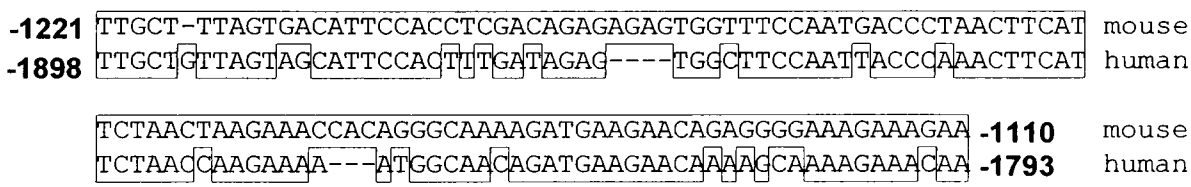

Figure 3.8: A potential enhancer region conserved between mouse and human StarD4.
This 5' non-coding sequence was conserved upstream of mouse and human StarD4, but not present elsewhere in the genome.

Identification of the StarD4 promoter SRE by reporter transfection studies: To identify a functional SRE, luciferase reporters driven by the StarD4 promoter were cloned and transfected into NIH 3T3 cells. Mouse StarD4 -350/+34 reporter activity decreased 9-fold upon culture in cholesterol and 25-hydroxycholesterol (sterols) and increased 3-fold upon culture in statin (Figure 3.9a). The positive control SREx3 reporter was similarly regulated, while the pGL3 empty vector was unregulated. Furthermore, the mouse StarD4 reporter showed dose dependent activity in response to both oxysterol (Figure 3.9b) and statin (Figure 3.9c). The -350/+34 mouse reporter contains all elements necessary for sterol regulation, as it showed similar activity and sterol regulation to longer reporter constructs (Figure 3.10).

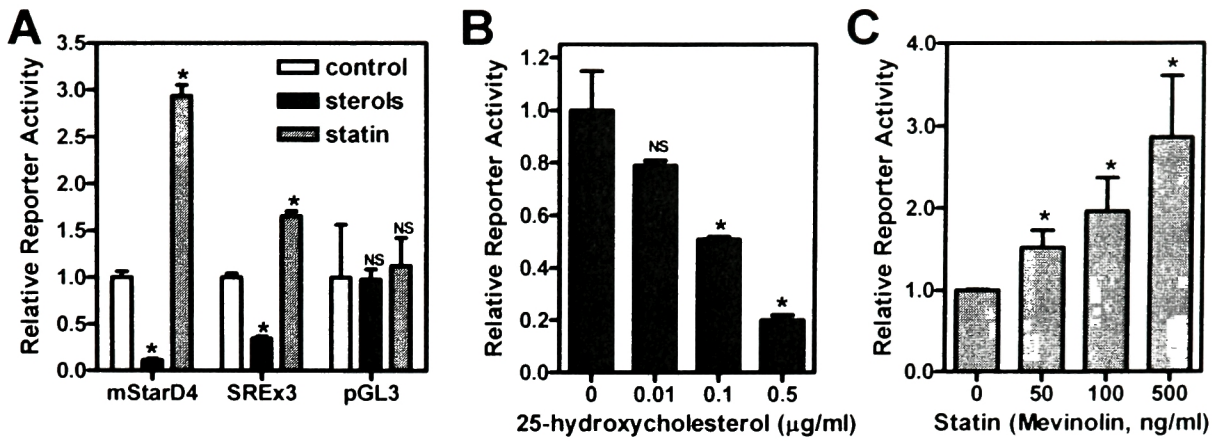

Figure 3.9: Regulation of the mouse StarD4 luciferase reporter by sterol and statin treatment. The mouse StarD4 -350/+34 luciferase reporter was transfected in NIH 3T3 cells, which were then cultured in lipoprotein-deficient media with sterols or statin as described above for 18-20 hours. (A) The mouse StarD4 reporter was regulated like the positive control SRE-regulated reporter (SREx3), while the empty luciferase vector (pGL3) was unregulated. The mouse StarD4 reporter activity showed dose dependent repression by oxysterol (B) and activation by statin (C). Luciferase values were normalized to β-galactosidase and control values were set equal to one. *P<0.05 vs. control.

The two constructs that spanned to –1335 included the putative enhancer element, but failed to show higher activity than shorter –350 constructs with only the proximal promoter. The human StarD4 reporter was regulated similarly to the mouse reporter, though its fold regulation was consistently less (only ~10-fold rather than ~20-fold comparing sterols to

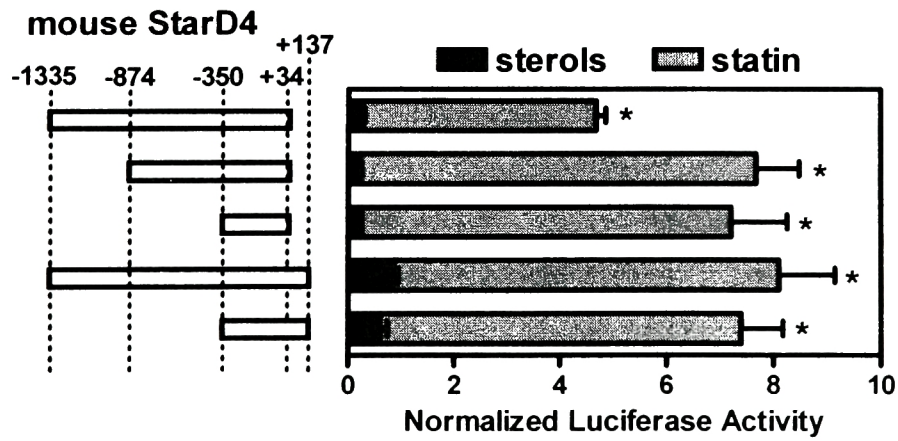

Figure 3.10: StarD4 luciferase reporters with longer promoters show similar regulation. The indicated lengths of mouse StarD4 promoter were used to generate luciferase reporters. All five, including the minimal -350/+34 reporter, showed significant activity differences in sterol- versus statin-treated NIH 3T3 cells. Luciferase activity was normalized to β-gal. *P<0.05, statin vs. sterols.

statin, see Figure 3.11a-b). Two different length of human promoter (-521/-8 and -282/-8) reporters also showed no differences in activity or regulation (data not shown).

We used site-directed mutagenesis to introduce point mutations into the potential SREs of the mouse and human StarD4 reporters (see Figure 3.7). SRE-A or SRE-C mutations had little effect on fold sterol regulation, while SRE-B mutations markedly decreased sterol regulation in both species (Figure 3.11a-b). In separate experiments with the mouse StarD4 reporter, overall regulation was less than typically observed, but mutations in potential SRE-D or SRE-E also did not affect sterol regulation (Figure 3.11c).

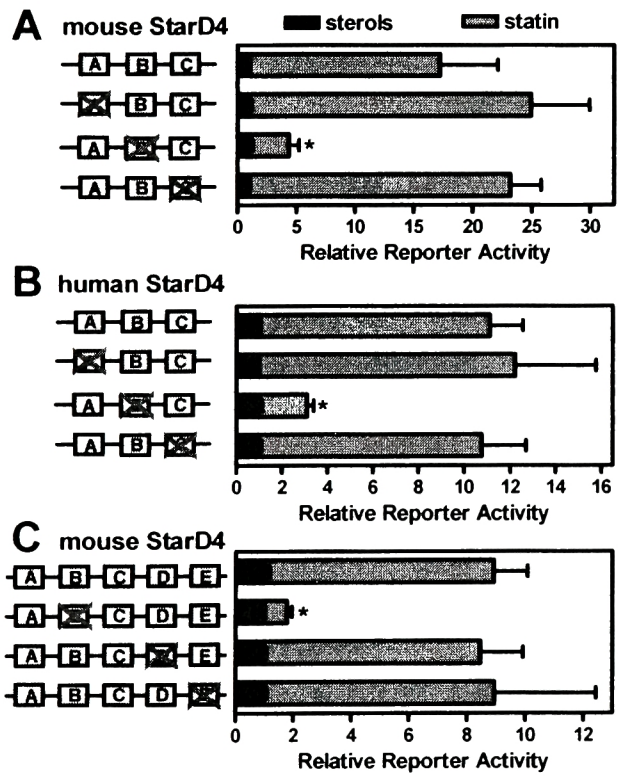

Figure 3.11: Regulation of StarD4 reporters with site-directed mutations in potential sterol regulatory elements.

Mutant StarD4 reporters were generated and transfected into NIH 3T3 cells, which were sterol- or statin-treated as before. (A) Mouse StarD4 wild type and SRE-A or SRE-C mutant reporters were regulated ~20-fold, while the SRE-B mutant was only regulated ~4-fold. (B) Human StarD4 wild type and SRE-A or SRE-C mutant reporters were regulated ~11-fold, while the SRE-B mutant was only regulated ~3-fold. (C) In another experiment, mouse StarD4 SRE-D and SRE-E mutant reporters were regulated like wild type, while the SRE-B mutant showed less regulation. Luciferase activity was normalized to β-gal, and sterol-treated activity for each reporter was set equal to one. *$P<0.05$, mutant vs. wild type (statin-treated).

Since SRE-B appears to be the functional element, we studied SRE-B mutant reporters in more detail. When SREBP cleavage was repressed by sterols, wild type and SRE-B mutant reporters had the same absolute activities (Figure 3.12a-b). However, when cells were cultured in the control media or in statin, the wild type reporters were strongly activated while the SRE-B mutant reporters were only weakly activated. Both the mouse and

human SRE-B mutant reporters showed residual regulation, with activity 4- to 5-fold higher in statin compared to sterols. However, in other experiments that compared sterol-containing to control media, there was no activation of SRE-B mutant reporters in the absence of sterols (Figure 3.12c).

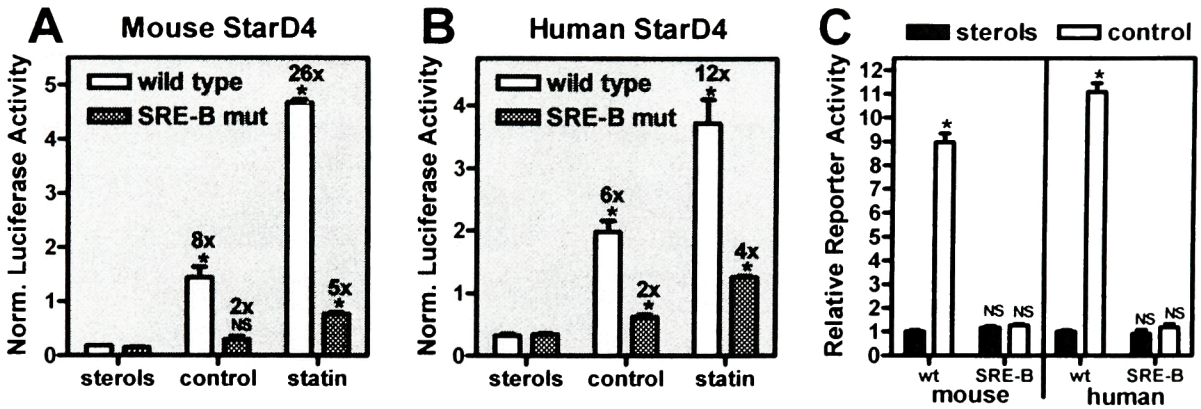

Figure 3.12: StarD4 SRE-B mutant reporters show defective sterol-regulation.
Mouse and human wild type or SRE-B mutant luciferase reporters were transfected into NIH 3T3 cells. (A, B) Cells were cultured in control medium, sterols, or statin as before. Luciferase activity was normalized to β-gal, and fold activation compared to sterol-treated cells is indicated. (C) In another experiment, cells were cultured in control medium or sterols. Luciferase activity was normalized to β-gal, and wild type activity in sterols was set equal to one. *P<0.05 vs. sterol-treated.

There were three possibilities for the residual activation SRE-B mutant reporters by statin treatment: (1) the SRE-B mutation may not have completely eliminated SREBP binding, (2) sequences in the pGL3 reporter vector may be SREBP-regulated, and (3) other potential StarD4 SREs may function in the absence of SRE-B. Consistent with the second possibility, it was reported that the pGL3 vector contains an E-box in its cloning polylinker that is SREBP-regulated in HepG2 cells (Annicotte et al., 2001). This E-box is unlikely to function in NIH 3T3 cells, as the empty pGL3 vector was not sterol-regulated (see Figure 3.8a). To rule out this artifact, we re-cloned the mouse wild type and SRE-B reporters using different restriction sites, thus eliminating the vector E-box. This modification did not affect regulation, as the wild type modified reporter was regulated 21-fold (statin compared to

sterols) and the SRE-B mutant was still regulated 4-fold (Figure 3.13). To test the third possibility that other SREs function in the absence of SRE-B, we generated double mutants of the modified mouse StarD4 reporter, each with mutations in SRE-B and a second potential SRE. Upon transfection, all the double mutants showed less regulation (1.3- to 2.4-fold) than the SRE-B alone mutant (4.4-fold, Figure 3.13). This result is difficult to interpret, but it implies that other SREs may have low levels of function. Nonetheless, most of the sterol regulation of mouse and human StarD4 is mediated by SRE-B.

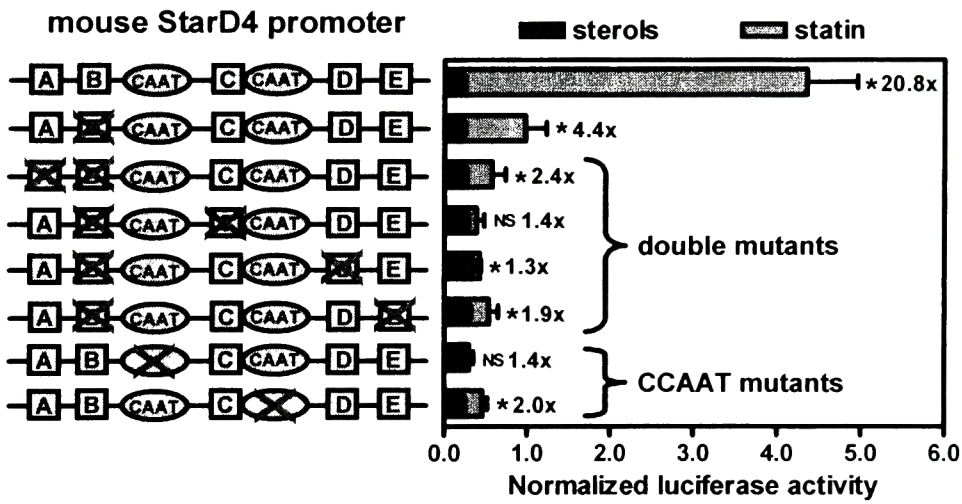

Figure 3.13: Additional mutagenesis studies of the mouse StarD4 promoter.

Mouse StarD4 -350/+34 was re-cloned into the *Sac*I and *Hind*III sites of the pGL3 reporter, thus eliminating the putative SREBP-binding E-box in the vector polylinker. This reporter showed similar activity and sterol-regulation to the previous *Bam*HI/*Hind*III reporter. Mutations were generated in various elements of the *Sac*I/*Hind*III reporter as indicated. Transfected cells were cultured in sterols or statin as before, and luciferase activity was normalized to β-gal. *P<0.05 sterols vs. statin.

We also generated mutations in two CCAAT boxes near SRE-B (see Figure 3.7), since these elements bind NF-Y and cooperate with SREBPs to activate transcription (Edwards et al., 2000). When the CCAAT box located 9 bp downstream of SRE-B was mutated, the reporter was virtually unregulated, with low activity even in the absence of sterols (Figure 3.13). Mutations in another CCAAT box after SRE-C, 40 bp from SRE-B, also blunted sterol regulation. Similar results were obtained with both CCAAT box

mutations in the human StarD4 reporter (data not shown). It appears that these CCAAT boxes, in addition to SRE-B, are necessary for maximally activated transcription from the StarD4 promoter.

StarD4 and StarD5 are not LXR target genes: Cholesterol can regulate gene expression via the SREBP and LXR transcription factors, so we also assayed for LXR regulation of StarD4 and StarD5. When mice were treated with the synthetic LXR agonist T0901317, liver expression of the known LXR-target gene ABCG5 was induced almost 3-fold, while StarD4 and StarD5 mRNA levels were unchanged (Figure 3.14a). By visual inspection, these mice developed the expected hepatic steatosis, indicating LXR activation of SREBP-1c and fatty acid synthesis (Lund et al., 2003). Since StarD4 was not induced, it appears to be a poor target for SREBP-1 in mouse liver, consistent with data from the SREBP-1a transgenic mice (see Figure 3.4).

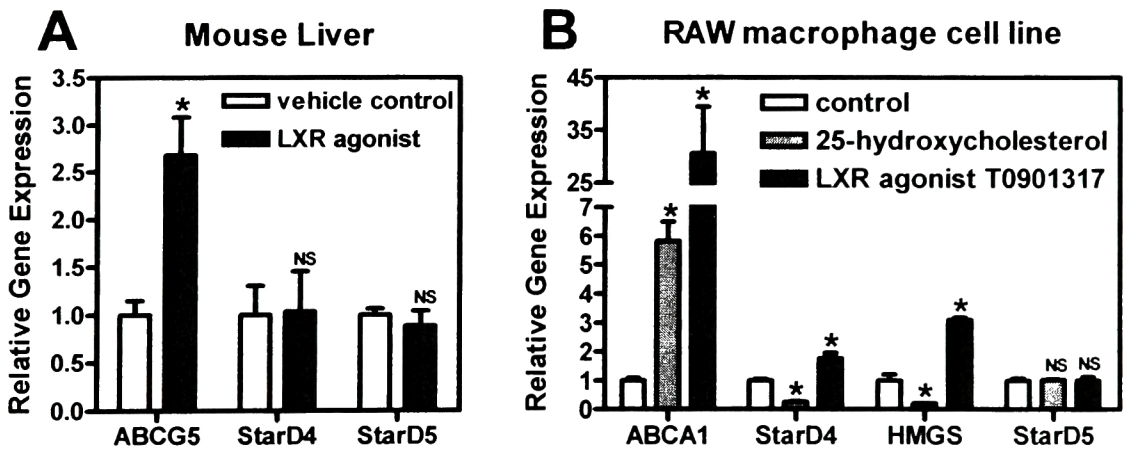

Figure 3.14: StarD4 and StarD5 are not LXR target genes.

(A) Mice were treated by gavage with the synthetic LXR agonist T0901317 or vehicle control (n=5 per group) for two days, and liver RNA was extracted. (B) RAW cells were treated for 18-20 hours with either 25-hydroxycholesterol or T090131 (n=3 per group) before RNA extraction. Gene expression was assayed by qPCR normalized to cyclophilin. ABCG5 and ABCA1 were control LXR targets, while HMG CoA synthase (HMGS) was a control SREBP-2 target. *P<0.05 vs. control.

We also treated the RAW mouse macrophage cell line with LXR ligands. As expected, ABCA1 mRNA levels were highly regulated (Costet et al., 2000), 6-fold by the weak LXR agonist 25-hydroxycholesterol and 30-fold by the strong agonist T0901317 (Figure 3.14b). It is also notable that PCTP expression was not activated by LXR agonists in these cells (data not shown), since this gene has been proposed to facilitate ABCA1-mediated lipid efflux (Baez et al., 2002). Expression of StarD4 was decreased four-fold by 25-hydroxycholesterol, consistent with its sterol regulation in NIH 3T3 and Hepa-1 cells (see Figures 3.2, 3.3). LXR agonist caused a two-fold increase in StarD4, but this regulation was also observed for another SREBP-2 target, HMGS. Conversely, StarD5 was unregulated by oxysterol or synthetic LXR ligands in RAW cells. Similar results were observed in Hepa-1 cells (data not shown). Therefore, StarD5 is not an LXR target gene, while there may be weak LXR activation of StarD4 consistent with SREBP-mediated effects.

StarD5 activation in cholesterol-loaded macrophages under ER stress: In addition to SREBPs and LXRs, a third transcriptional pathway can be activated by cholesterol. Tabas and coworkers recently demonstrated induction of various components of the ER stress response in free cholesterol-loaded macrophages (Feng et al., 2003a). To confirm these findings, we used a previously described RT-PCR assay for splicing of the Xbp1 mRNA (Calfon et al., 2002), an effect mediated by IRE-1 in response to ER stress (Yoshida et al., 2001a). As a control, treatment of NIH-3T3 cells with the ER stressor tunicamycin triggered Xbp1 processing (Figure 3.15a-b). In cDNA provided by Ira Tabas, processed Xbp1 appeared in free cholesterol-loaded macrophage, but not control or cholesterol-ester loaded macrophages, confirming ER stress activation (Figure 3.15c).

This macrophage cDNA was also assayed for expression of StarD4, StarD5, and the control ER-stress induced genes CHOP and BiP. Free cholesterol-loading activated

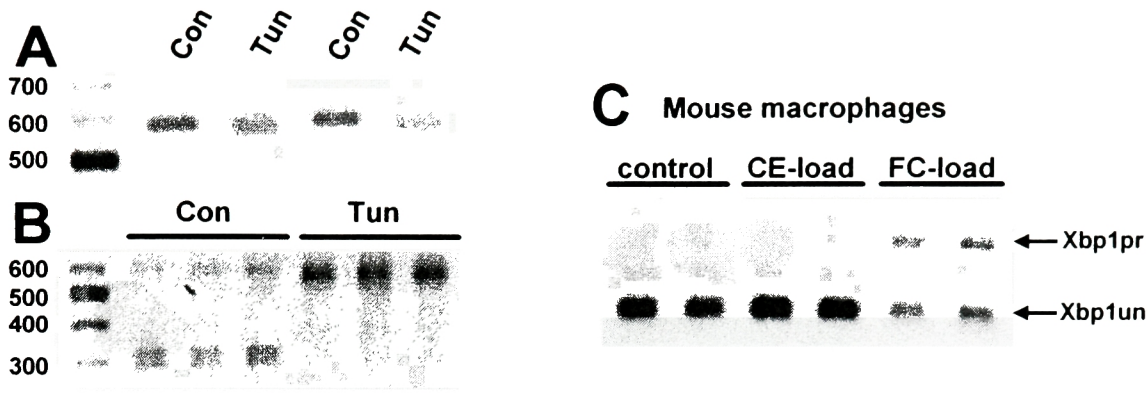

Figure 3.15: An Xbp1 splicing assay shows ER stress in free cholesterol-loaded macrophages.
(A) NIH 3T3 cells were cultured for 18 hours in control media or 2.5 μg/ml tunicamycin to induce ER stress. Xbp1 was RT-PCR amplified from these cells, giving a 601bp product in control cells but a smaller 575 bp product after ER stress-induced splicing of a non-traditional 26 bp intron. (B) PstI digest of these PCR products cleaves the unprocessed form (Xbp1un) into smaller 312 and 289 bp fragments, while the processed (Xbp1pr) form lacks the PstI site. (C) cDNA from control, cholesterol ester (CE) loaded, and free cholesterol (FC) loaded macrophage was likewise assayed for Xbp1 splicing by PCR and PstI digest.

expression of CHOP 50-fold and BiP 4.6-fold, while there was no significant effect of cholesterol ester-loading (Figure 3.16). The difference in fold regulation likely reflects a high baseline expression of BiP, which has a housekeeping role in ER protein folding, while the pro-apoptotic transcription factor CHOP is not expressed in unstressed cells (Ma et al., 2002). StarD4 expression was decreased 3-fold in response to loading of free cholesterol or esters, consistent with sterol regulation via SREBPs. StarD5 expression, however, was regulated similarly to BiP, with an almost 4-fold increase in free cholesterol-loaded

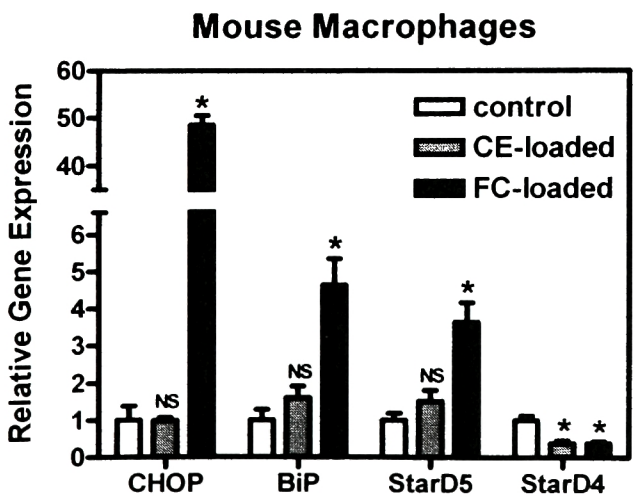

Figure 3.16: StarD5 expression is induced in free cholesterol-loaded macrophages.
cDNA from control, cholesterol ester (CE) loaded, and free cholesterol (FC) loaded macrophages (n=3 per condition) was assayed for gene expression by qPCR. Values were normalized to cyclophilin, and the control expression set equal to one for each gene. *P<0.05 vs. control.

macrophages. Since StarD5 was not activated by LXR agonists (see Figure 3.14), this suggests activation by the ER stress response.

StarD5 activation in ER stressed NIH-3T3 cells: To test whether StarD5 expression is indeed activated by ER stress, we treated NIH 3T3 cells with tunicamycin to induce the UPR. Tunicamycin activated CHOP (28-fold) and BiP (10-fold) as expected, while StarD5 was activated 8-fold and the negative control MLN64 was not regulated (Figure 3.17a). Northern blots of these samples showed both StarD5 mRNAs were activated by tunicamycin (Figure 3.17b). We also tested three additional agents that stress the ER by different mechanisms, as

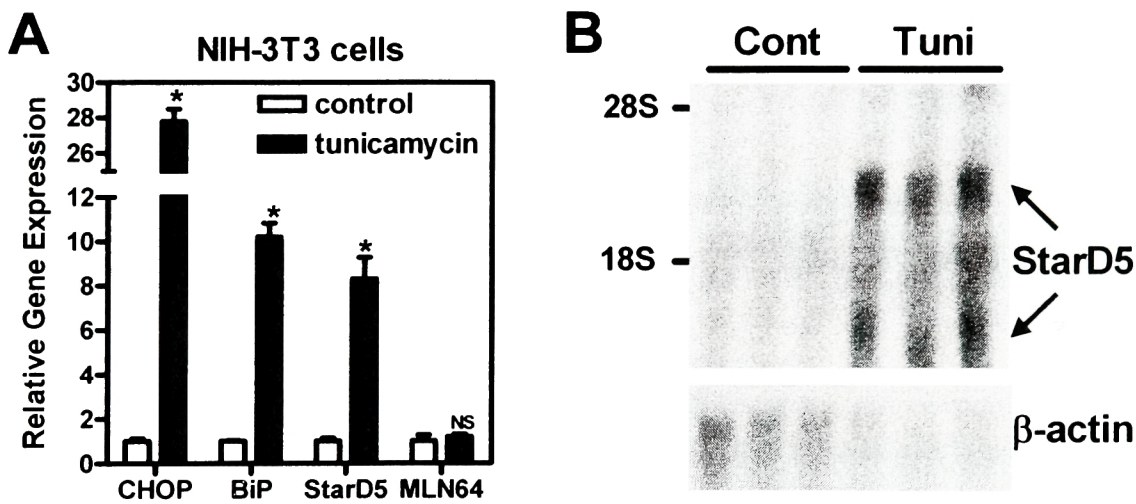

Figure 3.17: StarD5 expression is increased in NIH 3T3 cells by tunicamycin treatment.
NIH 3T3 cells were cultured 18-20 hours in control media or 2.5 μg/ml tunicamycin (n=3 wells each) to induce ER stress, and RNA was extracted. (A) qPCR analysis of gene expression, normalized to cyclophilin. *P<0.05 vs. control. (B) Northern blot probed for StarD5 or β-actin control.

described in the introduction. All four agents activated expression of BiP (9- to 17-fold) and StarD5 (~6-fold), confirming that ER stress activates StarD5 expression (Figure 3.18a). StarD4 expression showed small and inconsistent changes in response to ER stressors (only ~50% differences), perhaps due to effects on SREBP trafficking from the ER. To show that StarD5 expression was specific for ER stress as opposed to other stresses, cells were heat

shocked at 42°C. Heat shock protein 70 (Hsp70) was activated as expected, while BiP, StarD5, and StarD4 were not activated. Heat shock actually caused a 3-fold decrease in expression of StarD5 and BiP, again showing coordinate regulation of these genes. These results indicate that StarD5 expression is specifically induced by the ER stress response.

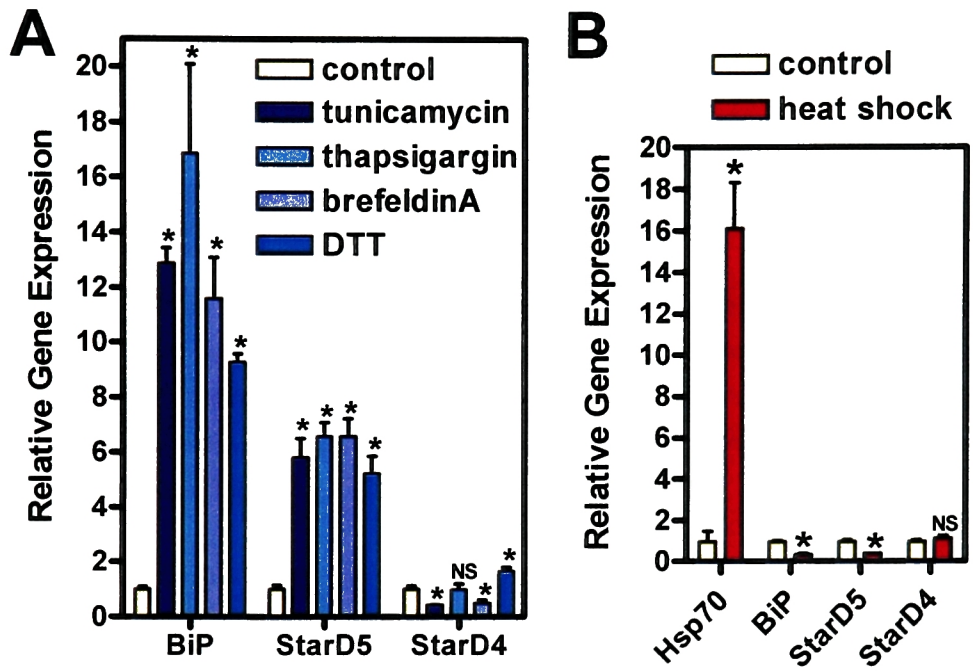

Figure 3.18: StarD5 is induced by ER stressors but not heat shock.

(A) NIH 3T3 cells were cultured in control media or ER stressed with 2.5μg/ml tunicamycin, 2.0μM thasigargin, 10μg/ml brefeldinA, or 2mM DTT (n=3 wells each). (B) NIH 3T3 cells were cultured at 37°C or 42°C to induce heat shock. Gene expressrision was assayed by qPCR and normalized to cyclophilin. *P<0.05 vs. control, NS=not significant.

StarD5 promoter reporter studies: The StarD5 promoter sequence from mouse and human was compared. Regions 400 bp upstream of the ATG translation start codon were conserved ~50% between species (Figure 3.19). A 100 bp region between -153 and -54 in mouse was 66% identical (between arrows), and contained three conserved promoter elements: two CCAAT boxes and one GC box. ER stress response elements (ERSE) have been identified in the promoters of BiP and other ER stress regulated genes (Roy and Lee, 1999), but there were no consensus ERSEs in the StarD5 proximal promoter.

Figure 3.19: The StarD5 proximal promoter lacks a consensus ER stress response element. Alignment of mouse and human StarD5 sequence around the ATG translation start codon (+1). The overall identity of upstream non-coding sequence was ~50% between the species. The sequence between the two arrows was ~66% identical. While upstream DNA included conserved CCAAT and GC boxes, there was no consensus ERSE.

Despite the absence of a consensus ERSE, the StarD5 proximal promoter could contain novel elements responsive to ER stress. We cloned a luciferase reporter driven by mouse StarD5 sequence from -400 to -1 from the ATG. For comparison, we also transfected two ER stress activated reporters, one driven by the BiP promoter and the other with five synthetic ATF6 consensus sites (5xATF6) (Lee et al., 2002). Upon treatment of cells with tunicamycin, the positive control reporters were activated, 5xATF6 by 16-fold and BiP by 2.5-fold, while the StarD5 reporter was actually repressed ~30% (Figure 3.20). The mouse StarD4 -350/+34 promoter was also slightly repressed by tunicamycin, as was a shorter StarD5 promoter -200/-1 reporter (data not shown). The failure of tunicamycin to activate these StarD5 promoter reporters, despite robust activation of the endogenous StarD5 gene in the same cell type (see Figure 3.16), suggests that the elements responsible for ER stress activation do not lie in the proximal 400 bp upstream of the ATG. The ER stress responsive elements in the StarD5 gene remain to be identified.

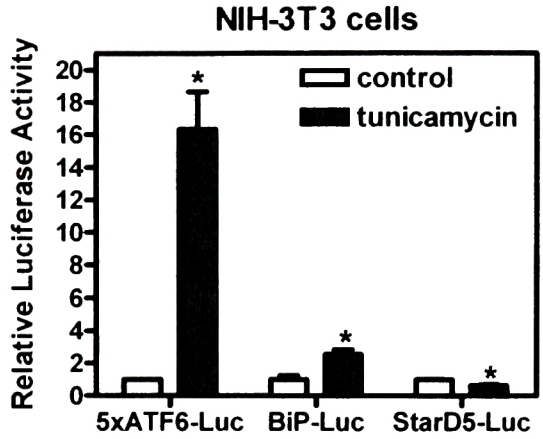

Figure 3.20: A mouse StarD5 proximal promoter luciferase reporter is not activated by ER stress. NIH 3T3 cells were transfected with luciferase (Luc) reporters driven by synthetic ATF6 sites (5xATF6), the BiP promoter, or the StarD5 promoter. After transfection, cells were cultured in control media or ER stressed with 1.0μg/ml tunicamycin. Luciferase activity was normalized to β-gal, and control was set equal to one for each reporter. *P<0.05 vs. control.

Chapter Summary: This chapter presents data that the widely expressed StarD4 and StarD5 genes are not regulated by steroidogenic stimulation like StAR, nor by LXRs which stimulate reverse cholesterol transport. StarD4 was shown to be sterol-regulated via SREBP-2, and a functional SRE was identified in the StarD4 promoter. StarD5 was not sterol-regulated, but it was activated by mutliple ER stressors, including free cholesterol-loading in macrophages, though the responsible promoter elements were not identified.

Localization of StarD4 and StarD5 throughout cells: If StarD4 subfamily proteins play roles in intracellular sterol transport, then subcellular localization may provide clues to function. StarD4, StarD5, and StarD6 consist entirely of START domains and lack other domains that could mediate localization. Since the isolated START domains N-62 StAR (Arakane et al., 1996), MLN64-START (Zhang et al., 2002b), and full length PCTP (de Brouwer et al., 2002) are found throughout the cell cytosol and nucleus, we hypothesized that StarD4 subfamily members would share this distribution. PROSITE (Falquet et al., 2002) and other protein sequence searches failed to identify any consensus localization signals in the StarD4 subfamily.

Mouse StarD4 was cloned as a fusion with enhanced green fluorescent protein (EGFP), such that the EGFP moiety was at the StarD4 N-terminus (rather than at the C-terminal α-helix lid). In transiently transfected HEK 293 or NIH 3T3 cells, the distribution of EGFP-mStarD4 was throughout the cytosol and nucleus, indistinguishable from EGFP alone (Figure 4.1). Some lipid binding proteins change their subcellular localization in

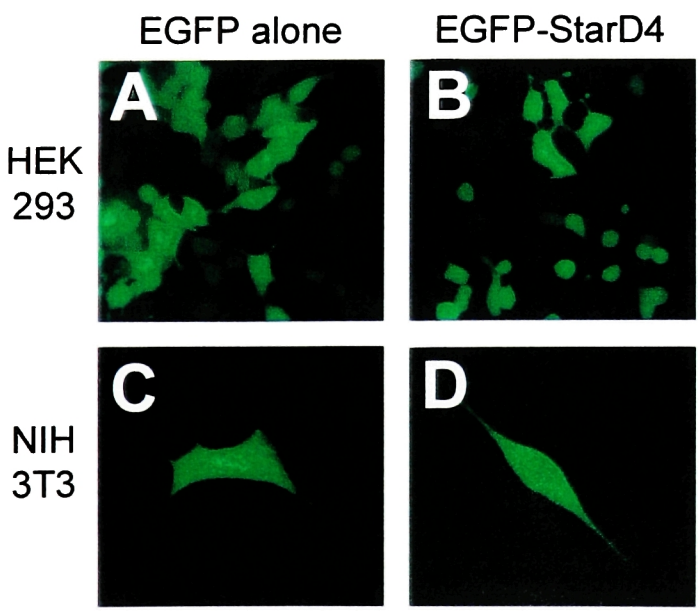

Figure 4.1: A GFP-StarD4 fusion protein localizes throughout cells. An expression plasmid for mouse StarD4 with an enhanced green fluorescent protein (EGFP) tag N-terminal to the START domain was cloned. Upon transient transfection of HEK 293 (B) or NIH 3T3 cells (D), the EGFP-StarD4 fusion protein was distributed evenly throughout the cell. The same distribution was observed for EGFP alone in these cells (A,C).

response to specific stimuli, as described in the introduction for PCTP and OSBP (de Brouwer et al., 2002; Lehto and Olkkonen, 2003). However, treatment of transfected cells with 25-hydroxycholesterol, lovastatin, or tunicamycin did not change the distribution of EGFP-StarD4 (data not shown).

FLAG epitope-tagged expression plasmids were cloned for six mouse START domains: the isolated START domains of StAR and MLN64, and the full-length proteins for PCTP, StarD4, StarD5, and StarD6. Upon transient transfection in HEK 293 cells and anti-FLAG immunofluorescence, StarD6 protein was barely detectable but the other five FLAG-START proteins showed similar localization. All were found throughout the cytosol and nucleus, and there was no punctuate staining to suggest a specific subcellular compartment. More detailed microscopy, and the response of these proteins to various treatments, has not been performed. However, the patterns observed were consistent with the prediction that isolated START domains distribute throughout the cell.

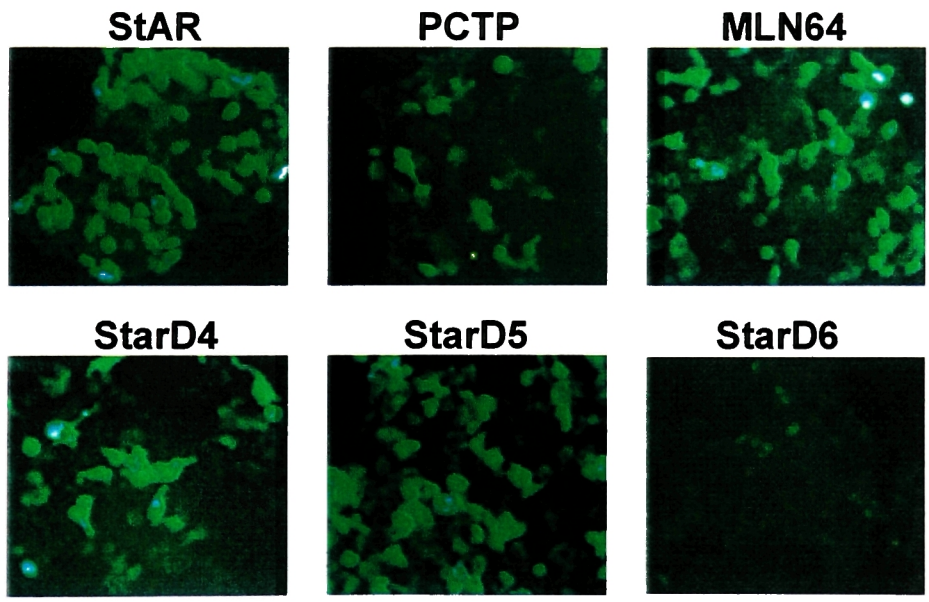

Figure 4.2: FLAG-tagged StarD4 and StarD5 proteins localize throughout cells

HEK 293 cells were transfected with N-terminal FLAG-tagged expression constructs for the six indicated mouse START domains. StAR and MLN64 were truncated proteins lacking the N-terminal domains that mediate localization of the full-length proteins. By anti-FLAG immunofluorescence, very little FLAG-StarD6 was detected, but the other five were similarly distributed throughout cells.

Cell culture assay for StAR-like steroidogenic activity: Several studies of StAR and MLN64 have used a cell culture steroidogenesis assay, in which non-steroidogenic COS-1 cells are transfected with an expression plasmid for the P450scc enzyme and its cofactors (Huang and Miller, 2001). The mitochondrial P450scc enzyme converts cholesterol into the first steroid pregnenolone, which can be assayed in the cell culture media (Sugawara et al., 1995a). However, it is more convenient to assay for progesterone, which is generated from pregnenolone by 3β-hydroxysteroid dehydrogenase (3β-HSD), so an expression plasmid for this enzyme is often co-transfected (Zhang et al., 2002b). Compared to the basal steroidogenesis by the two transfected enzymes, co-transfection of StAR increases progesterone production, presumably by delivering the substrate cholesterol to P450scc (Sugawara et al., 1995a). The isolated START domains of StAR and MLN64 are similarly active in this assay (Bose et al., 2000). Addition of the oxysterol 22(R)-hydroxycholesterol gives high levels of steroidogenesis even in the absence of StAR, apparently reaching the P450scc without need for an intracellular transport protein.

The FLAG-START expression constructs described earlier were tested in this steroidogenesis assay. 22(R)-hydroxycholesterol caused a 13-fold increase in progesterone production, while co-transfection of StAR in the absence of oxysterol resulted in an 11-fold increase. StarD4 showed StAR-like activity, increasing progesterone production 4-fold (Figure 4.3a). Further experiments tested all six FLAG-STARTs. As expected, the StAR and MLN64 START domains stimulated steroidogenesis, and PCTP was an inactive negative control. StarD4 and StarD5 both increased steroidogenesis 2- to 3-fold, but not to the same extent as StAR and MLN64, which gave 5- to 7-fold increases (Figure 4.3b). In repeated experiments, StarD4 and StarD5 consistently showed activity approximately one third of StAR activity. This disparity may reflect different protein expression levels, even though equal amounts of DNA were transfected. On anti-FLAG Western blots, transfected StAR,

PCTP, MLN64, and StarD5 were expressed to similar levels, while StarD4 showed much less expression (Figure 4.3c). Consistent with the immunofluorescence (see Figure 4.2), StarD6 protein expression was undetectable by Western, so its steroidogenic activity could not be determined. Lower StarD4 protein expression may account for its lower activity, but further dose response studies are necessary to address the relationship between protein expression levels and activity. Preliminary studies showed that decreasing the amount of transfected StAR by 5-fold did not affect its level of activity (data not shown). While specific conclusions regarding their relative activities cannot be reached, it is clear that StAR, MLN64, StarD4, and StarD5 START domains stimulated steroidogenesis in this assay. Therefore, StarD4 and StarD5 can function in intracellular cholesterol metabolism.

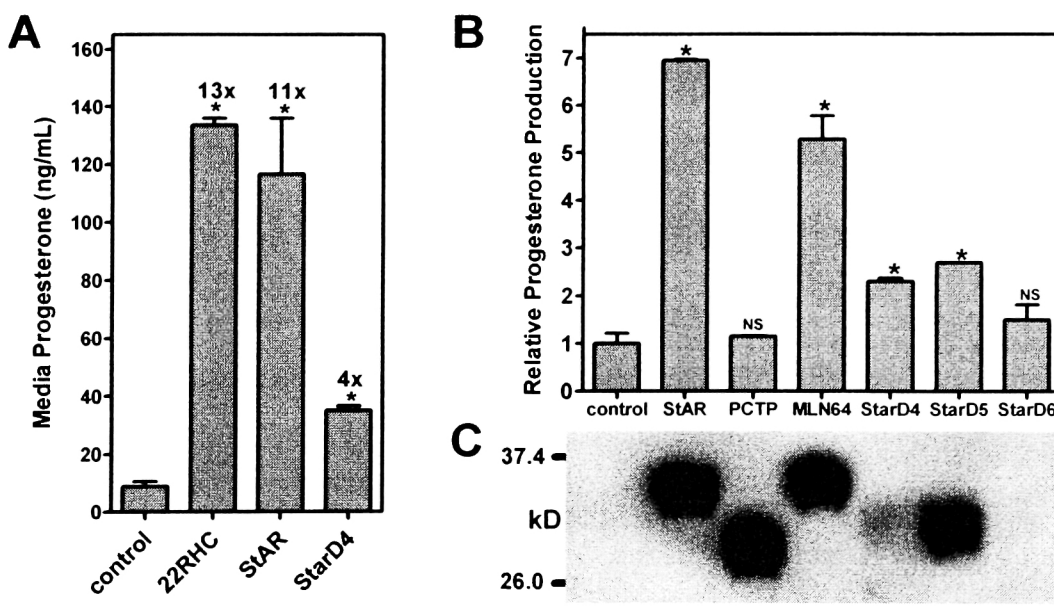

Figure 4.3: StarD4 and StarD5 have StAR-like activity in the cell culture steroidogenesis assay
(A) COS-1 cells were co-transfected with expression plasmids for two steroidogenic enzymes, P450scc and 3β-HSD, and the indicated FLAG-tagged START domain (n=3 wells each). Control cells were transfected with empty FLAG expression vector rather than START domains. After 48 hours, media progesterone levels were measured by enzyme linked immunosorbent assay (ELISA). Both StAR and StarD4 significantly stimulated progesterone production over control levels. The positive control was treatment of FLAG vector transfected cells with 1μg/ul 22(R)-hydroxycholesterol (22RHC), a StAR-independent substrate for steroidogenesis. (B) The same assay performed with additional START domains. Progesterone production in control FLAG vector transfected cells was set equal to one. *P<0.05 vs. control. (C) Anti-FLAG Western blot of FLAG-START transfected COS-1 cells.

Site-directed mutations in cavity salt bridges of StarD4 and MLN64: As described earlier, StAR and MLN64 have a unique salt bridge between charged amino acids in β5 and β6, rather than one in αC like the StarD4 subfamily and other START domains. These differences were proposed as lipid specificity determinants (Tsujishita and Hurley, 2000), so we performed site-directed mutagenesis of the FLAG-MLN64 and FLAG-StarD4 expression plasmids. When two charged residues in MLN64 were mutated to the corresponding uncharged residues in StarD4 (Asp332Tyr and Arg351Ser), the β5/β6 salt bridge was eliminated, yet this protein with neither salt bridge (*none*) had wild type steroidogenic activity (Figure 4.4a). When two more residues were mutated to agree with StarD4 (Met307Arg and Gln311Asp), such that the αC salt bridge was present (*switch*), activity decreased 25% but this difference was not significant. However, activity was decreased ~50% in MLN64 mutants with both salt bridges present (*both*) or with other combinations of substitutions (*A-D*, not significant for mutant *B*). Wild type MLN64 protein and its various mutants were expressed to similar levels based on an anti-FLAG Western blot (Figure 4.4b).

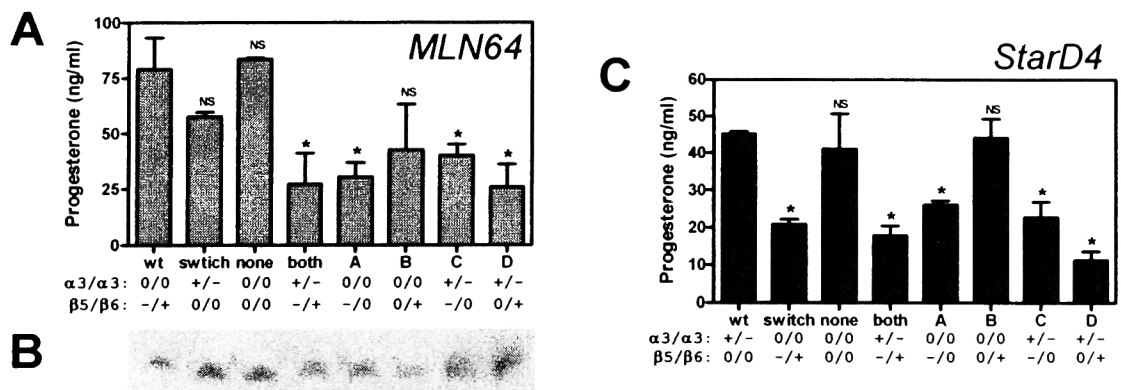

Figure 4.4: Steroidogenic activities of StarD4 and MLN64 salt bridge mutant proteins

The COS-1 steroidogenesis assay was performed as before, by co-transfecting expression plasmids for P450scc, 3β-HSD, and a FLAG-tagged START domain (n=2 wells each), then assaying for media progesterone after 48 hours. MLN64 and StarD4 mutants were generated with amino acid substitutions affecting the charged amino acids (+/-) that form salt bridges in α-helix 3 or between β-strands 5 and 6. (A) Progesterone production by wild type MLN64 and seven mutants. (B) Anti-FLAG Western blot showing similar expression levels for these MLN64 proteins. (C) Progesterone production by the corresponding StarD4 wild type and mutant proteins. *P<0.05 vs. wild type.

The corresponding set of StarD4 mutants was also generated: Arg92Met and Asp96Gln eliminated the αC salt bridge, while Tyr117Asp and Ser136Arg added the β5/β6 salt bridge. As with MLN64, the mutant with neither salt bridge (*none*) was fully active, while the mutant with *both* was only 50% active relative to wild type (Figure 4.5c). However, StarD4 with the β5/β6 salt bridge alone (*switch*) was also only 50% active, while mutant *B* with an unbalanced positive charge on β6 was fully active. Since the baseline progesterone production in the absence of START domains was typically 10-20 ng/ml, some of the StarD4 mutants were essentially inactive.

Several conclusions can be drawn based on the behavior of these StarD4 and MLN64 mutants. The salt bridges are not essential for function, since mutants with neither salt bridge (*none*) have the same steroidogenic activities as wild type proteins. The MLN64 mutant lacking the β5/β6 salt bridge but with the StarD4 αC salt bridge (*switch*) retained high activity, inconsistent with the hypothesis that the salt bridges determine differential ligand binding. The presence of both salt bridges in the same protein (*both*) reduced activity ~50%, perhaps due to excess charge in the predominantly hydrophobic cavity or altered protein folding. The unbalanced negative change on β5 in mutants *A* and *C* likewise decreased activity. However, an unbalanced positive change on β6 did not significantly affect activity in the absence of the αC salt bridge (mutant *B*), while activity was decreased in the presence of this salt bridge (mutant *D*). Notably, five START domains (PCTP, StarD7, StarD8, StarD10, and StarD13) have the salt bridge configuration of mutant *D* (see Figure 2.21), so this unbalanced positive charge can apparently be tolerated by the START structure.

Tom20 fusion proteins localizing START proteins to mitochondria: Miller and coworkers localized StAR to different parts of the mitochondria (OMM, IMM, intermembrane space, and matrix) by making fusions to various mitochondrial proteins (Bose et al., 2002). Only

the fusion to the C-terminus of Tom20, which places StAR on the cytosolic side of the outer mitochondrial membrane, was functional in steroidogenesis. Furthermore, Tom-StAR gave similar steroidogenesis to 22(R)-hydroxycholesterol, with twice the activity of full-length or N-62 StAR. They conclude that StAR functions at the outer mitochondrial membrane, and that artificial localization of the protein there results in maximum activity.

We generated FLAG-Tom-START chimeras by cloning mouse Tom20 into the FLAG-START expression plasmids for StAR, MLN64, StarD4, StarD5, and PCTP. FLAG-Tom-StAR was active as expected, though it was less active than FLAG-StAR (Figure 4.5a). This difference from the previous report may be due to the FLAG epitope tag or different protein expression levels. Indeed, anti-FLAG Western blots showed that Tom-START chimeras were expressed at much lower levels than START alone proteins, while expression was similar among the various Tom-START chimeras (Figure 4.5b). Tom-PCTP did not have significant steroidogenic activity, while the Tom fusions of StAR, MLN64, StarD4, and StarD5 all increased steroidogenesis 3.4- to 4.0-fold relative to Tom20 alone (Figure 4.5a).

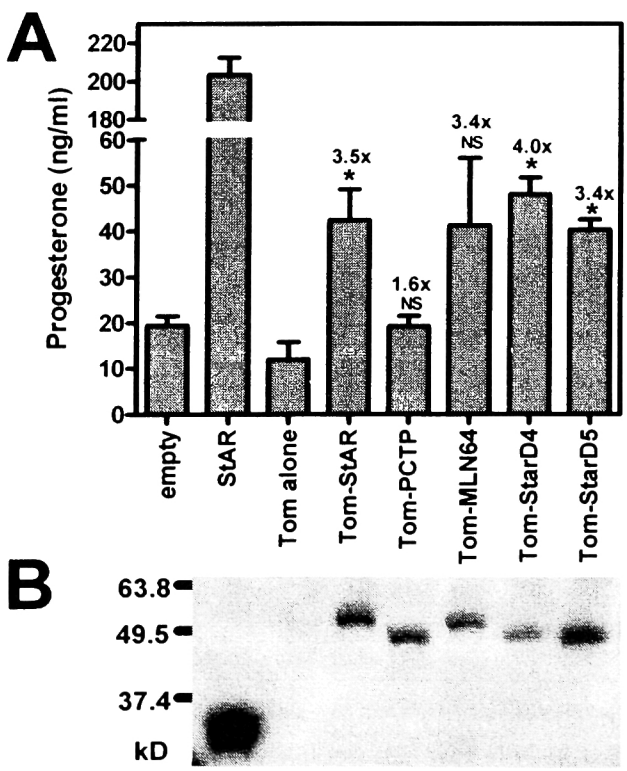

Figure 4.5: Steroidogenic activities of Tom20-START fusion proteins. FLAG-tagged fusions of the mitochondrial outer membrane protein Tom20 and START domains were generated. (A) These were tested in the COS-1 steroidogenesis assay as before. The FLAG empty and StAR plasmids were controls. The fold difference from the Tom alone control is indicated for each Tom-START. *P<0.05 vs Tom alone. (B) Anti-FLAG Western blot shows similar expression levels for the five Tom-STARTs, but lower expression than START alone proteins like StAR.

Therefore, in contrast to the FLAG-START results, in which StAR and MLN64 appeared more active than StarD4 and StarD5, these four FLAG-Tom-START fusions had nearly the same steroidogenic activities.

Effects of START domain overexpression on SREBP activity: The steroidogenesis assay is thought to measure cholesterol transfer to mitochondria, so we also sought to assay cholesterol transfer to the ER. SREBP processing is regulated by changes in ER cholesterol, so we used a luciferase reporter driven by three consensus SREs (SREx3) as an indirect measure. Activity of the SREx3 reporter in HEK 293 cells was decreased ~70% by co-transfection of the StAR or MLN64 START domains, compared to empty FLAG vector (Figure 4.6a). This repression of SRE activity was significant and similar to the effect of exogenous 25-hydroxycholesterol. StarD4 and StarD5 decreased SRE activity ~50%, while PCTP did not change activity. Repeat experiments confirmed that PCTP had no effect, while

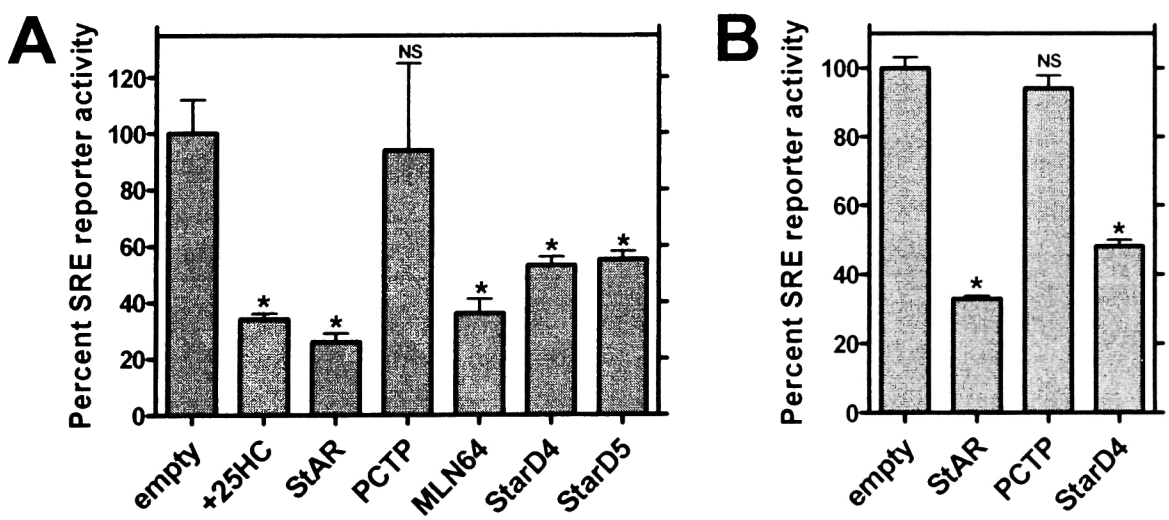

Figure 4.6: START proteins including StarD4 and StarD5 repress SRE reporter activity.
(A) HEK 293 cells were co-transfected with an SREBP-regulated luciferase reporter (SREx3 Luc) and the indicated FLAG-tagged START expression plasmid. Luciferase activity was normalized to β-gal, and activity with the control empty FLAG vector was set equal to 100%. As a positive control, adding 25-hydroxycholesterol (25HC) repressed SREBP activity as expected. Activity was also repressed by four START domains, but not PCTP. (B) A repeat experiment, also in HEK 293 cells, showed that StAR and StarD4 repress reporter activity, but PCTP had no effect. *$P<0.05$ vs. empty vector.

the other START domains repressed SRE reporter activity (Figure 4.6b and data not shown). Such a decrease suggests less SREBP processing, though this was not directly shown. These START proteins could either deliver cholesterol delivery directly to the ER or facilitate the conversion of cholesterol to oxysterols, which then feed back to the ER regulatory pool.

Effects of START domain overexpression on LXR activity: Since the START domains of StAR, MLN64, StarD4, and StarD5 affected SREBP activity, we also assayed for effects on LXR activity. COS-1 cells were transfected with an LXRE luciferase reporter, expression plasmids for human LXRα and RXRα, and the FLAG-STARTs. The StAR and MLN64 START domains both stimulated LXRE activity 5.5-fold, similar to effects of the synthetic LXR ligand T0907317 (Figure 4.7a). StarD4 and StarD5 likewise activated the LXRE reporter 3- to 4-fold, while PCTP had no effect. These START domains could activate

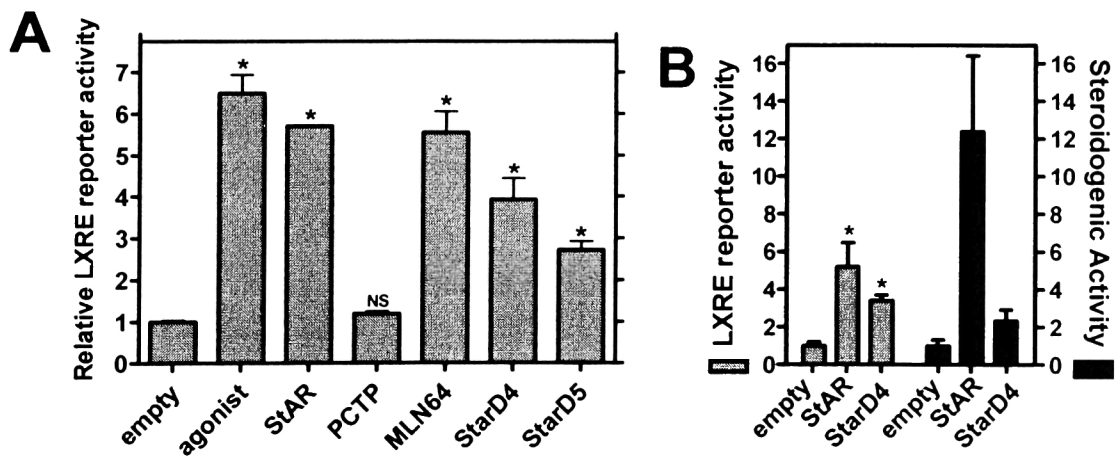

Figure 4.7: START proteins including StarD4 and StarD5 stimulate LXRE reporter activity.

(A) COS-1 cells were co-transfected with an LXR-regulated luciferase reporter (LXRE Luc) and expression plasmids for LXRα and RXRα, as well as the indicated FLAG-tagged START expression plasmid. Luciferase activity was normalized to β-gal, and activity of the control empty FLAG vector was set equal to one. As a positive control, adding the synthetic LXR agonist T0907317 (agonist) activated LXR activity as expected. Activity was also stimulated by four START domains, but not PCTP (B) Direct comparison between START domain activation of the LXRE reporter and steroidogenesis. One plate of COS-1 cells was transfected at the same time with the respective constructs, and both assays were performed as before. StAR was much more active than StarD4 in steroidogenesis, but their activities were more similar in activating LXR. *$P<0.05$ vs. empty vector.

LXRβ as well as LXRα (data not shown). StarD4 and StarD5 consistently stimulated LXRE activity almost as well as StAR and MLN64 START domains, while they appeared much less active in steroidogenesis assays (see Figure 4.3). This difference was confirmed in a combined experiment, assaying steroidogenic activity and LXR activation in COS-1 cells on the same plate transfected at the same time. In this experiment, StAR was 5-fold more active than StarD4 in steroidogenesis, but only 1.5-fold more in activating LXRs (Figure 4.7b).

The salt bridge mutants of StarD4 were also tested in this assay for LXR activation (Figure 4.8). The two mutants that were functional in the steroidogenesis assay (see Figure 4.4c), with neither salt bridge (*none*) or with an unbalanced positive charge on β6 (mutant *B*), activated the LXRE reporter like wild type. However, the other mutants with less steroidogenic activity were significantly less active or inactive in stimulating the LXRE reporter. Therefore, salt bridge mutations in StarD4 have similar effects on activity in the assays for steroidogenesis and LXRE activation.

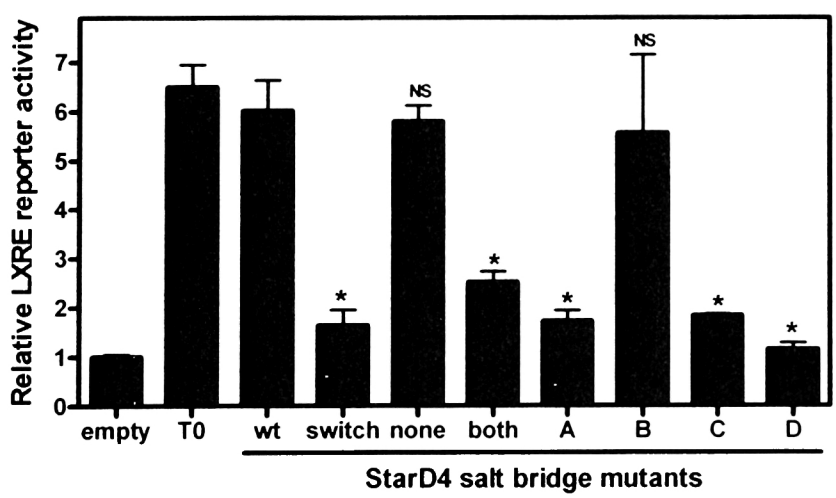

Figure 4.8: LXRE reporter stimulation activities of StarD4 salt bridge mutant proteins.
COS-1 cells were transfected as before with the LXRE luciferase reporter, LXRα, and RXRα. Expression plasmids for FLAG-tagged wild type (wt) StarD4 or the previously described salt bridge mutants (see Figure 4.4c) were co-transfected as indicated. Luciferase activity was normalized to β-gal, and activity of the control empty FLAG vector was set equal to one. As a positive control, the synthetic LXR agonist T0907317 (T0) activated LXR activity as expected. Certain StarD4 mutations affected activity. *P<0.05 StarD4 mutant vs. wild type.

We hypothesized that START domain overexpression activates LXRs by increasing levels of an oxysterol LXR ligand. The FLAG-Tom20-START chimeras, which presumably localize to mitochondria, showed similar effects on LXR activation as the cytosolic FLAG-STARTs (Figure 4.9). Therefore, one possibility is that START domains deliver cholesterol to mitochondrial Cyp27 to generate 27-hydroxycholesterol, analogous to pregnenolone generation by mitochondrial P450scc in steroidogenesis. Indeed, it was previously shown that StAR can deliver cholesterol to Cyp27 (Sugawara et al., 1995b). To determine whether

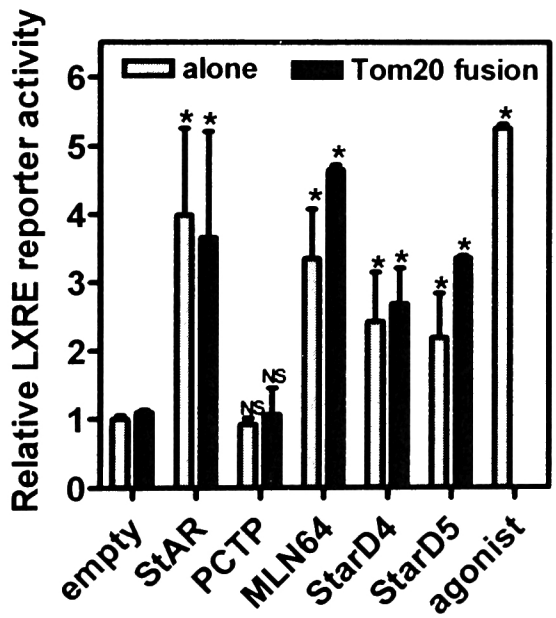

Figure 4.9: LXRE reporter stimulation by Tom20-START fusion proteins.
COS-1 cells were transfected as before with the LXRE luciferase reporter, LXRα, and RXRα. Expression plasmids for FLAG-STARTs (alone) and FLAG-Tom20-STARTs (fusion) were co-transfected as indicated. Luciferase activity was normalized to β-gal, and activity of the control empty FLAG vector was set equal to one. As a positive control, the synthetic LXR agonist T0907317 (agonist) activated LXR activity as expected. Fusions to the outer mitochondrial membrane protein Tom20 showed similar activity to START domains alone. *P<0.05 vs. empty vector.

an oxysterol LXR ligand accumulates in the media of START-transfected cells, we performed a conditioned media switch experiment. While Tom-StAR activated LXRs 2.5-fold in the transfected cells, conditioned media from these cells had no effect on other cells transfected with only the LXRE reporter and LXR/RXR (Figure 4.10). As a positive control, synthetic LXR ligand in the conditioned media was still effective. Therefore, any LXR ligand generated by START proteins failed to accumulate to high concentrations in media. Perhaps the putative LXR ligand is short-lived, or it may only function in a cell autonomous manner at high local concentrations.

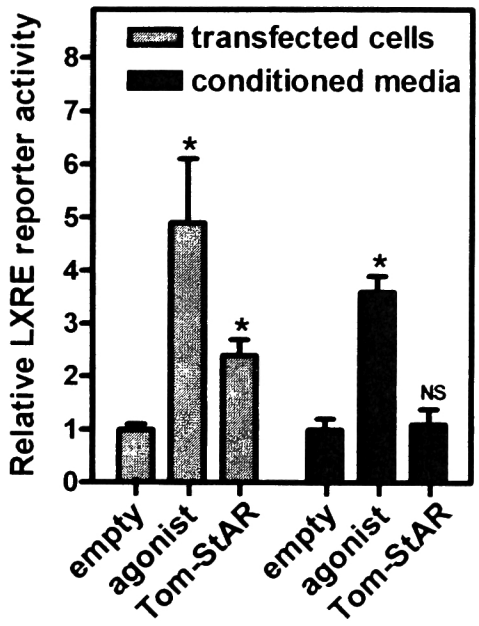

Figure 4.10: Conditioned media from START expressing cells does not stimulate an LXRE reporter in other cells.

Two groups of COS-1 cells were transfected as before with the LXRE luciferase reporter, LXRα, and RXRα. In the first group (gray), the LXR agonist T0907317 was added or FLAG-Tom20-StAR was co-transfected. After 24 hours, media from these cells was transferred to the group of cells (black) that did not receive these additional treatments. After another 24 hours, luciferase activity was measured as before. $P<0.05$ vs. empty vector.

Targeting construct for StarD4 knockout mice: The cell culture experiments described in this chapter show that overexpressed StarD4 or StarD5 have effects on intracellular cholesterol metabolism, but it is unknown whether they mediate such functions *in vivo*. Gene targeting by homologous recombination has been an invaluable tool for determining the physiological functions of many genes, so StarD4 and StarD5 knockout mice would be informative. We were unable to design a StarD5 targeting construct due to gaps in the available genomic sequences, but StarD4 was more amenable to this approach.

Since cholesterol is important for normal physiology and development, a traditional global knockout of StarD4 could cause embryonic lethality or other developmental defects. While such phenotypes would be interesting, we also sought to address the role of StarD4 in adult tissues. Therefore, a conditional targeting construct utilizing Cre-Lox technology (Nagy, 2000) was generated for StarD4 (Figure 4.11a-b). Exon 3 was targeted for deletion, since loss of this 50bp exon would cause a frameshift in the remaining sequence. An ~11 kB *Kpn*I fragment of StarD4 was generated by digesting the BAC AC020796. A LoxP site was cloned into the *Bss*SI site of intron 2, while a neomycin resistance cassette flanked by two

LoxP sites was cloned into the *Mfe*I site of intron 3. After homologous recombination of this construct in ES cells (Figure 4.11b), partial Cre-mediated excision of the neomycin resistance cassette would generate the targeted allele, with exon 3 flanked by two LoxP sites (Figure 4.11c). Mice carrying this allele would be crossed to transgenic mice expressing Cre in various tissues, such as liver or macrophage, resulting in tissue-specific excision of exon 3 and gene disruption. Global disruption of StarD4 could also be obtained by this strategy, either by crossing mice with the targeted allele to a germline Cre-expressing line, or by complete Cre recombination in the targeted ES cells (Figure 4.11d). Southern blot probes were generated to distinguish among these various StarD4 alleles in genomic DNA digested with *Pst*I or *Hpa*I. Unfortunately, the StarD4 targetting construct, with a long arm of ~9 kB and a short arm of ~1.5 kB, failed to give any homologous recombinants in almost 200 ES cell colonies. We decided to modify this construct by lengthening the short arm, and StarD4 knockout mice remain to be generated.

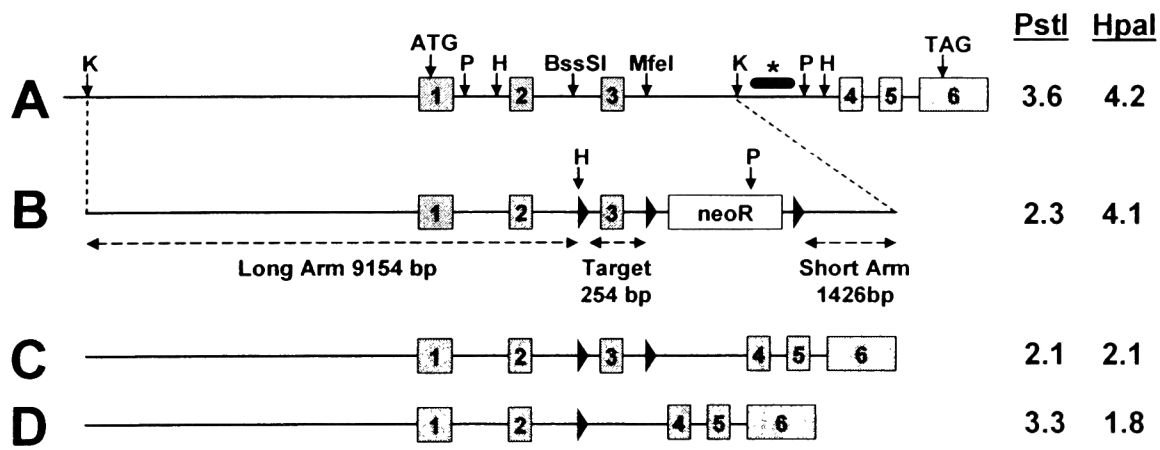

Figure 4.11: Targeting construct for a StarD4 conditional knockout mouse.

(A) The wild type mouse StarD4 gene has six exons. The start (ATG) and stop (TAG) codons are indicated, as well as certain restriction sites: *Bss*SI, *Mfe*I, K=*Kpn*I, P=*Pst*I, H=*Hind*III. (B) An ~11 kB *Kpn*I fragment of StarD4 was used to clone this targeting construct (see text for details). Triangles are LoxP sites. After homologous recombination in ES cells, partial Cre-mediated excision would generate this targeted allele (C), while complete Cre-mediated excision in ES cells or in mice would generate this knockout allele with exon 3 deleted (D). Southern blots with the probe shown (*) would distinguish among these four alleles (A-D) based on the size of *Pst*I or *Hpa*I fragments (in kB) as shown on the right.

Chapter Summary: This chapter describes three transient transfection cell culture assays in which overexpressed StarD4 and StarD5 showed activity: (1) StAR-like stimulation of steroidogenesis, (2) repression of an SREBP reporter, and (3) activation of and LXR reporter. StarD4 or StarD5 expression constructs from mouse or human showed similar activities (data not shown). These data strongly suggest that StarD4 and StarD5 function in intracellular sterol metabolism or transport. Consistent with this hypothesis, the known cholesterol-binding START domains of StAR and MLN64 were also active in these assays, while PCTP was an inactive negative control. All five START domains, which were expressed with FLAG epitope tags, appeared evenly distributed throughout the cell. In functional assays, we also tested mutant StarD4 and MLN64 proteins (with amino acid substitutions affecting salt bridges in the lipid binding cavity) and START domains fused to Tom20 (a mitochondrial outer membrane protein). A targeting construct for mouse StarD4 was cloned, though knockout mice have yet to be generated.

Chapter 5: StarD6 expression in male germ cells

StarD6 is not expressed in steroidogenic Leydig cells: The prototypical START gene, StAR, is highly expressed in steroidogenic cells of the testis, ovary, and adrenal (Stocco, 2001). Multiple tissue Northern blots showed StarD6 mRNA only in the testis (see Figure 2.12). Even sensitive RT-PCR assays failed to detect StarD6 expression in other tissues including ovary and adrenal (data not shown). Therefore, StarD6 is unlikely to function globally in steroidogenesis, but it may nonetheless be expressed in the androgen-producing Leydig cells of the testis. To test this hypothesis, we cultured MA-10 mouse Leydig tumor cells with and without steroidogenic stimulation. As expected, stimulation with a cAMP analog resulted in a 13-fold increase in production of the steroid pregnenolone (Figure 5.1a), and a corresponding large increase in both StAR mRNAs (Figure 5.1b). However, StarD6 mRNA was undetectable in these immortalized Leydig cells, regardless of steroidogenic stimulation, despite strong expression in whole mouse testis. Indeed, Northern blots of testis

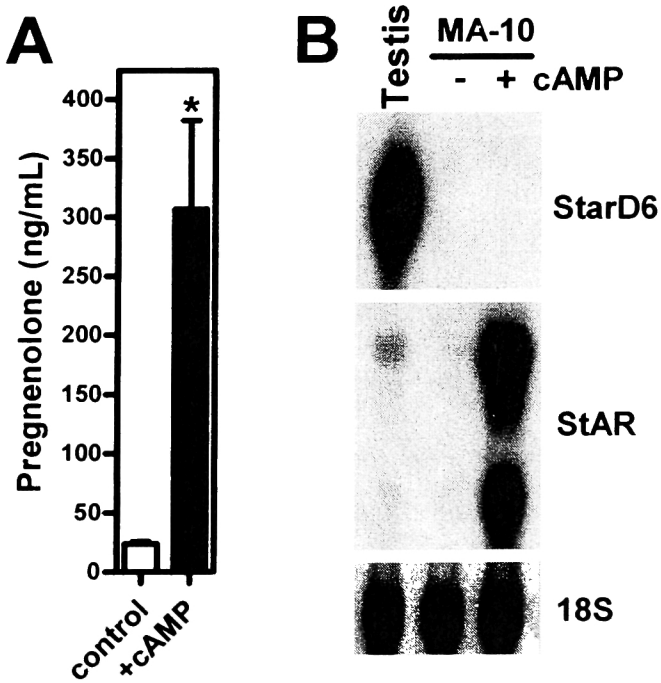

Figure 5.1: StarD6 is not expressed in the steroidogenically active MA-10 Leydig tumor cell line.
MA-10 cells were cultured for 24 hours in control media or with 8-bromo-cAMP to activate steroidogenesis (n=3 wells each). (A) Media pregnenolone levels were measured by ELISA. (B) Total RNA was extracted for Northern blotting with StarD6 and StAR probes. RNA from whole testis was a positive control for StarD6 expression. Ethidium bromide staining of 18S rRNA shows equal RNA loading in each lane.

total RNA probed for StarD6 gave good signals on radiographs after very short exposures (less than one hour), consistent with high basal expression levels Lack of detectable StarD6 in a steroidogenically active Leydig cell line strongly argues against StarD6 expression in this cell type of the testis.

StarD6 expression is absent in germ cell-deficient testis: There are three major cell types unique to the testis: the male germ cells and the somatic Leydig and Sertoli cells. The Sertoli cells are located in the seminiferous tubules with germ cells, where they play key roles in spermatogenesis. To determine whether StarD6 is expressed in germ cells, we obtained germ cell-deficient male mice with mutations in the receptor tyrosine kinase c-Kit. These sterile Kit W/Wv mice fail to maintain primordial germ cells, so the adult testis lacks virtually all germ cells (Ohta et al., 2003), while androgen production by Leydig cells is normal and Sertoli cells are present with relatively normal morphology (De Franca et al., 1994; Kurohmaru et al., 1992). StarD6 expression was undetectable in Kit W/Wv testis, but present in the wild type littermate control and C57BL/6 testis (Figure 5.2a). StAR, however, was still present in the Kit W/Wv testis consistent with expression in Leydig cells. The other controls were as expected: StarD6 and StAR were undetectable in liver, and the germ cell-specific GAPDH transcript was present in wild type testis but not Kit W/Wv. Expression of StAR and StarD6 in these mice was also analyzed by qPCR normalized to HPRT. The data showed ~3000-fold less StarD6 in the germ-cell deficient testis (Figure 5.2b).

This experiment strongly indicates that StarD6 mRNA is normally expressed in male germ cells. Kit W/Wv mice have been used by many other groups to distinguish between somatic and germ cell mRNA expression in testis (Chen et al., 1997; Sugihara et al., 1999). However, there are complex interactions among somatic and germ cells in the testis, some mediated by c-Kit: Sertoli cells express the ligand for c-Kit (Rossi et al., 2000), and Leydig

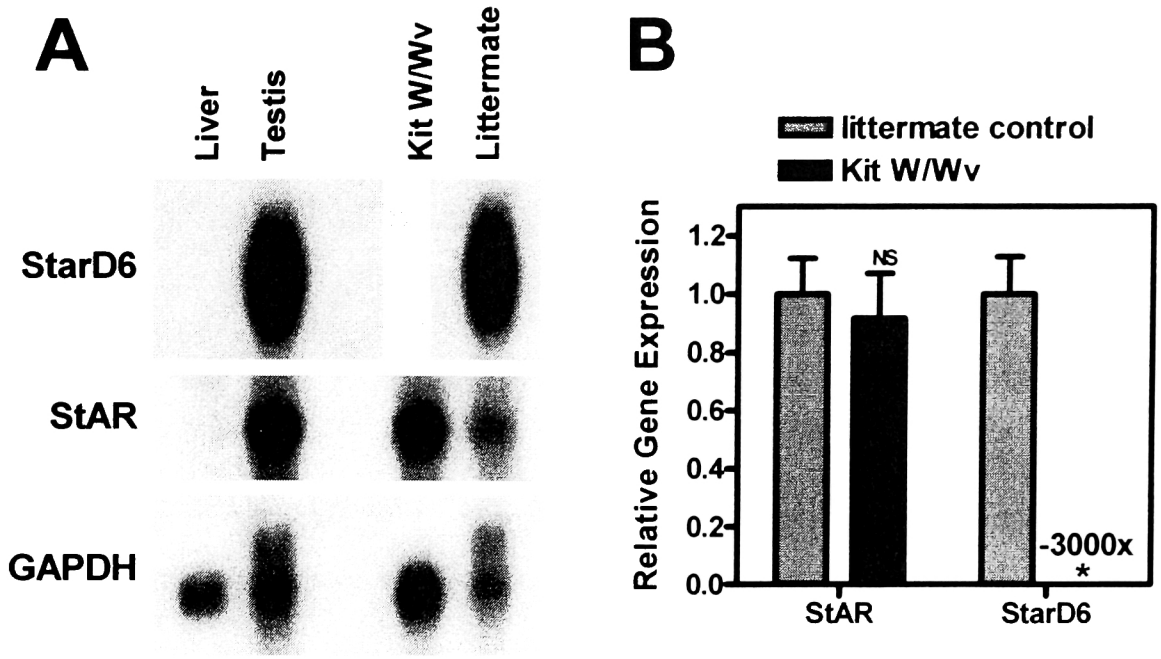

Figure 5.2: Testis StarD6 expression is absent in Kit W/Wv germ cell deficient mice.
(A) Total RNA was extracted from C57BL/6 mouse liver and testis, and from the testis of a Kit W/Wv germ cell deficient mouse and a wild type littermate. The Northern blot was probed for StarD6, StAR, and GAPDH. (B) qPCR analysis of gene expression of in testis of the Kit W/Wv and littermate control mice. Expression of StAR and StarD6 was normalized to hypoxanthine guanine phosphoribosyl transferase (HPRT), and the same cDNA sample was analyzed in quadruplicate. *P<0.05 vs. control.

cells normally express c-Kit (Yan et al., 2000). Therefore, it remained possible that StarD6 was expressed in other cell types in a germ cell- or c-Kit-dependent manner.

Expression of StarD6 in male germ cells: To confirm specific StarD6 expression in germ cells, we obtained several Northern blots from the laboratory of Patricia Morris and probed for StarD6 expression. First, whole testis StarD6 expression was assayed in rodents at various days of postnatal development. StarD6 mRNA was undetectable at early time points, expressed by day 20 in mice and day 25 in rats, and increased to adult levels thereafter (Figure 5.4). This developmental expression at puberty coincides with germ cell proliferation and the differentiation of specific germ cells at the onset of spermiogenesis (Yamanaka et al., 2000).

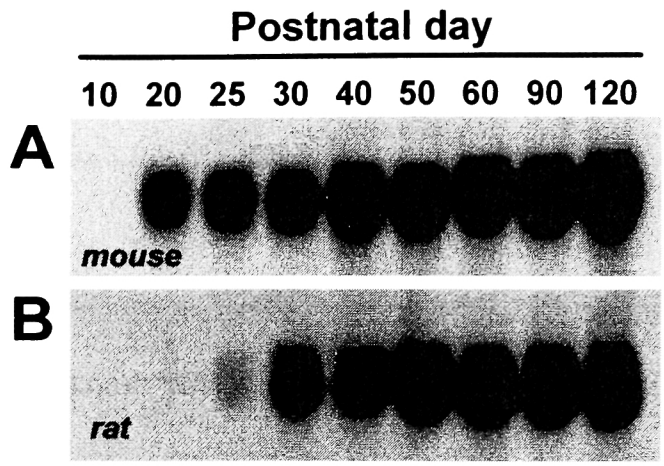

Figure 5.3: Testis StarD6 expression increases during puberty in mice and rats. The laboratory of Patricia Morris prepared Northern blots of whole testis total RNA at different times of postnatal development in mice (A) and rats (B). Equal RNA was loaded in each lane (data not shown). We hybridized these blots with a mouse StarD6 probe.

Next, StarD6 expression was assessed in total RNA from elutriator-purified populations of cells from rat testis (Figure 5.4a). StarD6 was strongly expressed in germ cells at different stages of development: the mitotic stem cells (spermatogonia), the meiotic cells (pachytene spermatocytes), and the haploid cells (round and elongated spermatids), which differentiate into spermatozoa. StarD6 mRNA was detected in the adult Sertoli cell preparation, but this preparation is typically contaminated with about 10% germ cells (mostly testicular sperm); StarD6 expression was not detected in three Sertoli cell lines (data not shown). StarD6 was also undetectable in freshly isolated Leydig cells (>98% pure),

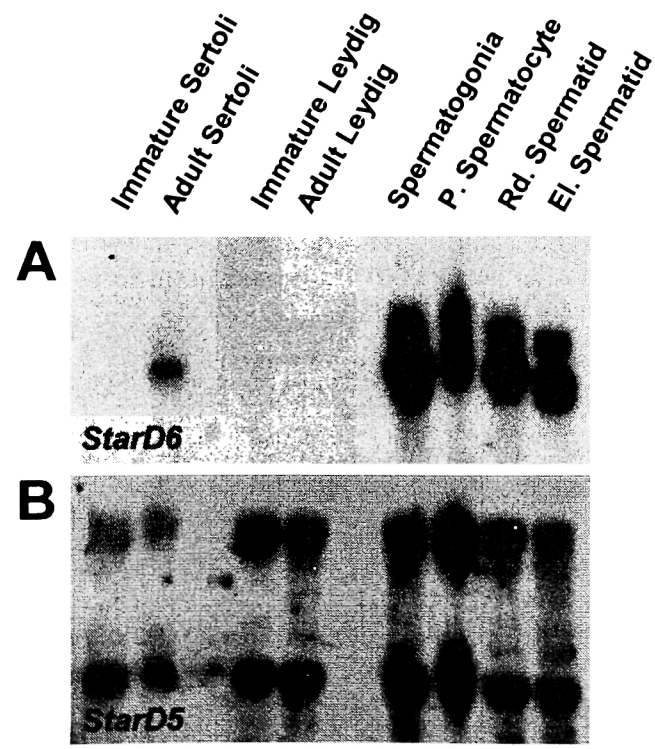

Figure 5.4: In isolated rat testis somatic and germ cells, StarD6 mRNA is expressed in germ cells at all stages of development. The laboratory of Patricia Morris elutriator-purified populations of somatic and germ cells from rat testis, extracted RNA, and prepared a Northern blot. Some closely associated cells types are difficult to separate, as the adult Sertoli cell preparation is typically contaminated with ~10% germ cells (data not shown). We hybridized this blot with probes for mouse StarD6 (A) or StarD5 (B).

consistent with the result in the MA-10 cell line (see Figure 5.1). In contrast, StarD5 expression was detected almost uniformly in Sertoli, Leydig, and germ cell populations (Figure 5.4b). StarD6 mRNA expression thus appears restricted to male germ cells.

Finally, StarD6 expression was assayed in mouse isolated germ cells and staged seminiferous tubules. Consistent with the result in rats, mouse StarD6 was expressed similarly in spermatogonia, pachytene spermatocytes, and round spermatids (Figure 5.5a). Likewise, there were no large differences in StarD6 expression in seminiferous tubules at different stages of spermatogenesis (Figure 5.5b). Therefore, StarD6 mRNA appears present in germ cells at all stages of development. However, this does not necessarily mean that the protein is also present at all stages. Germ cells often rely on translational regulation of mRNAs, since they become transcriptionally inactive during the later steps in spermiogenesis (Eddy, 1998). Indeed, the StarD6 mRNA is predicted to have long multi-exon 5'UTR with multiple upstream ATGs (see Figure 2.11), consistent with translational regulation (Morris and Geballe, 2000).

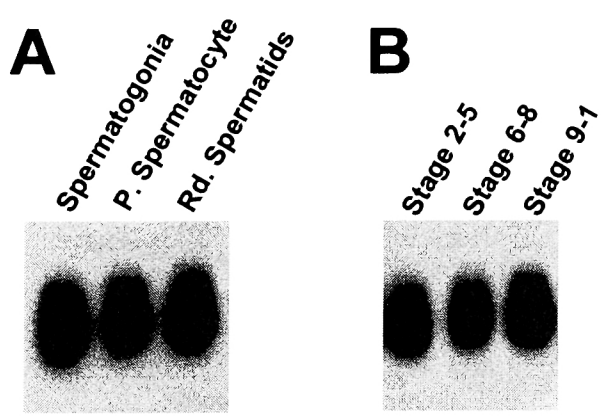

Figure 5.5: Mouse StarD6 mRNA is expressed in germ cells and seminiferous tubules at all stages. The laboratory of Patricia Morris prepared Northern blots of RNA from mouse elutriator-purified germ cells (A) or staged seminiferous tubules (B). Equal RNA was loaded in each lane (data not shown). We hybridized these blots with a mouse StarD6 probe.

5' RACE analysis of StarD6: To further characterize the 5' UTR of StarD6 and to identify the gene promoter, we performed a 5' RACE analysis of mouse and human StarD6. Mouse StarD6 had three non-coding exons upstream of the exon with the start codon, as predicted from available mouse ESTs, while human StarD6 had only two upstream exons (Figure

5.7a). ATG codons in these 5' exons give several upstream ORFs, but none extended into the StarD6 coding region due to an in-frame TAG stop codon immediately before the ATG start codon. Therefore, protein coding begins in mouse exon 4 and human exon 3.

5'-RACE also identified alternative first exons for both the mouse and human StarD6 genes. Exon 1b accounted for 7 of 12 mouse StarD6 RACE clones, while 3 clones had exon 1a and two had exon 1c (Figure 5.7b). Multiple transcription initiation sites were also found in each of these three first exons, which were near each other in the genomic sequence. For human StarD6, exon 1 predominated over exon 1' with 13 of 16 RACE clones, though there five different initiation sites in this exon (Figure 5.7c). Despite these complications, a +1 site for promoter numbering was designated in mouse and human StarD6 based on the most abundant initiation sites.

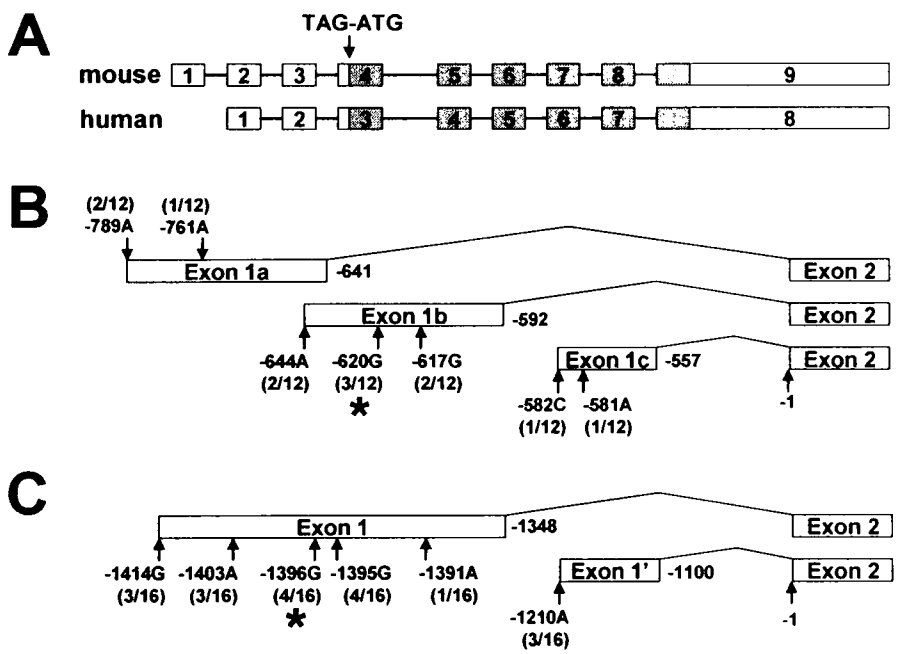

Figure 5.6: Rapid Amplification of cDNA ends (5' RACE) results for mouse and human StarD6. (A) In both mouse and human StarD6, the ATG translation initiation codon is immediately preceded by a TAG stop codon. Upstream of this, there are three non-coding exons in mice and two in humans. Alternate first exons and transcription initiation sites were identified for both the mouse (B) and human (C) StarD6 genes. The initiation sites are numbered based on their distance upstream of exon 2, and the number of RACE clones for each site is indicated (total n=12 for mouse, n=16 for human). For numbering the StarD6 promoter, the (*) initiation sites were designated as +1.

A problem was noted in the 5' RACE analysis of human but not mouse StarD6, as the cDNAs cloned could not encode the entire predicted StarD6 START protein. Using the gene specific RACE primer in exon 5, several products included predicted intron 3 sequence, while others had skipped exons (Figure 5.7a). Similar products were generated by RT-PCR of human StarD6 using primers in exons 2 and 8. Multiple bands were amplified, cloned, and sequenced, revealing the presence of intron 3 sequence or the absence of exons (Figure 5.7b). The template RNA for both 5'-RACE and RT-PCR was commercially available (Clontech) human testis RNA pooled from over 50 subjects. We saw similar problems in StarD4 RT-PCRs using human liver RNA from the same company (see Figure 2.4). There may be frequent mis-splicing human StarD4 and StarD6 RNAs, though we did not find this in mouse RNA prepared ourselves. Alternatively, the commercially available human RNAs may contain abundant heterogeneous nuclear RNAs rather than mature mRNAs.

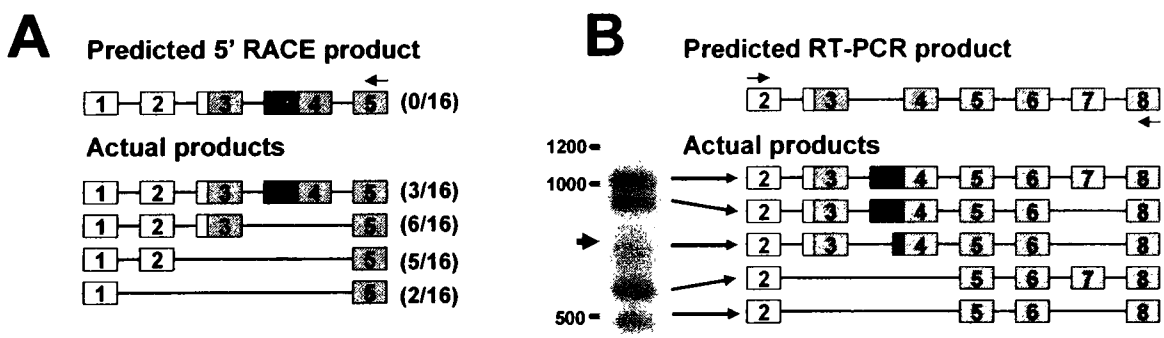

Figure 5.7: Mis-spliced human StarD6 RACE and RT-PCR products.
(A) 16 human StarD6 RACE products were generated with a gene specific primer in exon 5. Sequencing revealed that none could encode the full predicted START domain, due to unexpected splice patterns. (B) Primers in exons 2 and 8 were used to RT-PCR amplify StarD6 from the same commercial source of human testis RNA. Most RT-PCR products were longer or shorter than the predicted length (arrow). These products were sequenced, again revealing mis-spliced mRNAs.

The StarD6 promoter: The genomic sequence upstream of the designated +1 sites for mouse and human StarD6 was analyzed for potential promoter elements. A region of 120 bp was

highly conserved between mouse and human StarD6, with 76% identity (Figure 5.8a). This region was upstream of mouse exon 1b, but actually fell within mouse exon 1a. No human RACE products included this sequence, and there was no apparent sequence homology among the upstream exons of mouse and human StarD6. This is consistent with divergence of non-coding DNA in the upstream exons, so the conserved 120 bp was considered promoter and potential factor binding sites were identified using TRANSFAC (Matys et al., 2003). This analysis revealed a conserved strong consensus YY1 site on the negative DNA strand. This putative YY1 site agreed with the core consensus at 8 of 9 positions, including the requisite CCAT (Figure 5.8b). Though YY1 is a widely expressed transcription factor that acts at many promoters (Thomas and Seto, 1999), it has also been implicated in germ cell specific gene expression. Similar YY1 sites have been found in six germ cell-specific genes: proacrosin, protamines 1-3, and transition proteins 1-2 (Schulten et al., 1999). Other elements important for specific gene expression in germ cells remain to be identified in germ cell specific genes like StarD6.

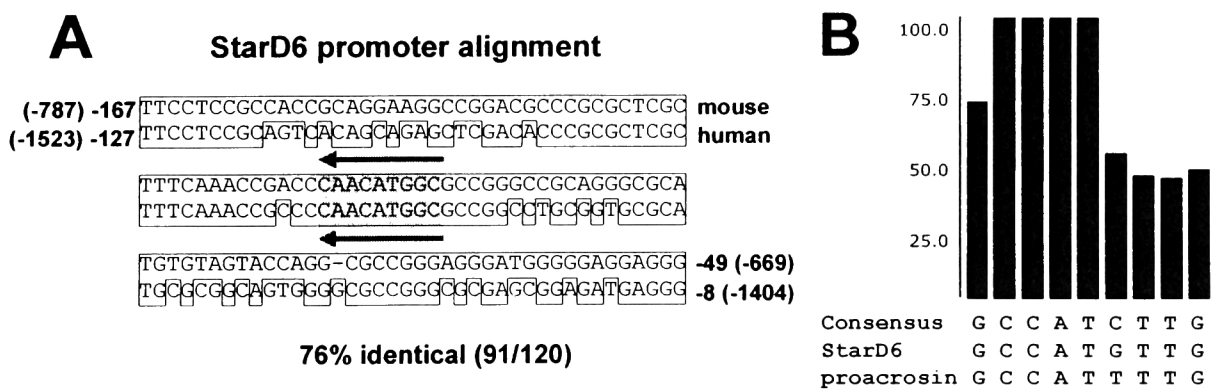

Figure 5.8: Conserved region of the mouse and human StarD6 proximal promoters.
This StarD6 upstream non-coding sequence was conserved between mice and humans, but not present elsewhere in the genome. The distances are indicated from the designated +1 sites as well as from the start of exon 2 (see Figure 5.6). A conserved putative YY1 site was identified on the negative DNA strand (arrows). (B) The potential YY1 site in the StarD6 promoter agreed well with the consensus and with the site in proacrosin, another male germ cell specific gene. The graph indicates the strength of the YY1 consensus based on many promoters from the TRANSFAC database (Matys et al., 2003).

Targeting construct for StarD6 knockout: Given its highly specific expression in male germ cells, StarD6 is likely to function in male fertility. Cholesterol and other sterols have been implicated in many aspects of male fertility, so there are several pathways where a putative sterol binding protein could act (see discussion, Figure 6.6). We hypothesized that male StarD6 knockout mice may be infertile, and the specific defect in sperm development or function would indicate the role of StarD6. Since this gene is only expressed in male germ cells, which are not essential for viabilty, there was no need to design a conditional knockout strategy. A traditional knockout construct was cloned to inactivate the gene on chromosome 18 (Figure 5.9). The long arm was a ~5.8 kB restriction fragment of StarD6 from the 5' flanking region to intron 3, while the short arm was a ~0.7 kB PCR product from intron 5. In this targeting construct, a neomycin resistance cassette replaced exons 4 and 5, which encode the N-terminal ~50 amino acids of the START domain. To identify ES cells with homologous recombination, a Southern blot probe was designed to detect different EcoRI fragments from wild type and knockout alleles. Unfortunately, almost 150 ES cell colonies were screened and no recombinants were detected. We decided to generate a new StarD6 construct by targeting different exons and lengthening the short arm.

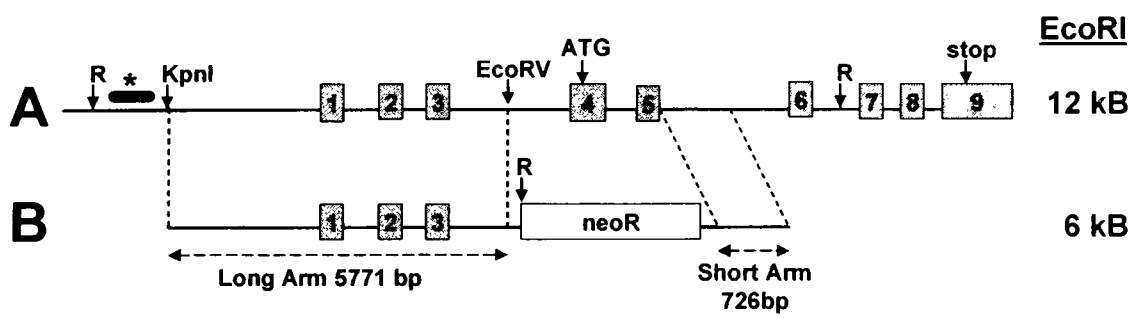

Figure 5.9: Targeting construct for a StarD6 knockout mouse.

(A) The wild type mouse StarD6 gene on chromosome 18 has six exons. The start (ATG) and stop codons are indicated, as well as certain restriction sites: KpnI, EcoRV, and R=EcoRI. (B) This targeting construct for StarD6 was cloned (see text for details). A StarD6 knockout allele would be generated by homologous recombination in ES cells (dashed lines). Southern blots with the probe shown (*) would distinguish wild type and knockout alleles based on the size of EcoRI fragments as shown on the right.

Chapter summary: This chapter describes the expression of StarD6 mRNA, which showed a much more limited tissue distribution than StarD4 and StarD5. Multiple lines of evidence indicate that StarD6 mRNA is specifically expressed in the germ cells of the testis. However, StarD6 was not expressed in the steroidogenic Leydig cells or the epithelial Sertoli cells, both somatic cells critical for germ cell development. The 5' end of the StarD6 mRNA in mice and humans had multiple non-coding exons and upstream ORFs, indicative of translational regulation. Therefore, even though StarD6 mRNA was present at all stages of germ cell development, protein expression may be regulated during spermatogenesis. A targeting construct was cloned to generate StarD6 knockout mice, which are predicted to have male fertility defects.

Chapter 6: Discussion and Future Directions

Here we describe a novel subfamily of three StAR-related lipid transfer proteins and the regulated gene expression for each one. StarD4 was activated by SREBP-2, an important transcription factor in cholesterol homeostasis (Horton et al., 2002), while StarD5 was activated by the ER stress response, a pathway recently implicated in apoptosis of cholesterol-loaded macrophages (Feng et al., 2003a). StarD6 expression was limited to the germ cells of the testis. To test the hypothesis that these proteins function in the intracellular metabolism or transport of sterols, we overexpressed START proteins in cultured cells.

Models of StarD4 and StarD5 activity in the three functional assays

StarD4 and StarD5 showed activity in three cell culture assays: (1) StAR-like activation of steroidogenesis, (2) repression of an SREBP reporter, and (3) activation of an LXR reporter (Figure 6.1). The cholesterol-binding START domains of StAR and MLN64 were active in these assays, while PCTP was an inactive negative control. The results of

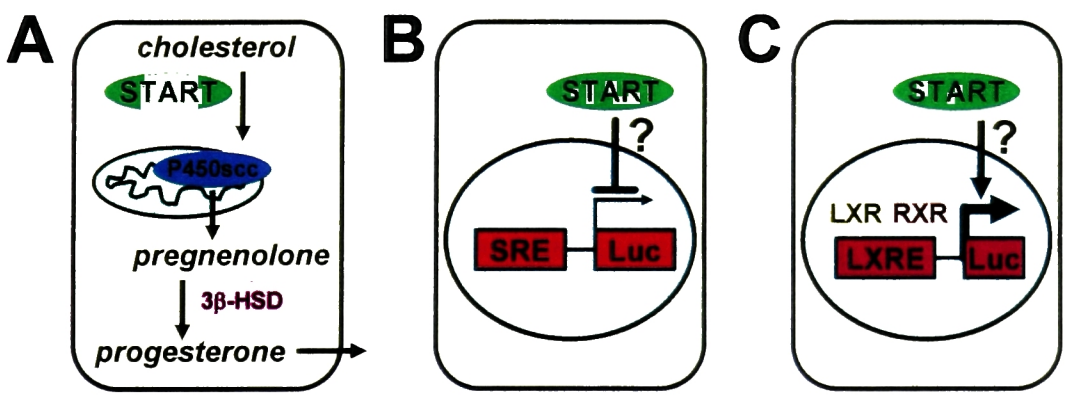

Figure 6.1: StarD4 and StarD5 showed activity in three functional assays.
In each assay, the cholesterol-binding START domains of StAR and MLN64 were also active, while PCTP was inactive. (A) When co-transfected with expression plasmids for the enzymes P450scc and 3β-hydroxysteroid dehydrogenase, they stimulated steroidogenesis. (B) When co-transfected with an SRE-regulated reporter, they decreased luciferase activity. (C) When co-transfected with an LXRE-regulated reporter and expression plasmids for LXRα and RXRα, they increased luciferase activity.

these experiments can be unified by a model involving cholesterol delivery to mitochondria. The P450scc enzyme localizes to the matrix side of the inner mitochondrial membrane, so StAR-like steroidogenic activity reflects delivery of cholesterol substrate to this compartment (Figure 6.1a). Sterol 27-hydroxylase (Cyp27) is another cholesterol-metabolizing enzyme at the same location as P450scc (Okuda, 1994). In contrast to the steroidogenic enzyme, Cyp27 is expressed in liver and many other cell types. Others have shown that StAR can deliver substrate to Cyp27 (Sugawara et al., 1995b), so it is likely that the MLN64 START domain, StarD4, and StarD5 share this activity. Generation of 27-hydroxycholesterol is consistent with the observed repression of SREBP activity and stimulation of LXR activity (Figure 6.2), since this oxysterol is an known inhibitor of SREBP processing and agonist of LXRs (Russell, 2000). 27-hydroxycholesterol also represents the first intermediate in hepatic alternative bile acid synthesis, and StAR overexpression in primary hepatocytes stimulates this pathway (Pandak et al., 2002). Since StAR is not expressed to high levels in liver, and MLN64 is localized to late endosomal membranes, StarD4 or StarD5 could therefore stimulate alternative bile acid synthesis *in vivo*.

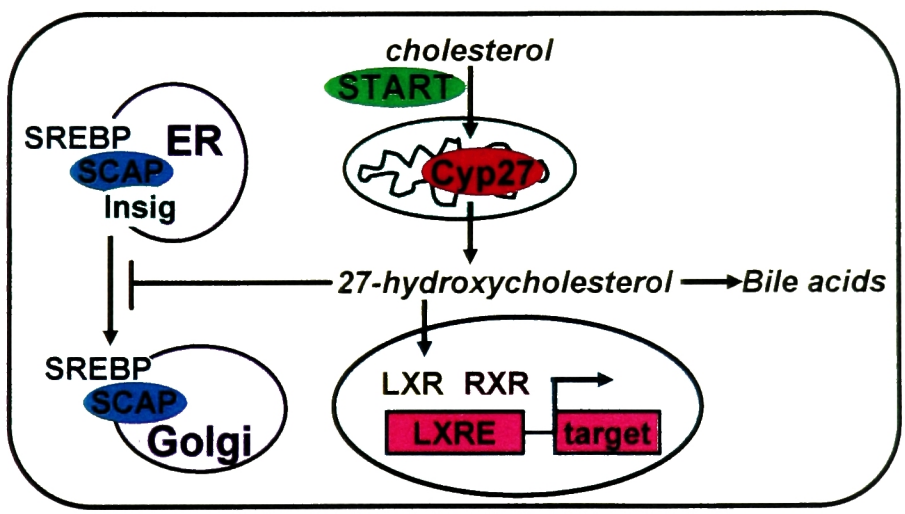

Figure 6.2: Model for StarD4 and StarD5 activity via generation of 27-hydroxycholesterol. Like the P450scc enzyme in steroidogenesis, cholesterol 27-hydroxylase (Cyp27) localizes to the matrix side of the inner mitochondrial membrane. 27-hydroxycholesterol can repress SREBPs, activate LXRs, and serve as the substrate for bile acid synthesis in liver by the alternative pathway.

Other models not involving mitochondrial Cyp27 could also account for some of the observed activities. For instance, START domains may deliver substrate to cholesterol 25-hydroxylase in ER and Golgi, and 25-hydroxycholesterol would repress SREBPs and activate LXRs like 27-hydroxycholesterol (Russell, 2000). Furthermore, 25-hydroxycholesterol can serve as a substrate for P450scc (Lukyanenko et al., 2001), so induction of steroidogenesis may proceed by this alternate route rather than direct delivery of cholesterol to mitochondria. Effects on cholesterol biosynthesis could also account for START domain regulation of SREBPs and LXRs, as cholesterol precursors can have effects on these transcription factors. The precursor desmosterol alters the conformation of SCAP similarly to cholesterol itself (Brown et al., 2002), while 24(S),25-epoxycholesterol derived from cholesterol biosynthesis is high affinity LXR ligand (Spencer et al., 2001). Finally, it is possible that these START domains have direct transcriptional effects as positive or negative cofactors for LXRs or SREBPs. There is a precedent for transcriptional activity by proteins not traditionally considered transcription factors, as the housekeeping enzyme glyceraldehyde-3-phosphate dehydrogenase (GAPDH) was recently shown to be a crucial component of a coactivator complex (Zheng et al., 2003). However, four different START domains showed activity, even though the StAR and StarD4 subfamilies share ~20% amino acid identity, arguing against specific cofactor activity for any one START protein. Given the extensive literature that StAR delivers cholesterol to mitochondria, it is more likely that these START domains are delivering cholesterol to Cyp27 as opposed to alternate models.

Comparison of the StarD4 subfamily to other START proteins

Unlike many other START proteins, StarD4, StarD5, and StarD6 lack additional domains for localization or enzymatic activity. StAR and MLN64 have N-terminal domains

that target the full-length proteins to mitochondria and late endosomes, respectively (Strauss et al., 2003). StarD4 subfamily members lack consensus localization signals and are predicted to be cytosolic like three other minimal START domains: full-length PCTP (de Brouwer et al., 2002) and the artificial START-only StAR and MLN64 proteins (Arakane et al., 1996; Zhang et al., 2002b). Consistent with this prediction, overexpressed EGFP-StarD4 and FLAG-tagged StarD4 and StarD5 showed even distributions through the cytoplasm and nucleus. Similar localization was observed for the FLAG-tagged PCTP and START domains of StAR and MLN64. However, these studies do not rule out specific localization of endogenous proteins or regulated re-localization in response to stimuli.

In other START proteins, lipid binding could serve a regulatory role, perhaps allosterically regulating N-terminal RhoGAP or thioesterase domains. The StarD4 subfamily lacks such domains, though it is possible that they interact with other proteins to regulate them upon lipid binding. However, we favor the hypothesis that StarD4, StarD5, and StarD6 function like StAR and PCTP, shuttling lipids between intracellular membranes. Interacting proteins could also play roles in lipid transport, either targeting lipid transfer to specific subcellular locations or facilitating loading or unloading of cavity lipids, which would require major conformation changes based on the START structure.

The X-ray crystal structure of StarD4 was described here, and the structures of the MLN64 START domain (Tsujishita and Hurley, 2000) and PCTP (Roderick et al., 2002) have also been solved. The three structures share a helix-grip fold with a predominantly hydrophobic lipid binding cavity. Charged residues in the cavities form salt bridges that may be important for protein folding or lipid binding specificity. StAR and MLN64 have a unique salt bridge between charged residues in β5 and β6, rather than one in αC like the StarD4 subfamily, PCTP, and most other START domains. The salt bridge in αC was predicted to help stabilize binding of zwitterionic phospholipid head groups (Tsujishita and

Hurley, 2000), but the PCTP structure showed Asp82 is too distant from the positive quaternary amine of PC to serve this function (Roderick et al., 2002). However, Arg82 in the PCTP αC salt bridge directly interacts with a phosphoryl group of PC, so this salt bridge was still considered a potential lipid specificity determinant (Roderick et al., 2002).

This salt bridge model predicts that the StarD4 subfamily would bind phospholipids, yet our functional data strongly suggest sterol transfer. Therefore, we performed site-directed mutagenesis of these salt bridges in StarD4 and MLN64. Surprisingly, proteins lacking both salt bridges (mutants designated *none*) showed equal activity to the corresponding wild type proteins in assays for steroidogenesis and LXR activation. This strongly indicates that cavity salt bridges are not essential for function. Others have reported loss of steroidogenic activity in the lipoid CAH StAR mutants Glu169Gly or Glu169Lys, which eliminate the negative charge of the β5/β6 salt bridge (Bose et al., 1996). Biophysical studies that preceded the START structures predicted misfolding of the StAR Glu169Gly mutant (Bose et al., 1998), but this mutant had an unbalanced positive charge in the cavity. This is analogous to the MLN64 mutant *B* generated here, which showed a trend towards lower activity, but when we also mutated the positive residue of this MLN64 salt bridge the double mutant protein (*none*) had full steroidogenic activity. Furthermore, StarD4 mutant *B*, with an Arg in β6 but Tyr rather than a negative charge in β5, showed its full activity, in contrast to the CAH StAR mutants with Gly or Lys substituted in β5. This may reflect the nature of the specific substitution, or differences among START domains in tolerance for substitutions. Overall, the role of salt bridges in START domains is much more complicated than previously appreciated. Additional structure-function studies, as well as more START crystal structures with lipid ligands, will be necessary to resolve these issues.

StarD4 subfamily functions appear distinct from StAR and steroidogenesis. While StAR expression is limited to steroidogenic cells, StarD4 and StarD5 are widely expressed,

and StarD6 is only expressed in germ cells, not Leydig cells, of the testis. StarD4 and StarD5 were expressed in MA-10 Leydig cells, but steroidogenic stimulation with a cAMP analog did not highly induce their expression like StAR, which was activated 50-fold. StarD4 and StarD5 were active in the transient transfection steroidogenesis assay, so they are candidates for the phenomenon of StAR-independent steroidogenesis (Miller and Strauss, 1999). However, they clearly cannot substitute for StAR function, as StAR mutations cause the disease lipoid CAH even with presumably intact StarD4 and StarD5 genes.

A connection between StarD4 or StarD5 and MLN64 is possible, though there is little evidence. All three are widely expressed, but MLN64 mRNA expression was not regulated by SREBPs like StarD4, by ER stress like StarD5, or by LXRs (data not shown). In ES cells heterozygous for inactivated MLN64, there is a two-fold increase in StarD4 mRNA suggesting potential functional compensation (Strauss et al., 2003). However, MLN64 is thought to function in cholesterol efflux from endosomes (Strauss et al., 2002), so StarD4 induction could reflect SREBP activation due to altered intracellular cholesterol trafficking. Homozygous deletion of MLN64 in knockout mice has yet to be reported. MLN64 localizes to the membranes of late endosomes (Alpy et al., 2001), but there is no evidence for StarD4 or StarD5 in this compartment. They could nonetheless function in an endosomal cholesterol efflux pathway, perhaps as cytosolic acceptors downstream of MLN64 and NPC proteins.

Several lines of evidence support the idea that StarD4 subfamily proteins bind and transfer cholesterol or other sterols: StarD4 is regulated by SREBP-2, the subfamily resembles StAR and MLN64, and the StarD4 and MLN64 lipid-binding cavities are similar in size and shape. Most convincing, StarD4 and StarD5 showed similar activity to the StAR and MLN64 START domains in three functional assays, while PCTP was inactive. Based on lipid transfer studies of StAR and PCTP, START domain are thought to be rather specific lipid binding proteins (Tsujishita and Hurley, 2000). This is in contrast to other proteins like

SCP-2 (Seedorf et al., 2000) and SPF (Panagabko et al., 2003), which bind promiscuously to many structurally different classes of lipids. StarD4 and StarD5 are likely involved in fundamental processes like intracellular sterol transport or cholesterol biosynthesis. This hypothesis is consistent with their ubiquitous expression, since all cells must handle cholesterol, as well as their abundance in liver, the central organ of cholesterol metabolism. In contrast, StarD6 expression was restricted to male germ cells, indicating a specialized role in fertility. The remaining discussion will address each StarD4 subfamily gene, proposing functions consistent with observed regulation and activities.

StarD4: an SREBP-2 target gene with potential roles in cholesterol synthesis or uptake

Like many other genes in cholesterol metabolism, StarD4 expression is regulated by sterols via SREBP transcription factors. StarD4 showed coordinate regulation with other SREBP target genes in three experimental systems. First, cholesterol feeding of wild type inbred mice decreased StarD4 expression in liver. Second, culturing cells with cholesterol and 25-hydroxycholesterol, a well-established treatment to inhibit SREBPs, likewise decreased StarD4 expression. This result was observed in fibroblast (NIH 3T3), hepatoma (Hepa-1), and macrophage (RAW) cell lines. Third, liver StarD4 expression was activated in transgenic mice overexpressing processed nuclear SREBP-2, but not significantly with SREBP-1a. This is consistent with the failure of LXR agonists, which activate SREBP-1c and lipogenesis in liver, to affect StarD4 expression. In liver, StarD4 thus appears to be a poor target for SREBP-1, with preferential activation by SREBP-2.

Further studies investigated the mouse and human StarD4 promoters in transient transfection reporter assays. 5' RACE revealed differences between the mouse and human StarD4 genes, with mouse exon 1 encoding 14 amino acids while human exon 1 included

only 5'UTR. These first exons were poorly conserved between the species, but both genes showed multiple +1 transcription start sites and lack of a consensus promoter TATA box. Two regions of upstream genomic sequence were highly conserved between species, the proximal promoter and a distal potential enhancer region over 1 kB upstream. Luciferase reporters driven by the mouse or human StarD4 promoters were sterol-regulated in NIH 3T3 fibroblasts, consistent with the regulation of the endogenous gene. Activity and regulation were observed for the mouse -350/+34 and human -281/-9 proximal promoter constructs, and the distal conserved region had no discernable effect on the mouse StarD4 reporter.

A consensus 9 bp SRE of Y-C-A-Y-C/A/G-Y-C-A-Y (Y=pyrimidine) was proposed (Magana and Osborne, 1996), and with some exceptions most SREs show good agreement with the consensus (Figure 6.3a) (Edwards et al., 2000). Three potential SREs (A-C) were conserved in the mouse and human StarD4 proximal promoters, and two additional potential SREs (D-E) were only present in mouse (Figure 6.3b). SRE-A (CCAgCCCAC) was the best

A

Hamster LDL receptor	TCACCCCAC
Human SREBP-2	TCACCCCAC
Hamster HMG CoA synthase	TCACCCCAC
	CCACCCCAC
Hamster HMG CoA reductase	CCGCACCAT
	TCTCACCAC
Rat FPP synthase	TCACACGAG
Human squalene synthase	TCACGCCAG
Rat fatty acid synthase	TCAGCCCAT
	CCACGCCAC
Mouse CTP:phohpocholine cytidylytransferase	TCACCCCAC
Mouse Glycerol-3-phosphate acyltransferase	TCAGCCTAG
Human ATP citrate lyase	TCAGGCTAG
Mouse acetyl CoA synthase 1	TCACTCCAC
	ACACCCCAT

B

Mouse/Human StarD4 SRE-A	CCAGCCCAC
Human StarD4 SRE-B	*TCATTCCAT
Mouse StarD4 SRE-B	*TCGGTCCAT
Human StarD4 SRE-C	CCGCGCCAG
Mouse StarD4 SRE-C	AGGCACCAG
Mouse StarD4 SRE-D	ACACCCCAC
Mouse StarD4 SRE-E	CCAAGGCAG

Figure 6.3: Alignment of known SREs with StarD4 functional SRE-B and other potential SREs. (A) Previously characterized SREs and (B) StarD4 potential SREs. Only SRE-B (*) in StarD4 was functional based on mutagenesis studies. Disagreements with the proposed 9 bp SRE consensus YCAY(C/A/G)YCAY (Y=pyrimidine) are indicated in red.

candidate since it was identical in mouse and human and differed from consensus only at position 4 (lower case). This G substitution is found in several SREs including rat fatty acid synthase (Magana and Osborne, 1996). Surprisingly, mutation of StarD4 SRE-A in either species did not change reporter sterol regulation, and mutations in SRE-C, SRE-D, and SRE-E likewise had no effect. However, sterol regulation was reduced by a factor of four to five upon mutating SRE-B in either mouse (20-fold to 4-fold) or human (12-fold to 3-fold), indicating this is a functional SRE. Interspecies conservation of SREs has been described for the human and hamster HMGS genes (Inoue et al., 1998), and there are presumably other examples. Human SRE-B (TCATtCCAT) agrees with the consensus except for T at the position 5, but this substitution was described in two SREs in mouse acetyl CoA synthase 1 (Ikeda et al., 2001). StarD4 SRE-B in mouse (TCggtCCAT) has two additional divergent bases: G in the position 4, like SRE-A, and G in position 3, which is also found in hamster HMG CoA reductase (Vallett et al., 1996). Residual low sterol regulation of SRE-B mutant reporters was often observed, particularly when statin drug treatment maximally activated SREBPs. This effect may be mediated by the other potential SREs in the StarD4 promoter, as double mutants of SRE-B and any of the other four SREs showed even less sterol regulation than SRE-B single mutants.

The activity of mouse SRE-B, despite relatively poor consensus agreement, likely reflects its position relative to other factor binding sites, particularly two downstream CCAAT boxes conserved in the human StarD4 promoter. Mutations in either CCAAT box, 10 bp or 40 bp downstream of SRE-B, nearly abolished sterol regulation, as these reporters showed similar low activity in the presence or absence of sterols. All known SRE-containing promoters have a site for NF-Y (CCAAT) or Sp1 (GC box) in close proximity, as SREBPs interact with these factors to activate transcription (Bennett and Osborne, 2000). The spacing of the CCAAT box from the SRE appears crucial, and these elements typically lie within 21

bp (Edwards et al., 2000). Sterol regulation is abrogated upon increasing the spacing beyond 17 bp in the HMGS promoter (Dooley et al., 1998) or beyond 20 bp in the FPP synthase promoter (Ericsson et al., 1996), and the optimal spacing for the SREBP-2 promoter was 16-20 bp (Inoue et al., 1998). Based on such reports, neither StarD4 CCAAT box appears optimally located at 10 and 40 bp from SRE-B. However, in the stearoyl-CoA desaturase-1 and -2 genes, CCAAT elements 5 and 48 bp from the SRE were functional (Tabor et al., 1999). Therefore, the spacing of elements may be promoter-specific, and CCAAT elements more distal from the SRE may be required for maximal activation of some promoters. From these studies, it is unclear why the StarD4 promoter is a preferential target for SREBP-2 rather than SREBP-1, but this is a major unresolved issue in the field of SREBP research.

All other known SREBP-2 target genes are involved in cholesterol synthesis (many biosynthetic enzymes) or its uptake from plasma (the LDL receptor) (Edwards et al., 2000), so we propose four models whereby StarD4 could also function in these pathways (Figure 6.4). First, as described in the introduction, the cholesterol precursors squalene, lanosterol, and every post-lanosterol sterol are hydrophobic molecules that may require a protein carrier such as StarD4. Cholesterol biosynthetic enzymes localize to the ER and peroxisomes (Olivier and Krisans, 2000), so StarD4 could shuttle the precursor between enzymes in different compartments or different membrane domains of one compartment (Figure 6.4a). Second, movement of nascent cholesterol from its primary site of synthesis in the ER to its major compartment in the PM can be considered the final step of cholesterol synthesis. This transport pathway from ER to PM is one of the best candidates for non-vesicular transport via lipid transfer proteins like StarD4 (Figure 6.4b). Third, cholesterol taken up via the LDL receptor must leave endosomes by the pathway involving the NPC proteins, MLN64, and possibly a cytosolic lipid transfer protein like StarD4. NPC1, NPC2, and MLN64 are not regulated by sterols, but SREBP-2 regulated genes such as the LDL receptor and StarD4 may

be rate-limiting in this transport pathway (Figure 6.4c). Finally, StarD4 overexpression repressed SRE reporters, consistent with generation of an oxysterol that decreases SREBP processing. If StarD4 serves this function *in vivo*, its activation by SREBP-2 could negatively feedback on SREBP processing, thus preventing excessive cholesterol synthesis or uptake (Figure 6.4d). Further experiments will be necessary to distinguish among these hypotheses for StarD4 function.

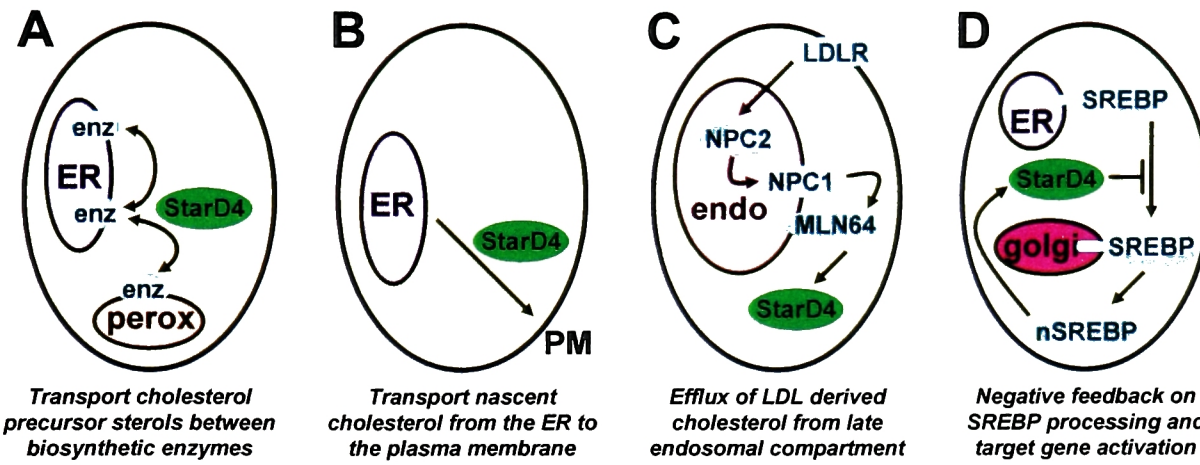

Figure 6.4: Four potential functions of StarD4 consistent with SREBP-2 gene regulation.
See text for further details.

StarD5: an ER stress activated gene with potential roles in ER function

StarD5 shows a similar tissue expression pattern to StarD4 and the proteins share 30% identity. However, StarD5 is not an SREBP target as its mRNA expression was unregulated by cholesterol feeding in mice, by truncated nuclear SREBPs in transgenic mice (data not shown), or by oxysterols or statin in cultured cells. StarD5 expression was also unaffected by LXR agonists in mouse liver and cultured cells. StarD5 expression was nonetheless increased 4-fold in free cholesterol-loaded macrophages relative to untreated or cholesterol ester-loaded cells. Tabas and coworkers have used Western blots to show activation of the ER stress response in these free cholesterol-loaded macrophages (Feng et

al., 2003a). We confirmed and extended these findings by showing increased Xbp1 splicing and increased mRNA for known ER stress target genes CHOP and BiP.

Since StarD5 was induced in free cholesterol-loaded macrophages but did not appear to be an LXR target, we investigated its regulation by classic inducers of ER stress. When NIH 3T3 cells were treated with agents known to cause ER protein misfolding (tunicamycin, thapsigargin, Brefeldin A, and DTT), StarD5 expression was consistently increased 6- to 8-fold. Control ER stress targets genes were also activated, while no consistent regulation was observed for StarD4 and MLN64. StarD5 activation was specific for ER stress, as the general protein folding stress of heat shock had no effect of StarD5 expression.

The gene regulatory elements responsible for ER stress activation of StarD5 were not localized. The proximal 400 bp upstream of the ATG was conserved between mouse and human StarD5, but no consensus sites for binding ER stress transcription factors were found. There were two conserved CCAAT boxes, but they lacked the other components of an ER stress response element (ERSE) or ERSE-II. Consistent with this, a luciferase reporter driven by this proximal 400 bp of mouse StarD5 was not activated by ER stress. Since the endogenous StarD5 mRNA is robustly induced by ER stress in the same cells, the responsible elements must lie elsewhere in the gene. ERSEs have only been described in proximal promoters, but these studies are based on a limited number of known target genes (Roy and Lee, 1999).

Several classes of genes are activated by the ER stress response, and these targets fall into two broad classes: (1) genes that help restore normal ER function and (2) genes that trigger apoptosis if ER function cannot be restored. Since the ER is the key regulatory compartment in cholesterol metabolism, we favor the hypothesis that StarD5 plays a protective rather than apoptotic role in ER-stressed cells. Since excess ER free cholesterol can cause ER stress (Feng et al., 2003a), we propose four models whereby StarD5 could

reduce ER free cholesterol levels (Figure 6.5). First, StarD5 could transport cholesterol from the ER to other compartments or to cellular efflux pathways, perhaps involving ABC transporters like ABCA1, ABCG5, and ABCG8 (Figure 6.5a). Second, StarD5 could deliver cholesterol for esterification by ER-localized ACAT, thus reducing free cholesterol levels (Figure 6.5b). Third, since overexpressed StarD5 activated LXRE reporters consistent with oxysterol generation, StarD5 *in vivo* may stimulate LXR activation of genes involved in cellular cholesterol efflux (Figure 6.5c). Fourth, oxysterol generation itself may be a means to unload cellular cholesterol, as more hydrophilic oxysterols are thought to leave cells more easily than cholesterol (Figure 6.5d). It remains to be determined whether StarD5 expression has any of these protective roles in ER-stressed cells.

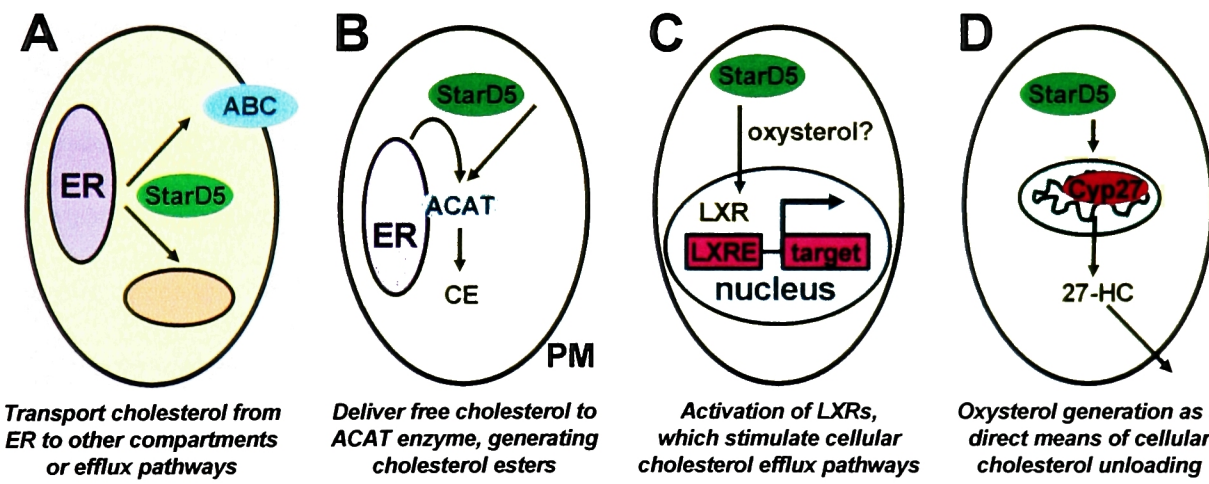

Figure 6.5: Four potential functions of StarD5 consistent with ER stress gene regulation.
ABC = ATP binding cassette transporter, CE = cholesterol esters, 27-HC = 27-hydroxycholesterol. See text for further details.

It is notable that the models for StarD4 function generally increase cellular cholesterol by synthesis or uptake, while the StarD5 models decrease cellular cholesterol by efflux or esterification. Even though StarD4 and StarD5 showed similar activities in the three overexpression assays, they could potentially have such opposing functions at endogenous expression levels *in vivo*. Cholesterol-depleted cells may activate StarD4 via

SREBP-2 to increase cholesterol levels, while cholesterol-loaded cells may activate StarD5 via the ER stress response to decrease cholesterol levels.

StarD6: a male germ cell specific gene with potential roles in fertility

Unlike StarD4 and StarD5, StarD6 expression was limited to the testis. A StAR-like role in steroidogenesis was unlikely since StarD6 was not expressed in other steroidogenic tissues, and further studies showed no StarD6 in steroidogenic Leydig cells of the testis. Rather, StarD6 mRNA was expressed in male germ cells at many stages of development, and expression was absent in germ cell-deficient mice. Germ cells themselves are not known to have steroidogenic capacity, but roles for StarD6 in steroid hormone metabolism cannot be ruled out. We were unable to test StarD6 function in transient transfection assays for steroidogenesis and transcriptional regulation, since expression of the FLAG-StarD6 construct was undetectable in several fibroblast cell lines. StarD6 may thus require germ-cell specific accessory proteins for protein stability. StarD6 may generate oxysterols, analogous to the potential activity of StarD4 and StarD5, which could be substrates for steroidogenesis in other cell types. For instance, 25-hydroxycholesterol produced by testicular macrophages can be converted to steroids by Leydig cells (Lukyanenko et al., 2001). Nonetheless, we favor non-steroidogenic roles for StarD6 in male germ cells.

The mouse genome includes an intron-less StarD6 gene on chromosome 10 nearly identical to the gene with introns on chromosome 18. The only coding difference in the intron-less gene is a deletion at +696 from the ATG, resulting in a frameshift right before the TAG stop and a longer ORF by 24 codons. This intron-less chromosome 10 gene is likely a processed pseudogene that is not transcribed, since it does not include the potential promoter elements of the chromosome 18 gene that are highly conserved in the syntenic human gene.

Furthermore, 5' RACE analysis of mouse StarD6 RNA showed three alternate first exons in StarD6 mRNA. All three alternate exons are on chromosome 18, while the intron-less chromosome 10 gene only has sequence for exon 1b. Alternate first exons were also identified in the human StarD6 gene, as well as multiple transcription start sites in each mouse and human first exon.

Another unusual feature of mouse and human StarD6 mRNAs was long 5' UTRs encoded by multiple exons, three non-coding initial exons in mice and two in humans. There was no apparent sequence conservation in these 5' UTRs, but both contain multiple AUG codons before the StarD6 ORF. None of the upstream ORFs could include this StarD6 START domain coding sequence, which has an in-frame stop codon immediately before the AUG codon. Ribosomes typically bind to the 5' mRNA cap and scan to the first start codon to initiate translation, but mRNAs with long 5' UTRs and upstream AUGs are often regulated translationally (Morris and Geballe, 2000). For instance, the Cyp27 mRNA was recently shown to have a long 5'UTR and upstream ORFs that regulate its translation in liver (Lodhi et al., 2003). Translational regulation is especially common in germ cells, which compact their nuclei and arrest most transcription during spermatogenesis (Eddy, 1998). Therefore, even though StarD6 mRNA was detected at all stages of germ cell development, protein expression may be restricted to specific stages.

Cholesterol and it biosynthetic precursor sterols have at least four important roles in sperm development and function, and each pathway could involve a putative sterol transfer protein like StarD6 (Figure 6.6). First, meiosis activating sterols (MAS) stimulate meiosis of germ cells (Byskov et al., 1998), and the precursor testis-MAS (T-MAS) accumulates in post-pubertal testis (Tacer et al., 2002). Second, other post-lanosterol sterols like 7-dehydrocholesterol are surprisingly abundant in testis and epididymis, where they may play roles in sperm maturation (Lindenthal et al., 2001). Third, the precursor desmosterol is

enriched in the membranes of sperm tails, where it is even more abundant than cholesterol and may increase membrane fluidity for sperm motility (Connor et al., 1998). Fourth, cholesterol efflux from the sperm head acrosomal membrane occurs during capacitation, a process necessary for fertilization (Travis and Kopf, 2002).

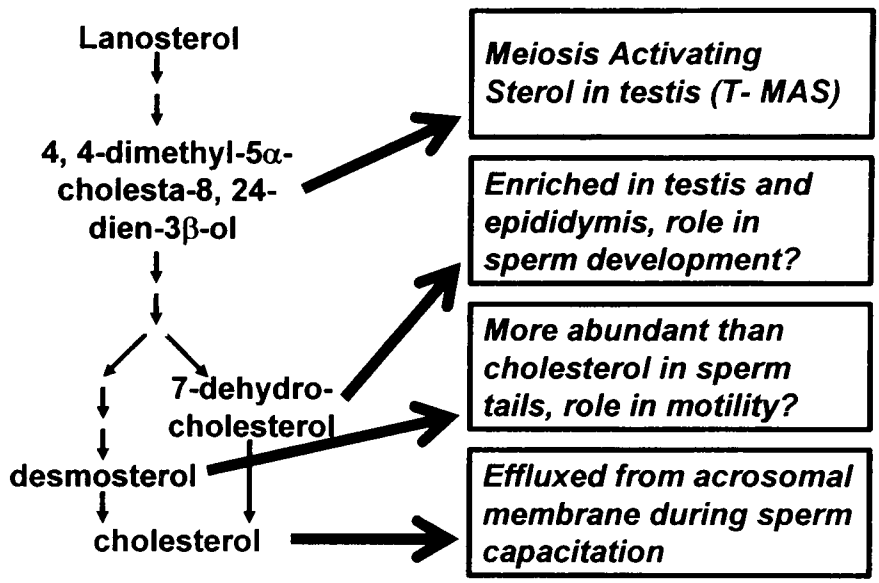

Figure 6.6: Four sterols with potential roles in male germ cells, perhaps requiring StarD6. See text for further details.

Using the anti-StarD6 antibody we generated, the laboratory of Patricia Morris has studied StarD6 protein expression. Preliminary data localizes StarD6 to the midpiece of mature spermatozoa in mice, rats, and humans (P. Morris, personal communication), making a role in capacitation unlikely. Another START domain protein of unknown function, StarD10 of the PCTP subfamily, is also expressed in sperm, but it localizes to sperm tails rather than midpiece (Yamanaka et al., 2000). The sperm midpiece is packed with mitochondria that generate energy for sperm motility, and mitochondrial dysfunction has been implicated in male infertility (Ruiz-Pesini et al., 1998). StarD6 in the midpiece may thus play a role in mitochondrial function and sperm motility, consistent with the model that START domains deliver sterols to mitochondria.

K02D3.2: The only StarD4 subfamily gene in *C. elegans*

While mammals have three StarD4 subfamily genes, the nematode *C. elegans* has only the K02D3.2 gene, and its six other START genes belong to other subfamilies. The fruit fly *Drosophila melanogaster*, another invertebrate whose genome has been completely sequenced, has only 4 START genes and no StarD4 subfamily member. K02D3.2 coding sequence was based on automated genome annotation, and the START domain was surprisingly interrupted by 60 non-START amino acids. We cloned the cDNA, revealing a START domain lacking these extra amino acids, and thus corrected the genomic annotation.

The K02D3.2 protein was more like the StarD4 subfamily than other START proteins, so we reasoned that K02D3.2 may be functionally orthologous to mammalian StarD4, StarD5, or StarD6. To test this hypothesis, we generated a K02D3.2 promoter GFP reporter worm line. This reporter was not expressed in male germ cells like mammalian StarD6, though there may be silencing of transgenes in the worm germline. Furthermore, reporter expression was not activated by cholesterol depletion or ER stress or like mammalian StarD4 or StarD5, respectively. While it is possible that this reporter lacked intronic, downstream, or distal gene regulatory elements, K02D3.2 did not appear to show gene regulation like any of the three mammalian genes.

The K02D3.2 reporter was expressed in seam cells of embryos and larvae, but not in adults. Seam cells are one of three major cell types of the nematode hypodermis, and they play crucial roles in development, organizing embryonic and larval morphogenesis and regulating body form (Koh and Rothman, 2001). There are ten bilateral pairs of seam cells at hatching, which then divide to form additional seams cells, other epidermal cells, and neurons. The main function of seam cells is the secretion of the cuticle or exoskeleton, an extracellular matrix composed primarily of small highly cross-linked collagens (Johnstone,

2000). Cuticle is essential for viability, as it maintains body shape, protects against environmental insults, and aids locomotion (Eschenlauer and Page, 2003). One percent of the *C. elegans* genome encodes over 150 cuticle collagens, as there are five stage-specific cuticles which are molted and replaced during embryonic and larval development (L1-L4). At the end of the final larvae stage L4, the individual seam cells fuse forming the seam syncytia in adults (Koh and Rothman, 2001). Loss of K02D3.2 expression at the transition between L4 and adults correlates with this homotypic seam cell fusion event. Certain ELT-family GATA transcription factors are essential for seam cell development and fusion (Koh and Rothman, 2001), so these factors are strong candidates for regulation of K02D3.2 expression.

Since seam cells are highly active in protein secretion, they may have physiological high levels of ER stress. In mammals, secretory cells (like insulin-producing pancreatic β-cells and antibody-producing plasma cells) are thought to constitutively activate the ER stress response to protect against ER overload (Harding et al., 2002). While the ER stress response is well characterized in *C. elegans*, its activation in individual cell types like seam cells has not been specifically described. An ER stress activated hsp-4 (BiP) GFP reporter is expressed in a bead-like pattern consistent with seam cells, but this is only apparent when expression elsewhere is blocked by mutations in upstream ER stress mediators IRE-1 or Xbp1 (Calfon et al., 2002). K02D3.2 is most similar to ER stress activated mammalian StarD5, so its expression may protect against ER stress. K02D3.2, however, did not appear to be an ER stress response target gene, as tunicamycin treatment failed to induce reporter expression. Consistent with this, a whole genome microarray analysis of tunicamycin-treated worms failed to show regulation of K02D3.2 (David Ron, personal communication). Even if K02D3.2 is not activated by ER stress *per se*, its very specific expression in the dedicated secretory seam cells could nonetheless indicate a role in ER function.

Based on a genome-wide RNAi screen, reduced expression of K02D3.2 causes decreased lipid storage and an altered pattern of lipid deposition in the gut lining cells of adult worms (Ashrafi et al., 2003). The K02D3.2 reporter, however, was not expressed in adult gut cells, so the RNAi phenotype could be secondary to a defect in seam cells or cuticle secretion. Such defects often give altered body shape, such as the dumpy (*Dpy*) phenotype of certain collagen mutations (Eschenlauer and Page, 2003), but this was not assayed in the RNAi screen. It is difficult to reconcile the RNAi phenotype in adult gut with exclusive expression in embryonic and larval seam cells.

It is also unclear how a putative sterol transfer protein could function in seam cells. A detailed review of cholesterol metabolism in *C. elegans* was recently published (Kurzchalia and Ward, 2003). Worms are incapable of *de novo* cholesterol synthesis but require sterols from the environment, so standard laboratory growth media includes cholesterol. When this cholesterol is omitted, there are mild defects in movement, gonad development, and, notably, shedding of cuticle during molting (Kurzchalia and Ward, 2003). When all sources of exogenous cholesterol are stringently excluded, first generation worms have decreased growth and fertility, while the second generation shows larval growth arrest (Merris et al., 2003). The vitellogenins, extracellular yolk proteins that resemble mammalian ApoB, have been implicated as sterol transfer proteins that deliver sterol to oocytes expressing specific receptors (Matyash et al., 2001). Nematodes appear to possess unique enzymatic machinery to converts cholesterol or plant sterols into their major sterol, 7-dehydrocholesterol. For instance, when sitosterol is the sole sterol source, it is converted to desmosterol, cholesterol, and finally 7-dehydrocholesterol (Choi et al., 2003). Worms grown in sitosterol and azacoprostane, a drug that blocks the conversion of desmosterol to cholesterol, show the expected sterol-depletion phenotypes in growth and fertility. In addition, these worms have defects in germ cell morphology, reduced motility, and poorly

developed cuticle (Choi et al., 2003). While cuticle defects could be secondary to other phenotypes, these sterol depletion experiments indicate that sterols may affect cuticle secretion in *C. elegans*, thus providing a potential role for K02D3.2 in seam cells.

Future Directions

The preceding discussion proposes multiple potential functions for each of the StarD4 subfamily members. These models are based on homology to the cholesterol-binding StAR and MLN64 proteins, the regulated expression of each gene, and the effects of overexpressing StarD4 or StarD5 in cultured cells by transient transfection. Future studies will address the hypotheses generated here.

Characterization of novel gene regulatory elements: StarD4 was shown to be an SREBP target gene with a functional SRE in its promoter. Regulated expression was also described for StarD5 and StarD6, by ER stress and germ cell factors, respectively, but the responsible regulatory elements were not identified. While SREs are relatively well defined, there have been many fewer studies of ER stress-responsive and germ cell-specific elements. Future investigation of such elements may use the StarD5 and StarD6 promoters as model systems.

Further studies of the* C. elegans *K02D3.2 gene: This StarD4 subfamily gene appears only expressed in hypodermal seam cells in embryos and larvae, inconsistent with a reported RNAi phenotype on lipid storage in the gut lining cells adults (Ashrafi et al., 2003). It would be useful to perform an independent RNAi study to confirm the gut phenotype, and look for other phenotypes such as defective cuticle secretion by seam cells.

Biochemical studies of recombinant proteins: The studies described here provide strong indirect evidence for sterol binding and transport by StarD4 and StarD5, but direct evidence

is lacking. Recombinant StarD4 protein was generated for the crystallographic studies, and bacterial expression plasmids were also cloned for StarD5 and StarD6. Similar to published studies of other lipid transfer proteins, *in vitro* experiments with recombinant StarD4 subfamily proteins could directly demonstrate sterol binding or sterol transfer between membranes.

Crosslinking of photoactive cholesterol: A photoaffinity cholesterol reagent has been developed, which is activated by ultraviolet light to covalently crosslink cholesterol-binding proteins *in vitro* or *in vivo* (Thiele et al., 2000). With the help of David Silver at Columbia University, we treated recombinant mouse proteins PCTP, StarD4, and MLN64 (prepared by Michael Romanowski) with photocholesterol dissolved in 0.1% ethanol in buffer. Surprisingly, the photocholesterol crosslinked to all three proteins, including PCTP which does not transfer cholesterol. Therefore, binding likely reflected non-specific association of the hydrophobic sterol with protein surfaces, rather than specific binding in the hydrophobic cavity. This experiment included no non-START control proteins, no competing proteins, and no membranes, which may be required for cavity lipid loading. The *in vitro* crosslinking experiment was therefore limited, so *in vivo* photocholesterol labeling of FLAG-START transfected cells may be more informative.

Ligand identification and oxysterol generation in stable overexpressing cell lines: Stable gene overexpression in permanent cell lines can overcome some limitations of transient transfection, such as low transfection efficiencies. We attempted to generate START-overexpressing stable cell lines without success, but further attempts are underway. Once this is accomplished, two experiments will be undertaken in which collaborators identify sterols by gas chromatography mass spectrometry. First, large amounts of the native overexpressed FLAG-START proteins will be immunoprecipitated and the putative sterol

ligand will be identified. Second, whole cell lipid extracts from control and overexpressing cells will be analyzed to determine whether any sterol or oxysterol peak is increased by START domain overexpression. This experiment may show that an oxysterol like 25- or 27-hydroxycholesterol is generated in StarD4- or StarD5-overexpressing cells, explaining the observed repression of SREBPs and activation of LXRs. This is a feasible approach, as similar studies of NPC cells recently showed defective oxysterol generation (Frolov et al., 2003). If stable cell lines cannot be generated, these studies can be performed by transient transfection using protocols optimized for greater than 90% efficiency.

Assaying the role of 27-hydroxycholesterol: We hypothesize that the mitochondrial sterol 27-hydroxylase enzyme Cyp27 mediates the effects of START domain overexpression on transcription. If this is the case, then co-transfection of a Cyp27 expression plasmid may stimulate the START domain effects on LXR activation or SREBP repression. Likewise, START domains may be inactive in Cyp27-deficient cells, from knockout mice or by RNAi. Similar experiments could test potential roles of cholesterol 25-hydroxylase or other genes.

Identification of interacting proteins: Protein-protein interactions could be essential for the function of StarD4 subfamily proteins, and identification of interacting partners may place these proteins in known cellular pathways. Immunoprecipitation of StarD4, StarD5, or StarD6 may co-precipitate interacting proteins, which would be identified by Western blotting of candidate proteins or tryptic-digest mass spectrometry of unknown bands. Yeast two-hybrid screens for interacting proteins are also being undertaken.

Further structure-function mutagenesis studies: We used site-directed mutagenesis to study the role of two different salt bridges in StarD4 and MLN64 based on their respective X-ray crystal structures. Corresponding mutations should be generated in StAR, as well as

the additional StAR mutations known to cause lipoid CAH (Bose et al., 1996). Additional structure-function relationships could also be tested in similar experiments.

Localization and expression of endogenous StarD4 subfamily proteins in cells and tissues: We have generated polyclonal anti-peptide antibodies against StarD4 and StarD6, and an anti-StarD5 antibody will also be generated. If these antibodies prove effective, they will be used in three experiments with endogenously expressed proteins. First, the cellular abundance of StarD4 subfamily proteins may be estimated by Western Blots, comparing cell extract levels to known dilutions of recombinant protein. Second, immunofluorescence may show the subcellular distributions of endogenous proteins, testing the hypothesis that they are soluble cytosolic proteins. Third, tissue immunostaining may reveal which cell types express the protein. For instance, high liver StarD4 mRNA expression presumably reflects expression in hepatocytes, and macrophages in atherosclerotic lesions may express high levels of StarD5 due to ER stress. Studies of StarD6 protein expression in testis and sperm are being carried out in the laboratory of Patricia Morris.

Mislocalization of START domains to specific subcellular compartments: The studies described here used mammalian FLAG-tagged overexpression vectors for isolated START domains as well as chimeric Tom20-STARTs. The former proteins localized throughout the cytoplasm and nucleus, while the latter presumably localized to the outer mitochondrial membrane. This prediction is based on studies of Tom-StAR by Miller and co-workers (Bose et al., 2002), but future studies must use immunofluorescence or cell fractionation to confirm mitochondrial localization of these chimeras. We also cloned chimeric proteins with the MLN64 N-terminal (MENTAL) domain fused to various START proteins, which should localize to the membranes of late endosomes like full-length MLN64. Other chimeric proteins could be generated to localize the START domain to other compartments, such as

ER, Golgi, or peroxisomes. Once localization is confirmed, these chimeras can be tested in the various functional assays. Localization to certain subcellular compartments may positively or negatively affect a given functional assay, perhaps indicating the relevant location for activity.

Transgenic mice: Similar to effects observed in transfected cells, overexpression of StarD4 or StarD5 in transgenic mice could affect cholesterol metabolism in the whole organism. We cloned transgenic constructs to express the human StarD4 or StarD5 ORFs in mouse liver via the human ApoE promoter and enhancer. This pLIV.7 transgenic expression construct was originally generated by the laboratory of John Taylor (Fan et al., 1998) and has been used to generate a number of transgenic mice and rabbits. No founder mice have been generated to date for StarD4 and StarD5, but injections are ongoing. In the future, it may also be fruitful to generate transgenic mice overexpressing StarD4 or StarD5 in non-hepatic cells, such as macrophages which are essential for atherosclerotic lesion formation.

Potential role in apoptosis: Unpublished observations in our lab and others suggest that overexpression of certain START domains may be toxic to cells. Transiently transfected cells appear to die after several days, and we have to date been unable to generate StarD4 or StarD5 stable cell lines or transgenic mice. High levels of certain START proteins may only be expressed physiologically when necessary, as StAR mRNA is highly regulated and the protein rapidly inactivated, and StarD4 and StarD5 are also regulated transcriptionally. These proteins could trigger apoptosis via several mechanisms, including oxysterol generation (Panini and Sinensky, 2001) and effects on mitochondrial function and cytochrome c release (Wang, 2001). Future studies may address the effects of StarD4 and StarD5 on apoptotic pathways in cell culture model systems.

Knockout mice: We designed and cloned targeting constructs for StarD4 and StarD6, but these failed to give homologous recombination in ES cells. The constructs are being modified and knockout mice for all three StarD4 subfamily members will be generated. StarD4- or StarD5-deficient mice may show obvious phenotypes in cholesterol metabolism, such as alterations in plasma lipoprotein profiles or tissue sterol levels. There may also be differences in response to high dietary cholesterol, bile acid pool depletion, or other dietary fat manipulations. Since cholesterol plays crucial roles in development, embryonic lethality or other developmental phenotypes are possible in complete knockouts, but these may be avoided in tissue-specific conditional knockouts. StarD6 knockout mice are predicted to be viable with potential male infertility. The normal function of StarD6 would be indicated by the specific defect in male fertility, such as altered sperm counts, morphology, or motility.

Knockout cells or RNA interference of StarD4 and StarD5: Cells isolated from StarD4 or StarD5 knockout mice, such as embryonic fibroblasts, peritoneal macrophages, or primary hepatocytes, may show defects in cellular cholesterol metabolism. There may be altered regulation of SREBP and LXR target genes, decreased cholesterol synthesis or esterification, defective cholesterol efflux, increased susceptibility to ER stress and apoptosis, or other phenotypes predicted by the models above. Prior to generation of knockout mice, similar studies could be performed using RNAi techniques to decrease StarD4 or StarD5 expression. We attempted small interfering RNA (siRNA), the transfection of double stranded RNA oligonucleotides (Elbashir et al., 2001), but failed to reduce StarD4 or StarD5 mRNA levels. Improvements in technology, such as DNA vectors that overexpress hairpin siRNAs via transfection or viral transduction (Shi, 2003), may allow more successful studies.

Effects of StarD4 and StarD5 on atherosclerosis: There are two prominent mouse models of atherosclerosis, the ApoE and LDL receptor deficient mice (Smith and Breslow, 1997).

To determine the effects of candidate genes on lesion development, genetically modified mice with transgenic overexpression or knockout of many candidate genes have been crossed to ApoE or LDL receptor deficient backgrounds (Glass and Witztum, 2001). Such studies will be performed with the StarD4 and StarD5 transgenic and knockout mice. If ER stress mediated macrophage apoptosis results in lesion progression, and StarD5 protects against this ER stress, then StarD5/ApoE double knockout mice may show worse lesions. Conversely, transgenic StarD5 overexpression in macrophages may protect against atherosclerosis. StarD4 may likewise have important effects on atherosclerosis.

Conclusion

The novel lipid-binding protein StarD4 was identified by microarray analysis of gene expression in cholesterol-fed mouse liver. StarD5 and StarD6 were then identified based on homology to StarD4, and the three genes were cloned and shown to form a subfamily within the START gene family. Functional data with overexpressed StarD4 and StarD5 proteins indicate that the StarD4 subfamily is involved in the intracellular metabolism of cholesterol or other sterols. The three subfamily members show specific regulated gene expression: StarD4 is an SREBP-2 target gene with a promoter SRE, StarD5 is activated by the ER stress response, while StarD6 is expressed exclusively in male germ cells. Since StarD4, StarD5, and StarD6 show different gene regulation and share only ~30% amino acid identity, each is likely to play a distinct role in sterol metabolism. Future studies, including biochemical assays, cell biological experiments, and analysis of genetically modified mouse models, will address these potential functions. Overall, the work described here has opened up a new field in the study of intracellular cholesterol metabolism and transport.

Chapter 7: Materials and Methods

Animals and diets: All animal protocols were approved by The Rockefeller University Animal Care and Use Committee. Mice were housed at the Rockefeller University Laboratory Animal Research Center in at the specific pathogen free, humidity- and temperature-controlled room with a 12 hour light-dark cycle. Wild type C57BL/6 mice (#00664) as well as the male KitW/Wv mouse and Kit+/+ littermate control (#100410) were obtained from the Jackson Laboratory.

For the initial cholesterol feeding cDNA microarray experiment, 6-week old C57BL/6 male mice were fed Picolab Rodent Chow 20 (5053), which contains 0.02% cholesterol (wt/wt), or the same diet supplemented to 0.50% cholesterol for three weeks. All subsequent feeding experiments used a semi-synthetic modified AIN76a diet containing 10% kcal as fat and 0.00% cholesterol (Clinton/Cybulsky Rodent Diet (Lichtman et al., 1999), Research Diets D12102N), which was fed to mice for one week before the start of each experiment. In additional cholesterol feeding studies, mice were fed either this control 0.00% cholesterol diet or this diet supplemented with 0.50% cholesterol (Research Diets D00083101) for one week. For the time course study performed by Kara Maxwell, twenty male C57BL/6 seven-week old mice were used. Four mice were sacrificed at day 0 on the 0.00% cholesterol diet, while the remaining mice were switched to a 0.50% cholesterol diet and groups of four were sacrificed at days 1, 2, 4 and 7.

Transgenic mice expressing truncated nuclear forms of human SREBP-1a (#002840) or SREBP-2 (#003311) were originally obtained from Jackson Laboratory and backcrossed to C57BL/6. Mice were genotyped by PCR from tail tip DNA using the primers in Table 7.1. N6/N7 generation SREBP-1a and N2/N3 SREBP-2 mice were used. Transgenic and littermate control male mice were fed standard rodent chow from birth to 8 weeks. They

were then switched to a 65% protein, 10% carbohydrate diet (Purina TestDiet 8092) for two weeks to induce maximal transgene expression, since the SREBP transgenes were under the control of the PEPCK promoter (Horton et al., 1998; Shimano et al., 1996).

Table 7.1: Primers for genotyping SREBP transgenic mice

Transgene	Primer	Sequence
hSREBP-1a	forward	GCAACCAGAAACTCAAGCAGG
	reverse	CTCCAAACCACCCCCCTC
hSREBP-2	forward	GCTGAGCCGGGCGATGGACGACAGC
	reverse	CTGGGGGCGGGGCTGAAGAATAGGAGTTGC

For the LXR agonist study performed by Beth Duncan and Kara Maxwell, seven-week old male C57BL/6 mice on the semisynthetic 0.00% cholesterol diet were gavaged with vehicle alone (5% ethanol, 95% sesame oil) or with 10 mg/kg TO901317 (Sigma T2320). This treatment was repeated after 24 hours and mice per were sacrificed later the same day.

At the end of all mouse experiments, food was removed from the cage early in the light cycle. Mice were fasted for 5-6 hours, sedated with ketamine/xylazine, and sacrificed. Harvested tissues were frozen in liquid nitrogen and stored at –80°C or stored in RNAlater (Ambion) according to manufacturer instructions. Liver total and free cholesterol (mg/g liver) was measured by gas chromatography with coprostanol as the internal standard, as previously described (Sehayek et al., 1998).

cDNA microarrays: Fluorescent cDNA probes were synthesized by reverse transcribing (Invitrogen Superscript II) 100 μg liver total RNA (Qiagen RNeasy) in the presence of Cy3 or Cy5 dUTP (AP Biotech). cDNA microarrays with ~9000 mouse ESTs were a generous gift of Dr. Raju Kucherlapati at Albert Einstein College of Medicine (Cheung et al., 1999). Standard protocols were used for preparation and hybridization of cDNA arrays, available online at http://sequence.aecom.yu.edu/bioinf/microarray/protocol4.html. Scanned arrays

were analyzed with Scanalyze (http://rana.lbl.gov/EisenSoftware.htm), and results were compiled using Microsoft Excel and Access software.

Real-Time Quantitative RT-PCR (qPCR): Total RNA was isolated from cultured cells using RNeasy kits (Qiagen), or from tissues using TRIzol reagent (Invitrogen) followed by RNeasy cleanup (Qiagen). RNA was treated with Dnase I (Ambion), and 5μg was reverse transcribed using Superscript II (Invitrogen) with oligo-dT and/or random hexamer primers. To perform relative quantification of gene expression with a standard curve, the genes of interest and the endogenous control gene (cyclophilin, β-actin, or HPRT) were amplified in separate tubes for each cDNA sample. Duplicate 50 μl PCR reactions were carried out with 1X Jumpstart PCR buffer, 1.00 U Jumpstart Taq (Sigma), 3.5 mM $MgCl_2$, 200 μM each dNTPs, 300 nM forward primer, 300 nM reverse primer, and 100 nM 6FAM-labeled TaqMan probe. TaqMan primer pairs and probes were typically designed using Primer Express (Applied Biosystems) to span splice junctions. The sequences are shown for all qPCR primers sets for housekeeping genes and START genes (Table 7.2), as well as control target genes for SREBPs, LXRs, and ER stress (Table 7.3). The template was 10 μl of a 1:100 or 1:250 dilution of cDNA, while the standards were a serial dilution of cDNA.

A 7700 Sequence Detection System (Applied Biosystems) was used with the default thermal cycling profile (95°C for 10 min; 40 cycles of 95°C 15s, 60°C 1min; 4°C soak). The quencher dye (TAMRA) was the passive reference. The threshold was set at 0.05 units of normalized fluorescence, and a threshold cycle (C_t) was measured in each well. Relative standard curves were plotted for each gene, and the mean C_t for each cDNA sample was expressed as an arbitrary value relative to standard. For each cDNA, values for genes of interest were normalized to the corresponding value for cyclophilin and expressed as a ratio.

Table 7.2: TaqMan quantitative RT-PCR primers for normalizer and START genes

Gene	Genbank	primer	sequence
Normalizers			
β-actin	X03672	forward	GAGAAGCTGTGCTATGTTGCTC
		reverse	AGGAAGAGGATGCGGCA
		probe	6FAM-AGACTTCGAGCAGGAGATGGCCA-TAMRA
cyclophilin A	X52803	forward	GGCCGATGACGAGCCC
		reverse	TGTCTTTGGAACTTTGTCTGCAA
		probe	6FAM-TGGGCCGCGTCTCCTTCGA-TAMRA
HPRT	AH003453	forward	GCAAACTTTGCTTTCCCTGG
		reverse	TTCGAGAGGTCCTTTTCACCA
		probe	6FAM-ACAGCCCCAAAATGGTTAAGGTTGCAA-TAMRA
START genes			
StarD1/StAR	AK019725	forward	CCGGAGCAGAGTGGTGTCA
		reverse	CAGTGGATGAAGCACCATGC
		probe	6FAM-CAGAGCTGAACACGGCCCCACC-TAMRA
StarD2/PCTP	NM008796	forward	CCTTTCCCACTGTCCAACAGA
		reverse	TCTTCCTCCTGTCCACATCCA
		probe	6FAM-CGTCTACACCCGCCAGCGCC-TAMRA
StarD3/MLN64	NM021547	forward	CACGCACAAATATGTCAGAGGG
		reverse	TTGTTGGCTGACTTGAGCACA
		probe	6FAM-AGAACGGCCCCGGAGGCTTCA-TAMRA
StarD4 ORF	AF480297	forward	GAGAGATGGCTGACCCTGAGA
		reverse	TCAGACAGTCCTTCCAGTTTGATC
		probe	6FAM-CCCGTGGTCACAGATTGGCAGGA-TAMRA
StarD4 3'UTR	BY677271	forward	TGCCGTGGTTTGCGG
		reverse	AGGCAGGAACATGGCTTCTCTA
		probe	6FAM-CTCTGCTCCTACCCTGTCAGCTCCATGA-TAMRA
StarD5	AF480302	forward	TGGCACCATCAGCTCCAAT
		reverse	TCTCACAAAACCGGGCTTTG
		probe	6FAM-CCCATGTGGAACATCCATTGTGTCCC-TAMRA
StarD6	AF480303	forward	AACTGTTTCCAGCAAGACCTCTAGA
		reverse	TGAGCTGCTGATTCTGGGATT
		probe	6FAM-TCCACGGAAACCTATACCGCGTTGAAG-TAMRA

Northern Blotting: Multiple tissue Northern blots were purchased from Clontech. Other blots were generated by running 10-20μg of total RNA per well on formaldehyde gels in MOPS buffer, followed by capillary transfer to positively charged nitrocellulose membranes (Roche). Radiolabeled DNA probes were synthesized from 20 ng of template DNA by random priming using the DECA prime II kit (Ambion) and ^{32}P-dATP (Perkin Elmer). Template DNA was typically the cloned START ORF cDNAs, which were generated using the primers in Table 7.7. Probes were purified from unincorporated nucleotides using ProbeQuant G-50 Micro columns (Amersham). Hybridization was performed with using Express Hyb rapid hybridization buffer (Clontech) according to manufacturer instructions.

Table 7.3: TaqMan quantitative RT-PCR primers for SREBP, LXR, and ER stress target genes

Gene	Genbank	primer	sequence
SREBP targets			
HMG CoA reductase	M62766	forward	GGGAGCATAGGCGGCT
		reverse	TGCGATGTAGATAGCAGTGACA
		probe	6FAM-CAACGCCCACGCAGCAACA-TAMRA
HMG CoA synthase	AA673053	forward	CTCTGTCTATGGTTCCCTGGCT
		reverse	TCCAATCCTCTTCCCTGCC
		probe	6FAM-TGTCCTGGCACAGTACTCACCTCAGCA-TAMRA
squalene epoxidase	BC042781	forward	GGAAGAGCCTCATCTCCAGTAAAG
		reverse	TGTGGTGCATCCTTCATAAGGA
		probe	6FAM-CTCCGTTTCTTCCCACTTCGTTGGC-TAMRA
LDLR receptor	X64414	forward	GGATGGCTATACCTACCCCTCAA
		reverse	CGGCTCTCCCGGCTG
		probe	6FAM-TCAGCCTGGAGGACGATGTGGCA-TAMRA
ATP citrate lyase	BC005533	forward	CACCCCGCTGCTCGACT
		reverse	TCAGGATAAGATTTGGCTTCTTGG
		probe	6FAM-TGCCCTGGAAGTGGAGAAGATTACCACC-TAMRA
Acetyl CoA carboxylase	BI250197	forward	CAGTCTACATCCGCTTGGCTG
		reverse	CAGCTCCTTCCGCTCAGTG
		probe	6FAM-CGATTGGGCACCCCAGAGCTAAGC-TAMRA
FABP5	X70100	forward	CGACAGCTGATGGCAGAAAA
		reverse	CCCATTGCTGGTGCTGG
		probe	6FAM-TGCACCTTCCAAGACGGTGCCCT-TAMRA
LXR targets			
ABCG5	AY195872	forward	TGGGATGTTCGGCAAGCT
		reverse	CGCATAATCACTGCCTGCTTATT
		probe	6FAM-TGTCCTGCTGAGGCGAGTAACAAGAAACTTAA-TAMRA
ABCA1	X75926	forward	ATTGCCAGACGGAGCCG
		reverse	TGCCAAAGGGTGGCACA
		probe	6FAM-CCAGCTGTCTTTGTTTGCATTGCC-TAMRA
ER stress targets			
BiP	AJ002387	forward	TCTGGTGATCAGGATACAGGTGAT
		reverse	TCCCACAGTTTCAATACCAAGTGTAA
		probe	6FAM-TGGTACTGCTTGATGTTTGTCCC-TAMRA
CHOP	X67083	forward	CCACCACACCTGAAAGCAGAA
		reverse	AGGTGAAAGGCAGGGACTCA
		probe	6FAM-CTGGTCCACGTGCAGTCATGG-TAMRA

General Cloning and PCR: Molecular cloning followed standard techniques using T4 DNA ligase from Invitrogen and other enzymes from New England BioLabs. All plasmid DNA was transformed into DH5α bacteria (Invitrogen) and prepared using Qiagen kits. Except where noted, PCR reagents were Advantage cDNA polymerase (Clontech), primers were from Genelink, and thermal cycling was on a Perkin Elmer 9700. Standard thermal cycling was 95°C for 10min, 40 cycles of 94°C 30s, 60°C 30s, and 72°C 1min, and a 4°C soak. TA

cloning of PCR products was carried out with pCR-2.1-TOPO (Invitrogen). DNA constructs were sequence-verified at the Rockefeller University DNA Sequencing Resource Center. DNA sequence was aligned and analyzed using the DNAStar software package. Human RNA from liver and testis was purchased from Clontech.

Rapid amplification of cDNA ends (RACE): The FirstChoice RLM-RACE kit (Ambion) was used according to manufacturer instructions. Briefly, total RNA (from liver for StarD4 and testis for StarD6) was treated with phosphatase to remove 5' phosphate groups from DNA, rRNA, tRNA, and degraded mRNAs. Next, the 5' caps of intact mRNAs were enzymatically removed, and a RACE adaptor sequence was ligated to the 5' ends of decapped mRNA. The RNA was reverse transcribed, and the resulting cDNA was template for nested PCRs with 5' inner and outer primers in the adaptor and 3' gene specific inner and outer primers. 5' gene specific primers served as controls, and the sequences of the gene specific RACE primer are shown in Table 7.4. RACE inner PCR products were TA cloned and sequenced.

Table 7.4: Primers for 5' RACE analysis of mouse and human StarD4 and StarD6

Gene	primer	sequence
mStarD4	outer	TCATCTTCTTTGATGCTGTGATACTGGAT
	inner	CCACGGGCTCTCAGGGTCAG
	5'	CTCTGGTACGGGACAGGAAGGAGG
hStarD4	outer	GGAACACAAAACCAACCACAGGGATG
	inner	GGTTATATCCTCGAACAAATTCTGGTCTC
	5'	ATGGAAGGCCTGTCTGATGTTGCTTC
mStarD6	outer	CAACGCGGTATAGGTTTCCGTG
	inner	GTTGGGCAATTGCCTTATAGTCCATC
	5'	GGGACAGGATATGAAGTGGGAAG
hStarD6	outer	GCCCACGGCAAAACTTTGTGTAATG
	inner	GCTGGTGATTCTGGAATTATCCCTTC
	5'	GTTAAGAGATATGGAGATTTCCACAAGG

Recombinant protein expression and crystallization: The mouse StarD4 ORF was RT-PCR amplified from liver cDNA using the PCR primers with *Bam*HI and *Xho*I restriction sites (Table 7.7). The product was cloned into these restriction sites of the pGEX-6P-1 plasmid and sequence verified with the pGEX 5' and 3' sequencing primers (Amersham). Glutathione S-transferase (GST)-tagged protein was expressed in Escherichia coli BL21 cells (Novagen) during overnight induction at 18°C. Fusion protein was purified by GST affinity chromatography. The N-terminal GST tag was removed by digestion with PreScission protease (Pharmacia), and StarD4 was separated from GST and uncleaved fusion protein on glutathione-agarose. After overnight dialysis in 20 mM Hepes (pH 8.4), 100 mM KCl, 5 mM DTT, the target protein was further purified by Q Sepharose ion-exchange chromatography, eluted with a 50-1000 mM KCl gradient. The final preparations were dialyzed against 20 mM Hepes (pH 7.5), 100 mM KCl, 5 mM DTT and concentrated to 1-20 mg/mL.

The molecular weight of purified StarD4 was verified by gel electrophoresis and matrix-assisted laser desorption ionization mass spectrometry (MALDI-MS). Size exclusion chromatography was also performed on a GF75 column (Pharmacia). The low molecular weight gel filtration standards (Pharmacia) chymotrypsinogen A (13.7 kD), ovalabumin (43 kD), and bovine serine albumin (67 kD) eluted from the column at 44.75, 50.75, and 57.33 mL, respectively, while StarD4 eluted at 56.6 mL.

Crystallization conditions for purified StarD4 protein were tested with Crystal Screen and Crystal Screen II (Hampton Research), and crystals formed in conditions 45 and 46 of Crystal Screen. Crystallization conditions were optimized, such that diffraction-quality StarD4 crystals were obtained at 4°C by sitting-drop vapor diffusion against a reservoir containing 0.1 M sodium cacodylate (pH 6.5), 0.2 M magnesium acetate, 16% (wt/vol) polyethylene glycol 8000, and 22% (vol/vol) glycerol.

For structure determination, selenomethionine-containing StarD4 crystals were generated. Michael Romanowski collected diffraction data and solved the X-ray crystal structure at 2.2 Å resolution as described (Romanowski et al., 2002). Residues 1-23, 223-224, and five residues from the N-terminal cloning artifact (Gly-Pro-Leu-Gly-Ser) were not visible in the electron density map and were omitted from refinement. Cavity volumes were measured and cavity plots generated with the VOIDOO program using a probe radius of 1.4 Å (Kleywegt and Jones, 1994). The structure was modeled and visualized using O (Jones et al., 1991) or PyMOL (Liang et al., 2003) software. The StarD4 structure has the Protein Data Bank (www.rcsb.org) identification 1JSS, while MLN64-START (Tsujishita and Hurley, 2000) and PCTP (Roderick et al., 2002) are 1EM2 and 1LN1-3, respectively.

C. elegans *K02D3.2 cloning and GFP reporter:* Four primers in the K02D3.2 ORF (Table 7.5) were used to amplify this cDNA from a *C. elegans* cDNA library (a gift of Shai Shaham). Products were TA cloned and sequenced. While the forward exon 1 ORF primer at +1 to +22 from the ATG gave PCR products with reverse primers, the –68 to –44 forward primer and the splice leader 1 (SL1) primer failed to amplify.

Table 7.5: RT-PCR primers for cloning the K02D3.2 cDNA

location	primer	sequence
exon 1 (ORF ATG)	forward	ATGCCTGCCACAGAGACCAGCG
exon 2 (ORF)	forward	GCGCATTCCGAACAGAACTTGTGCTG
exon 7 (ORF stop)	reverse	CTAGTTTTCCAAATGGGCAGCACACC
exon 5 (ORF)	reverse	GGGGATTAAGCATGAGAAGTGTGGGATAAG
-68/-44 from ATG	forward	ACAGTTCAGCGTCACATAATTCCAG
splice leader 1 (SL1)	forward	GGTTTAATTACCCAAGTTTGAG

To generate the K02D3.2 GFP reporter, a region spanning from –2700 from the ATG in the 5' flanking region to +114 in exon 1 was PCR amplified from *C. elegans* genomic DNA (a gift of Shai Shaham). The PCR primers (Table 7.6) gave the expected 2.8 kB

product with *Hind*III and *Bam*HI tails, which was TA cloned. This product was subcloned into the pPD95.69 GFP reporter vector (originally generated by the Andy Fire lab and a gift of Shai Shaham). At the 5' junction, the pPD95.69 *Xba*I was ligated to *Spe*I from the TA vector polylinker. The 3' junction in exon 1 was with *Bam*HI, giving an in frame fusion between exon 1 of K02D3.2 (encoding 38 amino acids) and the GFP reporter. Both junctions were sequence verified with the indicated primers (Table 7.6).

Table 7.6: Primers for the K02D3.2 GFP reporter

K02D3.2 reporter cloning primers:			
-2700	forward	*Hind*III	gtttaagcttCTGGAGCGATAAACGTTCCACCGGTC
+114	reverse	*Bam*HI	gtttggatccTTCGGAATGAAGTTGCCATTCCAAAGAGTGC
pPE95.69 sequencing primers:			
	upstream	forward	TCACTCACAACGATGGATACGC
	downstream	reverse	TTCACCCTCTCCACTGACAG

Elliot Perens co-injected worms with the pPD95.69-K02D3.2 reporter (25 ng/μl) and the dominant marker encoding *rol-6* (50 ng/μl) (Mello et al., 1991). Two *C. elegans* lines were generated, and both displayed fluorescence only in the seam cells of embryos and larvae. Worms were maintained on standard growth media that contains 5 μg/μl cholesterol. Media lacking added cholesterol (though trace amounts of cholesterol may be present in the agar or the bacterial lawn (Calfon et al., 2002)) or containing 5 μg/μl tunicamycin were also used, but did not affect the reporter expression pattern over two generations.

Cell Culture, media, and treatments: All cultured mammalian cells were grown at 37°C in 5% CO_2. MA-10 cells (a gift of Jonathan Smith) were cultured in Waymouth's media with 15% horse serum. To stimulate steroidogenesis, MA-10 cells were cultured in 1 μM 8-bromo-cAMP for three hours. Media was withdrawn and pregnenolone levels were

measured by ELISA (Diagnostic Biochem Canada). RNA was extracted for gene expression analysis by qPCR and Northern.

All other cell types (NIH 3T3, HEK 293, COS-1, RAW, and Hepa-1) were obtained from ATCC and maintained in Dulbecco modified Eagle's medium (DME) with 10% fetal bovine serum. NIH 3T3 cells were grown as fibroblast-like cells and were not differentiated to adipocytes. Lipoprotein-depleted serum (LPDS) was prepared from FBS by raising the density to 1.25 mg/mL with KBr and ultracentrifuging in a Ti60 rotor (Beckman) at 45,000 rpm overnight. The upper lipoprotein-containing fraction was removed, and LPDS was dialyzed against 150 mM NaCl to remove KBr and filtered sterilized (Nalgene).

Cells were treated with various drugs and agents from Sigma. To regulate SREBP activity with sterols and statin, 1000x stock solutions were made for cholesterol (10 mg/ml) and 25-hydroxycholesterol (1 mg/ml) in ethanol, as well as mevinolin/lovastatin (1 mg/ml). To ER stress cells, 1000x stocks were made for tunicamycin (2.5 mg/ml in methanol), thapsigargin (2 mM), Brefeldin A (10 mg/ml in ethanol), or DTT (2 M). Other 1000x stocks were 10 mM T0901317 and 1 mg/ml for 22(R)-hydroxycholesterol, both in ethanol. To treat cells, these agents were added to media containing LPDS or FBS at a final concentration of 1x, thus 1:1000th of the stock concentrations above. Vehicle control experiments showed no effect of 0.1% ethanol or methanol in the various assays. All treatments were preformed on subconfluent cells in six well plates for 18-20 hours, after which RNA was extracted.

Transient transfection experiments: Before all transfection assays, cells were split into 24 well plates at ~10^4 cells per well and grown overnight. The next day, each well of 50-80% confluent cells was transfected with 200-400 ng of total plasmid DNA using Lipofectamine PLUS reagent (Invitrogen).

For StarD4 and StarD5 reporter experiments, each well of NIH 3T3 cells was transfected with 200 ng of luciferase reporter and 20 ng of CMV-βgal expression vector for nomalization. After 3 hours, the serum-free transfection media was replaced with 0.5 ml of experimental media. For StarD4 reporter experiments, 3 media were used: control (DME with 10% LPDS), sterols (10 μg/ml cholesterol; 1 μg/ml 25-hydroxycholesterol), or statin (1 μg/ml mevinolin). In the StarD5 reporter ER stress assays, the media were control (DME with 10% FBS) versus tunicamycin (2.5 μg/ml). After 18-20 hours, cells were lysed with passive lysis buffer and assayed for luciferase and βgal activities (Promega). Luciferase relative light units were normalized to βgal units (absorbance at 420 nm), and results expressed as this ratio. Data are presented as mean and standard deviation of triplicate wells.

The other luciferase reporter experiments were peformed similarly. In the assays for START domain effects on SREBP reporters, each well of HEK 293 cells was transfected with 200 ng of SREx3 luciferase reporter, 20 ng of βgal, and 100 ng of FLAG-tagged START expression plasmid. In the assays for START domain effects on LXR reporters, each well of COS-1 cells was transfected with 200 ng of LXRE luciferase reporter, 50 ng of βgal, 25 ng of LXR, 25 ng of RXR, and 100 ng of FLAG-START. For both experiments, cells were cultured after transfection in DME with 10% FBS for 18-20 hours before lysis.

For the steroidogenesis assay, each well of COS-1 cells was transfected with 100 ng of F2/P450scc, 100 ng of 3β-HSD, and 100 ng of FLAG-START. After transfection, cells were grown in DME + 10% FBS for 48 hours. Media was withdrawn and progesterone levels were measured by ELISA (Diagnostic Biochem Canada).

START expression plasmids: START domain coding sequences were PCR amplified from liver or testis cDNA using the primers in Table 7.7, which had restriction site (italics) at their 5' tails. These PCR products were generally cloned into *Bam*HI and *Xho*I sites of the

pCMV-Tag2B epitope tagging mammalian expression vector (Stratagene). The mouse StarD5 sequence has an internal *Bam*HI site, so it was cloned using *Pst*I instead. Mouse StAR has an internal *Xho*I site, but was cloned using this enzyme by partial digestion. All expression plasmids were sequence verified using T3 and T7 primers to assure correct START domain sequence and in-frame fusion of the N-terminal FLAG epitope tag. Mouse StarD4 and PCTP had coding SNPs characteristic of the C57BL/6 strain (StarD4 A121, T152; PCTP G205, G324, G379). There were silent mutations in human StarD4 (A426G) and StarD5 (C21G), and all other START domains agreed with predicted sequence.

Table 7.7: Primers for cloning the FLAG-START expression plasmids

gene	type	primer	tail	sequence
mStarD4	ORF	forward	*Bam*HI	gtcgt*ggatcc*ATGGCTGACCCTGAGAGCCCG
		reverse	*Xho*I	gtcgt*ctcgag*TCATGCCTTGCGTAGACCTTTTCG
mStarD5	ORF	forward	*Pst*I	gtcgt*ctgcag*ATGGACCCGTCCTGGGCCACGCAAG
		reverse	*Xho*I	gtcgt*ctcgag*TCAGTGATGGAACTTCCTCACTGCCTTC
mStarD6	ORF	forward	*Bam*HI	gtcgt*ggatcc*ATGGACTATAAGGCAATTGCCCAACAAAC
		reverse	*Xho*I	gtcgt*ctcgag*CTACGGTTTAATGGCAGAATGTCCTTC
hStarD4	ORF	forward	*Bam*HI	gtcgt*ggatcc*ATGGAAGGCCTGTCTGATGTTG
		reverse	*Xho*I	gtcgt*ctcgag*TCATAAAGCTTTTCGTAAATCACCATAG
hStarD5	ORF	forward	*Bam*HI	gtcgt*ggatcc*ATGGACCCGGCGCTGGCAGC
		reverse	*Xho*I	gtcgt*ctcgag*TTACTCATGGAATTGCTTCACTGCTTTCTG
mStAR	START	forward	*Bam*HI	gtcgt*ggatcc*GAAGCAACACTCTATAGTGACCAGG
		reverse	*Xho*I	gtcgt*ctcgag*TTAACACTGGGCCTCAGAGGCAGG
mPCTP	ORF	forward	*Bam*HI	gtcgt*ggatcc*ATGGCGGGGGCCGCATGCTGCTT
		reverse	*Xho*I	gtcgt*ctcgag*TTAGGTTTTCTTGTGGTAGTTCTGACACG
mMLN64	START	forward	*Bam*HI	gtcgt*ggatcc*GGGTCTGACAATGAATCAGATGAGG
		reverse	*Xho*I	gtcgt*ctcgag*TCAAGCTCGGGCCCCCAGCTC
MLN64	MENTAL	forward	*Bam*HI	gtcgt*ggatcc*ATGAGCAAGCGACCTGGTGATCTGGC
		reverse	*Bam*HI	gtcgt*ggatcc*TGCAAAGGATTCTGGGGGAGAGTAGAAC
Tom20	ORF	forward	*Bam*HI	gtcgt*ggatcc*ATGGTGGGCCGGAACAGCGCC
	no stop	reverse	*Bam*HI	gtcgt*ggatcc*TTCCACATCATCTTCAGCCAAGCTCTG

To generate the FLAG-Tom20-START fusions, the mouse Tom20 coding sequence was PCR amplified from liver cDNA with primers lacking the 3' stop codon but with *Bam*HI tails at both ends (Table 7.7). This Tom20 product was cloned into FLAG-START plasmids at the *Bam*HI site between the FLAG tag and START domain (for mouse StAR, PCTP, MLN64, StarD4, and StarD6, as well as human StarD5). *Sac*II digests identified clones with

the correct orientation of Tom20, and these were sequence verified for the correct Tom20 sequence and in-frame fusion. To generate FLAG-MENTAL-START fusions, the mouse MLN64 N-terminal (MENTAL) domain was likewise RT-PCR amplified from liver cDNA with *Bam*HI tailed primers (Table 7.7), and cloned into FLAG-STARTs via *Bam*HI. *Kpn*I digests identified clones with the correct MENTAL orientation before sequence verification.

To generate the mouse StarD4 and MLN64 salt bridge mutant expression plasmids, the FLAG-START vectors were modified using the QuikChange II site-directed mutagenesis kit (Stratagene). Briefly, a pair of oppositely directed primers with the desired mutation(s) was used to replicate both plasmid strands with a high fidelity *Pfu* DNA polymerase. The methylated parental DNA was digested with DpnI, while the mutant strands were transformed into bacteria for nick repair, generating mutant plasmids. Three types of mutagenic primers were designed for each gene, one targeting both residues of the αC salt bridge, and two others targeting the charged β5 and β6 residues individually. The six forward mutagenic primers are shown in Table 7.8, and the six corresponding reverse primers were complementary. In addition to the desired changes for amino acid substituitons (underlined), the primers also introduced silent mutations (lower case) that added or removed restriction sites. This allowed screening for mutants based on restriction fragment length polymorphisms (RFLPs), though this was not ultimately necessary as mutagenesis efficiency

Table 7.8: Mutagenic primers for StarD4 and MLN64 salt bridge mutants

gene	substitution(s)	RFLP	forward primer
StarD4	R92M, D96N	-AgeI	CCAGGGCCCTGGATGTTGGACTGGAAtCGGTTAATGACC
	Y177D	+BspHI	GAGAATTGTTGTGTcATGaGaGACACCACTGCTGGGC
	S136R	+SalI	CCGAGAGAGTTTGTcGAcTTCCGCTATACTGTGGGC
MLN64	M307R, N311D	+MluI	GCAGCCTGAGAGaCGCGTGCTGTGGGACAAGACGGTGAC
	D332Y	-BspEI	CCTTGTCTCCTATTATGTGTCATCaGGAGCTGCAGGTGG
	R351S	+XhoI	GACTTTGTGAATGTCTCGaGaATTGAGCGGCGCAGAG

was >90%. To generate the double and triple mutations, mutant plasmids were subjected to additional rounds of mutagenesis. All mutations were confirmed by DNA sequencing.

StarD4 and Star5 luciferase reporters: The mouse StarD4 proximal promoter was PCR amplified from C57BL/6 genomic DNA using a forward primer at –1335 and reverse primers at either +34 or +137 (Table 7.9). The forward primer had a *Sac*I tail, and the reverse primers had *Hind*III tails. These PCR products were TA cloned. To generate the –1335 StarD4 reporters, the entire *Sac*I/*Hind*III fragment was subcloned into these sites in the pGL3 basic luciferase vector (Promega). To generate –874 reporters, *Bgl*II (which cuts at –874) and *Hind*III digested fragments were cloned into these sites of pGL3. To generate –350 reporters, such as the –350/+34 reporter used in most experiments, *Bam*HI (which cuts at –350) and *Hind*III digested fragments were cloned into the *Bgl*II/*Hind*III sites of pGL3. The human StarD4 proximal promoter from –521 to –8 was similarly PCR amplified from genomic DNA with *Bam*HI and *Hind*III tails, and cloned into pGL3.

Table 7.9: PCR Primers for cloning StarD4 and StarD5 reporters

gene	location	primer	tail	sequence
mStarD4	-1335	forward	*Sac*I	gcttct*gagctc*GAGTGCGTGTGCATGTTCAGACATTG
	-350	forward	*Sac*I	gcttct*gagctc*GGATCCAATCCTACAAACCCTTACGCTTAGG
	+34	reverse	*Hind*III	gcttct*aagctt*GGATGTCAGGCGGTCAACAACTCC
	+137	reverse	*Hind*III	gcttct*aagctt*CTCTCTCCCCTCTACAGGGGGCAGC
hStarD4	-521	forward	*Bam*HI	gcttct*ggatcc*GTCAGGCTAAGCAGGAGGCAGAGAGC
	-282	forward	*Sac*I	gcttct*gagctc*CCCAACCAATCCAAACCTGCAGGC
	-8	reverse	*Hind*III	gcttct*aagctt*TCGCAGCCAACTGGAAGGCAC
mStarD5	-1 from ATG	reverse	*Hind*III	gcttc*aagctt*CCGCCAACGTGCAGGCTCCC
	-200 from ATG	forward	*Kpn*I	gcttc*ggtacc*GAGCTGCCTGAGACCCGCCCAGAG
	-400 from ATG	forward	*Kpn*I	gcttc*ggtacc*TGGTGTGTACCCCTCCTGCCTAC

Mutations were generated in the mouse –350/+34 and human –521/-8 reporters using the GeneEditor *in vitro* Site-Directed Mutagenesis System (Promega) according to manufacturer instructions. Briefly, double stranded plasmid template was denatured, and a

mutant strand was synthesized using one oligo to mutagenize the region of interest and another to alter the ampicillin resistance cassette. The chimeric DNA with both mutant and wild type strands was transformed into mismatch repair deficient bacteria. Bacteria were grown in the GeneEditor antibiotic selection mix, which selected for the modified ampicillin resistance. DNA from these cells was isolated and normal bacteria were transformed to produce mutant plasmids. The mouse and human StarD4 mutagenic oligos to eliminate potential sterol regulatory elements (SREs) are indicated in Table 7.10. The mutations were designed to add or remove restriction sites so mutant clones could be identified by RFLPs. All wild type and mutant reporter constructs were sequence-verified.

Table 7.10: Mutagenic primers for StarD4 promoter elements

reporter	site	RFLP	mutagenic primer
mStarD4	SRE-A	-EaeI	CTGGCTCCGGCACGCCCACACGCAC
	SRE-B	+BamHI	GCACGCGGAATCGGTGGATCCTCGGAGGCCAA
	SRE-C	+EaeI	TTCACGCTGAGGCACTGGCCAATCCCAGCGAAC
	SRE-D	+StyI	CTCCCGCTAACACCCTAGGGAAGTTCCCCTCC
	SRE-E	+BamHI	CTCGCCTTCACCAAGGATCCCTTCTGCCTTCTGATTG
	CCAAT-B	+StuI	CATCCTCGGAGGCCTGTCGGCTCCCTTCAC
	CCAAT-C	+BamHI	GCTGAGGCACCAGCGGATCCCAGCGAACACAC
hStarD4	SRE-A	+ApaI	CGGCTCGGGCGGGCCCACACCCA
	SRE-B	+BamHI	CACACCCACGCGGAATGGATCCATTTATCGGCCAC
	SRE-C	+EaeI	CACACGCTCCCGCGCTGGCCAATCCGAACAAG
	CCAAT-B	+PmlI	CCATTTATCGGCCACGTGTCAGCCCTCCACACGC
	CCAAT-C	+BamHI	CTCCCGCGCCAGCGGATCCGAACAAGCG

A potential SREBP-binding E box was reported in the pGL3 polylinker, between the *Sac*I and *Bgl*II sites (Annicotte et al., 2001). The mouse –350/+34 and human –521/–8 StarD4 reporters were previously cloned into the *Bgl*II and *Hind*III sites and included this potentially confounding element. Therefore, additional forward primers with *Sac*I tails for mouse –350 and human –282 (Table 7.9) were generated to PCR amplify and re-clone these

reporters. These modified *Sac*I/*Hind*III cloned wild type and SRE-B mutant reporters showed the same activity and regulation as the previous *Bgl*II/*Hind*III versions. Additional mutations were generated in the modified reporters using GeneEditor as before: CCAAT boxes were eliminated from the wild type reporter, and additional SRE mutations were added to SRE-B mutant mouse StarD4 reporters.

StarD5 luciferase reporters were also generated, though 5' RACE was not performed to identify the true transcription start site. The putative StarD5 proximal promoter was amplified from C57BL/6 genomic DNA, using forward primers at –400 or –200 from the ATG and a reverse primer at –1 (Table 7.9). The forward primers had a *Kpn*I tails, and the reverse primer had *Hind*III, so the products were subcloned into these sites of pGL3 basic.

Other reporter and expression plasmids: The SREx3 luciferase reporter was a gift of Doug Thewke and Michael Sinensky, and was generated by subcloning the sterol-regulated promoter region from the pTK(Kx3) CAT reporter (Dawson et al., 1988) into pGL2 basic (Promega). The LXRE luciferase reporter, as well as the expression plasmids for human LXRα and RXRα, were gifts of Jonathan Smith and originally generated in the laboratory of Ron Evans (Forman et al., 1997). The two ER stress activated pGL3 reporters, BiP promoter and the artificial 5xATF6 (Ye et al., 2000), were gifts of Ron Prywes. For the steroidogenesis assay, the F2 expression plasmid for P450scc and its electron transporters (Harikrishna et al., 1993) was a gift of Walter Miller, and the 3β-HSD expression plasmid (Zhang et al., 2002b) was a gift of Jerry Strauss.

Antibodies, Western blots, and immunofluorescence: Two antigenic peptides were designed for mouse StarD4 based on their locations in the X-ray crystal structure and

predictions of antigenicity (using DNAStar Protean software). The epitopes were conserved between mouse and human StarD4, but not in other START proteins. Bethyl Laboratory synthesized the 52-67 and 153-168 peptides, conjugated them to KLH, and immunized rabbits with both peptides in adjuvant. Immune serum was generated and each antibody was affinity-purified over a cyanogen-bromide linked peptide column. Likewise, two affinity purified rabbit antibodies against mouse StarD6 peptides 29-44 and 154-169 were also generated.

For Western Blots, whole cell lysates were prepared in lysis buffer with protease inhibitor cocktail (Sigma). Cultured cells were scraped from the plate with a rubber policeman, or liver tissue was homogenized. Protein concentrations were measured using BCA reagent (Pierce) relative to a standard curve of bovine serum albumin (BSA). 40-50 μg of protein was loaded in each well of pre-cast 8% or 12% polyacrylamides gels (Invitrogen) for SDS-PAGE. Proteins were transferred to nitrocellulose membranes (Invitrogen), and blots were blocked in PBS-casein (Pierce). For StarD4 Western blots, the primary antibody was anti-StarD4 52-67 (1:250) and the secondary was goat anti-rabbit HRP (1:2000, Sigma). For FLAG Western blots, the primary antibody was anti-FLAG M2 (1:500 Sigma) and secondary was goat anti-mouse IgG HRP (1:2000, Sigma). Blots were washed in PBS-Tween and developed using NEN Renaissance Chemiluminenscence Reagent (Perkin Elmer).

For immunofluorescence, HEK 293 cells were grown on chamber slides and transfected with FLAG-START expression plasmids. After overnight incubation, cells were rinsed with PBS, fixed and permeabilized with methanol at -20°C, rinsed with PBS, and blocked with PBS casein (Pierce). The primary antibody was anti-FLAG M2 (1:1000, Sigma) and the secondary antibody was Cy3-coupled goat anti-mouse IgG (1:10,000, Sigma). Cells were mounted and viewed on a fluorescence microscope.

Additional methods: To generate the EGFP-StarD4 fusion, the mouse StarD4 ORF was PCR amplified using the primers in Table 7.7, except both primers had BamHI tails. The product was cloned into the BglII and BamHI sites of pEGFP-C1 (Clonetech), and the proper direction and in-frame GFP fusion were confirmed by sequencing. Six well plates of NIH 3T3 or HEK 293 cells were transfected using 1μg of DNA per well, and cells were imaged the next day by fluorescence microscopy. Table 7.11 shows additional RT-PCR primers for Xbp1 (see Figure 3.15) and human StarD6 (see Figure 5.7).

Table 7.11: Additional RT-PCR primers for mouse Xbp1 and human StarD6

Primers for Xbp1 splicing assay:		
Xbp1	forward	AAACAGAGTAGCAGCGCAGACTGC
Xbp1	reverse	GGGATCTCTAAAACTAGAGGCTTGGTG
Primer for RT-PCR of human StarD6:		
exon 2 (5'UTR)	forward	GGATTTGGAGAGGAGCCCCAGTAGTTAC
exon 3 (ORF)	forward	ATGGACTTCAAGGCAATTGCCCAACAAAC
exon 8 (ORF)	reverse	TCATGAATGACTATTATGATGAAATCCACGTC

Knockout and transgenic mouse constructs: To generate the conditional StarD4 knockout construct (see Figure 4.11), the BAC AC020796 containing the 129 strain mouse StarD4 gene was obtained from Lawrence Berkely Laboratories. This BAC was digested with *KpnI*, and the ~11 kB fragment of StarD4, spanning from the 5' flanking region into intron 3, was cloned into the *Kpn*I site of pSP72 vector (Promega). A LoxP site flanked by two restriction sites on each side (*Bss*SI-*Hpa*I-LoxP-*Pst*I-*Bss*SI) was generated by synthesizing the complemenatary oligos in Table 7.12. This double stranded oligo with *Bss*SI sticky ends was cloned into the *Bss*SI site in StarD4 intron 2. The neomycin resistance cassette flanked by two LoxP sites (LoxP-neo-LoxP) from the vector pKSloxPNT (Hanks et al., 1995) was subcloned into the *Kpn*I and *Cla*I sites of pBluescript(KS+) (Strategene), then a the LoxP-neo-LoxP fragment was generated by *Eco*RI digest. The *Eco*RI fragment was cloned into the

*Mfe*I site of StarD4 intron 3. This generated the targeting construct with a long arm of 9154 bp, a short arm of 1426 bp, and a targeting region of 254 bp including exon 3. Both cloning junctions and the LoxP site orientations were sequence-verified, using forward and reverse sequencing primers in introns 2 and 3 and in the neomycin resistance cassette (Table 7.12). The targeting construct was transfected into 129 strain ES cells by the Rockefeller University Gene Targeting Facility. To screen for ES clones with homologous recombination, a Southern blot probe in StarD4 intron 3 downstream of the targeting construct was designed. The 289 bp probe template was generated by PCR using the primers in Table 7.12. Southern Blot of genomic DNA from ES cells showed only the wild type 3.6 kB *Pst*I fragment, and none of almost 200 clones showed the targeted 2.3 kB fragment.

To generate the StarD6 knockout construct (see Figure 5.9), the BAC RP23-5B18 containing the C57BL/6 strain mouse StarD6 gene was obtained from Research Genetics. This BAC was digested with *Kpn*I and *Eco*RV, and the ~5.8 kB KpnI fragment of StarD6, spanning from the 5' flanking region into intron 3, was cloned into the *Kpn*I/*Eco*RV sites of pBluescript(KS+) (Strategene). This was the long arm of the targetting construct. The short arm, a 726 bp fragment of intron 5, was generated by PCR from C57/BL6 genomic DNA using the primers in Table 7.12. The forward primer had an *Spe*I site and the reverse primer had a *Sac*I site, so the short arm fragment was cloned into these sites downstream of the long arm in pBluescript. Finally, the neomycin resistance cassette *Eco*RI fragment (described above for the StarD4 knockout), was cloned between the long and short arm in the *Eco*RI site of pBluescript. The targetting construct thus replaced exons 4 and 5 of StarD6, including the start codon, with a neomycin cassette. Cloning junctions were sequence-verified with the neomycin cassette primers described above. The targeting construct was transfected into C57BL/6 strain ES cells by the Rockefeller University Gene Targeting Facility. To screen for ES clones with homologous recombination, a Southern blot probe in the 5' flanking

region upstream of the targeting construct was designed. The 293 bp probe template was generated by PCR using the primers in Table 7.12. Southern Blot of genomic DNA from ES cells showed only the wild type 12 kB *Eco*RI fragment, and none of almost 150 clones showed the targeted 6 kB fragment.

To generate transgenic mice overexpressing StarD4 or StarD5 in liver, human StarD4 and StarD5 ORFs were PCR amplified using the primers in Table 7.7, except with a *Kpn*I tail on the forward primer and *Xho*I on the reverse primer. The human sequences were used so that transgene mRNA expression could be distinguished from the endogenous mouse genes. These ORFs were cloned into the *Kpn*I/*Xho*I sites of pLIV.7, a transgene construct in which liver expression is driven by the human ApoE promoter and enhancer (Fan et al., 1998). Both constructs were sequence verified using primers in the pLIV.7 vector (Table 7.12). *Sac*II and *Spe*I digestion isolated the linear ~6.5 kB transgene fragments from the vector. The fragments were purified by ethanol precipitation such that the OD 260/280 was greater than

Table 7.12: Primers for knockout targeting constructs and transgenes

Primers for StarD4 knockout:			
LoxP site oligo	forward	acg*agttaac*ATAACTTCGTATAATGTATGCTATACGAAGTTAT*ctgcagc*	
	reverse	tcgtg*ctgcag*ATAACTTCGTATAGCATACATTATACGAAGTTAT*gttaac*	
intron 3 probe	forward	GGTACCCTGTTAGTGTATATTTAATTCCAGGGAAG	
	reverse	GGATCCAGGAGTTTGCTGTGAGACC	
intron 2 sequence	forward	GAAGTCATTGGATCCCTGAGCTACTG	
	reverse	GTACATGGTGATTGTCACATAGGTGG	
intron 3 sequence	forward	CCTCAGAAGAGTTTAATGGGTATCTG	
	reverse	AAATTCAGATCTGTATCTGTCTACTGC	
neomycin sequence	forward	GCTAAAGCGCATGCTCCAGAC	
	reverse	CCAAGTTCTAATTCCATCAGAAGCTG	
Primers for StarD6 knockout:			
intron 5 short arm	forward	gact*actagt*ACATCTTCCCATTTACAGCCATCGTCG	(*Spe*I tail)
	reverse	gtca*gagctc*CTAGATACAAACACAGGTAAACTTCAGTAAG	(*Sac*I tail)
5' probe	forward	CTCTGCCAGTGTTCAGTAGAGTTTATGAATTC	
	reverse	GTCCTTGGAGAAGACACAGGTACC	
Primers for pLIV.7 transgene sequencing:			
hApoE exon 4	forward	TAGGGTCCACCCCAGGAG	
pLIV.7 downstream	reverse	GCAGATGCGTGAAACTTGGTGAATC	

1.9 and the the OD 260/230 ratio was greater than 1.6. Pronuclear injection of transgene DNA was carried out at the Rockefeller University Transgenic Facility, and 33 potential founder mice were generated. Genotyping of tail tip DNA by PCR with the respective human StarD4 or StarD5 ORF primers failed to reveal any founders.

Data analysis and statistics: For all quantitative assays, the control and experimental groups were compared by a two-tailed type 2 Students T-test, with the threshold for significance at $P<0.05$. Data was analyzed in Microsoft Exel and graphed in Prism (Graphpad). All bar graphs show the mean with standard deviation error bars.

References

Adams, S. H., Chui, C., Schilbach, S. L., Yu, X. X., Goddard, A. D., Grimaldi, J. C., Lee, J., Dowd, P., Colman, S., and Lewin, D. A. (2001). BFIT, a unique acyl-CoA thioesterase induced in thermogenic brown adipose tissue: cloning, organization of the human gene and assessment of a potential link to obesity. Biochem J *360*, 135-142.

Agellon, L. B., Drover, V. A., Cheema, S. K., Gbaguidi, G. F., and Walsh, A. (2002). Dietary cholesterol fails to stimulate the human cholesterol 7alpha-hydroxylase gene (CYP7A1) in transgenic mice. J Biol Chem *277*, 20131-20134.

Agellon, L. B., and Torchia, E. C. (2000). Intracellular transport of bile acids. Biochim Biophys Acta *1486*, 198-209.

Akiyama, N., Sasaki, H., Ishizuka, T., Kishi, T., Sakamoto, H., Onda, M., Hirai, H., Yazaki, Y., Sugimura, T., and Terada, M. (1997). Isolation of a candidate gene, CAB1, for cholesterol transport to mitochondria from the c-ERBB-2 amplicon by a modified cDNA selection method. Cancer Res *57*, 3548-3553.

Alpy, F., Stoeckel, M. E., Dierich, A., Escola, J. M., Wendling, C., Chenard, M. P., Vanier, M. T., Gruenberg, J., Tomasetto, C., and Rio, M. C. (2001). The Steroidogenic Acute Regulatory Protein Homolog MLN64, a Late Endosomal Cholesterol-binding Protein. J Biol Chem *276*, 4261-4269.

Alpy, F., Wendling, C., Rio, M. C., and Tomasetto, C. (2002). MENTHO, a MLN64 homologue devoid of the START domain. J Biol Chem.

Amemiya-Kudo, M., Shimano, H., Hasty, A. H., Yahagi, N., Yoshikawa, T., Matsuzaka, T., Okazaki, H., Tamura, Y., Iizuka, Y., Ohashi, K., *et al.* (2002). Transcriptional activities of nuclear SREBP-1a, -1c, and -2 to different target promoters of lipogenic and cholesterogenic genes. J Lipid Res *43*, 1220-1235.

Annicotte, J. S., Schoonjans, K., Haby, C., and Auwerx, J. (2001). An E-box in pGL3 reporter vectors precludes their use for the study of sterol regulatory element-binding proteins. Biotechniques *31*, 993-994, 996.

Arakane, F., Kallen, C. B., Watari, H., Stayrook, S. E., Lewis, M., and Strauss, J. F., 3rd (1998). Steroidogenic acute regulatory protein (StAR) acts on the outside of mitochondria to stimulate steroidogenesis. Endocr Res *24*, 463-468.

Arakane, F., Sugawara, T., Nishino, H., Liu, Z., Holt, J. A., Pain, D., Stocco, D. M., Miller, W. L., and Strauss, J. F., 3rd (1996). Steroidogenic acute regulatory protein (StAR) retains activity in the absence of its mitochondrial import sequence: implications for the mechanism of StAR action. Proc Natl Acad Sci U S A *93*, 13731-13736.

Ashrafi, K., Chang, F. Y., Watts, J. L., Fraser, A. G., Kamath, R. S., Ahringer, J., and Ruvkun, G. (2003). Genome-wide RNAi analysis of Caenorhabditis elegans fat regulatory genes. Nature *421*, 268-272.

Atshaves, B. P., Storey, S. M., and Schroeder, F. (2003). Sterol carrier protein-2/sterol carrier protein-x expression differentially alters fatty acid metabolism in L-cell fibroblasts. J Lipid Res.

Baez, J. M., Barbour, S. E., and Cohen, D. E. (2002). Phosphatidylcholine transfer protein promotes apolipoprotein A-I-mediated lipid efflux in Chinese hamster ovary cells. J Biol Chem *277*, 6198-6206.

Bennett, M. K., and Osborne, T. F. (2000). Nutrient regulation of gene expression by the sterol regulatory element binding proteins: increased recruitment of gene-specific coregulatory factors and selective hyperacetylation of histone H3 in vivo. Proc Natl Acad Sci U S A *97*, 6340-6344.

Bernlohr, D. A., Simpson, M. A., Hertzel, A. V., and Banaszak, L. J. (1997). Intracellular lipid-binding proteins and their genes. Annu Rev Nutr *17*, 277-303.

Bjorkhem, I. (2002). Do oxysterols control cholesterol homeostasis? J Clin Invest *110*, 725-730.

Blanchette-Mackie, E. J. (2000). Intracellular cholesterol trafficking: role of the NPC1 protein. Biochim Biophys Acta *1486*, 171-183.

Blanchette-Mackie, E. J., and Pentchev, P. G. (1998). Cholesterol distribution in Golgi, lysosomes, and endoplasmic reticulum. In Intracellular Cholesterol Trafficking, T. Y. Chang, and D. A. Freeman, eds. (Boston, Kluwer Academic Publishing), pp. 53-74.

Blom, T. S., Linder, M. D., Snow, K., Pihko, H., Hess, M. W., Jokitalo, E., Veckman, V., Syvanen, A. C., and Ikonen, E. (2003). Defective endocytic trafficking of NPC1 and NPC2 underlying infantile Niemann-Pick type C disease. Hum Mol Genet *12*, 257-272.

Bose, H., Lingappa, V. R., and Miller, W. L. (2002). Rapid regulation of steroidogenesis by mitochondrial protein import. Nature *417*, 87-91.

Bose, H. S., Baldwin, M. A., and Miller, W. L. (1998). Incorrect folding of steroidogenic acute regulatory protein (StAR) in congenital lipoid adrenal hyperplasia. Biochemistry *37*, 9768-9775.

Bose, H. S., Sugawara, T., Strauss, J. F., 3rd, and Miller, W. L. (1996). The pathophysiology and genetics of congenital lipoid adrenal hyperplasia. International Congenital Lipoid Adrenal Hyperplasia Consortium. N Engl J Med *335*, 1870-1878.

Bose, H. S., Whittal, R. M., Huang, M. C., Baldwin, M. A., and Miller, W. L. (2000). N-218 MLN64, a protein with StAR-like steroidogenic activity, is folded and cleaved similarly to StAR. Biochemistry *39*, 11722-11731.

Brown, A. J., Sun, L., Feramisco, J. D., Brown, M. S., and Goldstein, J. L. (2002). Cholesterol addition to ER membranes alters conformation of SCAP, the SREBP escort protein that regulates cholesterol metabolism. Mol Cell *10*, 237-245.

Brown, M. S., and Goldstein, J. L. (1999). A proteolytic pathway that controls the cholesterol content of membranes, cells, and blood. Proc Natl Acad Sci U S A *96*, 11041-11048.

Brown, P. O., and Botstein, D. (1999). Exploring the new world of the genome with DNA microarrays. Nat Genet *21*, 33-37.

Byskov, A. G., Baltsen, M., and Andersen, C. Y. (1998). Meiosis-activating sterols: background, discovery, and possible use. J Mol Med *76*, 818-823.

Calfon, M., Zeng, H., Urano, F., Till, J. H., Hubbard, S. R., Harding, H. P., Clark, S. G., and Ron, D. (2002). IRE1 couples endoplasmic reticulum load to secretory capacity by processing the XBP-1 mRNA. Nature *415*, 92-96.

Caron, K. M., Soo, S. C., and Parker, K. L. (1998). Targeted disruption of StAR provides novel insights into congenital adrenal hyperplasia. Endocr Res *24*, 827-834.

Chang, T. Y., Chang, C. C. Y., and Lee, O. (1998). The sterol-specific regulation of ACAT-1 and SREBPs in mammalian cells and liver. In Intracellular Cholesterol Trafficking, T. Y. Chang, and D. A. Freeman, eds. (Boston, Kluwer Academic Publishing), pp. 1-14.

Chen, L., Sato, M., Inoko, H., and Kimura, M. (1997). Molecular cloning and analysis of novel cDNAs specifically expressed in adult mouse testes. Biochem Biophys Res Commun *240*, 261-268.

Cheng, B., Hsu, D. K., and Kimura, T. (1985). Utilization of intramitochondrial membrane cholesterol by cytochrome P-450-dependent cholesterol side-chain cleavage reaction in bovine adrenocortical mitochondria: steroidogenic and non-steroidogenic pools of cholesterol in the mitochondrial inner membranes. Mol Cell Endocrinol *40*, 233-243.

Cheung, V. G., Morley, M., Aguilar, F., Massimi, A., Kucherlapati, R., and Childs, G. (1999). Making and reading microarrays. Nat Genet *21*, 15-19.

Choi, B. K., Chitwood, D. J., and Paik, Y. K. (2003). Proteomic changes during disturbance of cholesterol metabolism by azacoprostane treatment in Caenorhabditis elegans. Mol Cell Proteomics.

Choi, Y. S., and Freeman, D. A. (1998). The movement of plasma membrane cholesterol through the cell. In Intracellular Cholesterol Trafficking, T. Y. Chang, and D. A. Freeman, eds. (Boston, Kluwer Academic Publishing), pp. 109-121.

Choinowski, T., Hauser, H., and Piontek, K. (2000). Structure of sterol carrier protein 2 at 1.8 A resolution reveals a hydrophobic tunnel suitable for lipid binding. Biochemistry *39*, 1897-1902.

Choudhury, A., Dominguez, M., Puri, V., Sharma, D. K., Narita, K., Wheatley, C. L., Marks, D. L., and Pagano, R. E. (2002). Rab proteins mediate Golgi transport of caveola-internalized

glycosphingolipids and correct lipid trafficking in Niemann-Pick C cells. J Clin Invest *109*, 1541-1550.

Christensen, K., Bose, H. S., Harris, F. M., Miller, W. L., and Bell, J. D. (2001). Binding of steroidogenic acute regulatory protein to synthetic membranes suggests an active molten globule. J Biol Chem *276*, 17044-17051.

Cohen, D. E., Green, R. M., Wu, M. K., and Beier, D. R. (1999). Cloning, tissue-specific expression, gene structure and chromosomal localization of human phosphatidylcholine transfer protein. Biochim Biophys Acta *1447*, 265-270.

Connor, W. E., Lin, D. S., Wolf, D. P., and Alexander, M. (1998). Uneven distribution of desmosterol and docosahexaenoic acid in the heads and tails of monkey sperm. J Lipid Res *39*, 1404-1411.

Costet, P., Luo, Y., Wang, N., and Tall, A. R. (2000). Sterol-dependent transactivation of the ABC1 promoter by the liver X receptor/retinoid X receptor. J Biol Chem *275*, 28240-28245.

Cruz, J. C., and Chang, T. Y. (2000). Fate of endogenously synthesized cholesterol in Niemann-Pick type C1 cells. J Biol Chem *275*, 41309-41316.

Cruz, J. C., Sugii, S., Yu, C., and Chang, T. Y. (2000). Role of Niemann-Pick type C1 protein in intracellular trafficking of low density lipoprotein-derived cholesterol. J Biol Chem *275*, 4013-4021.

Davies, J. P., Chen, F. W., and Ioannou, Y. A. (2000). Transmembrane molecular pump activity of Niemann-Pick C1 protein. Science *290*, 2295-2298.

Dawson, P. A., Hofmann, S. L., van der Westhuyzen, D. R., Sudhof, T. C., Brown, M. S., and Goldstein, J. L. (1988). Sterol-dependent repression of low density lipoprotein receptor promoter mediated by 16-base pair sequence adjacent to binding site for transcription factor Sp1. J Biol Chem *263*, 3372-3379.

de Brouwer, A. P., Westerman, J., Kleinnijenhuis, A., Bevers, L. E., Roelofsen, B., and Wirtz, K. W. (2002). Clofibrate-induced relocation of phosphatidylcholine transfer protein to mitochondria in endothelial cells. Exp Cell Res *274*, 100-111.

De Franca, L. R., Bartke, A., Borg, K. E., Cecim, M., Fadden, C. T., Yagi, A., and Russell, L. D. (1994). Sertoli cells in testes containing or lacking germ cells: a comparative study of paracrine effects using the W (c-kit) gene mutant mouse model. Anat Rec *240*, 225-232.

DeBose-Boyd, R. A., Ou, J., Goldstein, J. L., and Brown, M. S. (2001). Expression of sterol regulatory element-binding protein 1c (SREBP-1c) mRNA in rat hepatoma cells requires endogenous LXR ligands. Proc Natl Acad Sci U S A *98*, 1477-1482.

DeGrella, R. F., and Simoni, R. D. (1982). Intracellular transport of cholesterol to the plasma membrane. J Biol Chem *257*, 14256-14262.

Diatchenko, L., Lau, Y. F., Campbell, A. P., Chenchik, A., Moqadam, F., Huang, B., Lukyanov, S., Lukyanov, K., Gurskaya, N., Sverdlov, E. D., and Siebert, P. D. (1996).

Suppression subtractive hybridization: a method for generating differentially regulated or tissue-specific cDNA probes and libraries. Proc Natl Acad Sci U S A *93*, 6025-6030.

Dietschy, J. M., and Turley, S. D. (2002). Control of cholesterol turnover in the mouse. J Biol Chem *277*, 3801-3804.

Dobrosotskaya, I. Y., Seegmiller, A. C., Brown, M. S., Goldstein, J. L., and Rawson, R. B. (2002). Regulation of SREBP processing and membrane lipid production by phospholipids in Drosophila. Science *296*, 879-883.

Dooley, K. A., Millinder, S., and Osborne, T. F. (1998). Sterol regulation of 3-hydroxy-3-methylglutaryl-coenzyme A synthase gene through a direct interaction between sterol regulatory element binding protein and the trimeric CCAAT-binding factor/nuclear factor Y. J Biol Chem *273*, 1349-1356.

Ebisuno, S., Isohashi, F., Nakanishi, Y., and Sakamoto, Y. (1988). Acetyl-CoA hydrolase: relation between activity and cholesterol metabolism in rat. Am J Physiol *255*, R724-730.

Eddy, E. M. (1998). Regulation of gene expression during spermatogenesis. Semin Cell Dev Biol *9*, 451-457.

Edwards, P. A., and Ericsson, J. (1999). Sterols and isoprenoids: signaling molecules derived from the cholesterol biosynthetic pathway. Annu Rev Biochem *68*, 157-185.

Edwards, P. A., Tabor, D., Kast, H. R., and Venkateswaran, A. (2000). Regulation of gene expression by SREBP and SCAP. Biochim Biophys Acta *1529*, 103-113.

Elbashir, S. M., Harborth, J., Lendeckel, W., Yalcin, A., Weber, K., and Tuschl, T. (2001). Duplexes of 21-nucleotide RNAs mediate RNA interference in cultured mammalian cells. Nature *411*, 494-498.

Ennis, H. L., Dao, D. N., Pukatzki, S. U., and Kessin, R. H. (2000). Dictyostelium amoebae lacking an F-box protein form spores rather than stalk in chimeras with wild type. Proc Natl Acad Sci U S A *97*, 3292-3297.

Ericsson, J., Jackson, S. M., and Edwards, P. A. (1996). Synergistic binding of sterol regulatory element-binding protein and NF-Y to the farnesyl diphosphate synthase promoter is critical for sterol-regulated expression of the gene. J Biol Chem *271*, 24359-24364.

Eschenlauer, S. C., and Page, A. P. (2003). The Caenorhabditis elegans ERp60 homolog protein disulfide isomerase-3 has disulfide isomerase and transglutaminase-like cross-linking activity and is involved in the maintenance of body morphology. J Biol Chem *278*, 4227-4237.

Falquet, L., Pagni, M., Bucher, P., Hulo, N., Sigrist, C. J., Hofmann, K., and Bairoch, A. (2002). The PROSITE database, its status in 2002. Nucleic Acids Res *30*, 235-238.

Fan, J., Ji, Z. S., Huang, Y., de Silva, H., Sanan, D., Mahley, R. W., Innerarity, T. L., and Taylor, J. M. (1998). Increased expression of apolipoprotein E in transgenic rabbits results in

reduced levels of very low density lipoproteins and an accumulation of low density lipoproteins in plasma. J Clin Invest *101*, 2151-2164.

Farnegardh, M., Bonn, T., Sun, S., Ljunggren, J., Ahola, H., Wilhelmsson, A., Gustafsson, J. A., and Carlquist, M. (2003). The three dimensional structure of the liver X receptor beta reveals a flexible ligand binding pocket that can accommodate fundamentally different ligands. J Biol Chem.

Feng, B., Yao, P. M., Li, Y., Devlin, C. M., Zhang, D., Harding, H. P., Sweeney, M., Rong, J. X., Kuriakose, G., Fisher, E. A., *et al.* (2003a). The endoplasmic reticulum is the site of cholesterol-induced cytotoxicity in macrophages. Nat Cell Biol.

Feng, B., Zhang, D., Kuriakose, G., Devlin, C. M., Kockx, M., and Tabas, I. (2003b). Niemann-Pick C heterozygosity confers resistance to lesional necrosis and macrophage apoptosis in murine atherosclerosis. Proc Natl Acad Sci U S A.

Feng, L., Chan, W. W., Roderick, S. L., and Cohen, D. E. (2000). High-level expression and mutagenesis of recombinant human phosphatidylcholine transfer protein using a synthetic gene: evidence for a C-terminal membrane binding domain. Biochemistry *39*, 15399-15409.

Ferguson, K. C., Heid, P. J., and Rothman, J. H. (1996). The SL1 trans-spliced leader RNA performs an essential embryonic function in Caenorhabditis elegans that can also be supplied by SL2 RNA. Genes Dev *10*, 1543-1556.

Field, F. J., Born, E., Murthy, S., and Mathur, S. N. (1998). Transport of cholesterol from the endoplasmic reticulum to the plasma membrane is constitutive in CaCo-2 cells and differs from the transport of plasma membrane cholesterol to the endoplasmic reticulum. J Lipid Res *39*, 333-343.

Forman, B. M., Ruan, B., Chen, J., Schroepfer, G. J., Jr., and Evans, R. M. (1997). The orphan nuclear receptor LXRalpha is positively and negatively regulated by distinct products of mevalonate metabolism. Proc Natl Acad Sci U S A *94*, 10588-10593.

Friedland, N., Liou, H. L., Lobel, P., and Stock, A. M. (2003). Structure of a cholesterol-binding protein deficient in Niemann-Pick type C2 disease. Proc Natl Acad Sci U S A *100*, 2512-2517.

Frolkis, V. V., and Tanin, S. A. (1999). Peculiarities of axonal transport of steroid hormones (hydrocortisone, testosterone) in spinal root fibres of adult and old rats. Neuroscience *92*, 1399-1404.

Frolov, A., Srivastava, K., Daphna-Iken, D., Traub, L. M., Schaffer, J. E., and Ory, D. S. (2001). Cholesterol overload promotes morphogenesis of a Niemann-Pick C (NPC)-like compartment independent of inhibition of NPC1 or HE1/NPC2 function. J Biol Chem *276*, 46414-46421.

Frolov, A., Zielinski, S. E., Crowley, J. R., Dudley-Rucker, N., Schaffer, J. E., and Ory, D. S. (2003). NPC1 and NPC2 regulate cellular cholesterol homeostasis through generation of low density lipoprotein cholesterol-derived oxysterols. J Biol Chem *278*, 25517-25525.

Fu, X., Menke, J. G., Chen, Y., Zhou, G., MacNaul, K. L., Wright, S. D., Sparrow, C. P., and Lund, E. G. (2001). 27-hydroxycholesterol is an endogenous ligand for liver X receptor in cholesterol-loaded cells. J Biol Chem *276*, 38378-38387.

Fuchs, M. (2003). Bile acid regulation of hepatic physiology: III. Regulation of bile acid synthesis: past progress and future challenges. Am J Physiol Gastrointest Liver Physiol *284*, G551-557.

Fuchs, M., Hafer, A., Munch, C., Kannenberg, F., Teichmann, S., Scheibner, J., Stange, E. F., and Seedorf, U. (2001). Disruption of the sterol carrier protein 2 gene in mice impairs biliary lipid and hepatic cholesterol metabolism. J Biol Chem *276*, 48058-48065.

Fujise, H., Annoura, T., Sasawatari, S., Ikeda, T., and Ueda, K. (2002). Transepithelial transport and cellular accumulation of steroid hormones and polychlorobiphenyl in porcine kidney cells expressed with human P-glycoprotein. Chemosphere *46*, 1505-1511.

Gagescu, R., Demaurex, N., Parton, R. G., Hunziker, W., Huber, L. A., and Gruenberg, J. (2000). The recycling endosome of Madin-Darby canine kidney cells is a mildly acidic compartment rich in raft components. Mol Biol Cell *11*, 2775-2791.

Gallegos, A. M., Atshaves, B. P., Storey, S. M., Starodub, O., Petrescu, A. D., Huang, H., McIntosh, A. L., Martin, G. G., Chao, H., Kier, A. B., and Schroeder, F. (2001). Gene structure, intracellular localization, and functional roles of sterol carrier protein-2. Prog Lipid Res *40*, 498-563.

Gan, X., Kaplan, R., Menke, J. G., MacNaul, K., Chen, Y., Sparrow, C. P., Zhou, G., Wright, S. D., and Cai, T. Q. (2001). Dual mechanisms of ABCA1 regulation by geranylgeranyl pyrophosphate. J Biol Chem *276*, 48702-48708.

Glass, C. K., and Witztum, J. L. (2001). Atherosclerosis. the road ahead. Cell *104*, 503-516.

Goodwin, B., Jones, S. A., Price, R. R., Watson, M. A., McKee, D. D., Moore, L. B., Galardi, C., Wilson, J. G., Lewis, M. C., Roth, M. E., *et al.* (2000). A regulatory cascade of the nuclear receptors FXR, SHP-1, and LRH-1 represses bile acid biosynthesis. Mol Cell *6*, 517-526.

Granot, Z., Silverman, E., Friedlander, R., Melamed-Book, N., Eimerl, S., Timberg, R., Hales, K. H., Hales, D. B., Stocco, D. M., and Orly, J. (2002). The life cycle of the steroidogenic acute regulatory (StAR) protein: from transcription through proteolysis. Endocr Res *28*, 375-386.

Grober, J., Zaghini, I., Fujii, H., Jones, S. A., Kliewer, S. A., Willson, T. M., Ono, T., and Besnard, P. (1999). Identification of a bile acid-responsive element in the human ileal bile acid-binding protein gene. Involvement of the farnesoid X receptor/9-cis-retinoic acid receptor heterodimer. J Biol Chem *274*, 29749-29754.

Hamosh, A., Scott, A. F., Amberger, J., Bocchini, C., Valle, D., and McKusick, V. A. (2002). Online Mendelian Inheritance in Man (OMIM), a knowledgebase of human genes and genetic disorders. Nucleic Acids Res *30*, 52-55.

Hanks, M., Wurst, W., Anson-Cartwright, L., Auerbach, A. B., and Joyner, A. L. (1995). Rescue of the En-1 mutant phenotype by replacement of En-1 with En-2. Science *269*, 679-682.

Hao, M., Lin, S. X., Karylowski, O. J., Wustner, D., McGraw, T. E., and Maxfield, F. R. (2002). Vesicular and non-vesicular sterol transport in living cells. The endocytic recycling compartment is a major sterol storage organelle. J Biol Chem *277*, 609-617.

Harding, H. P., Calfon, M., Urano, F., Novoa, I., and Ron, D. (2002). Transcriptional and translational control in the Mammalian unfolded protein response. Annu Rev Cell Dev Biol *18*, 575-599.

Harikrishna, J. A., Black, S. M., Szklarz, G. D., and Miller, W. L. (1993). Construction and function of fusion enzymes of the human cytochrome P450scc system. DNA Cell Biol *12*, 371-379.

Harris, T. W., Lee, R., Schwarz, E., Bradnam, K., Lawson, D., Chen, W., Blasier, D., Kenny, E., Cunningham, F., Kishore, R., *et al.* (2003). WormBase: a cross-species database for comparative genomics. Nucleic Acids Res *31*, 133-137.

Hauet, T., Liu, J., Li, H., Gazouli, M., Culty, M., and Papadopoulos, V. (2002). PBR, StAR, and PKA: partners in cholesterol transport in steroidogenic cells. Endocr Res *28*, 395-401.

Heino, S., Lusa, S., Somerharju, P., Ehnholm, C., Olkkonen, V. M., and Ikonen, E. (2000). Dissecting the role of the golgi complex and lipid rafts in biosynthetic transport of cholesterol to the cell surface. Proc Natl Acad Sci U S A *97*, 8375-8380.

Hirano, Y., Murata, S., Tanaka, K., Shimizu, M., and Sato, R. (2003). Sterol regulatory element-binding proteins are negatively regulated through SUMO-1 modification independent of the ubiquitin/26 S proteasome pathway. J Biol Chem *278*, 16809-16819.

Hirano, Y., Yoshida, M., Shimizu, M., and Sato, R. (2001). Direct demonstration of rapid degradation of nuclear sterol regulatory element-binding proteins by the ubiquitin-proteasome pathway. J Biol Chem *276*, 36431-36437.

Hogenboom, S., Romeijn, G. J., Houten, S. M., Baes, M., Wanders, R. J., and Waterham, H. R. (2002). Absence of functional peroxisomes does not lead to deficiency of enzymes involved in cholesterol biosynthesis. J Lipid Res *43*, 90-98.

Hojmann Larsen, A., Frandsen, A., and Treiman, M. (2001). Upregulation of the SERCA-type Ca2+ pump activity in response to endoplasmic reticulum stress in PC12 cells. BMC Biochem *2*, 4.

Holtta-Vuori, M., Tanhuanpaa, K., Mobius, W., Somerharju, P., and Ikonen, E. (2002). Modulation of cellular cholesterol transport and homeostasis by Rab11. Mol Biol Cell *13*, 3107-3122.

Homma, Y., and Emori, Y. (1995). A dual functional signal mediator showing RhoGAP and phospholipase C-delta stimulating activities. Embo J *14*, 286-291.

Hornick, C. A., Hui, D. Y., and DeLamatre, J. G. (1997). A role for retrosomes in intracellular cholesterol transport from endosomes to the plasma membrane. Am J Physiol *273*, C1075-1081.

Horton, J. D., Goldstein, J. L., and Brown, M. S. (2002). SREBPs: activators of the complete program of cholesterol and fatty acid synthesis in the liver. J Clin Invest *109*, 1125-1131.

Horton, J. D., Shimomura, I., Brown, M. S., Hammer, R. E., Goldstein, J. L., and Shimano, H. (1998). Activation of cholesterol synthesis in preference to fatty acid synthesis in liver and adipose tissue of transgenic mice overproducing sterol regulatory element-binding protein-2. J Clin Invest *101*, 2331-2339.

Hu, X., Li, S., Wu, J., Xia, C., and Lala, D. S. (2003). Liver x receptors interact with corepressors to regulate gene expression. Mol Endocrinol *17*, 1019-1026.

Huang, M. C., and Miller, W. L. (2001). Creation and activity of COS-1 cells stably expressing the F2 fusion of the human cholesterol side-chain cleavage enzyme system. Endocrinology *142*, 2569-2576.

Hubank, M., and Schatz, D. G. (1999). cDNA representational difference analysis: a sensitive and flexible method for identification of differentially expressed genes. Methods Enzymol *303*, 325-349.

Hunt, M. C., and Alexson, S. E. (2002). The role Acyl-CoA thioesterases play in mediating intracellular lipid metabolism. Prog Lipid Res *41*, 99-130.

Ide, T., Shimano, H., Yoshikawa, T., Yahagi, N., Amemiya-Kudo, M., Matsuzaka, T., Nakakuki, M., Yatoh, S., Iizuka, Y., Tomita, S., *et al.* (2003). Cross-talk between peroxisome proliferator-activated receptor (PPAR) alpha and liver X receptor (LXR) in nutritional regulation of fatty acid metabolism. II. LXRs suppress lipid degradation gene promoters through inhibition of PPAR signaling. Mol Endocrinol *17*, 1255-1267.

Ikeda, Y., Yamamoto, J., Okamura, M., Fujino, T., Takahashi, S., Takeuchi, K., Osborne, T. F., Yamamoto, T. T., Ito, S., and Sakai, J. (2001). Transcriptional regulation of the murine acetyl-CoA synthetase 1 gene through multiple clustered binding sites for sterol regulatory element- binding proteins and a single neighboring site for Sp1. J Biol Chem *276*, 34259-34269.

Imachi, H., Murao, K., Sayo, Y., Hosokawa, H., Sato, M., Niimi, M., Kobayashi, S., Miyauchi, A., Ishida, T., and Takahara, J. (1999). Evidence for a potential role for HDL as an important source of cholesterol in human adrenocortical tumors via the CLA-1 pathway. Endocr J *46*, 27-34.

Ince, T. A., and Scotto, K. W. (1995). A conserved downstream element defines a new class of RNA polymerase II promoters. J Biol Chem *270*, 30249-30252.

Inoue, J., Sato, R., and Maeda, M. (1998). Multiple DNA elements for sterol regulatory element-binding protein and NF-Y are responsible for sterol-regulated transcription of the genes for human 3-hydroxy-3-methylglutaryl coenzyme A synthase and squalene synthase. J Biochem (Tokyo) *123*, 1191-1198.

Iyer, L. M., Koonin, E. V., and Aravind, L. (2001). Adaptations of the helix-grip fold for ligand binding and catalysis in the START domain superfamily. Proteins *43*, 134-144.

Janowski, B. A., Grogan, M. J., Jones, S. A., Wisely, G. B., Kliewer, S. A., Corey, E. J., and Mangelsdorf, D. J. (1999). Structural requirements of ligands for the oxysterol liver X receptors LXRalpha and LXRbeta. Proc Natl Acad Sci U S A *96*, 266-271.

Janowski, B. A., Willy, P. J., Devi, T. R., Falck, J. R., and Mangelsdorf, D. J. (1996). An oxysterol signalling pathway mediated by the nuclear receptor LXR alpha. Nature *383*, 728-731.

Javitt, N. B., Lee, Y. C., Shimizu, C., Fuda, H., and Strott, C. A. (2001). Cholesterol and hydroxycholesterol sulfotransferases: identification, distinction from dehydroepiandrosterone sulfotransferase, and differential tissue expression. Endocrinology *142*, 2978-2984.

Jefcoate, C. (2002). High-flux mitochondrial cholesterol trafficking, a specialized function of the adrenal cortex. J Clin Invest *110*, 881-890.

Jeong, J., and McMahon, A. P. (2002). Cholesterol modification of Hedgehog family proteins. J Clin Invest *110*, 591-596.

Johansson, M., Bocher, V., Lehto, M., Chinetti, G., Kuismanen, E., Ehnholm, C., Staels, B., and Olkkonen, V. M. (2003). The Two Variants of Oxysterol Binding Protein-related Protein-1 Display Different Tissue Expression Patterns, Have Different Intracellular Localization, and Are Functionally Distinct. Mol Biol Cell *14*, 903-915.

Johnson, W. J., and Reinhart, M. P. (1994). Lack of requirement for sterol carrier protein-2 in the intracellular trafficking of lysosomal cholesterol. J Lipid Res *35*, 563-573.

Johnstone, I. L. (2000). Cuticle collagen genes. Expression in Caenorhabditis elegans. Trends Genet *16*, 21-27.

Jones, T. A., Zou, J. Y., Cowan, S. W., and Kjeldgaard (1991). Improved methods for building protein models in electron density maps and the location of errors in these models. Acta Crystallogr A *47 (Pt 2)*, 110-119.

Kallen, C. B., Billheimer, J. T., Summers, S. A., Stayrook, S. E., Lewis, M., and Strauss, J. F., 3rd (1998). Steroidogenic acute regulatory protein (StAR) is a sterol transfer protein. J Biol Chem *273*, 26285-26288.

Kaplan, M. R., and Simoni, R. D. (1985). Transport of cholesterol from the endoplasmic reticulum to the plasma membrane. J Cell Biol *101*, 446-453.

Kaufman, R. J. (2002). Orchestrating the unfolded protein response in health and disease. J Clin Invest *110*, 1389-1398.

Kellner-Weibel, G., Geng, Y. J., and Rothblat, G. H. (1999). Cytotoxic cholesterol is generated by the hydrolysis of cytoplasmic cholesteryl ester and transported to the plasma membrane. Atherosclerosis *146*, 309-319.

Kim, H. J., Kim, J. E., Ha, M., Kang, S. S., Kim, J. T., Park, I. S., Paek, S. H., Jung, H. W., Kim, D. G., Cho, G. J., and Choi, W. S. (2003). Steroidogenic acute regulatory protein expression in the normal human brain and intracranial tumors. Brain Res *978*, 245-249.

Kim, J. H., Lee, J. N., and Paik, Y. K. (2001). Cholesterol biosynthesis from lanosterol. a concerted role for sp1 and nf-y-binding sites for sterol-mediated regulation of rat 7-dehydrocholesterol reductase gene expression. J Biol Chem *276*, 18153-18160.

King, S. R., Manna, P. R., Ishii, T., Syapin, P. J., Ginsberg, S. D., Wilson, K., Walsh, L. P., Parker, K. L., Stocco, D. M., Smith, R. G., and Lamb, D. J. (2002). An essential component in steroid synthesis, the steroidogenic acute regulatory protein, is expressed in discrete regions of the brain. J Neurosci *22*, 10613-10620.

Ko, D. C., Gordon, M. D., Jin, J. Y., and Scott, M. P. (2001). Dynamic movements of organelles containing Niemann-Pick C1 protein: NPC1 involvement in late endocytic events. Mol Biol Cell *12*, 601-614.

Koh, K., and Rothman, J. H. (2001). ELT-5 and ELT-6 are required continuously to regulate epidermal seam cell differentiation and cell fusion in C. elegans. Development *128*, 2867-2880.

Koh, P. O., Kim, Y. S., Cheon, E. W., Kang, S. S., Cho, G. J., and Choi, W. S. (2002). Expression of steroidogenic acute regulatory protein mRNA in rat placenta during mid-late pregnancy. Mol Cells *14*, 355-360.

Kokame, K., Kato, H., and Miyata, T. (2001). Identification of ERSE-II, a new cis-acting element responsible for the ATF6-dependent mammalian unfolded protein response. J Biol Chem *276*, 9199-9205.

Kurohmaru, M., Kanai, Y., and Hayashi, Y. (1992). A cytological and cytoskeletal comparison of Sertoli cells without germ cell and those with germ cells using the W/WV mutant mouse. Tissue Cell *24*, 895-903.

Kurzchalia, T. V., and Ward, S. (2003). Why do worms need cholesterol? Nat Cell Biol *5*, 684-688.

Laffitte, B. A., Joseph, S. B., Chen, M., Castrillo, A., Repa, J., Wilpitz, D., Mangelsdorf, D., and Tontonoz, P. (2003). The phospholipid transfer protein gene is a liver X receptor target expressed by macrophages in atherosclerotic lesions. Mol Cell Biol *23*, 2182-2191.

Laffitte, B. A., Joseph, S. B., Walczak, R., Pei, L., Wilpitz, D. C., Collins, J. L., and Tontonoz, P. (2001). Autoregulation of the human liver X receptor alpha promoter. Mol Cell Biol *21*, 7558-7568.

Lagace, T. A., Byers, D. M., Cook, H. W., and Ridgway, N. D. (1997). Altered regulation of cholesterol and cholesteryl ester synthesis in Chinese-hamster ovary cells overexpressing the oxysterol-binding protein is dependent on the pleckstrin homology domain. Biochem J *326 (Pt 1)*, 205-213.

Lange, Y. (1998). Intracellular cholesterol movement and homeostasis. In Intracellular Cholesterol Trafficking, T. Y. Chang, and D. A. Freeman, eds. (Boston, Kluwer Academic Publishers), pp. 15-28.

Lange, Y., Echevarria, F., and Steck, T. L. (1991). Movement of zymosterol, a precursor of cholesterol, among three membranes in human fibroblasts. J Biol Chem *266*, 21439-21443.

Lange, Y., Ye, J., Rigney, M., and Steck, T. (2000). Cholesterol movement in Niemann-Pick type C cells and in cells treated with amphiphiles. J Biol Chem *275*, 17468-17475.

Lange, Y., Ye, J., Rigney, M., and Steck, T. L. (1999). Regulation of endoplasmic reticulum cholesterol by plasma membrane cholesterol. J Lipid Res *40*, 2264-2270.

Lange, Y., Ye, J., Rigney, M., and Steck, T. L. (2002). Dynamics of lysosomal cholesterol in Niemann-Pick type C and normal human fibroblasts. J Lipid Res *43*, 198-204.

Lavery, D. J., Lopez-Molina, L., Fleury-Olela, F., and Schibler, U. (1997). Selective amplification via biotin- and restriction-mediated enrichment (SABRE), a novel selective amplification procedure for detection of differentially expressed mRNAs. Proc Natl Acad Sci U S A *94*, 6831-6836.

Lee, K., Tirasophon, W., Shen, X., Michalak, M., Prywes, R., Okada, T., Yoshida, H., Mori, K., and Kaufman, R. J. (2002). IRE1-mediated unconventional mRNA splicing and S2P-mediated ATF6 cleavage merge to regulate XBP1 in signaling the unfolded protein response. Genes Dev *16*, 452-466.

Lee, M. L., Kuo, F. C., Whitmore, G. A., and Sklar, J. (2000). Importance of replication in microarray gene expression studies: statistical methods and evidence from repetitive cDNA hybridizations. Proc Natl Acad Sci U S A *97*, 9834-9839.

Lehto, M., and Olkkonen, V. M. (2003). The OSBP-related proteins: a novel protein family involved in vesicle transport, cellular lipid metabolism, and cell signalling. Biochim Biophys Acta *1631*, 1-11.

Li, Y., Bolten, C., Bhat, B. G., Woodring-Dietz, J., Li, S., Prayaga, S. K., Xia, C., and Lala, D. S. (2002). Induction of human liver X receptor alpha gene expression via an autoregulatory loop mechanism. Mol Endocrinol *16*, 506-514.

Liang, M. P., Banatao, D. R., Klein, T. E., Brutlag, D. L., and Altman, R. B. (2003). WebFEATURE: An interactive web tool for identifying and visualizing functional sites on macromolecular structures. Nucleic Acids Res *31*, 3324-3327.

Liang, P., and Pardee, A. B. (1992). Differential display of eukaryotic messenger RNA by means of the polymerase chain reaction. Science *257*, 967-971.

Lichtman, A. H., Clinton, S. K., Iiyama, K., Connelly, P. W., Libby, P., and Cybulsky, M. I. (1999). Hyperlipidemia and atherosclerotic lesion development in LDL receptor-deficient mice fed defined semipurified diets with and without cholate. Arterioscler Thromb Vasc Biol *19*, 1938-1944.

Lindenthal, B., Aldaghlas, T. A., Kelleher, J. K., Henkel, S. M., Tolba, R., Haidl, G., and von Bergmann, K. (2001). Neutral sterols of rat epididymis. High concentrations of dehydrocholesterols in rat caput epididymidis. J Lipid Res *42*, 1089-1095.

Liscum, L. (1998). Analysis of somatic cell mutants that express defective intracellular cholesterol transport. In Intracellular Cholesterol Trafficking, T. Y. Chang, and D. A. Freeman, eds. (Boston, Kluwer Academic Publishing), pp. 75-92.

Liscum, L., and Collins, G. J. (1991). Characterization of Chinese hamster ovary cells that are resistant to 3-beta-[2-(diethylamino)ethoxy]androst-5-en-17-one inhibition of low density lipoprotein-derived cholesterol metabolism. J Biol Chem *266*, 16599-16606.

Liscum, L., and Munn, N. J. (1999). Intracellular cholesterol transport. Biochim Biophys Acta *1438*, 19-37.

Liu, P., Rudick, M., and Anderson, R. G. (2002). Multiple functions of caveolin-1. J Biol Chem *277*, 41295-41298.

Lodhi, K. M., Ozdener, M. H., and Shayiq, R. M. (2003). The upstream open reading frame mediates constitutive effects on translation of cytochrome P-450c27 from the 7th in-frame AUG codon in rat liver. J Biol Chem.

Lu, T. T., Makishima, M., Repa, J. J., Schoonjans, K., Kerr, T. A., Auwerx, J., and Mangelsdorf, D. J. (2000). Molecular basis for feedback regulation of bile acid synthesis by nuclear receptors. Mol Cell *6*, 507-515.

Lukyanenko, Y. O., Chen, J. J., and Hutson, J. C. (2001). Production of 25-hydroxycholesterol by testicular macrophages and its effects on Leydig cells. Biol Reprod *64*, 790-796.

Lund, E. G., Kerr, T. A., Sakai, J., Li, W. P., and Russell, D. W. (1998). cDNA cloning of mouse and human cholesterol 25-hydroxylases, polytopic membrane proteins that synthesize a potent oxysterol regulator of lipid metabolism. J Biol Chem *273*, 34316-34327.

Lund, E. G., Menke, J. G., and Sparrow, C. P. (2003). Liver x receptor agonists as potential therapeutic agents for dyslipidemia and atherosclerosis. Arterioscler Thromb Vasc Biol *23*, 1169-1177.

Luo, S., Baumeister, P., Yang, S., Abcouwer, S. F., and Lee, A. S. (2003). Induction of grp78/BiP by translational block: Activation of the Grp78 promoter by ATF4 through an upstream ATF/CRE site independent of the endoplasmic reticulum stress elements. J Biol Chem.

Luo, Y., and Tall, A. R. (2000). Sterol upregulation of human CETP expression in vitro and in transgenic mice by an LXR element. J Clin Invest *105*, 513-520.

Lusa, S., Heino, S., and Ikonen, E. (2003). Differential mobilization of newly synthesized cholesterol and biosynthetic sterol precursors from cells. J Biol Chem *278*, 19844-19851.

Ma, Y., Brewer, J. W., Diehl, J. A., and Hendershot, L. M. (2002). Two distinct stress signaling pathways converge upon the CHOP promoter during the mammalian unfolded protein response. J Mol Biol *318*, 1351-1365.

Magana, M. M., and Osborne, T. F. (1996). Two tandem binding sites for sterol regulatory element binding proteins are required for sterol regulation of fatty-acid synthase promoter. J Biol Chem *271*, 32689-32694.

Mak, P. A., Laffitte, B. A., Desrumaux, C., Joseph, S. B., Curtiss, L. K., Mangelsdorf, D. J., Tontonoz, P., and Edwards, P. A. (2002). Regulated expression of the apolipoprotein E/C-I/C-IV/C-II gene cluster in murine and human macrophages. A critical role for nuclear liver X receptors alpha and beta. J Biol Chem *277*, 31900-31908.

Malerod, L., Juvet, L. K., Hanssen-Bauer, A., Eskild, W., and Berg, T. (2002). Oxysterol-activated LXRalpha/RXR induces hSR-BI-promoter activity in hepatoma cells and preadipocytes. Biochem Biophys Res Commun *299*, 916-923.

Mathieu, A. P., Fleury, A., Ducharme, L., Lavigne, P., and LeHoux, J. G. (2002). Insights into steroidogenic acute regulatory protein (StAR)-dependent cholesterol transfer in mitochondria: evidence from molecular modeling and structure-based thermodynamics supporting the existence of partially unfolded states of StAR. J Mol Endocrinol *29*, 327-345.

Matsunaga, T., Isohashi, F., Nakanishi, Y., and Sakamoto, Y. (1985). Physiological changes in the activities of extramitochondrial acetyl-CoA hydrolase in the liver of rats under various metabolic conditions. Eur J Biochem *152*, 331-336.

Matyash, V., Geier, C., Henske, A., Mukherjee, S., Hirsh, D., Thiele, C., Grant, B., Maxfield, F. R., and Kurzchalia, T. V. (2001). Distribution and transport of cholesterol in Caenorhabditis elegans. Mol Biol Cell *12*, 1725-1736.

Matys, V., Fricke, E., Geffers, R., Gossling, E., Haubrock, M., Hehl, R., Hornischer, K., Karas, D., Kel, A. E., Kel-Margoulis, O. V., *et al.* (2003). TRANSFAC: transcriptional regulation, from patterns to profiles. Nucleic Acids Res *31*, 374-378.

Maxfield, F. R., and Wustner, D. (2002). Intracellular cholesterol transport. J Clin Invest *110*, 891-898.

Maxwell, K. N., Soccio, R. E., Duncan, E. M., Sehayek, E., and Breslow, J. L. (2003). Novel putative SREBP and LXR target genes identified by microarray analysis in liver of cholesterol-fed mice. J Lipid Res.

Mello, C. C., Kramer, J. M., Stinchcomb, D., and Ambros, V. (1991). Efficient gene transfer in C.elegans: extrachromosomal maintenance and integration of transforming sequences. Embo J *10*, 3959-3970.

Menon, A. K. (2002). Introduction: lipid transport--an overview. Semin Cell Dev Biol *13*, 159-162.

Merris, M., Wadsworth, W. G., Khamrai, U., Bittman, R., Chitwood, D. J., and Lenard, J. (2003). Sterol effects and sites of sterol accumulation in Caenorhabditis elegans: developmental requirement for 4alpha-methyl sterols. J Lipid Res *44*, 172-181.

Millatt, L. J., Bocher, V., Fruchart, J. C., and Staels, B. (2003). Liver X receptors and the control of cholesterol homeostasis: potential therapeutic targets for the treatment of atherosclerosis. Biochim Biophys Acta *1631*, 107-118.

Miller, W. L. (2002). Androgen biosynthesis from cholesterol to DHEA. Mol Cell Endocrinol *198*, 7-14.

Miller, W. L., and Strauss, J. F., 3rd (1999). Molecular pathology and mechanism of action of the steroidogenic acute regulatory protein, StAR. J Steroid Biochem Mol Biol *69*, 131-141.

Mohammadi, A., Perry, R. J., Storey, M. K., Cook, H. W., Byers, D. M., and Ridgway, N. D. (2001). Golgi localization and phosphorylation of oxysterol binding protein in Niemann-Pick C and U18666A-treated cells. J Lipid Res *42*, 1062-1071.

Moog-Lutz, C., Tomasetto, C., Regnier, C. H., Wendling, C., Lutz, Y., Muller, D., Chenard, M. P., Basset, P., and Rio, M. C. (1997). MLN64 exhibits homology with the steroidogenic acute regulatory protein (STAR) and is over-expressed in human breast carcinomas. Int J Cancer *71*, 183-191.

Morris, D. R., and Geballe, A. P. (2000). Upstream open reading frames as regulators of mRNA translation. Mol Cell Biol *20*, 8635-8642.

Mukherjee, S., and Maxfield, F. R. (1999). Cholesterol: stuck in traffic. Nat Cell Biol *1*, E37-38.

Mukherjee, S., Zha, X., Tabas, I., and Maxfield, F. R. (1998). Cholesterol distribution in living cells: fluorescence imaging using dehydroergosterol as a fluorescent cholesterol analog. Biophys J *75*, 1915-1925.

Munn, N. J., Arnio, E., Liu, D., Zoeller, R. A., and Liscum, L. (2003). Deficiency in ethanolamine plasmalogen leads to altered cholesterol transport. J Lipid Res *44*, 182-192.

Murphy, E. J. (2002). Sterol carrier protein-2: not just for cholesterol any more. Mol Cell Biochem *239*, 87-93.

Nagase, T., Kikuno, R., Ishikawa, K. I., Hirosawa, M., and Ohara, O. (2000). Prediction of the coding sequences of unidentified human genes. XVI. The complete sequences of 150 new cDNA clones from brain which code for large proteins in vitro. DNA Res *7*, 65-73.

Nagy, A. (2000). Cre recombinase: the universal reagent for genome tailoring. Genesis *26*, 99-109.

Nakanishi, Y., Okamoto, K., and Isohashi, F. (1993). Effects of chronic administration of the peroxisome proliferator, clofibrate, on cytosolic acetyl-CoA hydrolase in rat liver. Biochem Pharmacol *45*, 1403-1407.

Naureckiene, S., Sleat, D. E., Lackland, H., Fensom, A., Vanier, M. T., Wattiaux, R., Jadot, M., and Lobel, P. (2000). Identification of HE1 as the second gene of Niemann-Pick C disease. Science *290*, 2298-2301.

Neufeld, E. B. (1998). What the Niemann-Pick type C gene has taught us about cholesterol transport. In Intracellular Cholesterol Trafficking, T. Y. Chang, and D. A. Freeman, eds. (Boston, Kluwer Academic Publishers), pp. 93-107.

Neufeld, E. B., Cooney, A. M., Pitha, J., Dawidowicz, E. A., Dwyer, N. K., Pentchev, P. G., and Blanchette-Mackie, E. J. (1996). Intracellular trafficking of cholesterol monitored with a cyclodextrin. J Biol Chem *271*, 21604-21613.

Ng, I. O., Liang, Z. D., Cao, L., and Lee, T. K. (2000). DLC-1 is deleted in primary hepatocellular carcinoma and exerts inhibitory effects on the proliferation of hepatoma cell lines with deleted DLC-1. Cancer Res *60*, 6581-6584.

Nilsson, I., Ohvo-Rekila, H., Slotte, J. P., Johnson, A. E., and von Heijne, G. (2001). Inhibition of protein translocation across the endoplasmic reticulum membrane by sterols. J Biol Chem *276*, 41748-41754.

Ohta, H., Tohda, A., and Nishimune, Y. (2003). Proliferation and differentiation of spermatogonial stem cells in the W/Wv mutant mouse testis. Biol Reprod.

Okuda, K. I. (1994). Liver mitochondrial P450 involved in cholesterol catabolism and vitamin D activation. J Lipid Res *35*, 361-372.

Olivier, L. M., Kovacs, W., Masuda, K., Keller, G. A., and Krisans, S. K. (2000). Identification of peroxisomal targeting signals in cholesterol biosynthetic enzymes. AA-CoA thiolase, hmg-coa synthase, MPPD, and FPP synthase. J Lipid Res *41*, 1921-1935.

Olivier, L. M., and Krisans, S. K. (2000). Peroxisomal protein targeting and identification of peroxisomal targeting signals in cholesterol biosynthetic enzymes. Biochim Biophys Acta *1529*, 89-102.

Ou, J., Tu, H., Shan, B., Luk, A., DeBose-Boyd, R. A., Bashmakov, Y., Goldstein, J. L., and Brown, M. S. (2001). Unsaturated fatty acids inhibit transcription of the sterol regulatory element-binding protein-1c (SREBP-1c) gene by antagonizing ligand-dependent activation of the LXR. Proc Natl Acad Sci U S A *98*, 6027-6032.

Panagabko, C., Morley, S., Hernandez, M., Cassolato, P., Gordon, H., Parsons, R., Manor, D., and Atkinson, J. (2003). Ligand specificity in the CRAL-TRIO protein family. Biochemistry *42*, 6467-6474.

Pandak, W. M., Ren, S., Marques, D., Hall, E., Redford, K., Mallonee, D., Bohdan, P., Heuman, D., Gil, G., and Hylemon, P. (2002). Transport of Cholesterol into Mitochondria Is Rate-limiting for Bile Acid Synthesis via the Alternative Pathway in Primary Rat Hepatocytes. J Biol Chem *277*, 48158-48164.

Panini, S. R., and Sinensky, M. S. (2001). Mechanisms of oxysterol-induced apoptosis. Curr Opin Lipidol *12*, 529-533.

Parker, R., Phan, T., Baumeister, P., Roy, B., Cheriyath, V., Roy, A. L., and Lee, A. S. (2001). Identification of TFII-I as the endoplasmic reticulum stress response element binding factor ERSF: its autoregulation by stress and interaction with ATF6. Mol Cell Biol *21*, 3220-3233.

Peet, D. J., Turley, S. D., Ma, W., Janowski, B. A., Lobaccaro, J. M., Hammer, R. E., and Mangelsdorf, D. J. (1998). Cholesterol and bile acid metabolism are impaired in mice lacking the nuclear oxysterol receptor LXR alpha. Cell *93*, 693-704.

Petrescu, A. D., Gallegos, A. M., Okamura, Y., Strauss, J. F., 3rd, and Schroeder, F. (2001). Steroidogenic acute regulatory protein binds cholesterol and modulates mitochondrial membrane sterol domain dynamics. J Biol Chem *276*, 36970-36982.

Phillips, J. E., and Johnson, W. J. (1998). Efflux and plasma transport of biosynthetic sterols. In Intracellular Cholesterol Trafficking, T. Y. Chang, and D. A. Freeman, eds. (Boston, Kluwer Academic Publishers), pp. 147-167.

Pichler, H., Gaigg, B., Hrastnik, C., Achleitner, G., Kohlwein, S. D., Zellnig, G., Perktold, A., and Daum, G. (2001). A subfraction of the yeast endoplasmic reticulum associates with the plasma membrane and has a high capacity to synthesize lipids. Eur J Biochem *268*, 2351-2361.

Pol, A., Luetterforst, R., Lindsay, M., Heino, S., Ikonen, E., and Parton, R. G. (2001). A caveolin dominant negative mutant associates with lipid bodies and induces intracellular cholesterol imbalance. J Cell Biol *152*, 1057-1070.

Ponting, C. P., and Aravind, L. (1999). START: a lipid-binding domain in StAR, HD-ZIP and signalling proteins. Trends Biochem Sci *24*, 130-132.

Porter, F. D. (2002). Malformation syndromes due to inborn errors of cholesterol synthesis. J Clin Invest *110*, 715-724.

Portincasa, P., Moschetta, A., Calamita, G., Margari, A., and Palasciano, G. (2003). Pathobiology of cholesterol gallstone disease: from equilibrium ternary phase diagram to agents preventing cholesterol crystallization and stone formation. Curr Drug Targets Immune Endocr Metabol Disord *3*, 87-68.

Prinz, W. (2002). Cholesterol trafficking in the secretory and endocytic systems. Semin Cell Dev Biol *13*, 197-203.

Puglielli, L., Rigotti, A., Amigo, L., Nunez, L., Greco, A. V., Santos, M. J., and Nervi, F. (1996). Modulation of intrahepatic cholesterol trafficking: evidence by in vivo antisense treatment for the involvement of sterol carrier protein-2 in newly synthesized cholesterol transport into rat bile. Biochem J *317 (Pt 3)*, 681-687.

Puglielli, L., Tanzi, R. E., and Kovacs, D. M. (2003). Alzheimer's disease: the cholesterol connection. Nat Neurosci *6*, 345-351.

Raya, A., Revert, F., Navarro, S., and Saus, J. (1999). Characterization of a novel type of serine/threonine kinase that specifically phosphorylates the human goodpasture antigen. J Biol Chem *274*, 12642-12649.

Raya, A., Revert-Ros, F., Martinez-Martinez, P., Navarro, S., Rosello, E., Vieites, B., Granero, F., Forteza, J., and Saus, J. (2000). Goodpasture antigen-binding protein, the kinase that phosphorylates the goodpasture antigen, is an alternatively spliced variant implicated in autoimmune pathogenesis. J Biol Chem *275*, 40392-40399.

Reid, P. C., Sugii, S., and Chang, T. Y. (2003). Trafficking defects in endogenously synthesized cholesterol in fibroblasts, macrophages, hepatocytes, and glial cells from Niemann-Pick type C1 mice. J Lipid Res *44*, 1010-1019.

Reinhart, M. P., Billheimer, J. T., Faust, J. R., and Gaylor, J. L. (1987). Subcellular localization of the enzymes of cholesterol biosynthesis and metabolism in rat liver. J Biol Chem *262*, 9649-9655.

Repa, J. J., Liang, G., Ou, J., Bashmakov, Y., Lobaccaro, J. M., Shimomura, I., Shan, B., Brown, M. S., Goldstein, J. L., and Mangelsdorf, D. J. (2000a). Regulation of mouse sterol regulatory element-binding protein-1c gene (SREBP-1c) by oxysterol receptors, LXRalpha and LXRbeta. Genes Dev *14*, 2819-2830.

Repa, J. J., and Mangelsdorf, D. J. (2000). The role of orphan nuclear receptors in the regulation of cholesterol homeostasis. Annu Rev Cell Dev Biol *16*, 459-481.

Repa, J. J., and Mangelsdorf, D. J. (2002). The liver X receptor gene team: potential new players in atherosclerosis. Nat Med *8*, 1243-1248.

Repa, J. J., Turley, S. D., Lobaccaro, J. A., Medina, J., Li, L., Lustig, K., Shan, B., Heyman, R. A., Dietschy, J. M., and Mangelsdorf, D. J. (2000b). Regulation of absorption and ABC1-mediated efflux of cholesterol by RXR heterodimers. Science *289*, 1524-1529.

Reynolds, G. A., Basu, S. K., Osborne, T. F., Chin, D. J., Gil, G., Brown, M. S., Goldstein, J. L., and Luskey, K. L. (1984). HMG CoA reductase: a negatively regulated gene with unusual promoter and 5' untranslated regions. Cell *38*, 275-285.

Ridgway, N. D., Badiani, K., Byers, D. M., and Cook, H. W. (1998a). Inhibition of phosphorylation of the oxysterol binding protein by brefeldin A. Biochim Biophys Acta *1390*, 37-51.

Ridgway, N. D., Dawson, P. A., Ho, Y. K., Brown, M. S., and Goldstein, J. L. (1992). Translocation of oxysterol binding protein to Golgi apparatus triggered by ligand binding. J Cell Biol *116*, 307-319.

Ridgway, N. D., Lagace, T. A., Cook, H. W., and Byers, D. M. (1998b). Differential effects of sphingomyelin hydrolysis and cholesterol transport on oxysterol-binding protein phosphorylation and Golgi localization. J Biol Chem *273*, 31621-31628.

Ridley, A. J. (2001). Rho family proteins: coordinating cell responses. Trends Cell Biol *11*, 471-477.

Roderick, S. L., Chan, W. W., Agate, D. S., Olsen, L. R., Vetting, M. W., Rajashankar, K. R., and Cohen, D. E. (2002). Structure of human phosphatidylcholine transfer protein in complex with its ligand. Nat Struct Biol *9*, 507-511.

Romanowski, M. J., Soccio, R. E., Breslow, J. L., and Burley, S. K. (2002). Crystal structure of the Mus musculus cholesterol-regulated START protein 4 (StarD4) containing a StAR-related lipid transfer domain. Proc Natl Acad Sci U S A *99*, 6949-6954.

Rossi, P., Sette, C., Dolci, S., and Geremia, R. (2000). Role of c-kit in mammalian spermatogenesis. J Endocrinol Invest *23*, 609-615.

Roy, B., and Lee, A. S. (1999). The mammalian endoplasmic reticulum stress response element consists of an evolutionarily conserved tripartite structure and interacts with a novel stress-inducible complex. Nucleic Acids Res *27*, 1437-1443.

Ruiz-Pesini, E., Diez, C., Lapena, A. C., Perez-Martos, A., Montoya, J., Alvarez, E., Arenas, J., and Lopez-Perez, M. J. (1998). Correlation of sperm motility with mitochondrial enzymatic activities. Clin Chem *44*, 1616-1620.

Russell, D. W. (2000). Oxysterol biosynthetic enzymes. Biochim Biophys Acta *1529*, 126-135.

Saito, H., Dhanasekaran, P., Nguyen, D., Holvoet, P., Lund-Katz, S., and Phillips, M. C. (2003). Domain structure and lipid interaction in human apolipoproteins A-I and E, a general model. J Biol Chem *278*, 23227-23232.

Schoonjans, K., Brendel, C., Mangelsdorf, D., and Auwerx, J. (2000). Sterols and gene expression: control of affluence. Biochim Biophys Acta *1529*, 114-125.

Schroeder, F., Gallegos, A. M., Atshaves, B. P., Storey, S. M., McIntosh, A. L., Petrescu, A. D., Huang, H., Starodub, O., Chao, H., Yang, H., *et al.* (2001). Recent advances in membrane microdomains: rafts, caveolae, and intracellular cholesterol trafficking. Exp Biol Med (Maywood) *226*, 873-890.

Schroeder, F., Jefferson, J. R., Powell, D., Incerpi, S., Woodford, J. K., Colles, S. M., Myers-Payne, S., Emge, T., Hubbell, T., Moncecchi, D., and et al. (1993). Expression of rat L-FABP in mouse fibroblasts: role in fat absorption. Mol Cell Biochem *123*, 73-83.

Schroeder, F., Zhou, M., Swaggerty, C. L., Atshaves, B. P., Petrescu, A. D., Storey, S. M., Martin, G. G., Huang, H., Helmkamp, G. M., and Ball, J. M. (2003). Sterol carrier protein-2 functions in phosphatidylinositol transfer and signaling. Biochemistry *42*, 3189-3202.

Schulten, H. J., Engel, W., Nayernia, K., and Burfeind, P. (1999). Yeast one-hybrid assay identifies YY1 as a binding factor for a proacrosin promoter element. Biochem Biophys Res Commun *257*, 871-873.

Schultz, J. R., Tu, H., Luk, A., Repa, J. J., Medina, J. C., Li, L., Schwendner, S., Wang, S., Thoolen, M., Mangelsdorf, D. J., *et al.* (2000). Role of LXRs in control of lipogenesis. Genes Dev *14*, 2831-2838.

Seedorf, U., Ellinghaus, P., and Roch Nofer, J. (2000). Sterol carrier protein-2. Biochim Biophys Acta *1486*, 45-54.

Sehayek, E., Ono, J. G., Shefer, S., Nguyen, L. B., Wang, N., Batta, A. K., Salen, G., Smith, J. D., Tall, A. R., and Breslow, J. L. (1998). Biliary cholesterol excretion: a novel mechanism that regulates dietary cholesterol absorption. Proc Natl Acad Sci U S A *95*, 10194-10199.

Sekimata, M., Kabuyama, Y., Emori, Y., and Homma, Y. (1999). Morphological changes and detachment of adherent cells induced by p122, a GTPase-activating protein for Rho. J Biol Chem *274*, 17757-17762.

Sever, N., Yang, T., Brown, M. S., Goldstein, J. L., and DeBose-Boyd, R. A. (2003). Accelerated degradation of HMG CoA reductase mediated by binding of insig-1 to its sterol-sensing domain. Mol Cell *11*, 25-33.

Shen, W. J., Patel, S., Natu, V., Hong, R., Azhar, S., and Kraemer, F. B. (2003). Interaction of hormone-sensitive lipase with steroidogenic acute regulatory protein: Facilitation of cholesterol transfer in adrenal. J Biol Chem.

Sheng, Z., Otani, H., Brown, M. S., and Goldstein, J. L. (1995). Independent regulation of sterol regulatory element-binding proteins 1 and 2 in hamster liver. Proc Natl Acad Sci U S A *92*, 935-938.

Shi, Y. (2003). Mammalian RNAi for the masses. Trends Genet *19*, 9-12.

Shibata, N., Arita, M., Misaki, Y., Dohmae, N., Takio, K., Ono, T., Inoue, K., and Arai, H. (2001). Supernatant protein factor, which stimulates the conversion of squalene to lanosterol, is a cytosolic squalene transfer protein and enhances cholesterol biosynthesis. Proc Natl Acad Sci U S A *98*, 2244-2249.

Shimano, H., Horton, J. D., Hammer, R. E., Shimomura, I., Brown, M. S., and Goldstein, J. L. (1996). Overproduction of cholesterol and fatty acids causes massive liver enlargement in transgenic mice expressing truncated SREBP-1a. J Clin Invest *98*, 1575-1584.

Shimano, H., Horton, J. D., Shimomura, I., Hammer, R. E., Brown, M. S., and Goldstein, J. L. (1997). Isoform 1c of sterol regulatory element binding protein is less active than isoform 1a in livers of transgenic mice and in cultured cells. J Clin Invest *99*, 846-854.

Shimomura, I., Bashmakov, Y., Shimano, H., Horton, J. D., Goldstein, J. L., and Brown, M. S. (1997). Cholesterol feeding reduces nuclear forms of sterol regulatory element binding proteins in hamster liver. Proc Natl Acad Sci U S A *94*, 12354-12359.

Simons, K., and Ehehalt, R. (2002). Cholesterol, lipid rafts, and disease. J Clin Invest *110*, 597-603.

Simons, K., and Ikonen, E. (2000). How cells handle cholesterol. Science *290*, 1721-1726.

Skiba, P. J., Zha, X., Maxfield, F. R., Schissel, S. L., and Tabas, I. (1996). The distal pathway of lipoprotein-induced cholesterol esterification, but not sphingomyelinase-induced cholesterol esterification, is energy-dependent. J Biol Chem *271*, 13392-13400.

Smart, E. J., Ying, Y., Donzell, W. C., and Anderson, R. G. (1996). A role for caveolin in transport of cholesterol from endoplasmic reticulum to plasma membrane. J Biol Chem *271*, 29427-29435.

Smith, J. D., and Breslow, J. L. (1997). The emergence of mouse models of atherosclerosis and their relevance to clinical research. J Intern Med *242*, 99-109.

Soccio, R. E., Adams, R. M., Romanowski, M. J., Sehayek, E., Burley, S. K., and Breslow, J. L. (2002). The cholesterol-regulated StarD4 gene encodes a StAR-related lipid transfer protein with two closely related homologues, StarD5 and StarD6. Proc Natl Acad Sci U S A *99*, 6943-6948.

Soccio, R. E., and Breslow, J. L. (2003). StAR-related lipid transfer (START) proteins: mediators of intracellular lipid metabolism. J Biol Chem *278*, 22183-22186.

Song, C., Hiipakka, R. A., and Liao, S. (2001). Auto-oxidized cholesterol sulfates are antagonistic ligands of liver X receptors: implications for the development and treatment of atherosclerosis. Steroids *66*, 473-479.

Soukas, A., Cohen, P., Socci, N. D., and Friedman, J. M. (2000). Leptin-specific patterns of gene expression in white adipose tissue. Genes Dev *14*, 963-980.

Spencer, T. A., Li, D., Russel, J. S., Collins, J. L., Bledsoe, R. K., Consler, T. G., Moore, L. B., Galardi, C. M., McKee, D. D., Moore, J. T., *et al.* (2001). Pharmacophore analysis of the nuclear oxysterol receptor LXRalpha. J Med Chem *44*, 886-897.

Starodub, O., Jolly, C. A., Atshaves, B. P., Roths, J. B., Murphy, E. J., Kier, A. B., and Schroeder, F. (2000). Sterol carrier protein-2 localization in endoplasmic reticulum and role in phospholipid formation. Am J Physiol Cell Physiol *279*, C1259-1269.

Steinberg, D., and Gotto, A. M., Jr. (1999). Preventing coronary artery disease by lowering cholesterol levels: fifty years from bench to bedside. Jama *282*, 2043-2050.

Stocco, D. M. (2001). StAR protein and the regulation of steroid hormone biosynthesis. Annu Rev Physiol *63*, 193-213.

Stocker, A., Tomizaki, T., Schulze-Briese, C., and Baumann, U. (2002). Crystal structure of the human supernatant protein factor. Structure (Camb) *10*, 1533-1540.

Storey, M. K., Byers, D. M., Cook, H. W., and Ridgway, N. D. (1998). Cholesterol regulates oxysterol binding protein (OSBP) phosphorylation and Golgi localization in Chinese hamster ovary cells: correlation with stimulation of sphingomyelin synthesis by 25-hydroxycholesterol. Biochem J *336 (Pt 1)*, 247-256.

Strauss, J. F., 3rd, Kishida, T., Christenson, L. K., Fujimoto, T., and Hiroi, H. (2003). START domain proteins and the intracellular trafficking of cholesterol in steroidogenic cells. Mol Cell Endocrinol *202*, 59-65.

Strauss, J. F., Liu, P., Christenson, L. K., and Watari, H. (2002). Sterols and intracellular vesicular trafficking: lessons from the study of NPC1. Steroids *67*, 947-951.

Suematsu, N., Okamoto, K., Shibata, K., Nakanishi, Y., and Isohashi, F. (2001). Molecular cloning and functional expression of rat liver cytosolic acetyl-CoA hydrolase. Eur J Biochem *268*, 2700-2709.

Sugawara, T., Holt, J. A., Driscoll, D., Strauss, J. F., 3rd, Lin, D., Miller, W. L., Patterson, D., Clancy, K. P., Hart, I. M., Clark, B. J., and et al. (1995a). Human steroidogenic acute regulatory protein: functional activity in COS-1 cells, tissue-specific expression, and mapping of the structural gene to 8p11.2 and a pseudogene to chromosome 13. Proc Natl Acad Sci U S A *92*, 4778-4782.

Sugawara, T., Lin, D., Holt, J. A., Martin, K. O., Javitt, N. B., Miller, W. L., and Strauss, J. F., 3rd (1995b). Structure of the human steroidogenic acute regulatory protein (StAR) gene: StAR stimulates mitochondrial cholesterol 27-hydroxylase activity. Biochemistry *34*, 12506-12512.

Sugawara, T., Shimizu, H., Hoshi, N., Nakajima, A., and Fujimoto, S. (2003). Steroidogenic acute regulatory protein binding-protein cloned by a yeast two-hybrid system. J Biol Chem.

Sugihara, T., Wadhwa, R., Kaul, S. C., and Mitsui, Y. (1999). A novel testis-specific metallothionein-like protein, tesmin, is an early marker of male germ cell differentiation. Genomics *57*, 130-136.

Sugii, S., Reid, P. C., Ohgami, N., Du, H., and Chang, T. Y. (2003). Distinct endosomal compartments in early trafficking of low density lipoprotein-derived cholesterol. J Biol Chem *278*, 27180-27189.

Tabas, I. (2002a). Cholesterol in health and disease. J Clin Invest *110*, 583-590.

Tabas, I. (2002b). Consequences of cellular cholesterol accumulation: basic concepts and physiological implications. J Clin Invest *110*, 905-911.

Tabor, D. E., Kim, J. B., Spiegelman, B. M., and Edwards, P. A. (1999). Identification of conserved cis-elements and transcription factors required for sterol-regulated transcription of stearoyl-CoA desaturase 1 and 2. J Biol Chem *274*, 20603-20610.

Tabunoki, H., Sugiyama, H., Tanaka, Y., Fujii, H., Banno, Y., Jouni, Z. E., Kobayashi, M., Sato, R., Maekawa, H., and Tsuchida, K. (2002). Isolation, characterization, and cDNA sequence of a carotenoid binding protein from the silk gland of Bombyx mori larvae. J Biol Chem *277*, 32133-32140.

Tacer, K. F., Haugen, T. B., Baltsen, M., Debeljak, N., and Rozman, D. (2002). Tissue-specific transcriptional regulation of the cholesterol biosynthetic pathway leads to accumulation of testis meiosis-activating sterol (T-MAS). J Lipid Res *43*, 82-89.

Tall, A. R., Costet, P., and Wang, N. (2002). Regulation and mechanisms of macrophage cholesterol efflux. J Clin Invest *110*, 899-904.

Tansey, T. R., and Shechter, I. (2000). Structure and regulation of mammalian squalene synthase. Biochim Biophys Acta *1529*, 49-62.

Taylor, F. R., and Kandutsch, A. A. (1985). Oxysterol binding protein. Chem Phys Lipids *38*, 187-194.

Thiele, C., Hannah, M. J., Fahrenholz, F., and Huttner, W. B. (2000). Cholesterol binds to synaptophysin and is required for biogenesis of synaptic vesicles. Nat Cell Biol *2*, 42-49.

Thomas, M. J., and Seto, E. (1999). Unlocking the mechanisms of transcription factor YY1: are chromatin modifying enzymes the key? Gene *236*, 197-208.

Tomasetto, C., Regnier, C., Moog-Lutz, C., Mattei, M. G., Chenard, M. P., Lidereau, R., Basset, P., and Rio, M. C. (1995). Identification of four novel human genes amplified and overexpressed in breast carcinoma and localized to the q11-q21.3 region of chromosome 17. Genomics *28*, 367-376.

Tontonoz, P., and Mangelsdorf, D. J. (2003). Liver x receptor signaling pathways in cardiovascular disease. Mol Endocrinol *17*, 985-993.

Travers, K. J., Patil, C. K., Wodicka, L., Lockhart, D. J., Weissman, J. S., and Walter, P. (2000). Functional and genomic analyses reveal an essential coordination between the unfolded protein response and ER-associated degradation. Cell *101*, 249-258.

Travis, A. J., and Kopf, G. S. (2002). The role of cholesterol efflux in regulating the fertilization potential of mammalian spermatozoa. J Clin Invest *110*, 731-736.

Tsujishita, Y., and Hurley, J. H. (2000). Structure and lipid transport mechanism of a StAR-related domain. Nat Struct Biol *7*, 408-414.

Tuckey, R. C., Headlam, M. J., Bose, H. S., and Miller, W. L. (2002). Transfer of cholesterol between phospholipid vesicles mediated by the steroidogenic acute regulatory protein (StAR). J Biol Chem.

Uittenbogaard, A., Everson, W. V., Matveev, S. V., and Smart, E. J. (2002). Cholesteryl ester is transported from caveolae to internal membranes as part of a caveolin-annexin II lipid-protein complex. J Biol Chem *277*, 4925-4931.

Uittenbogaard, A., and Smart, E. J. (2000). Palmitoylation of caveolin-1 is required for cholesterol binding, chaperone complex formation, and rapid transport of cholesterol to caveolae. J Biol Chem *275*, 25595-25599.

Uittenbogaard, A., Ying, Y., and Smart, E. J. (1998). Characterization of a cytosolic heat-shock protein-caveolin chaperone complex. Involvement in cholesterol trafficking. J Biol Chem *273*, 6525-6532.

Underwood, K. W., Andemariam, B., McWilliams, G. L., and Liscum, L. (1996). Quantitative analysis of hydrophobic amine inhibition of intracellular cholesterol transport. J Lipid Res *37*, 1556-1568.

Underwood, K. W., Jacobs, N. L., Howley, A., and Liscum, L. (1998). Evidence for a cholesterol transport pathway from lysosomes to endoplasmic reticulum that is independent of the plasma membrane. J Biol Chem *273*, 4266-4274.

Urbani, L., and Simoni, R. D. (1990). Cholesterol and vesicular stomatitis virus G protein take separate routes from the endoplasmic reticulum to the plasma membrane. J Biol Chem *265*, 1919-1923.

Vallett, S. M., Sanchez, H. B., Rosenfeld, J. M., and Osborne, T. F. (1996). A direct role for sterol regulatory element binding protein in activation of 3-hydroxy-3-methylglutaryl coenzyme A reductase gene. J Biol Chem *271*, 12247-12253.

van der Sanden, M. H., Houweling, M., van Golde, L. M., and Vaandrager, A. B. (2003). Inhibition of phosphatidylcholine synthesis induces expression of the endoplasmic reticulum stress and apoptosis-related protein CCAAT/enhancer-binding protein-homologous protein (CHOP/GADD153). Biochem J *369*, 643-650.

van Helvoort, A., de Brouwer, A., Ottenhoff, R., Brouwers, J. F., Wijnholds, J., Beijnen, J. H., Rijneveld, A., van der Poll, T., van der Valk, M. A., Majoor, D., *et al.* (1999). Mice without phosphatidylcholine transfer protein have no defects in the secretion of phosphatidylcholine into bile or into lung airspaces. Proc Natl Acad Sci U S A *96*, 11501-11506.

Velculescu, V. E., Zhang, L., Vogelstein, B., and Kinzler, K. W. (1995). Serial analysis of gene expression. Science *270*, 484-487.

Venkateswaran, A., Repa, J. J., Lobaccaro, J. M., Bronson, A., Mangelsdorf, D. J., and Edwards, P. A. (2000). Human white/murine ABC8 mRNA levels are highly induced in lipid-loaded macrophages. A transcriptional role for specific oxysterols. J Biol Chem *275*, 14700-14707.

Wagner, B. L., Valledor, A. F., Shao, G., Daige, C. L., Bischoff, E. D., Petrowski, M., Jepsen, K., Baek, S. H., Heyman, R. A., Rosenfeld, M. G., *et al.* (2003). Promoter-specific roles for liver X receptor/corepressor complexes in the regulation of ABCA1 and SREBP1 gene expression. Mol Cell Biol *23*, 5780-5789.

Wang, X. (2001). The expanding role of mitochondria in apoptosis. Genes Dev *15*, 2922-2933.

Watari, H., Arakane, F., Moog-Lutz, C., Kallen, C. B., Tomasetto, C., Gerton, G. L., Rio, M. C., Baker, M. E., and Strauss, J. F., 3rd (1997). MLN64 contains a domain with homology to the steroidogenic acute regulatory protein (StAR) that stimulates steroidogenesis. Proc Natl Acad Sci U S A *94*, 8462-8467.

Watari, H., Blanchette-Mackie, E. J., Dwyer, N. K., Sun, G., Glick, J. M., Patel, S., Neufeld, E. B., Pentchev, P. G., and Strauss, J. F., 3rd (2000). NPC1-containing compartment of

human granulosa-lutein cells: a role in the intracellular trafficking of cholesterol supporting steroidogenesis. Exp Cell Res *255*, 56-66.

Werstuck, G. H., Lentz, S. R., Dayal, S., Hossain, G. S., Sood, S. K., Shi, Y. Y., Zhou, J., Maeda, N., Krisans, S. K., Malinow, M. R., and Austin, R. C. (2001). Homocysteine-induced endoplasmic reticulum stress causes dysregulation of the cholesterol and triglyceride biosynthetic pathways. J Clin Invest *107*, 1263-1273.

Wirtz, K. W. (1991). Phospholipid transfer proteins. Annu Rev Biochem *60*, 73-99.

Wojtanik, K. M., and Liscum, L. (2003). The transport of low density lipoprotein-derived cholesterol to the plasma membrane is defective in NPC1 cells. J Biol Chem *278*, 14850-14856.

Wustner, D., Herrmann, A., Hao, M., and Maxfield, F. R. (2002). Rapid nonvesicular transport of sterol between the plasma membrane domains of polarized hepatic cells. J Biol Chem *277*, 30325-30336.

Xie, C., Turley, S. D., and Dietschy, J. M. (2000). Centripetal cholesterol flow from the extrahepatic organs through the liver is normal in mice with mutated Niemann-Pick type C protein (NPC1). J Lipid Res *41*, 1278-1289.

Xu, J., Cho, H., O'Malley, S., Park, J. H., and Clarke, S. D. (2002). Dietary polyunsaturated fats regulate rat liver sterol regulatory element binding proteins-1 and -2 in three distinct stages and by different mechanisms. J Nutr *132*, 3333-3339.

Xu, X. X., and Lambeth, J. D. (1989). Cholesterol sulfate is a naturally occurring inhibitor of steroidogenesis in isolated rat adrenal mitochondria. J Biol Chem *264*, 7222-7227.

Yamaguchi, A., Hori, O., Stern, D. M., Hartmann, E., Ogawa, S., and Tohyama, M. (1999). Stress-associated endoplasmic reticulum protein 1 (SERP1)/Ribosome-associated membrane protein 4 (RAMP4) stabilizes membrane proteins during stress and facilitates subsequent glycosylation. J Cell Biol *147*, 1195-1204.

Yamanaka, M., Koga, M., Tanaka, H., Nakamura, Y., Ohta, H., Yomogida, K., Tsuchida, J., Iguchi, N., Nojima, H., Nozaki, M., *et al.* (2000). Molecular cloning and characterization of phosphatidylcholine transfer protein-like protein gene expressed in murine haploid germ cells. Biol Reprod *62*, 1694-1701.

Yan, W., Kero, J., Huhtaniemi, I., and Toppari, J. (2000). Stem cell factor functions as a survival factor for mature Leydig cells and a growth factor for precursor Leydig cells after ethylene dimethane sulfonate treatment: implication of a role of the stem cell factor/c-Kit system in Leydig cell development. Dev Biol *227*, 169-182.

Yang, T., Espenshade, P. J., Wright, M. E., Yabe, D., Gong, Y., Aebersold, R., Goldstein, J. L., and Brown, M. S. (2002). Crucial step in cholesterol homeostasis: sterols promote binding of SCAP to INSIG-1, a membrane protein that facilitates retention of SREBPs in ER. Cell *110*, 489-500.

Ye, J., Rawson, R. B., Komuro, R., Chen, X., Dave, U. P., Prywes, R., Brown, M. S., and Goldstein, J. L. (2000). ER stress induces cleavage of membrane-bound ATF6 by the same proteases that process SREBPs. Mol Cell *6*, 1355-1364.

Yoder, M. D., Thomas, L. M., Tremblay, J. M., Oliver, R. L., Yarbrough, L. R., and Helmkamp, G. M., Jr. (2001). Structure of a multifunctional protein. Mammalian phosphatidylinositol transfer protein complexed with phosphatidylcholine. J Biol Chem *276*, 9246-9252.

Yoshida, H., Haze, K., Yanagi, H., Yura, T., and Mori, K. (1998). Identification of the cis-acting endoplasmic reticulum stress response element responsible for transcriptional induction of mammalian glucose-regulated proteins. Involvement of basic leucine zipper transcription factors. J Biol Chem *273*, 33741-33749.

Yoshida, H., Matsui, T., Hosokawa, N., Kaufman, R. J., Nagata, K., and Mori, K. (2003). A time-dependent phase shift in the mammalian unfolded protein response. Dev Cell *4*, 265-271.

Yoshida, H., Matsui, T., Yamamoto, A., Okada, T., and Mori, K. (2001a). XBP1 mRNA is induced by ATF6 and spliced by IRE1 in response to ER stress to produce a highly active transcription factor. Cell *107*, 881-891.

Yoshida, H., Okada, T., Haze, K., Yanagi, H., Yura, T., Negishi, M., and Mori, K. (2001b). Endoplasmic reticulum stress-induced formation of transcription factor complex ERSF including NF-Y (CBF) and activating transcription factors 6alpha and 6beta that activates the mammalian unfolded protein response. Mol Cell Biol *21*, 1239-1248.

Yoshikawa, T., Ide, T., Shimano, H., Yahagi, N., Amemiya-Kudo, M., Matsuzaka, T., Yatoh, S., Kitamine, T., Okazaki, H., Tamura, Y., *et al.* (2003). Cross-talk between peroxisome proliferator-activated receptor (PPAR) alpha and liver X receptor (LXR) in nutritional regulation of fatty acid metabolism. I. PPARs suppress sterol regulatory element binding protein-1c promoter through inhibition of LXR signaling. Mol Endocrinol *17*, 1240-1254.

Yu, L., York, J., von Bergmann, K., Lutjohann, D., Cohen, J. C., and Hobbs, H. H. (2003). Stimulation of cholesterol excretion by the liver X receptor agonist requires ATP-binding cassette transporters G5 and G8. J Biol Chem *278*, 15565-15570.

Yuan, B. Z., Zhou, X., Durkin, M. E., Zimonjic, D. B., Gumundsdottir, K., Eyfjord, J. E., Thorgeirsson, S. S., and Popescu, N. C. (2003). DLC-1 gene inhibits human breast cancer cell growth and in vivo tumorigenicity. Oncogene *22*, 445-450.

Zha, X., Pierini, L. M., Leopold, P. L., Skiba, P. J., Tabas, I., and Maxfield, F. R. (1998). Sphingomyelinase treatment induces ATP-independent endocytosis. J Cell Biol *140*, 39-47.

Zhang, M., Liu, P., Dwyer, N. K., Christenson, L. K., Fujimoto, T., Martinez, F., Comly, M., Hanover, J. A., Blanchette-Mackie, E. J., and Strauss, J. F., 3rd (2002a). MLN64 mediates mobilization of lysosomal cholesterol to steroidogenic mitochondria. J Biol Chem.

Zhang, M., Liu, P., Dwyer, N. K., Christenson, L. K., Fujimoto, T., Martinez, F., Comly, M., Hanover, J. A., Blanchette-Mackie, E. J., and Strauss, J. F., 3rd (2002b). MLN64 mediates

mobilization of lysosomal cholesterol to steroidogenic mitochondria. J Biol Chem *277*, 33300-33310.

Zhang, Y., Yu, C., Liu, J., Spencer, T. A., Chang, C. C., and Chang, T. Y. (2003). Cholesterol is superior to 7-ketocholesterol or 7 alpha-hydroxycholesterol as an allosteric activator for acyl-coenzyme A:cholesterol acyltransferase 1. J Biol Chem *278*, 11642-11647.

Zheng, L., Roeder, R. G., and Luo, Y. (2003). S phase activation of the histone H2B promoter by OCA-S, a coactivator complex that contains GAPDH as a key component. Cell *114*, 255-266.

Publications and Manuscripts

Research Articles:

Soccio, R. E., Adams, R. M., Romanowski, M. J., Sehayek, E., Burley, S. K., and Breslow, J. L. (2002). The cholesterol-regulated StarD4 gene encodes a StAR-related lipid transfer protein with two closely related homologues, StarD5 and StarD6. Proc Natl Acad Sci U S A *99*, 6943-6948.

Romanowski, M. J., Soccio, R. E., Breslow, J. L., and Burley, S. K. (2002). Crystal structure of the Mus musculus cholesterol-regulated START protein 4 (StarD4) containing a StAR-related lipid transfer domain. Proc Natl Acad Sci U S A *99*, 6949-6954.

Soccio, R. E., Maxwell, K. N., Adams, R. M., and Breslow, J. L. Differential gene regulation of the StarD4 and StarD5 cholesterol transfer proteins: activation of StarD4 by SREBP-2 and StarD5 by endoplasmic reticulum stress. *(in preparation).*

Soccio, R. E., Vigodner, M., Hwang, K., Huang, H., Breslow, J. L., and Morris, P. L. StarD6 expression and localization in male germ cells. *(in preparation).*

Review Articles:

Soccio, R. E., and Breslow, J. L. Intracellular Cholesterol Transport. Arterioscler Thromb Vasc Biol *(in preparation).*

Soccio, R. E., and Breslow, J. L. (2003). StAR-related lipid transfer (START) proteins: mediators of intracellular lipid metabolism. J Biol Chem *278*, 22183-22186.